

NON-CONTACT PREDICTION OF SOIL MOISTURE
PROFILES USING RADIO WAVE REFLECTION

By

DUANE LEE NEEDHAM

Bachelor of Science
University of Nebraska-Lincoln
Lincoln, Nebraska
1998

Master of Science
Oklahoma State University
Stillwater, Oklahoma
2000

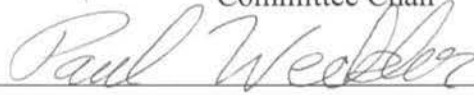
Submitted to the Faculty of the
Graduate College of the
Oklahoma State University
in partial fulfillment of
the requirements for
the Degree of
DOCTOR OF PHILOSOPHY
August, 2003

NON-CONTACT PREDICTION OF SOIL MOISTURE
PROFILES USING RADIO WAVE REFLECTION

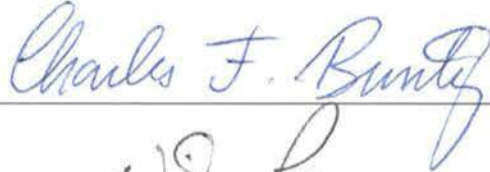
Thesis Approved:



Committee Chair



Dissertation Adviser



Dean of the Graduate College

ACKNOWLEDGMENTS

So many thanks are owed to people for my education at Oklahoma State University. I am deeply indebted to my committee chairman and friend Marvin Stone for his guidance throughout my graduate program. Throughout my travels in life, he and his wife Bonnie will always be in my heart. To the other members of my committee: Paul Weckler, John Solie, Bill Raun, and Charles Bunting, I express my appreciation for their valuable advice in research and in life. Their knowledge and positive attitude have been an invaluable part of my experience at Oklahoma State. I would also like to thank Wayne, Harshman, Rocky, and Veldman for help with all of my projects and for the advice in “real life”.

Very special thanks must be directed to Dale and Gwen Needham, my parents, for their endless love and support through all of my endeavors. No matter how far I travel, I’ll always know the direction of home. Finally, I would like to thank Angelika, the love of my life, for she is the driving force that kept me studying, working, and striving to be my best.

TABLE OF CONTENTS

Chapter	Page
I. INTRODUCTION	1
II. LITERATURE REVIEW	5
Soil Dielectric Properties	5
Electromagnetic Wave Propagation.....	8
Soil Effects on Radio Wave Propagation.....	12
Layered Earth.....	14
Profile Restoration Algorithms.....	20
Summery	22
III. DETECTION THEORY AND PHYSICAL ASSEMBLY	24
Introduction.....	24
Preliminary Calculations.....	24
Field Test Apparatus.....	26
IV. INSTRUMENT CALIBRATIONS	37
Introduction.....	37
Neutron Probe Calibration	37
Neutron Probe Calibration Results	40
Dielectric Property Coaxial Cell Calibration.....	42
Coaxial Cell Calibration Results.....	50
Field Apparatus Calibration.....	58
Field Apparatus Calibration Results	63
V. SOIL DIELECTRIC VARIABILITY.....	71
Introduction.....	71
Soil Density.....	71
Soil Particle Size.....	74
Dielectric Properties.....	74
VI. SOIL MOISTURE AND DIELECTRIC PROPERTY RELATIONSHIPS..	77
Procedure	77
Soil Moisture-Dielectric Relationship	78

VII. SIMULATION OF REFLECTION COEFFICIENTS	90
Procedure	90
Profiles of Constant Moisture	92
Two-Layer Moisture Profiles.....	95
Profiles Acquired via Neutron Probe Measurements.....	101
VIII. FIELD MEASUREMENTS	102
Procedure	102
Field Trial Measurement Results.....	105
Comparisons of Reflection Coefficients.....	109
Correlation of Reflection Coefficients to Moisture	112
IX. PROFILE RESTORATION ALGORITHM.....	119
Procedure	119
Results of Profile Restoration Algorithm	122
X. CONCLUSIONS AND RECOMENDATIONS.....	128
Summary	128
Conclusions.....	130
Recommendations for Further Research.....	132
BIBLIOGRAPHY	135

APPENDICES	139
APPENDIX A— INTERFERING ELECTROMAGNETIC ENERGY MEASURED BY THE DISCONE ANTENNA	140
APPENDIX B—NEUTRON PROBE CALIBRATION DATA	141
APPENDIX C—MATLAB CODE: COAXIAL CELL DIELECTRIC ITTERATION ALGORITHM	142
APPENDIX D—COAXIAL CELL CALIBRATION DATA.....	146
APPENDIX E—MATLAB CODE: FIELD INSTRUMENT REFLECTION CALCULATIONS	148
APPENDIX F—FIELD INSTRUMENT CALIBRATION DATA	150
APPENDIX G—SOIL HOMOGENEITY DATA	154
APPENDIX H—MOISTURE / DIELECTRIC RELATIONSHIP DATA ...	157
APPENDIX I—MATLAB CODE: SIMULATION OF RADIO WAVE REFLECTIONS FROM DIELECTRIC PROFILES	169
APPENDIX J— SIMULATION AND FIELD MEASUREMENTS.....	171
APPENDIX K—MATLAB CODE: PROFILE RESTORATION ALGORITHM.....	175

LIST OF TABLES

Table		Page
1.	Calculated wavelengths and skin depths.....	25
2.	Calculated reflection coefficients	25
3.	Error in network analyzer measurements and resulting dielectric error	57
4.	Reflection coefficient error of offset steel plates	68
5.	Analysis of variance of density in plots and at depth	72
6.	Depth profile of average soil density	73
7.	Analysis of variance of percent sand by plot and by depth	74
8.	ANOVA of soil permittivity with frequency, in plots, and at depth.....	75
9.	ANOVA of soil conductivity with frequency, in plots, and at depth	76
10.	Soil permittivity at specific moistures, in depth layers and within each frequency range.....	81
11.	Soil conductivity at specific moistures, in depth layers and within each frequency range	82
12.	Characteristic equations relating moisture content to dielectric properties ...	86
13.	Calculated skin depths of topsoil at various moistures.....	87
14.	ANOVA of magnitude of reflection from simulated profiles with constant moisture.....	92
15.	ANOVA of phase of simulated reflection from constant moisture profiles ..	93

16.	Magnitude and phase of simulated reflection coefficients from simulated profiles with constant moisture at a frequency of 793 MHz.....	94
17.	Average soil moisture at each depth for eight selected profiles as measured by the neutron probe	105
18.	ANOVA of simulated reflection magnitude from field profile measurements	109
19.	ANOVA of simulated reflection phase from field profile measurements	111
20.	Volumetric moisture content vs. average reflection magnitudes.....	112
21.	Volumetric moisture content vs. average reflection phase	114
22.	Volumetric moisture content vs. reflection magnitude at specific frequencies	115
23.	Volumetric moisture content vs. reflection phase at specific frequencies.....	117
24.	Algorithm predicted moisture from simulated reflections of profiles with constant moisture	123
25.	Predicted and actual moisture from simulated reflection of 2-layer moisture profiles	124
26.	Moisture profiles from simulated and measured reflections from field trials	125

LIST OF FIGURES

Figure	Page
1. Parallel polarized uniform plane wave	9
2. Parallel polarized uniform plane wave	28
3. Multiple reflections between dielectric layers	30
4. Geometry of wooden structure and antennas.....	32
5. Predicted shape of the soil surface detected by the antennas.....	33
6. Test plot pattern with soil cores	38
7. Neutron probe measurement of volumetric soil moisture.....	39
8. Relationship between neutron measurements and VMC.....	40
9. Variation in neutron probe measurements (normal speed setting)	41
10. Coaxial cell used in soil dielectric measurements (Arnold, 1992)	43
11. Exponential propagation characterizing the cable and lower cell (Prop)	51
12. Exponential propagation characterizing the upper cell (Prop2)	52
13. Terminating impedance Z_{cap}	53
14. Theoretical and measured permittivity of reagent grade n-propanol.....	54
15. Theoretical and measured conductivity of reagent grade n-propanol.....	55
16. Theoretical and measured permittivity of air.....	56
17. Theoretical and measured conductivity of air.....	56
18. Antenna configuration for isolation calibration.....	60

19.	Configuration of 16-gage steel calibration sheets.....	62
20.	Reflection from sky (impedance mismatch at antenna).....	64
21.	Transmission via the sky (antenna crosstalk)	65
22.	Reflection frequency response (F1).....	66
23.	Transmission frequency response (F2)	67
24.	Reflection coefficient magnitude as measured by network analyzer transmission	69
25.	Reflection coefficient phase of offset steel plates as measured by network analyzer transmission.....	69
26.	Depth profile of average soil density	69
27.	Permittivities of topsoil with various moisture contents	79
28.	Conductivities of topsoil with various moisture contents.....	79
29.	Moisture content—permittivity relationship of bottom layer.....	83
30.	Moisture content / permittivity relationship of topsoil	84
31.	Moisture content / conductivity relationship of topsoil	85
32.	Skin depths of topsoil at various moistures	88
33.	Magnitude and phase of reflection coefficients from simulated profiles with constant moisture at a frequency of 793 MHz.....	94
34.	Magnitude of simulated reflection from two-layer (dry over wet) profiles with several boundary depths.....	96

35.	Phase of simulated reflection from two-layer (dry over wet) profiles with several boundary depths.....	97
36.	Magnitude of simulated reflection from two-layer (wet over dry) profiles with several boundary depths.....	98
37.	Phase of simulated reflection from two-layer (wet over dry) profiles with several boundary depths.....	98
38.	Line diagrams of Tukey's comparisons of simulated profiles with dry soil on top of wet soil	99
39.	Line diagrams of Tukey's comparisons of simulated profiles with wet soil on top of dry soil	100
40.	Geometry of irrigation sprinkler system	104
41.	Average absolute volumetric moisture at depth (Profiles 1-4 measured with the neutron probe).....	106
42.	Average absolute volumetric moisture at depth (Profiles 5-8 measured with the neutron probe).....	106
43.	MATLAB simulated reflection coefficient of moisture profile number 2	107
44.	Measured soil reflection coefficient of moisture profile number 2	108
45.	Line diagrams of Tukey's comparisons of reflection magnitude (field trials).....	110
46.	Line diagrams of Tukey's comparisons of reflection phase (field trials)	111
47.	Volumetric moisture content vs. average reflection magnitudes.....	113

48.	Volumetric moisture content vs. average reflection phases.....	106
49.	Volumetric moisture content vs. reflection magnitude at specific frequencies	111
50.	Volumetric moisture content vs. reflection phase at specific frequencies.....	111
51.	Soil moisture predictions in top 30.5 cm from simulated and measured reflection coefficients.....	111
52.	Soil moisture predictions in lower 30.5 cm from simulated and measured reflection coefficients.....	111

NOMENCLATURE

ANOVA	Analysis of Variance
EM	Electromagnetic
ϵ	Permittivity
FCC	Federal Communications Commission
Γ	Reflection Coefficient
GPR	Ground-penetrating radar
PVC	Poly-vinyl Chloride
τ	Transmission Coefficient
TE	Transverse-electric
TM	Transverse-magnetic
VHF	Very High Frequency
VMC	Volumetric Moisture Content
VSWR	Voltage Standing Wave Ratio
UHF	Ultra High Frequency

CHAPTER I

INTRODUCTION

In the hydrologic cycle, one of the largest storage components for fresh water is soil. The amount of water in the soil influences all aspects of the environment of a particular area. Knowledge of the distribution of water in the soil allows the prediction of dynamic changes in water movement used in models for hydrology, meteorology, hydraulics, and agriculture. Among motivations for these models is the large-scale management of resources. Fresh water is becoming a scarce resource in many areas of the world, and the value of water conservation continues to increase. One of the largest consumers of water from the soil is production agriculture. Quantifying the water in soil would allow changes in farming practices to reduce water use in irrigation (Zur et al., 1994), reduce groundwater contamination from leaching nutrients (Vellidis et al., 1990), increase germination and emergence of seed (Bowers et al., 1975), and aid in the prediction of sources of plant stress. Irrigation scheduling and control of other agricultural operations i.e. tillage depend on the availability of soil moisture information concerning spatial and depth distribution of moisture.

Although soil moisture is a valuable ingredient for the prediction of crop needs, it is a difficult parameter to routinely measure over a large area. Individual locations can be sampled using sensors that measure soil moisture per unit mass, volume, or pressure. Many different types of sensing methods exist. Nevertheless, several are destructive and almost all of the methods rely on sensors that contact the soil.

In general, measurements made by sensors that rely on physical contact require more time than non-contact sensors. In order to implement a real-time system that utilizes moisture sensors, speed of the measurement is important. Time-domain reflectometry probes can make rapid surface moisture measurements but still require physical contact. The contact with the soil would add difficulty to the implementation on a moving machine and would rapidly fatigue the probes. Moisture profiles, as opposed to surface moisture, are even more difficult to measure because several sensor measurements at varied depths must be taken to get an adequate profile prediction. Neutron probes, which measure moisture at depth, also require access tubes for the measurement. Still, if moisture gradients could be measured quickly with adequate accuracy, the measurements could be very valuable for the management of resources in agricultural operations.

It is widely known that moisture in soil affects the soil's electrical properties. The change in electrical properties is the basis for many of the moisture sensors in existence, including time-domain reflectometry probes. The moisture-induced electrical property changes alter the behavior of electromagnetic fields in and around the soil. By transmitting electromagnetic waves toward the soil, and detecting the reflection, a measurement of moisture in the soil can be made.

This study investigated the potential of non-contact measurement of volumetric soil moisture profiles by detecting reflected VHF and UHF radio waves. (Volumetric moisture is the ratio of the volume of water in a volume of soil). The specific objectives of the study were:

1. To determine analytically if electromagnetic reflection coefficients within the frequency range of 80 MHz to 1 GHz. can detect volumetric moisture and moisture boundaries at depth in Oklahoma soil with hypothetical and existent moisture profiles.
2. To verify through measurement that electromagnetic reflection coefficients within the frequency range of 80 MHz to 1 GHz can detect volumetric moisture from Oklahoma soil containing various moisture profiles.
3. To develop a “moisture profile restoration algorithm” and test if it can estimate soil moisture content within layered depths from continuous wave electromagnetic reflection coefficients of multiple frequencies.

In order to test the objectives, two mathematical models were developed. The first model simulated electromagnetic reflection coefficients from hypothetical and existent profiles in soil. The second predicted moisture profiles in layers from electromagnetic reflection coefficients. The two models operated on an assumption that the soil electrical characteristics varied primarily with depth. To validate the assumption, variability of soil characteristics that affect electrical properties was tested. The algorithms also required relationships between moisture content and soil dielectric properties. Measurements were made in a coaxial cell that related soil moisture content to permittivity and conductivity. Soil reflections were simulated in a MATLAB program using homogeneous dielectric layers. The layers in the model were determined directly from moisture-dielectric relationships measured in the coaxial cell. Predicted reflections were analyzed, as were reflections measured in a field experiment in which radio waves

were transmitted by a log-periodic antenna, reflected by the soil surface and subsurface layers of dissimilar moisture, and detected by a receiving antenna. The profile restoration algorithm utilized the moisture-dielectric relationships to estimate moisture in layers from electromagnetic reflection coefficients.

CHAPTER II

LITERATURE REVIEW

Soil Dielectric Properties

Researchers have long known that the changing complex dielectric constants of the soil interact with radio wave propagation. Predictions of the dielectric constant of soil have been made since Ratcliffe and Shaw in 1929 (1929). In 1935, Smith-Rose (1935) measured the electrical properties of soil from 1 to 100 megacycles per second in two coaxial soil sample condensers. In the study, the moisture content of the soil was shown to affect the dielectric properties. The results also revealed that the measured quantities appeared different at different frequencies. Since that time, many researchers (Arulanandan and Smith, 1973; Hallikainen et al., 1985; Hipp, 1974; Hoekstra and Delaney, 1974; Nelson, 1983; Topp et al., 1980; Wang, 1980) have conducted studies on the dielectric constants of soil and have shown them to be functions of several soil characteristics.

Given that all materials contain charged particles, all materials possess certain electrical and magnetic properties. Three primary properties of a material control the relationship between electromagnetic fields and resulting currents in the material. Permittivity is the ratio of the electric flux density to the electric field intensity. Permittivity, also known as the real part of the dielectric constant, in free space is:

$$\epsilon = 8.854 \times 10^{-12} \frac{\text{farads}}{\text{meter}} \quad (1)$$

Permeability, which relates magnetic flux density to magnetic field intensity, in free space has the value:

$$\mu = 4\pi \times 10^{-7} \frac{\text{henries}}{\text{meter}} \quad (2)$$

Conductivity, which is the relation between the conduction current density and the electric field intensity, in free space is:

$$\sigma = 0 \frac{\text{siemens}}{\text{meter}} \quad (3)$$

Relative permittivity is the permittivity of a material with respect to free space. Dry soil has a relative permittivity of about 3. Pure water has a relative permittivity of about 81. Researchers have used these characteristics to relate the permittivity to the quantity of water in the soil. The permeability of both soil and water are similar to that of free space.

Researchers have shown that the permittivity and conductivity of soil can be related to moisture content. Electrical moisture sensors are based on these properties. Babb (1951) designed a radio-frequency moisture meter that relied on a material's change in permittivity as the amount of water in the sample varied. The change in the sample's permittivity caused the resonant frequency of his circuit to change. By measuring the resonant frequency, the moisture of the material was determined. Permittivity and conductivity have both been shown to be strong functions of soil moisture. However, conductivity is also influenced by several other factors. McNeill (1980) analyzed the electrical conductivity of soils and rocks using VLF radio waves in the 20-kHz range. He determined that the conductivity in soil was a function of porosity, moisture, electrolytes, temperature, and colloids in the soil.

Electromagnetically, soil can be modeled as a four component dielectric mixture consisting of air, bulk soil, bound water, and free water. Volumetric moisture content is the preferred measurement because the relation to permittivity is a function of the water volume fraction in the mixture. The quantity of water in the first molecular layer adjoining the soil particles is proportional to the surface area of the particles, which is a function of the soil particle size and mineralogy ($d > 0.005$ is sand, $0.002 < d < 0.005$ is silt, and $d < 0.002$ is clay) (Hallikainen et al., 1985).

The complex dielectric constant is:

$$\epsilon_c = \epsilon + \frac{\sigma}{\omega} = \epsilon' - j\epsilon'' \quad (4)$$

where ϵ is the permittivity, σ is the conductivity, ω is the radian frequency, ϵ' is the real part of the dielectric constant (permittivity $\epsilon = \epsilon'$), and ϵ'' is the imaginary part of the dielectric constant. The complex dielectric constants of bound and free water are functions of electromagnetic frequency, temperature, and ion concentration. (Curtis, 1998). The permittivity of bound water is much less than that of free water. As soil moisture content is increased gradually from zero, the permittivity of the soil will increase slowly. As the soil becomes saturated, and water content continues to increase, the effect of free water will increase permittivity at a greater rate.

Other factors besides water content can affect the permittivity of soil. For instance, soil density has been shown to slightly affect the permittivity (Hipp, 1974). Additionally, the permittivity will change with frequency. In the presence of an electric field, charges accumulate between clay particles and the surrounding solution. The build up takes time so as the frequency increases, the system's ability to store energy reduces, decreasing the dielectric constant. This decrease is called a Maxwell-Wagner relaxation

(Arulanandan and Smith, 1973). Arulanandan and Smith (1973) reported that this change occurs primarily at frequencies less than 100 MHz. Hoekstra (1974) concluded from his experiments that constant permittivity exists at frequencies above the Maxwell-Wagner relaxation and at frequencies less than 200 MHz. He also reported that an additional dielectric relaxation following the Debye equation (Debye, 1829) occurs at frequencies above 200 MHz. The Debye equation is:

$$\epsilon' - \epsilon'' = \epsilon_{\infty} + \frac{\epsilon_0 - \epsilon_{\infty}}{1 + j\omega \left(\frac{1}{2\pi f_c} \right)} \quad (5)$$

where ϵ_0 is the static dielectric constant, ϵ_{∞} is the high frequency dielectric constant, f_c is the relaxation frequency of the dielectric material, ϵ' is the permittivity of the dielectric material, and ϵ'' is the imaginary part of the dielectric constant. This dielectric relaxation is attributed to the presence of water in the soil and is similar to a relaxation that occurs in pure water. If this relaxation were to occur at the same frequency in all soils, a simple model could be used to predict permittivities as they relate to moisture only. However, Wang (1982) reported that because the Debye-type relaxation involved the molecular arrangement of water around soil particles, different sized particles undergo relaxation at different frequencies. The interaction with particle size indicated that the relaxations could induce soil type differences in permittivity values.

Electromagnetic Wave Propagation

The electrical parameters of conductivity and permittivity of the earth can be measured by electromagnetic wave propagation. An electromagnetic wave consists of two separate fields that are perpendicular to each other: the electric field (E) and the magnetic field

(H). Depending on the orientation of the antennas with the ground, the EM wave can have parallel polarization (Figure 1) when the electric field is parallel to the plane of incidence, or perpendicular polarization, when the electric field is perpendicular to the plane of incidence.

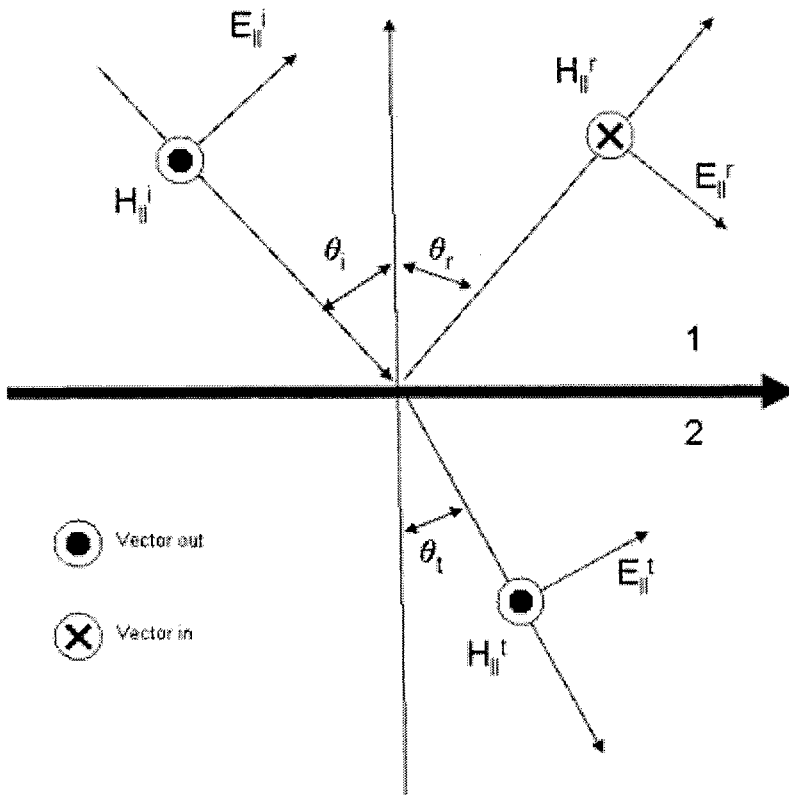


Figure 1. Parallel polarized uniform plane wave

Additionally, a plane wave traveling at an incident angle θ to a plane boundary between two low-loss media will reflect at an angle θ . Assuming the incident angle θ is not zero, the electromagnetic interaction with the boundary can be described by the transverse-electric mode or the transverse-magnetic mode.

The magnitude and phase of the wave interactions at the interface are functions of the dielectric properties of the two media. Balanis (1989) defined the equations that

describe electromagnetic wave propagation through the media as given below. An electric field propagates through a material following the equation:

$$E = E_0 e^{j\omega t - \gamma x} \quad (6)$$

where E_0 is the initial electric field intensity, ω is the frequency, γ is the propagation constant, t is time, and x is distance. The equation of the propagation constant is:

$$\gamma = \alpha + j\beta = \sqrt{j\omega\mu(\sigma + j\omega\epsilon)} \quad (7)$$

and can be separated into an attenuation constant:

$$\alpha = \omega\sqrt{\mu\epsilon} \left\{ 0.5 \left[\sqrt{1 + \left(\frac{\sigma}{\omega\epsilon}\right)^2} - 1 \right] \right\}^{0.5} \quad (8)$$

and a phase constant.

$$\beta = \omega\sqrt{\mu\epsilon} \left\{ 0.5 \left[\sqrt{1 + \left(\frac{\sigma}{\omega\epsilon}\right)^2} + 1 \right] \right\}^{0.5} \quad (9)$$

Knowledge of the electrical characteristics of a material will allow the prediction of the wave behavior in the material. When an electromagnetic wave propagates from one medium to another, having dissimilar electric and magnetic properties, a portion of the wave is transmitted and a portion is reflected. As the wave propagates through a medium, the wave will be attenuated based on the lossy dielectric properties of the material. The reflected field intensity is the proportion of the incident wave (Γ) that is reflected and can be computed as:

$$\Gamma = \frac{\eta_2 - \eta_1}{\eta_1 + \eta_2} \quad (10)$$

where Γ is the reflection coefficient. The proportion of the transmitted field intensity is:

$$\tau = \frac{2\eta_2}{\eta_1 + \eta_2} \quad (11)$$

where τ is the transmission coefficient, η_1 is the intrinsic impedance of material 1, and η_2 is the intrinsic impedance of material 2. The intrinsic impedance of a material η is:

$$\eta = \sqrt{\frac{j\omega\mu}{\sigma + j\omega\epsilon}} \quad (12)$$

The distance that the wave will travel in a lossy medium at which its intensity is reduced to 36.8%, that is, $100\left(\frac{1}{e}\right)\%$ of its initial value is the skin depth, which is expressed as:

$$\delta = \frac{1}{\alpha} \quad (13)$$

The naming systems of the radio and microwave bands in the literature can cause confusion. For clarification, the microwave naming system (ref) uses letters as follows:

P-band	0.3 to 1 GHz
L-band	1 to 2 GHz
S-band	2 to 4 GHz
C-band	4 to 8 GHz
X-band	8 to 12.5 GHz
Ku-band	12.5 to 18 GHz
K-band	18 to 26.5 GHz
Ka-band	26.5 to 40 GHz

For use in this study, the radio naming system will be used.

VLF	Very low frequency	3 to 30 kHz
LF	Low frequency	30 to 300 kHz
MF	Medium frequency	0.3 to 3 MHz
HF	High frequency	3 to 30 MHz
VHF	Very high frequency	30 to 300 MHz
UHF	Ultra high frequency	300 to 3 GHz

Soil Moisture Effects on Radio Wave Propagation

Many researchers have studied the influences of properties of the ground such as moisture, temperature, topography, and vegetation on radio wave propagation. The analytical calculations made by Josephson and Blomquist (1958) indicated that the properties of the ground near transmitting and receiving antennas affected the received signal with an influence that was equivalent to a change in the efficiencies of the antennas. In their study, field strength was shown to change as much as 14 dB over ground due to changes in moisture content.

While the dielectric properties of air are similar to that of free space, a measured electromagnetic reflection from the surface of a homogeneous soil would allow a determination of the dielectric properties of that soil. Such experiments with the assumption of homogeneous soil have been conducted by several researchers (Batlivala and Ulaby, 1977; Chanzy, 1996; Lundien, 1966). The outcomes of those experiments were greatly influenced by the frequencies that were selected for testing. In 1966, NASA was interested in launching satellites destined for the moon and other planets to sense dielectric properties of the surfaces. As part of the preparation for this test program, Lundien conducted experiments on the detection of soil moisture using pulsed radar with frequencies of 297, 5870, 9375, and 34543 MHz. The tests were designed to detect the dielectric properties of soil at various moistures and measure the effect of a stand of wheat on the sensed dielectric properties. In the experiment, the pairs of parabolic antennas, 1 transmitting and 1 receiving for each frequency were aimed toward the center of the top surface of a crate filled with soil. The angle of incidence was varied from 0 degrees to more than 60 degrees. The power of the received signal was monitored and

recorded. The VHF-band (297 MHz) penetrated the soil, and power reflections were strong functions of soil permittivity, which related closely with soil moisture. The higher frequencies had poor penetration into the soil, high noise associated with surface roughness, and poor correlation to moisture. The reason that the electromagnetic energy in the mid-microwave range was so sensitive to factors such as surface roughness and vegetation was that the wavelengths were less than 1 cm long. Thus, small changes on the soil surface result in large shifts in phase of the reflected waves. Further, the skin depth of microwave propagation in moist soil is also small so the reflection coefficient at microwave frequencies is almost entirely due to the reflection from the surface, detecting only surface moisture. The moisture in the top 1 cm of soil is probably not representative of the average soil moisture. Since that time researchers have used similar frequencies from NASA satellites to conduct reflection coefficient tests and relate them to soil moisture.

One of the critical aspects of detection of soil dielectric properties using radio wave propagation is the selection and calibration of antennas. Ulaby (1974) conducted a test with a frequency-modulated continuous-wave radar system with 2 parabolic dish antennas, with 0.762-meter diameters, attached to a 22.8-meter truck-mounted boom to measure soil reflections of 10 frequency points across a 4-8 GHz band. Two types of calibration were used: a delay line calibration that bypassed the antennas and allowed a direct detection of the transmission signal, and a Luneberg Lens calibration with which a metallic sphere was placed in the antennas' main beam and reflected evenly over a wide angular range.

Another method for antenna calibration was conducted to establish a reflectance reference for highway materials (Lundien, 1972). The system transmitted swept-frequencies over octave bands from a 7.6-meter high parabolic dish antenna and received the reflected signal with an identical antenna designed to transmit/receive over the range of 300 MHz to 3 GHz. The system was calibrated using a metal target that covered the sensed area. The 3.35-m² metal surface acted as a radio wave mirror to reflect 100 percent of the signal in the detected area to the receiving antenna. The reference of perfect reflection was used as a correction for all other measurements. Magnitudes of reflections from the highway materials were divided by the reference reflection magnitudes at each frequency. In this way, the bias of frequency response of the system was removed from the measured reflections.

Layered Earth

When analyzing the reflections of electromagnetic energy from a non-homogeneous layered earth, the model becomes slightly more complicated. In nature, the soil dielectric values vary with soil density, soil particle size, and moisture. Further, the moisture of the soil often varies widely with depth beneath the surface. Liquid water flow occurs as a response to a hydraulic potential gradient, which forms from gravity and capillary forces. When water content is plotted as a function of depth, there are normally sharp discontinuities in the curve at the boundaries between layers (Hanks and Ashcroft, 1980). These boundaries are referred to as wetting fronts and drying fronts, which are unique to porous material. McNeill, (1980) explains that a soil moisture profile typically has four major regions. In the top pendular region, pores are primarily filled with vapor;

no continuous path of liquid water exists. In the second layer, the funicular stage, liquid films become continuous through the pore space. The third layer is the capillary stage (Vadose zone) where all pore spaces are filled. Finally, the phreatic stage is the water table. The soil being analyzed in a root zone of the top two meters will likely contain the first three of the four major regions.

Hanks and Ashcroft (1980) outline that the shape of a typical moisture profile will vary depending if the soil is in a period of infiltration or a period of evaporation. During infiltration, the volumetric moisture content of the soil will be greater at the surface and will decrease to the initial moisture with increased depth. During evaporation, the volumetric moisture content will be low at the surface and increase with increased depth.

Because moisture content varies with depth, and it varies spatially throughout an agricultural field, a likely concern is knowledge of the spatial distribution of the moisture and the number of samples that must be taken in order to have an accurate measurement of moisture. Rao and Ulaby (1977) conducted a study on the required spatial sampling of moisture so that accurate averages could be compared with microwave reflectance. Soil samples were collected and moisture contents were averaged from fields that ranged from 2.5 to 40 acres and depths from the surface to 45cm. Two basic sampling procedures were used: random sampling and stratified sampling. Random sampling considered each depth individually and assumed that moisture was normally distributed at that depth. Stratified sampling recognized the dependency of moisture at one layer on moisture at adjacent layers. The study found that the number of samples required in random sampling did not significantly decrease with smaller sized resolution cells. The results indicated that to find the average moisture to 15cm depth of a 2.5-acre area, 4 moisture

samples must be collected. For a 40-acre area, a minimum of 8 samples must be collected.

The vertical infiltration rate of water through soil is an important aspect to consider for the temporal resolution of soil moisture sampling. During redistribution, the moisture content in the top two meters can change dramatically in the first 48 hours after irrigation. During evaporation, the volumetric moisture content changes slower and may require 100 hours or more to achieve very dry conditions. Vellidis et al. (1990) detected wetting front movements with a broadband pulse modulated ground-penetrating radar (GPR) before and after irrigations. GPR systems typically emit a single electromagnetic pulse and detect the reflected fields with time-domain techniques. Statistical analysis showed a relationship between the 120 MHz reflection and the wetting front. In one trial, data was taken prior to irrigation and 1h, 7h and 25h after irrigation. Another trial involved data collection at 3h intervals after irrigation. Soil samples were collected to a depth of 1.8 meters in 150mm increments.

The layered dielectric properties that are introduced by moisture gradients complicate the analysis of electromagnetic reflections. Gradients are difficult to analyze with electromagnetics because the propagation of waves through a non-homogeneous medium are very complicated mathematically. Yet, a gradient can be divided into several discrete layers of homogeneous material and the interfaces can be considered smooth provided that the layer thickness is small compared to the wavelength of the electromagnetic wave. The specific relationship known as the Rayleigh criterion is:

$$h < \lambda / (8 \cos \alpha) \quad (14)$$

where h is the average height of surface irregularities, λ is the wavelength of the incident pulse and α is the incidence angle (Chanzy et al., 1996). With layered effects, multiple reflections of the electromagnetic energy will occur. Several researchers have used a layered earth model in the estimation of average moisture content in the soil (Boisvert et al., 1997; Maley, 1963; Nikodem, 1966). Boisvert et al. (1997) used a surface diffusion model to predict the mean soil moisture from stratified layers caused by irrigation and evaporation. In order to evaluate the effect of a layered profile on a reflected signal, incoherent reflectivity and Fresnel reflectivity were used to predict the reflection contribution from each layer. Irrigation management was used to create wetting and drying fronts and moisture gradients. Measurements at frequencies of 12.8 GHz, 5.17 GHz, and 1.5 GHz were collected with a truck mounted scatterometer. Complex dielectric constant measurements were made with a portable 1.5 GHz dielectric probe, and gravimetric soil moisture was measured at intervals 0-1, 2-3, 4-5, 6-7, 8-9, and 10-11 cm. Nikodem (1966) discussed the results of a theoretical study that used VHF radio waves (300 MHz) to detect soil moisture to a depth of two feet. Results showed that when no subsurface reflections were present, the reflection coefficient could be used to derive the dielectric constant. However, subsurface reflections had a dramatic effect on the quantity of energy reflected. He concluded that standard monochromatic pulsed-radar systems are not suitable for measuring subsurface soil conditions. Swept-frequency systems are needed.

Other researchers have developed simulations to predict soil-column moisture using only the surface layer measurements of microwave and infrared reflections (Entekhabi et al., 1994; Jackson, 1980). Jackson (1980) used a predetermined soil matrix

potential, and a predicted hydraulic head of the surface layer, to predict the moisture of each layer in the top meter of soil. Hydraulic equilibrium was assumed for all of the 0.1-meter thick layers. Entekhabi et al. (1994) used reflection observations from the top few centimeters of soil to predict the profile down to several tens of centimeters. A learning algorithm was used in which an initial guess at state profiles was updated. The algorithm was based on soil storage and transport processes that are functions of moisture and temperature. By measuring moisture at the surface and temperature at the surface, the algorithm predicted the hydraulic conductivity of the soil and used these predictions to update the model with respect to the state profiles.

Some electromagnetic remote sensing methods have been proposed to identify the properties of individual dielectric layers. As electromagnetic waves reflect from more than one surface, the phase of the apparent reflection depends on the distance the waves travel. The magnitudes of the apparent reflections depend on reflection coefficients at each boundary between layers and attenuation of the fields within the layers. The sum of these reflections create one resulting reflection in which it is possible for the magnitudes of the reflections to add, if the waves are in phase, or to subtract, if the waves are out of phase. The phasing of the reflections depends on the ratio of the layer thickness to the wavelengths used. Chudobiak et al. (1979), Hallikainen et al. (1985), Nikodem (1966), and Lundien (1972) observed these interference patterns. Nikodem showed that a soil with a layered profile and a transition zone thickness within an order of 4 percent of the electromagnetic wavelength in the material resulted with an erratic power reflection measurement due to the interference patterns of the multiple reflections (Nikodem, 1966). Lundien (1972) conducted a study to determine the thickness of highway materials using

multi-frequency radar in the 500 MHz to 2 GHz range. The system transmitted swept-frequencies over octave bands. The harmonic oscillations described by the interference patterns from the multiple reflections of the three-layered highway were used to predict layer thickness.

Although used as a measurement indicator in Lundien's project, the reflection interference patterns from multiple boundaries could cause problems when trying to use reflection coefficients from specific frequencies to determine moisture content within the soil. The attenuation of the electromagnetic waves through the soil would likely limit the depth of penetration. But, reflections from boundaries that exist within the penetration depth could significantly interfere with reflections at the soil surface. The interference would likely shift the prediction of moisture high or low depending on the addition or subtraction of subsurface reflectance patterns.

Ulaby's experiment in which a radar system measured soil reflections across a 4-8 GHz band demonstrated some interference problems (Ulaby, 1974). The study showed that the reflections were very sensitive to surface roughness, frequency, and angle of incidence. The wavelengths of the high frequencies (4-8 GHz) were small enough so that the roughness of the soil allowed phase shifts of the reflected fields. The shifts in phase introduced interference in the reflections, which affected the apparent magnitudes of reflection coefficients of the soil.

Moghaddam et al. (2002) proposed the use of UHF and VHF (435MHz and 118 MHz) reflections to detect moisture in soil covered with thick canopies of vegetation. The proposed study utilized the two frequencies to numerically separate reflectance from

the vegetation and reflection from the soil. The frequencies were also estimated to penetrate the soil to a depth of 1 meter.

The electromagnetic skin depth of soil layers may be used to estimate volumetric soil moisture profiles with adequate accuracy for many agricultural applications. Holdem et al. (2000) conducted a computer simulation of an in situ measurement of soil moisture gradients using reflection coefficients of continuous radio waves at several discrete frequencies. The penetration depth was regulated by the frequency of the wave and the moisture content of the soil. The lowest frequency chosen was 10 MHz. The highest frequency depended on the number of layers in the moisture profile. Four moisture profiles were simulated including a smooth sigmoid, a stepped sigmoid, a smooth linear gradient, and a stepped linear gradient. The sigmoid profiles were gradients in which moisture changed rapidly within a short distance in the middle of the profile. Linear gradients involved moisture change at a constant rate throughout the profile. The smooth gradients were simulated by digitizing them at 300 intervals between the surface and 1.5 meters in depth. The results showed that the profiles could be estimated to reasonable accuracy and provide support to a field system that utilizes skin depth and reflection coefficients to estimate in situ soil moisture profiles.

Profile Restoration Algorithms

A soil sensor that estimates layers of moisture content must relate the measured data to the desired output. If the measured data includes the reflected magnitude and phase of several frequencies of radio waves, and the desired output is a layered profile of soil moisture, then a restoration algorithm must be implemented to calculate moisture at

depth from radio wave reflection coefficients. Several researchers have developed similar algorithms for other uses. Lager and Lytle (1977) tested three neural network type data-inversion algorithms on the reconstruction of subsurface electromagnetic profiles using the propagation of radio waves from one drill hole to another. The waves, originating and terminating at many different depths, were transmitted through rectangular zones of differing dielectric properties. The transmission coefficients were used in iterative reconstruction equations to resolve each zone's dielectric properties. When considering the algorithms, an equation of this type can be underdetermined, square, or overdetermined based on the number of cells versus the number of measurements. If the number of cells is greater than the number of measurements, the system is underdetermined. If the number of cells is equal to the number of measurements, the system is square. If the number of cells is less than the number of measurements, the system is overdetermined. Lager and Lytle (1977) concluded that for a learning algorithm to converge in a reasonable number of iterations, the equation must be square or overdetermined.

In an experiment that involved the detection of dielectric properties in layers of highway materials, a type of reconstruction algorithm was used to convert reflected electromagnetic energy at swept-frequencies to dielectric constants and layer thicknesses (Lundien, 1972). The material properties were determined by a five-step procedure. First, the dielectric constant of the top layer was estimated using the average reflection over the entire frequency range. Second, the electrical thickness of the concrete layer was determined using the harmonic frequency of reflected maxima from the strongest oscillating reflection. Third, the electrical thickness and the estimate dielectric constant

were used to calculate the actual thickness of the top layer. Fourth, the electrical thickness of the second layer was predicted using the harmonic frequency of the reflected maxima from the second most dominant oscillating interference pattern. Finally, the electrical thickness and a guess at the dielectric constant of the second layer were used to estimate the actual thickness of the second layer. Although this algorithm results in a good prediction of electrical thickness of the layers, it requires knowledge of the dielectric properties of the layers to measure actual thickness.

Another algorithm type that does not involve an iterative process was developed to determine the depth profiles of conductivity and permittivity of a layered earth using a set of complex surface impedance measurements over a few frequency decades (Assal and Mahmoud, 1986). In their model, the surface reflection coefficient at each frequency was expressed as a ratio of two polynomials involving the summation of reflection coefficients from each contributing boundary. When the number of different frequencies equaled $(2N-1)$, where N was the number of layers in the earth, the permittivity and conductivity can be solved exactly from the reflection coefficients. The model required very distinct boundaries and homogeneous media within the dielectric layers.

Summary

The existence of moisture gradients in the soil gives rise to the desire to predict moisture as a function of depth. The literature has shown that moisture content directly influences a soil's dielectric properties. In general, increases in volumetric moisture content increase soil permittivity and increase soil conductivity. Electromagnetic theory indicates that changes in dielectric properties will influence reflection coefficients of

radio waves at boundaries between dissimilar dielectric media. Further, electromagnetic waves of different frequencies are attenuated differently within a dielectric material. Utilizing soil dielectric properties as they relate to moisture, and electromagnetic field attenuation as it relates to frequency, reflection coefficients of multiple frequencies can be used with a profile restoration algorithm to estimate moisture of the soil at various depths.

CHAPTER III

DETECTION THEORY AND PHYSICAL ASSEMBLY

Introduction

This chapter contains theory of radio wave reflections from the soil containing moisture profiles. Included are a discussion of preliminary calculations that led to the selection of a frequency range, a description of the physical assembly used in field measurements of radio wave reflection, and a discussion of various concerns regarding electromagnetic sensitivity and interference.

Preliminary Calculations

The results of the reflection studies conducted at the US Army Engineers Waterway Experiment Station for NASA in 1966 showed that a 297 MHz wave penetrated more than 2 feet into the soil, and microwave frequencies above 5 GHz did not penetrate a measurable amount (Lundien, 1966). The results of the experiment demonstrated the importance of frequency selection in order to achieve the proper penetration into the soil. Electromagnetic waves of different frequencies exhibit different skin depths and can be used to detect layering effects of moisture in the ground. However, as Lundien's experiment showed, frequencies used will drastically affect the results. In order to select the proper range, permittivity and conductivity values taken from the literature (Curtis, 1998) were used to calculate predictions of skin depths and reflection coefficients at various frequencies. Based on the far-field analysis of EM

waves propagating normal to the soil surface, the wavelengths, skin depths, and reflection coefficients were calculated for soil at different moistures based on the dielectric data from Curtis. The computation results are shown in Table 1 and Table 2.

Table 1. Calculated wavelengths and skin depths

Frequency (MHz)	Wavelength (m)			Skin Depth (m)	
	in air	soil MC=5%	soil MC=40%	soil MC=5%	soil MC=40%
50	6.00	3.68	1.28	5.77	1.31
100	3.00	1.87	0.67	3.70	1.02
205	1.46	0.93	0.34	2.46	0.74
910	0.33	0.22	0.08	1.35	0.28

Table 2. Calculated reflection coefficients

Frequency (MHz)	Reflection Coefficients		
	air to MC=5%	air to MC=40%	MC=5% to MC=40%
50	-0.24 + 0.05i	-0.65 + 0.04i	-0.49 + 0.02i
100	-0.23 + 0.04i	-0.64 + 0.03i	-0.47 + 0.01i
205	-0.22 + 0.03i	-0.63 + 0.02i	-0.47 + 0.01i
910	-0.21 + 0.01i	-0.62 + 0.01i	-0.47 + 0.01i

The dielectric properties of the Mississippi soil from Curtis's data were compared to properties from Oklahoma soils (Arnold, 1992) at 50 MHz and 100 MHz. The permittivities and conductivities appeared to be similar, indicating that similar skin depths and reflection coefficients could be expected from Oklahoma soils. An operational frequency range of 80 MHz to 1 GHz was selected for estimation of moisture profiles in the top 2 meters of soil. The range was selected using the preliminary skin depth calculations and knowledge of the range of frequencies typically available in log-periodic antennas.

Field Test Apparatus

The soil moisture measurement apparatus utilized an Agilent Technologies 8712ET network analyzer, two A. H. Systems SAS-517 log-periodic antennas, RG-58 coaxial cables with type N connectors, 3.18-cm (1.25-inch) aluminum conduits that housed the cables, and a wooden structure that supported the equipment. During operation, the network analyzer, from port one, transmitted a swept frequency continuous voltage wave. The first log-periodic antenna transmitted the resulting EM wave toward the center of the test plot. The EM fields reflected from the air-soil interface and other subsurface boundaries of dissimilar moisture. The reflected electric fields were detected as surface currents on both log-periodic antennas with resultant voltage waves that were detected by the network analyzer. Given proper calibration of the instrument, the detected waves were used to calculate a reflection coefficient for the ground. Reflection coefficients that resulted from several frequencies were used to predict soil moisture at depth.

In order to maintain predictable reflection patterns from the soil, the EM fields were assumed to propagate as plane waves toward the air-soil and moisture layer boundaries. For this assumption to remain accurate, the wooden structure was made large enough so that the surface of the ground existed in the far-field region around the antennas and so that there was little inductive energy transmitted between the two antennas. Far fields exist in the region sufficiently far from the antenna such that only radiating field components are present and angular field distribution is independent of distance. EM energy can be characterized as plane waves in the far field if the following condition exists:

$$R \geq \frac{2D^2}{\lambda} \quad (15)$$

where R is the distance from a radiating antenna, D is the largest dimension of the antenna, and λ is the wavelength of the transmission through the surrounding media. The longest wavelength in the experiment occurred at 80 MHz and in free space was 3.75 meters. The antenna width (D) was 1.84 meters. Thus, a distance (R) of 1.80 meters was required between the ground and each antenna's center emission point. Because the distance from each antenna's mounting bracket to the antenna's emission center was 0.73 meters, the wooden structure was made more than 2.53 meters tall to maintain far-field reflections by the ground. In addition to the height restrictions, the wooden structure also had minimum width requirements. In order to sufficiently isolate the two antennas, the second antenna needed to be mounted outside the reactive near field of the first. The reactive near field is associated with non-propagating, quasi-static fields that are primarily electric or magnetic. To remain outside the reactive near field, the distance (R) between the antennas must adhere to the following condition:

$$R \geq 0.62 \sqrt{\frac{D^3}{\lambda}} \quad (16)$$

where D is the largest dimension of the antenna and λ is the wavelength. The antenna dipole rods were turned end to end in order to minimize the radiation path between them. However, even though the second antenna was positioned outside the transmission pattern of the first, a minimum space of 0.80 meters was used to ensure that signal transmission remained outside the reactive near field. The wooden structure was made wide enough to accommodate the width of both antennas and the intermediate distance R. The calculated minimum width of the structure was 4.48 meters.

The antenna orientation created electromagnetic fields that reflected from the surface with parallel/vertical polarization. In the parallel polarization, the electric field was parallel to the plane of incidence as shown in Figure 2.

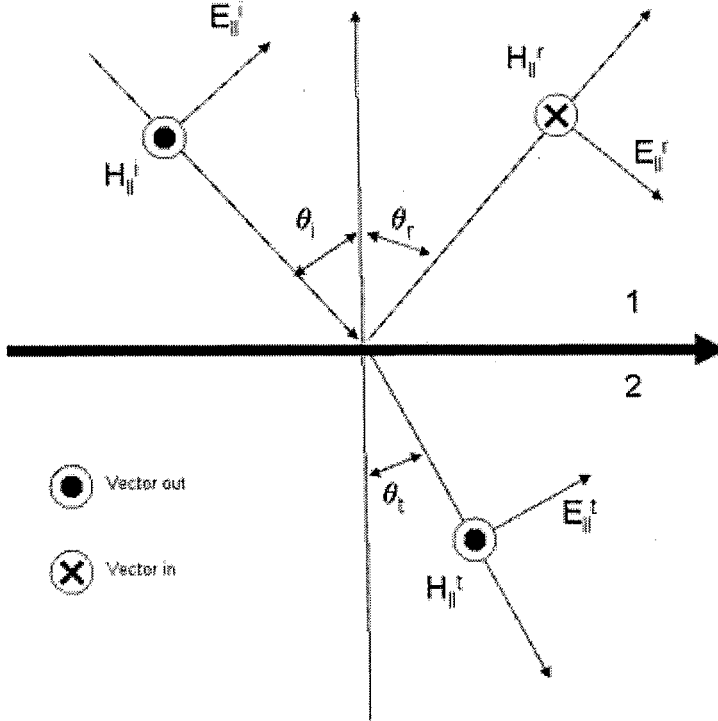


Figure 2. Parallel polarized uniform plane wave

The transverse-magnetic mode reflection coefficient that resulted from the parallel polarization of the antenna was:

$$\Gamma = \frac{-\eta_1 \cos \theta_i + \eta_2 \cos \theta_t}{\eta_1 \cos \theta_i + \eta_2 \cos \theta_t} \quad (17)$$

where η_1 was the intrinsic impedance of layer 1, η_2 was the intrinsic impedance of layer 2, θ_i was the angle of incidence, θ_t was the transmission angle, and:

$$\beta_1 \sin \theta_i = \beta_2 \sin \theta_t \quad (18)$$

where β_1 and β_2 were the phase constants of the respective layers. With the same conditions, the transmission coefficient was:

$$\tau = \frac{2\eta_2 \cos \theta_i}{\eta_1 \cos \theta_i + \eta_2 \cos \theta_t} \quad (19)$$

Although the cosine terms were considered for the air-soil boundary, they were ignored for boundaries of dissimilar moisture beneath the soil surface. Using Snell's law of refraction:

$$\beta_1 \sin \theta_i = \beta_2 \sin \theta_t \quad (20)$$

where β_1 was the phase constant of air (free space), θ_i was the angle of incidence (20°), and β_2 was the phase constant of soil at 5% volumetric moisture content, the transmitted angle θ_t was calculated as:

$$\theta_t = \arcsin\left(\frac{\omega\sqrt{\mu\epsilon_0} \sin(20^\circ)}{\omega\sqrt{\mu\epsilon_1}}\right) = \arcsin\left(\frac{\sin(20^\circ)}{\sqrt{11}}\right) = 5.9^\circ \quad (21)$$

The cosine of 5.9° is 0.995. Thus, the cosine terms had very little effect on the reflection and transmission coefficients of subsurface boundaries. Further, top layers with higher volumetric moisture contents would have even smaller transmitted angles.

In nature, soil moisture profiles are continuous functions of hydraulic potential gradients. Although the soil may contain large discontinuities, moisture content often changes gradually with depth. In order to model this non-homogeneous medium, the top 1.98 meters of soil were divided into 15.2 cm thick lossy dielectric slabs that were assumed to have homogeneous permittivity, permeability, and conductivity within each layer.

Although the homogeneous medium with several boundaries simplified the model, one complexity that was introduced involved electromagnetic waves within dielectric slabs that underwent multiple reflections from each boundary (Figure 3).

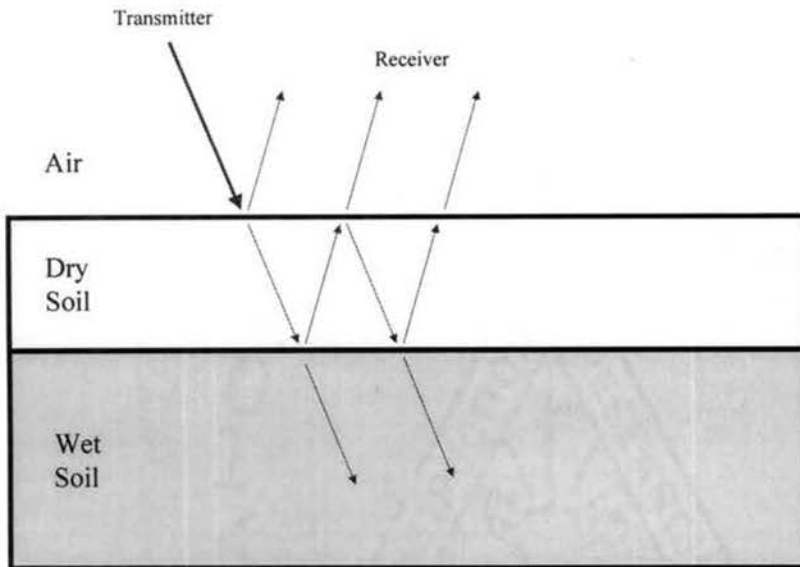


Figure 3. Multiple reflections between dielectric layers

However, Balanis (1989) outlined that in the analysis of reflections from multiple layers, a single reflection may be considered if the magnitudes of the reflection coefficients at each boundary were small compared to unity. In the soil moisture profile, the small changes in permittivity and conductivity resulted in small reflection coefficients so that the only reflection coefficient that approached unity was the air-soil interface, which resulted from a single reflection.

The soil attributes and surrounding area were influential in the selection of a suitable field test site. The variability within the soil and the potential for electromagnetic reflections from nearby structures were considered when selecting the test location. A field was selected in the Cow Creek Bottom located on the west side of

the Oklahoma State Agronomy Research Station. The field contained what was believed to be a very deep sandy loam soil that had supported alfalfa the previous year. The specific site was selected far from buildings, machinery, and other structures that could change the transmission properties between the antennas. In March 2003, four 3.2 meter x 3.2 meter test plots were flagged in the middle of the sandy loam field.

The antennas were placed at 20 degree angles and each was bore-sighted toward the center of the 3.2 meter x 3.2 meter test plot 1 meter below the soil surface. Because the antenna cables could interfere with each antenna's radiation pattern, the cables were routed on the structure through 3.18-cm (1.25-inch) aluminum conduits. Although the conduits did reflect electromagnetic fields, they were made immovable, mounted to the wooden structure, so that the reflection effect could be removed during calibration. The network analyzer was situated in the same plane as the antenna dipoles in order to minimize interference with the antenna patterns. Figure 4 shows the geometry of the apparatus with the actual dimensions of the wooden structure and electrical components.

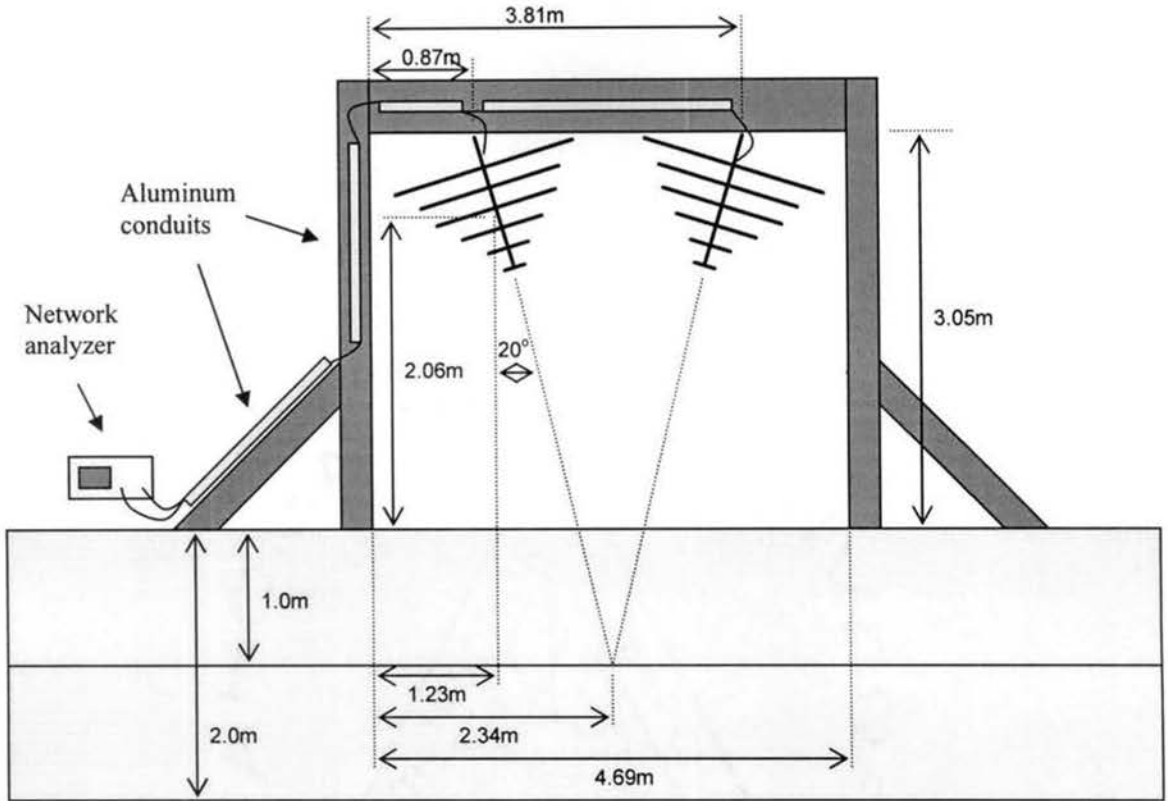


Figure 4. Geometry of wooden structure and antennas

Cheng (1983) showed that the intensity of the electric field surrounding a center-fed half-wave linear dipole with sinusoidal current distribution is:

$$E = j \frac{I_m \eta_o e^{-j\beta r}}{2\pi r} \frac{\cos\left[\frac{\pi}{2} \cos\theta\right]}{\sin\theta} \quad (22)$$

where E is the resulting electric field intensity, I_m is the magnitude of the current phasor, η_o is the intrinsic impedance of air, r is the distance from the antenna, β is the phase constant of air, and θ is the angle from the dipole axis. The dipole intensity pattern was applied to the log periodic antennas, along with an assumption that surface roughness and random dispersion in soil resulted in Lambertian reflectance. The assumptions were made in order to predict the largest possible antenna pattern projected on the ground.

Note that the actual pattern was most likely smaller than the predicted pattern because the antennas exhibited a numeric gain greater than a half-wave dipole and the reflection from soil was not truly Lambertian. The predicted pattern was a nearly circular shape of which the electric field intensity on the edges was 0.5 times the intensity of the center of the plot. A plot of the predicted area is shown in Figure 5.

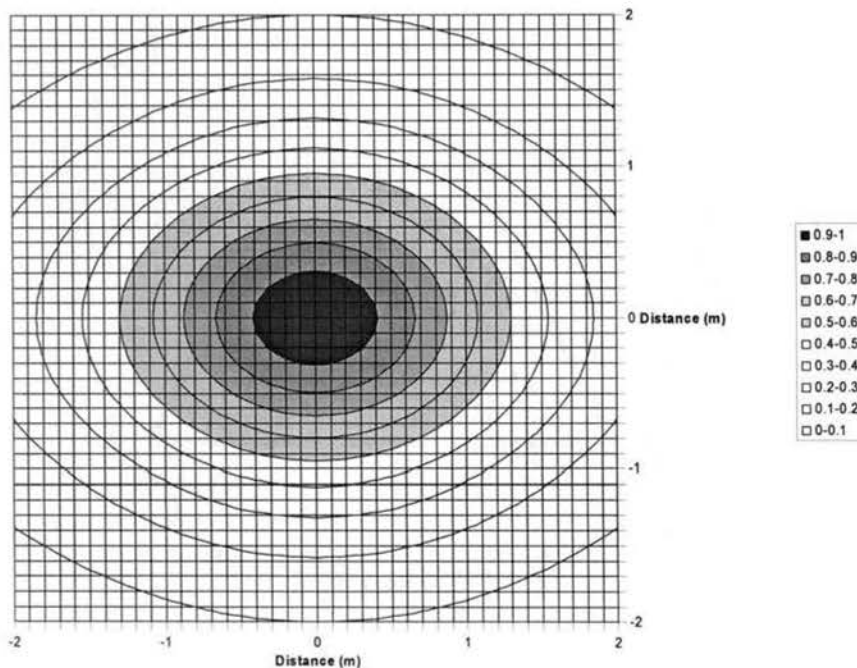


Figure 5. Predicted shape of the soil surface detected by the antennas.

The Agilent Technologies 8712ET network analyzer is a two port instrument designed to test electrical devices between the frequencies of 300 kHz and 1.3 GHz. It has the capability to produce an outgoing traveling wave (source) that passes through a wave guide to port 1. It also receives incoming voltage waves from port 1, which pass through the waveguide and are measured as reflections from the device under test. A voltage wave that enters port 2 is measured as a transmitted wave through the device

under test. In the application of moisture layer sensing, the network analyzer and antenna apparatus measured reflection coefficients from the ground in two ways. On the one hand, port 1 experienced returning voltage waves from impedance mismatch in the antenna and from a voltage wave induced on the antenna by electromagnetic fields reflected from the ground. The reflected wave detected by the analyzer indirectly measured the reflection coefficient of the ground. On the other hand, the sourced wave on the first antenna transmitted electromagnetic fields to the ground. The ground reflected the fields to the second antenna. The reflected electromagnetic fields induced a voltage wave on the second antenna, which was measured via port 2 of the network analyzer. The transmitted wave yielded an indirect measure of the reflection coefficient of the ground.

The SAS-517 log-periodic antennas used with the network analyzer transmitted an attenuated amount of power supplied by the instrument. The prediction of the attenuation that occurred between the network analyzer output and the signal that was emitted by the antenna enabled calculation of the maximum supply power that could be used without FCC approval. The percentage of electrical energy that was transmitted from the antenna was regulated by the gain of the antenna. Antenna gain (G_t), which was provided by the manufacturer, represents the ratio of the transmission intensity in a specific direction to the intensity that would be transmitted if the electrical power accepted by the antenna were radiated isotropically ($P_e/4\pi$). Because the antenna gain was recorded using the ANSI C63.5 standard, it also includes the power lost to impedance mismatch in the calculation. Thus, the power transmitted by the antenna was calculated as:

$$P_i = P_o \left(\frac{G_t}{4\pi} \right) \quad (23)$$

The maximum power that could be transmitted without FCC approval was 100 mW. The most efficient power transfer occurred at a frequency of 950 MHz with a gain of 4.35. Thus, the maximum acceptable power supplied by the network analyzer was 288 mW. However, the network analyzer was not capable of supplying a 288 mW signal. Instead, a setting of 16 dBm or 40 mW was used.

The amount of attenuation between the supplied voltage wave and the wave detected by the network analyzer was also predicted. The field intensity of the wave would attenuate linearly with the distance from the transmitting antenna and power would attenuate with the square of distance. The wave would then partially reflect from the ground and again attenuate with distance to the receiving antenna. From reciprocity, we know that the gain of the receiving antenna was equal to the gain of the transmitting antenna. Thus, the power of the wave received by the network analyzer was defined by the Friis equation as:

$$P_i = P_o (\Gamma)^2 \left(\frac{G_t}{4\pi} \right)^2 \left(\frac{\lambda}{2D} \right)^2 \quad (24)$$

where D was the distance from the antenna to the center of the plot surface (m), λ was the wavelength (m), and Γ was the magnitude of the reflection coefficient of the ground. At a frequency of 800 MHz, a soil moisture content of 5%, and a distance (D) of 2.19 meters, the manufacturer's recordings of antenna gain were used to calculate a maximum power attenuation of -49.0 dB. In contrast, a lower attenuation of -22.5 dB was attained at a frequency of 170 MHz and a soil moisture content of 40%.

The selected range of frequencies that were used contained many specific communication bands specified by the Federal Communications Commission. In order to identify the potential electromagnetic noise from outside sources, omni-directional measurements were made with a Radio Shack outdoor scanner/ham Discone antenna with a receiving range from 25 to 1300 MHz and an HP 8590B spectrum analyzer. The standing wave characteristics of the Discone antenna were measured using the Agilent Technologies 8712ET Network Analyzer to verify that the antenna was adequately sensitive to all frequencies within the range of 80 MHz to 1 GHz. The gain of the antenna was assumed to be 1.64, that of a half-wave dipole.

The 16 dBm voltage wave produced by the network analyzer was predicted to undergo a maximum attenuation of -49dB. The power of specific frequencies was determined sufficient to cause significant interference with the signals produced for the measurement of moisture. However, during the field moisture measurements, minimal wave detection occurred from the antenna connected to port two of the network analyzer when the transmitting antenna was disconnected from port one. The lack of any significant wave on the receiving antenna indicated that the directionality of the antennas minimized detection of these spurious communication signals. The spectrum analyzer's measurements of electromagnetic power, the network analyzer's measurements of the antenna's standing wave ratio, and the calculated EM power in the air are displayed in Appendix A.

CHAPTER IV

INSTRUMENT CALIBRATIONS

Introduction

Three primary instruments were used in this study: a neutron probe was used to measure volumetric moisture in soil, a coaxial sample holder was used with a network analyzer to measure soil dielectric properties, and log-periodic antennas were used with the network analyzer to measure electromagnetic reflection coefficients from soil in the field. This section outlines the calibration procedures and the calibration procedural results for the three instruments.

Neutron Probe Calibration

Within each of four 3.2 meter x 3.2 meter plots, four soil cores with 4.45 cm diameters were collected with a Giddings coring tool to depths of 2.59 meters in the pattern shown in Figure 6.

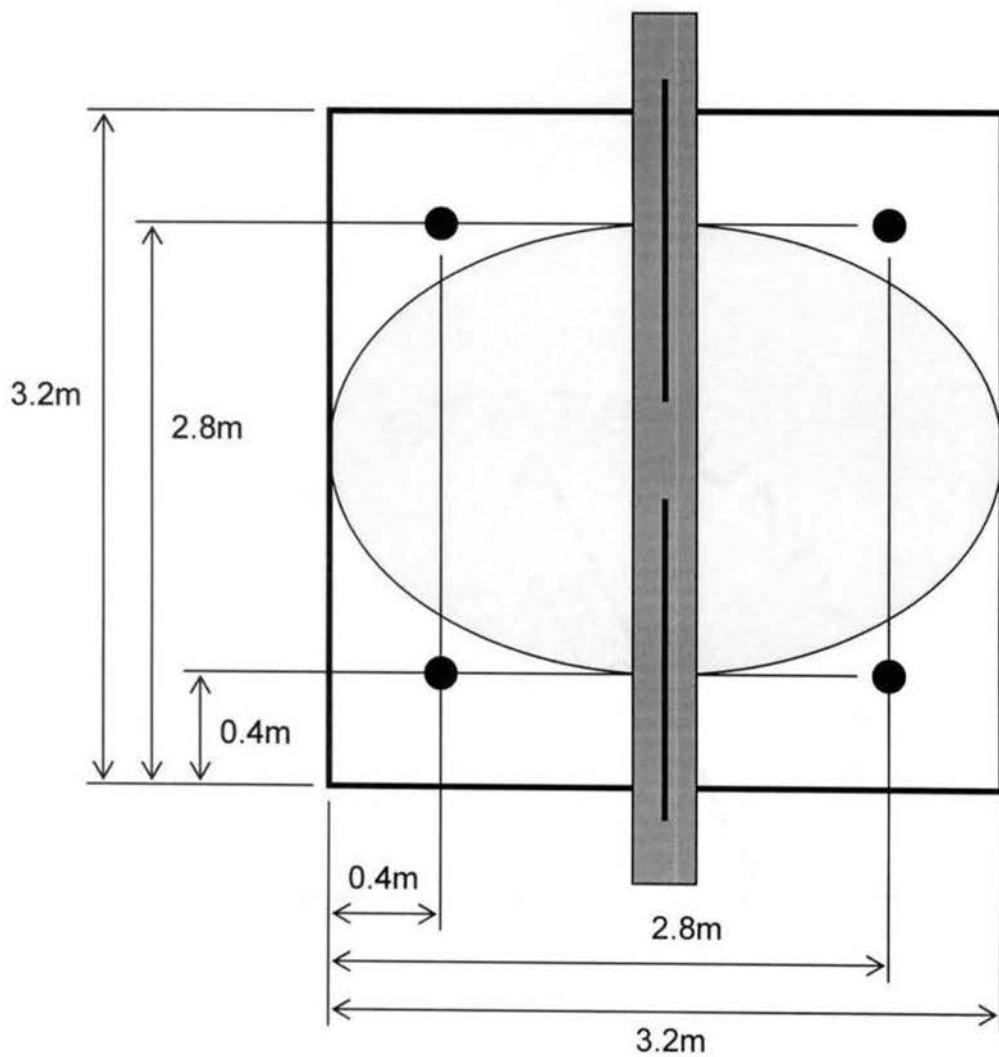


Figure 6. Test plot pattern with soil cores

The 2.59-meter cores were divided into seventeen 15.2-cm samples. Thin-wall PVC neutron probe access tubes, 2.25 meters long and 3.81-cm dia. (1.5-inch), were inserted into the core holes. Fast neutron reflection measurements were made with a Troxler neutron “depth probe” in 15.2 cm increments to a depth of 2.1 meters (Figure 7).



Figure 7. Neutron probe measurement of volumetric soil moisture

Each instance of neutron probe measurements began with the collection of a standard count on the slow data collection speed. Neutron counts at all 14 depths in all 16 holes were collected at the normal speed setting. Within each 15 cm soil core sample, weights and lengths were recorded for a portion of the core. The recorded portions were then dried and weighed. The measurements of length, diameter, wet mass, and dry mass were used to calculate the volumetric moisture and soil density of each 15 cm sample. It was found that significant compaction had occurred when collecting some of the soil cores.

To remove the bias resulting from the compaction, the 2 least compacted cores from each plot were correlated to the neutron measurements in order to calibrate the neutron depth probe for use in volumetric moisture measurement in PVC tubes. In addition to the field measurements of volumetric soil moisture, a 55 gallon barrel was fitted with an identical PVC tube, and the reflectance of fast neutrons in air (0% volumetric moisture), and water (100% volumetric moisture) were also used to calibrate the neutron probe.

Neutron Probe Calibration Results

Measurements of neutron counts and calculations of volumetric moisture were used to establish a calibration relationship. Simple correlation was used to fit a quadratic equation to the volumetric moisture and neutron probe measurements (Figure 8). The correlated volumetric moisture content and neutron probe measurements in soil, air, and water can be found in Appendix B.

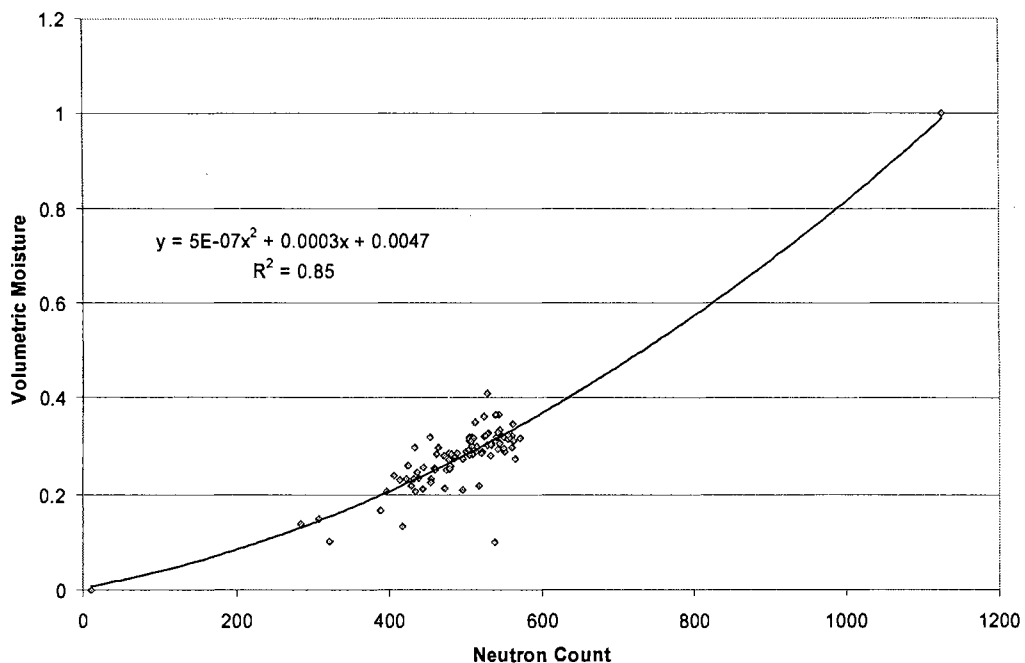


Figure 8. Relationship between neutron measurements and volumetric moisture content

As the curve in Figure 8 shows, the neutron probe measurements related closely to the volumetric moisture in the soil. However, some error was present in each measurement. In order to determine if the error was due primarily to a sampling error in the neutron probe or error in the volume and weight measurements of the soil, the precision of the instrument was tested. Three neutron probe measurements from each depth in five of the access tubes were made. Three measurements were also conducted in water. Figure 9 shows the relationship of the mean neutron count vs. moisture content with error bars representing one standard deviation of the neutron probe measurement.

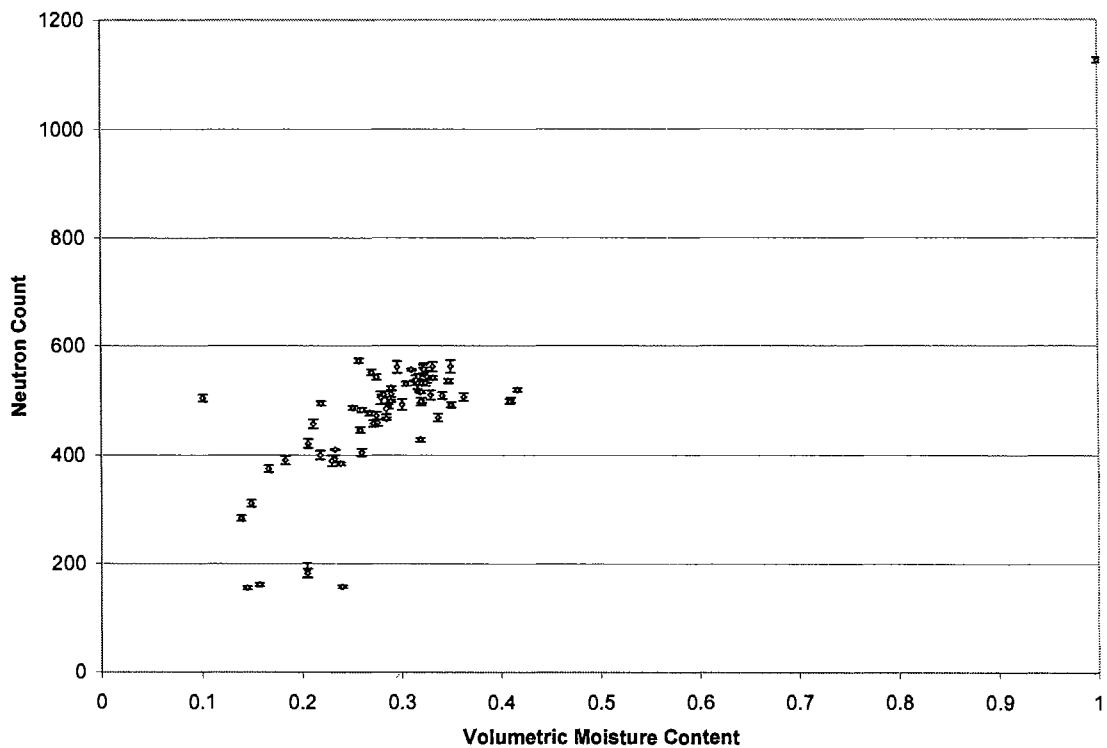


Figure 9. Variation in neutron probe measurements (normal speed setting)

The figure indicates that the primary source of error did not result from lack of precision in the instrument. In fact, the average standard deviation of the neutron counts was 5.77, and at a volumetric moisture content of 26%, one standard deviation would result in an error of 0.0045 in moisture content prediction.

The accuracy of the instrument was also verified with a comparison between water measurements (100% moisture content) in PVC and in a steel tube. The water measurement in the PVC tube was exactly 85% of that in a steel tube, which exactly matched the ratio predicted in the literature (Vlotman, 1985).

Dielectric Property Coaxial Cell Calibration

Information regarding the relationship between moisture content of the soil at the test site and the respective dielectric properties were needed so that the association could later be used for prediction of moisture using radio wave reflections. A method that had been proven to adequately relate permittivity and conductivity to moisture utilized radio wave propagation in a soil-filled coaxial cell. One particular cell, designed by Jorgensen et al. (1970) for measurement of dielectric properties of grain, utilized specific inner and outer dimensions resulting in a transmission line with a 50-ohm characteristic impedance when the cell was filled with air. Arnold (1992) used a modified version of the cell design (Figure 10) for moisture measurement of soil between 1 MHz and 100 MHz.

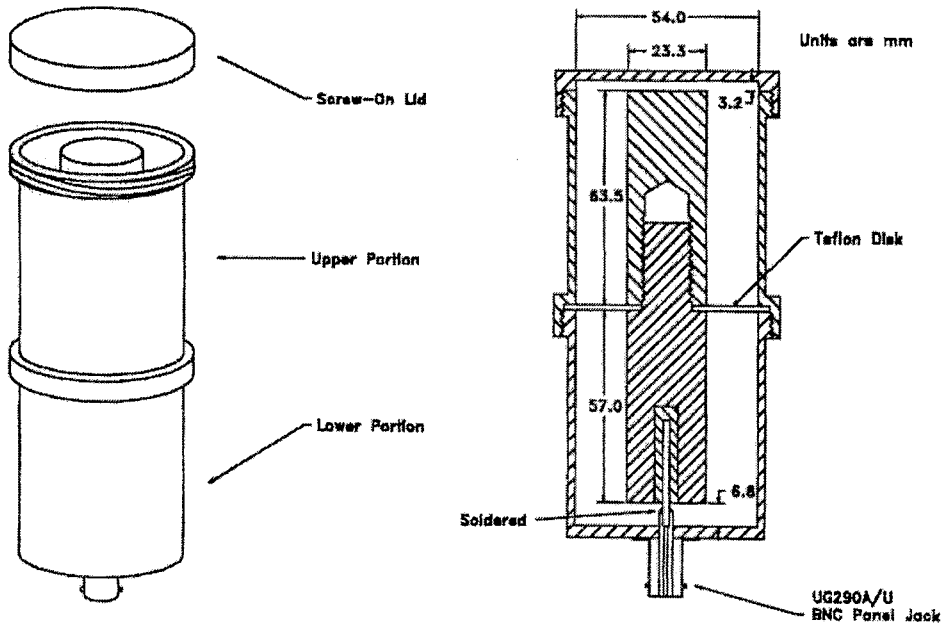


Figure 10. Coaxial cell used in soil dielectric measurements (Arnold, 1992)

Arnold's cell, which was used in this study, consisted of a center cylinder conductor and an outer cylinder conductor (both silver-plated brass), a Teflon ring that separated the lower and upper halves of the cell, a BNC type connector, and a screw-on cap. When modeled as a transmission line, the impedance of the cell was used to calculate the permittivity and conductivity of the dielectric material. The complex characteristic impedance per unit length of a coaxial transmission line is:

$$Z_s = \frac{j\omega\mu}{2\pi\gamma_s} \ln \frac{b}{a} \quad (25)$$

where ω is the radian frequency, μ is the permeability of the dielectric material, γ_s is the complex propagation constant of the dielectric material, a is the inner diameter of the dielectric material, and b is the outer diameter of the dielectric material (Cheng, 1983).

Additionally, the impedance Z_L measured at the input of a transmission line, which is terminated by a load Z_{cap} is:

$$Z_L = Z_s \frac{Z_{cap} + Z_s \tanh(\gamma_s d)}{Z_s + Z_{cap} \tanh(\gamma_s d)} \quad (26)$$

where Z_s is the characteristic impedance of the transmission line, γ_s is the complex propagation constant of the transmission line, and d is the length of the transmission line.

By connecting the cell to port 1 of the Agilent Technologies 8712ET network analyzer using a 50-ohm cable with type-N connectors and a type-N to BNC adapter, EM reflection coefficients from the cell network were measured. In transmission line theory, the voltage wave that propagates through a dielectric medium is shown to be:

$$V = V_o e^{-\gamma l} \quad (27)$$

where V is the voltage wave at a distance l from the source, V_o is the voltage wave at the source, and γ is the complex propagation constant of the medium.

If the voltage wave encounters a boundary of dissimilar dielectric media, a partial phase-shifted reflection occurs. The reflection coefficient from transmission lines with different characteristic impedances is:

$$\Gamma = \frac{Z_L - Z_o}{Z_L + Z_o} \quad (28)$$

where Z_o is the characteristic impedance of the first transmission line, and Z_L is the input impedance of the second transmission line. Because the network analyzer, the cable, and the lower half of the coaxial cell all had characteristic impedances of 50 ohms, the voltage wave reflection measured at port 1 of the network analyzer was:

$$\Gamma_{in} = \frac{V}{V_o} = \Gamma_{cell} e^{-2\gamma_1 l_1} e^{-2\gamma_2 l_2} \quad (29)$$

where Γ_{cell} was the reflection coefficient between the lower and upper halves of the cell, γ_1 was the complex propagation constant of the coaxial cable and connectors, l_1 was the length of the coaxial cable and connectors, γ_2 was the complex propagation constant of the lower half of the coaxial cell, l_2 was the length of the lower half of the cell, and:

$$\Gamma_{cell} = \frac{Z_L - 50}{Z_L + 50} \quad (30)$$

where Z_L was the input impedance of the upper half of the coaxial cell.

A metal disk, cut to the same dimensions as the Teflon disk, was inserted into the cell on the top side of the Teflon disk ($Z_L = 0$). Ten reflection measurements were made and the average was used to calculate the constant (Prop) representing propagation through the cable and the lower-half of the coaxial cell.

$$\text{Prop} = e^{-2\gamma_1 l_1} e^{-2\gamma_2 l_2} = \frac{\Gamma_{in}}{\Gamma_{cell}} \quad (31)$$

$$\Gamma_{cell} = \frac{0 - 50}{0 + 50} = -1 \quad (32)$$

The metal disk was then placed on the cap end of the cell to short the center conductor to the outer cylinder of the cell. In this configuration, the terminating impedance Z_{cap} equaled zero. Ten reflection measurements were averaged and used to calculate the constant (Prop2) representing propagation through the upper-half of the coaxial cell.

$$\text{Prop2} = e^{-2\gamma_s d} = \frac{\Gamma_{in}}{\Gamma_{cell} \text{Prop}} \quad (33)$$

$$\Gamma_{cell} = \frac{0 - 50}{0 + 50} = -1 \quad (34)$$

Additional measurements were made in which the coaxial cell was filled with air and the cap was screwed on to leave a 3.2 mm gap between the center conductor and the surface of the cap. The average of 10 reflection measurements was used with equations 28 and 33 to calculate the terminating impedance that resulted from the cap.

$$\Gamma_{end} = \frac{\Gamma_{in}}{\text{Prop}(\text{Prop}2)} \quad (35)$$

$$Z_{cap} = 50 \frac{1 + \Gamma_{end}}{1 - \Gamma_{end}} \quad (36)$$

With all of the constant portions of the cell network characterized, a voltage wave reflection from the cell with the upper portion filled with a dielectric material was measured and the input impedance of the upper half of the cell was calculated directly.

In addition to the calculation of the cell's input impedance from the resulting reflection, the input impedance was easily calculated from the permittivity and conductivity of the dielectric material in the cell. The propagation constant was related to the two properties by:

$$\gamma_s = \sqrt{j\omega\mu(\sigma + j\omega\varepsilon)} \quad (37)$$

where ω was the radian frequency, μ was the permeability of the dielectric material, σ was the conductivity of the dielectric material, ε was the permittivity of the dielectric material, γ_s was the complex propagation constant of the dielectric material. The intrinsic impedance of the sample was related to the propagation constant by:

$$Z_s = \frac{j\omega\mu}{2\pi\gamma_s} \ln \frac{b}{a} \quad (38)$$

and, the input impedance of the cell was:

$$Z_L = Z_s \frac{Z_{cap} + Z_s \tanh(\gamma_s d)}{Z_s + Z_{cap} \tanh(\gamma_s d)} \quad (39)$$

However, the opposite problem was not so straightforward. The goal of this calibration was not to enable calculation of impedance from known dielectric properties, but to enable calculation of dielectric properties from measured impedance. The literature proposes multiple methods including bilinear transformations (Lawrence et al., 1989) and iterative algorithms (Scott and Smith, 1986) to solve this problem. But, special conditions must exist for these strategies to work. The bilinear transformation relies on the limitation that for each value of cell impedance exactly one corresponding permittivity and one conductivity exist. For smaller coaxial cells or lower frequencies, this remains the case. But, larger cells and higher frequencies don't exhibit such characteristics. Scott and Smith (1986) discussed the difficulty of solving the inverse function for a cell of generic length because the input impedance is multivalued. For the cell used in this study, at frequencies up to 1 GHz, there can be more than one set of realistic dielectric values that result with the same input impedance to the cell. For an iterative algorithm to converge to the correct value, the method and initial conditions must be chosen carefully. The algorithm used to solve this problem utilized the following procedural steps.

1. Soil permittivity and conductivity values from the literature were used as the initial guess.
2. The propagation constant (γ_s) and intrinsic impedance (Z_s) of the soil were calculated from the predicted values.
3. The propagation constant and soil impedance were then used with the cap impedance (Z_{cap}) to predict the input impedance of the cell (Z_L').

4. The distance between the predicted input impedance and the measured value was calculated adding the differences of the squared values of the real and imaginary parts:

$$dist = \sqrt{(real(Z_L') - real(Z_L))^2 + (imag(Z_L') - imag(Z_L))^2} \quad (40)$$

5. Nearest neighbor increments of 0.01 were added to and subtracted from the initial permittivity value, and nearest neighbor increments of 0.001 were added to and subtracted from the initial conductivity value. The eight nearest points to the initial dielectric values were all used to calculate the eight resulting input impedances.
6. Complex distances from the measured values were determined and the permittivity and conductivity values that resulted in the minimum impedance difference were selected as the new initial guess.

The process was repeated approximately 600 times until the predicted impedance converged to the measured impedance. Although the process was slow, it successfully calculated the permittivities and conductivities of the dielectric material in the cell.

In order to verify that the measurements of the dielectric properties were accurate, measurements with air and reagent grade n-propanol were used to check the calibration of the coaxial cell. The analytical permittivity and conductivity values of air were assumed to be that of free space. The analytical values of propanol were calculated for each frequency implementing the Debye equation (Debye, 1829) and using static and high frequency dielectric properties and the relaxation frequency published by Buckley and Maryott (1958). The Debye equation is:

$$\varepsilon' - j\varepsilon'' = \varepsilon_\infty + \frac{\varepsilon_0 - \varepsilon_\infty}{1 + j\omega \left(\frac{1}{2\pi f_c} \right)} \quad (41)$$

where ε_0 is the static dielectric constant, ε_∞ is the high frequency dielectric constant, f_c is the relaxation frequency of the dielectric material, ε' is the permittivity of the dielectric material, ε'' is the imaginary part of the dielectric constant, and:

$$\sigma = \omega\varepsilon'' \quad (42)$$

Using the analytical permittivities and conductivities of propanol, and measuring the reflection coefficients from the cell, the bias errors of the cell measurement were quantified. Because permittivity and conductivity of propanol were close in value to those of soil, the quantified bias errors from propanol were subtracted from dielectric measurements of soil.

An additional calibration check was conducted to predict permittivity and conductivity of air. The equations below outline the calculation of the cell impedance to be used with the iterative algorithm.

$$\Gamma_{cell} = \frac{\Gamma_{in}}{\text{Prop}} \quad (43)$$

where Γ_{cell} is the reflection from the upper coaxial cell, Γ_{in} is the reflection measured by the network analyzer, and Prop is the constant representing propagation through the cable and the lower-half of the coaxial cell.

$$Z_L = 50 \frac{1 + \Gamma_{cell}}{1 - \Gamma_{cell}} \quad (44)$$

where Z_L is the input impedance of the upper cell.

$$\gamma_s = \gamma_{\text{freespace}} = 0 - j\omega\sqrt{\mu\epsilon} \quad (45)$$

where γ_s is the complex propagation constant of the sample, ω is the radian frequency, μ is the permeability of the sample, and ϵ is the permittivity of the sample

$$Z_s = \frac{j\omega\mu}{2\pi\gamma_s} \ln \frac{b}{a} \quad (46)$$

where Z_s is the impedance of the sample, a is the inner diameter of the sample, and b is the outer diameter of the sample

$$Z_L = Z_s \frac{Z_{\text{cap}} + Z_s \tanh(\gamma_s d)}{Z_s + Z_{\text{cap}} \tanh(\gamma_s d)} \quad (47)$$

where Z_{cap} is the terminating impedance from the cap and d is the length of the dielectric sample.

Coaxial Cell Calibration Results

Recall that the calibration of the cell included a three step process. First, a metal disk was inserted into the cell on the top side of the Teflon disk ($Z_L = 0$), and reflection measurements were used to calculate propagation through the cable and the lower-half of the coaxial cell (Prop). Second, the metal disk was inserted on the cap end of the cell ($Z_{\text{cap}} = 0$), and reflection measurements were used to characterize propagation in the upper half of the cell (Prop2). Finally, measurements were made in which the metal disk was removed, and the cap was screwed onto the coaxial cell. Average reflection measurements were used to calculate the terminating impedance (Z_{cap}). The MATLAB code used to execute the calibration in post-processed data is displayed in Appendix C and the calibration data is in Appendix D. Figure 11 displays the magnitude and phase of

the term representing average propagation through the cable and the lower coaxial cell (Prop).

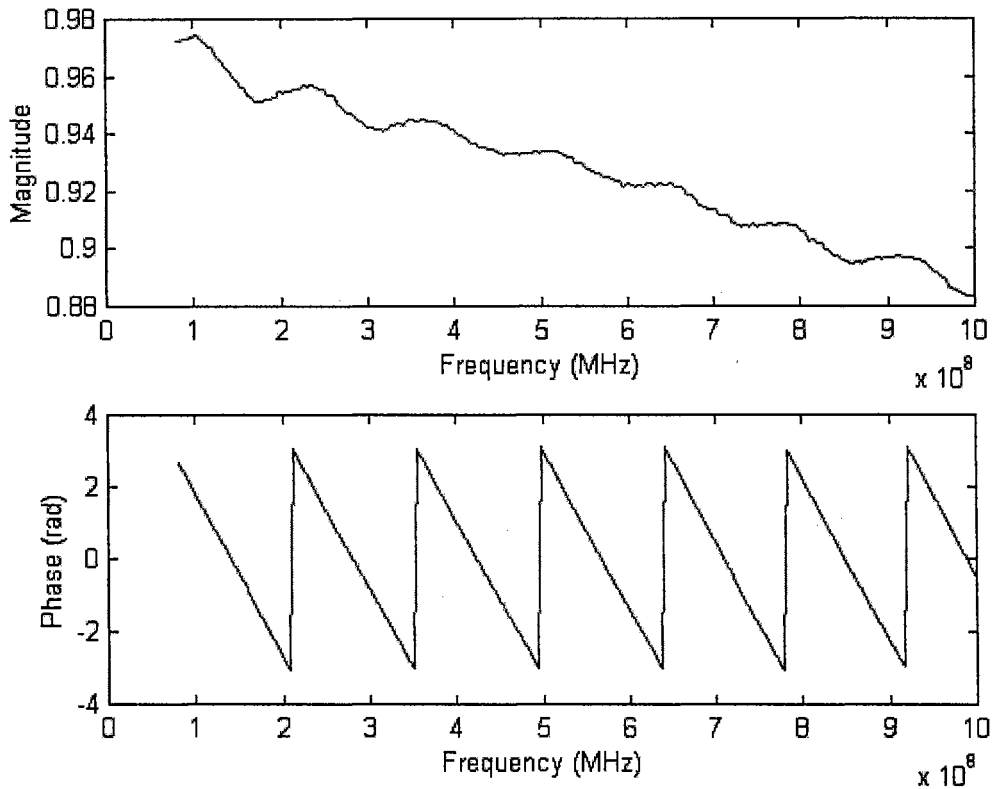


Figure 11. Exponential propagation characterizing the cable and lower cell (Prop)

The figure shows that the primary effect of the cable's frequency response was a shift in phase. The figure also shows that attenuation through the cable increased with increasing frequency. The interference ripple in the magnitude matches the shift in phase. This interference pattern indicates that the impedance of the cable and the lower cell are matched reasonably well, but the impedances are slightly different than the input impedance of the network analyzer. Although the intent of the calibration was to remove this systematic error, a hint of the interference ripple can be observed in many of the cell measurements.

Figure 12 displays the magnitude and phase of the term representing propagation through the upper half of the air-filled coaxial cell (Prop2).

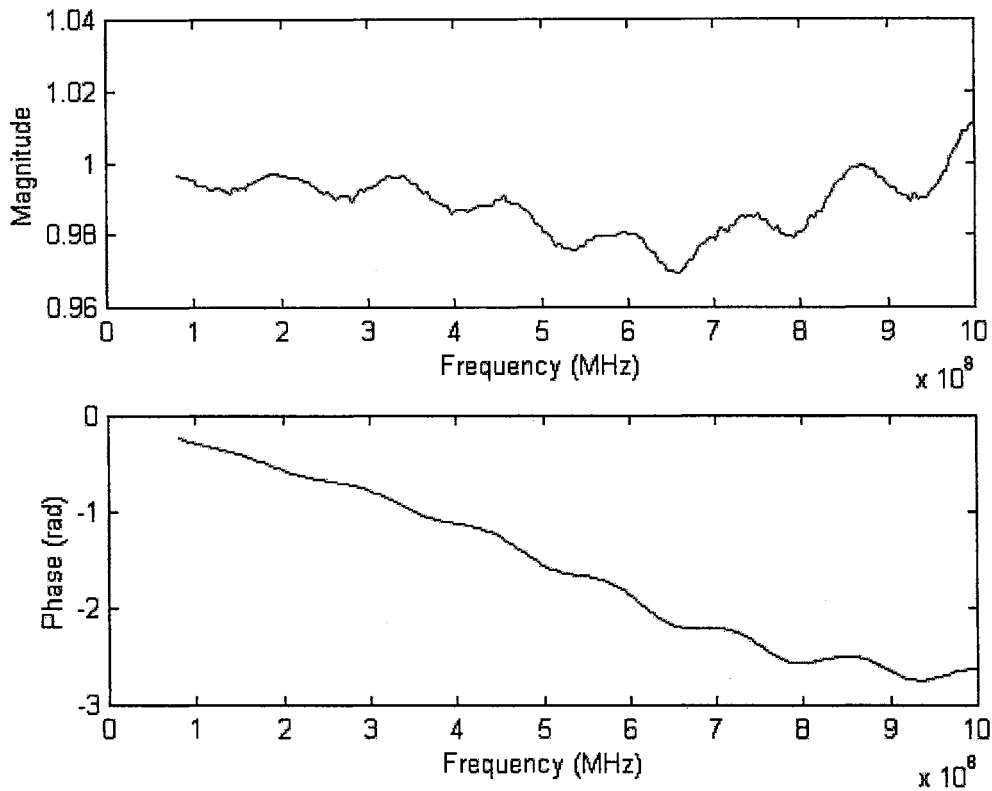


Figure 12. Exponential propagation characterizing the upper cell (Prop2)

The plot shows that the primary effect of this term was a phase shift with frequency. It also contains some systematic error. The ripple was systematic error induced by the impedance mismatch between the cable and the network analyzer. The shift in magnitude is also systematic error resulting from part of the calibration process. In theory, the magnitude should remain exactly 1 at every frequency. This error was also observed in the calibration check when calculating the dielectric properties of air.

Figure 13 displays the magnitude and phase of the terminating impedance (Z_{cap}).

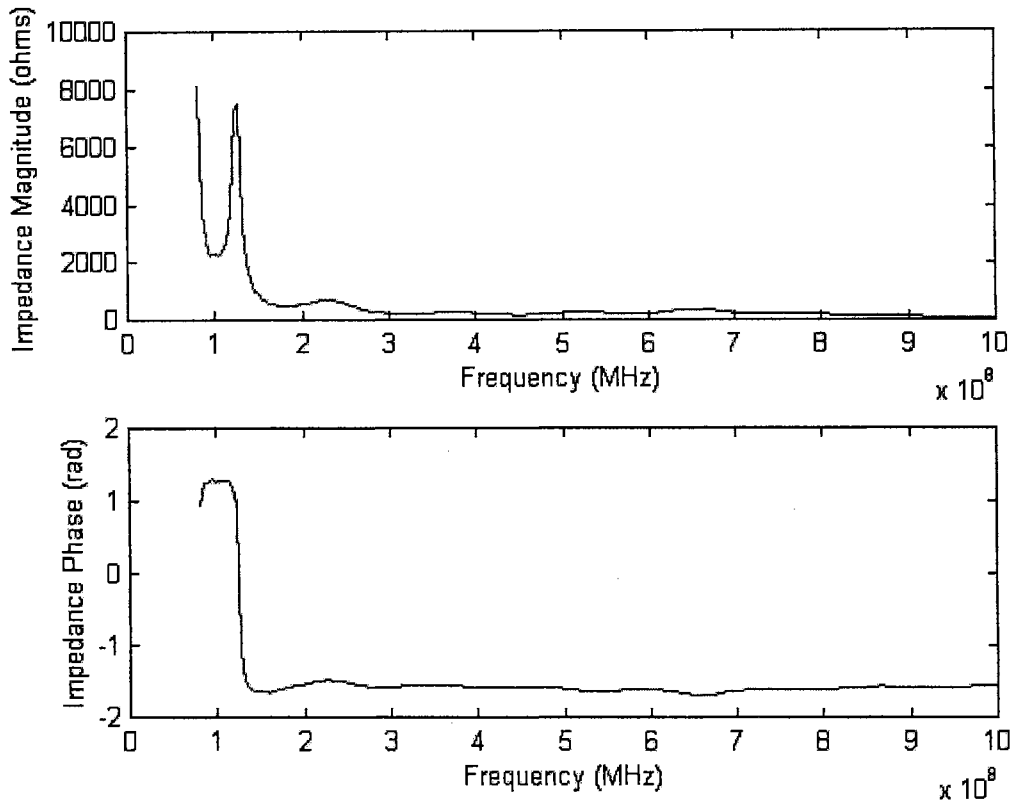


Figure 13. Terminating impedance Z_{cap}

The magnitude and phase of the complex terminating impedance (Z_{cap}) shows a very high impedance at frequencies below 130 MHz and low impedance at higher frequencies. The impedance at a frequency of 100 MHz had a phase of approximately 1.57 radians indicating that Z_{cap} was primarily inductive. At frequencies above 130 MHz, Z_{cap} had an approximate phase of -1.57 radians indicating that the impedance was primarily capacitive. The calculated propagation terms, Prop and Prop2, and terminating impedance Z_{cap} are listed in Appendix D.

With all of the constant portions of the cell network characterized, materials with known theoretical dielectric properties were used to test the calibration. The analytical permittivity and conductivity values of propanol calculated with the Debye equation were

compared with the average values detected by the cell. Average measured permittivities and conductivities of n-propanol are displayed with the theoretical values in Figures 14 and 15. The error bars represent a random error of one standard deviation from the mean.

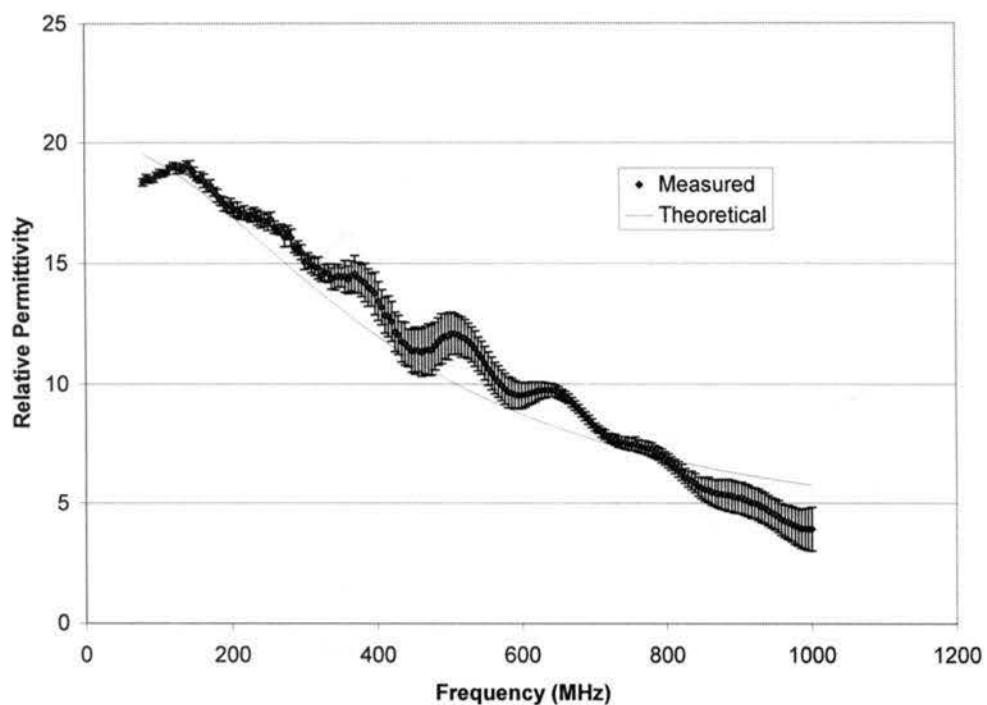


Figure 14. Theoretical and measured permittivity of reagent grade n-propanol

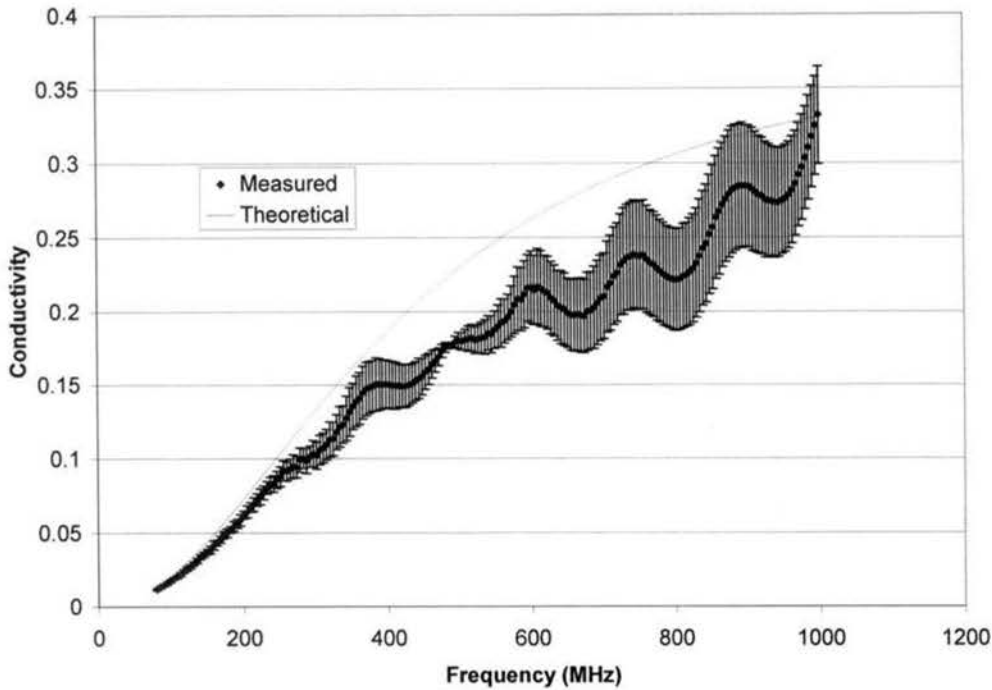


Figure 15. Theoretical and measured conductivity of reagent grade n-propanol

The average bias error between the theoretical and measured permittivity of n-propanol was 0.958. The average bias error of propanol conductivity was 0.042. The bias errors from the propanol measurements were used as part of the calibration procedure and subtracted from each measurement of permittivity and conductivity from soil. Note that the systematic error (ripple) from the impedance mismatch at the network analyzer exists in the measurements of permittivity and conductivity.

The theoretical dielectric properties of air were assumed to be that of free space and were compared with the measured values. Average measured permittivities and conductivities of air are displayed with the theoretical values in Figures 16, and 17. The error bars represent one standard deviation from the mean.

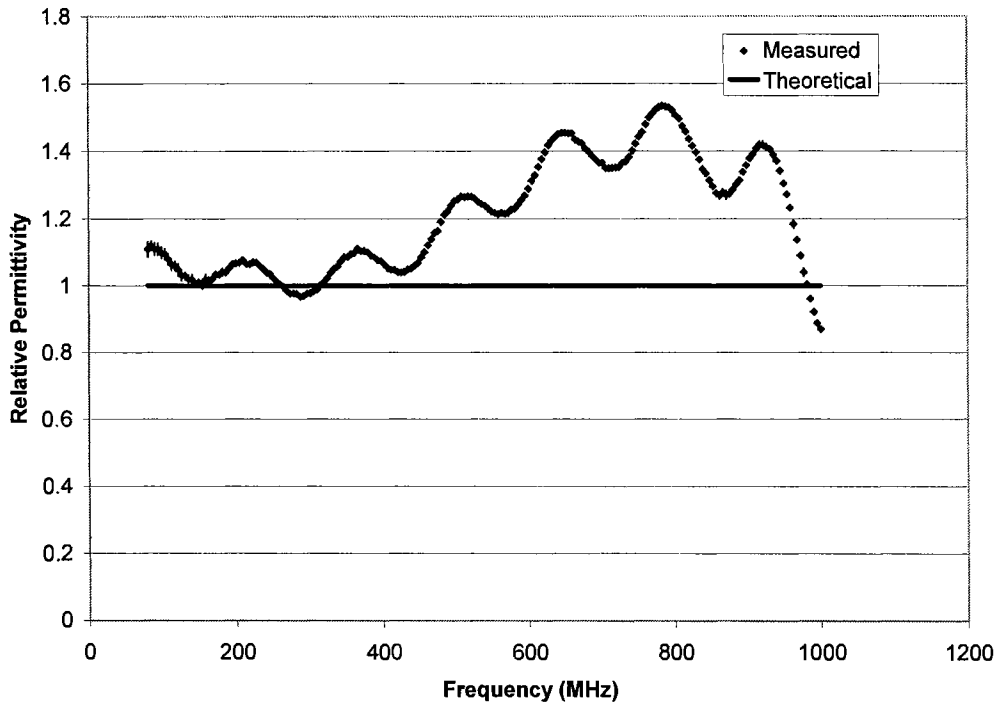


Figure 16. Theoretical and measured permittivity of air

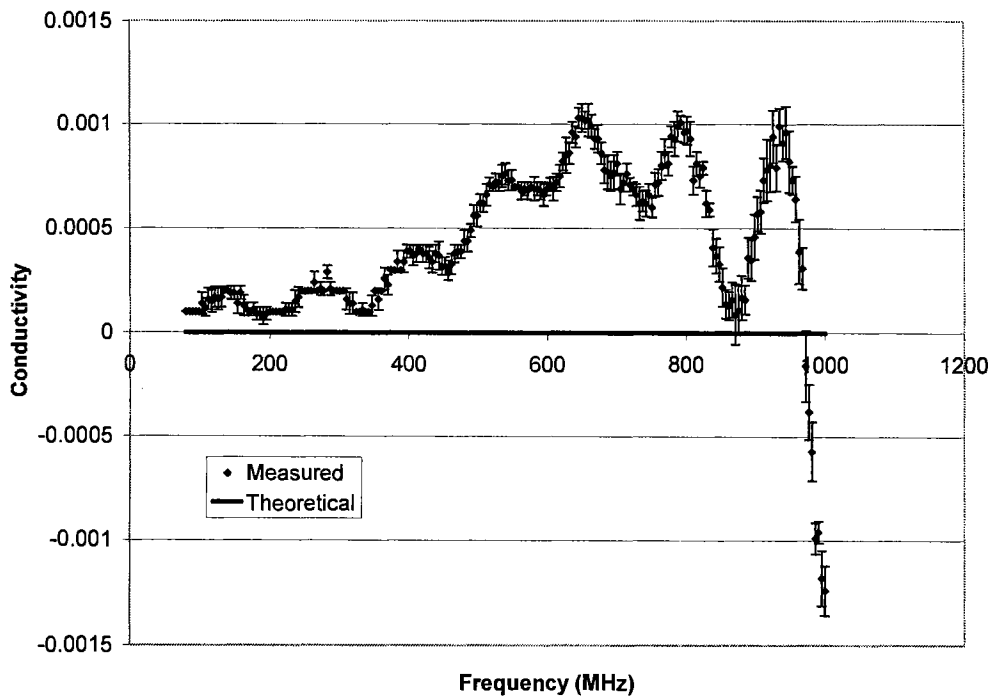


Figure 17. Theoretical and measured conductivity of air

The average bias error of permittivity and conductivity in air were 0.214 and 0.0005 respectively. The large systematic error resulted from a slightly inaccurate calibration of the propagation through the upper cell (Prop2). Because the soil dielectric measurements were corrected with the bias error from propanol, the bias error from the air measurement was disregarded. However, caution should be taken when measuring materials with dielectric properties near those of free space.

Random error was also observed in the propanol and air tests. The random error was analyzed as error in the magnitude and phase measurements of the instrument and the error that resulted in the calculated permittivity and conductivity values. The standard deviations at each frequency were averaged to yield a measure of random error for each of the measured and calculated values. The average standard deviations are shown in Table 3.

Table 3. Error in network analyzer measurements and resulting dielectric property error

	Magnitude	Average Standard Deviation		
		Phase (deg)	Permittivity	Conductivity
Propanol	0.014	3.190	0.473	0.020
Air	0.00083	0.24735	0.00725	0.00005

Note: The standard deviation of phase error from the propanol measurements increased with frequency.

At 80 MHz: $\sigma = 0.35$, at 1GHz: $\sigma = 6.20$

The error in the phase measurement of propanol increased with frequency. Error in the phase measurement appeared to be the primary source of random error in the calculated permittivity and conductivity values.

Field Apparatus Calibration

Under normal circumstances, vector network analyzers are used to characterize the reflection and transmission coefficients of a device between the network ports. When used to sense soil moisture profiles, the instrument's measured voltage waves indirectly measured the reflection coefficient of the ground. Because the ground reflection was only a small part of the complex electrical network, and far removed from the direct measurements made by the instrument, it was important that a calibration minimize the effects of all of the network characteristics except soil reflectance. The calibration process essentially treated the effects from the other components as a portion of the systematic error in the measurement. Systematic error, bias that is predictable and time invariant, in radio wave instruments typically includes signal leakage, reflections from mismatched sources and loads, and frequency response errors.

The network analyzer's measurement of reflection contained two primary influences, a reflection from the impedance mismatch of the transmitting antenna, and the voltage wave induced on the antenna by radio waves reflected from the soil. The antenna impedance mismatch reflection was modeled as:

$$\Gamma_1 = \Gamma_a e^{-2\gamma_l l_1} \quad (48)$$

where Γ_a was the reflection coefficient at the antenna, γ_l was the complex propagation constant of the coaxial cable, and l_1 was the length of the coaxial cable.

The reflection resulting from antenna transmission, soil reflection, and antenna reception was:

$$\Gamma_2 = F_1 \Gamma_s \quad (49)$$

where Γ_s was the reflection coefficient of the soil and F_1 was complex function representing propagation through the cable, antenna, and air. The concept of superposition was used to add the two reflections to yield the total reflection detected by the network analyzer.

$$\Gamma_{in} = \Gamma_1 + F_1\Gamma_s \quad (50)$$

The network analyzer's detection of radio wave transmission was modeled in a similar way. The transmission through the first cable, into the first antenna, through the air to the second antenna (in all paths except a direct reflection from the soil), and through the second cable was expressed as a transmission coefficient τ_1 . The transmission of the wave from port 1 to port 2 via a direct reflection from the soil surface was expressed as:

$$\tau_2 = F_2\Gamma_s \quad (51)$$

where Γ_s was the reflection coefficient of the soil and F_2 was the complex function representing wave propagation through the cables, antennas, and air. Again using superposition, the transmission coefficients were added to yield:

$$\tau_{in} = \tau_1 + F_2\Gamma_s \quad (52)$$

The calibration of the network analyzer/antenna apparatus required four static calibrations in order to isolate soil reflection from the effects of the other network components. The effects that were removed through calibration had equivalent systematic error: reflection signal leakage (Γ_1), antenna crosstalk (τ_1), reflection element frequency response (F_1), and transmission element frequency response (F_2). In each of the four static calibrations, the magnitude and phase of the signal were recorded at each frequency. In each instance of soil reflection measurement, the calibration measurements

were recorded, and saved for removal of systematic errors in post-processing. The following is a list of the static calibrations conducted and the errors that were removed.

1. Reflection signal leakage: Both antennas were aimed at the sky 20 degrees inward (Figure 18), which was an inverted configuration of the downward geometry used for the soil moisture tests (note: see Figure 4).

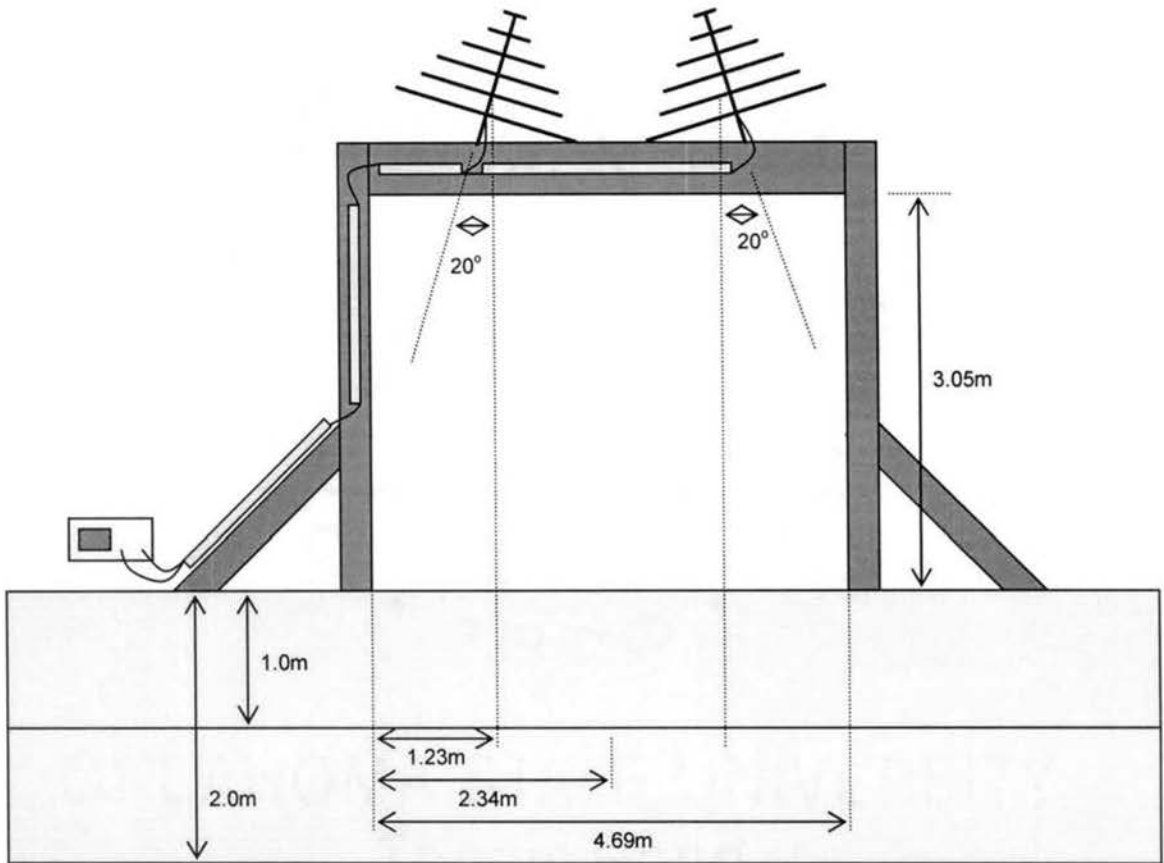


Figure 18. Antenna configuration for isolation calibration

The network analyzer output a voltage wave to the transmitting antenna. The magnitude and phase of the reflection were recorded ($\Gamma_s = 0$, $\Gamma_{in} = \Gamma_1$) as the frequency was swept from 80 MHz to 1 GHz. The measurement was used to

remove the portion of the reflection that resulted from mismatched antenna impedance (Γ_1).

2. Antenna isolation: Both antennas were directed toward the sky 20 degrees from vertical. The network analyzer transmitted a signal via antenna 1. The magnitude and phase of the signal in port 2 of the network analyzer were recorded ($\Gamma_s = 0$, $\tau_{in} = \tau_1$) as the frequency was swept from 80 MHz to 1 GHz. The antenna isolation measured crosstalk error between the antennas that resulted from radiated energy traveling to the second antenna through a path other than a direct reflection from the targeted soil (τ_1).
3. Maximum soil reflection: 4 1.52 x 1.52 meter sheets of 16-gage steel were placed over the surface of the target soil in the configuration shown in Figure 19.

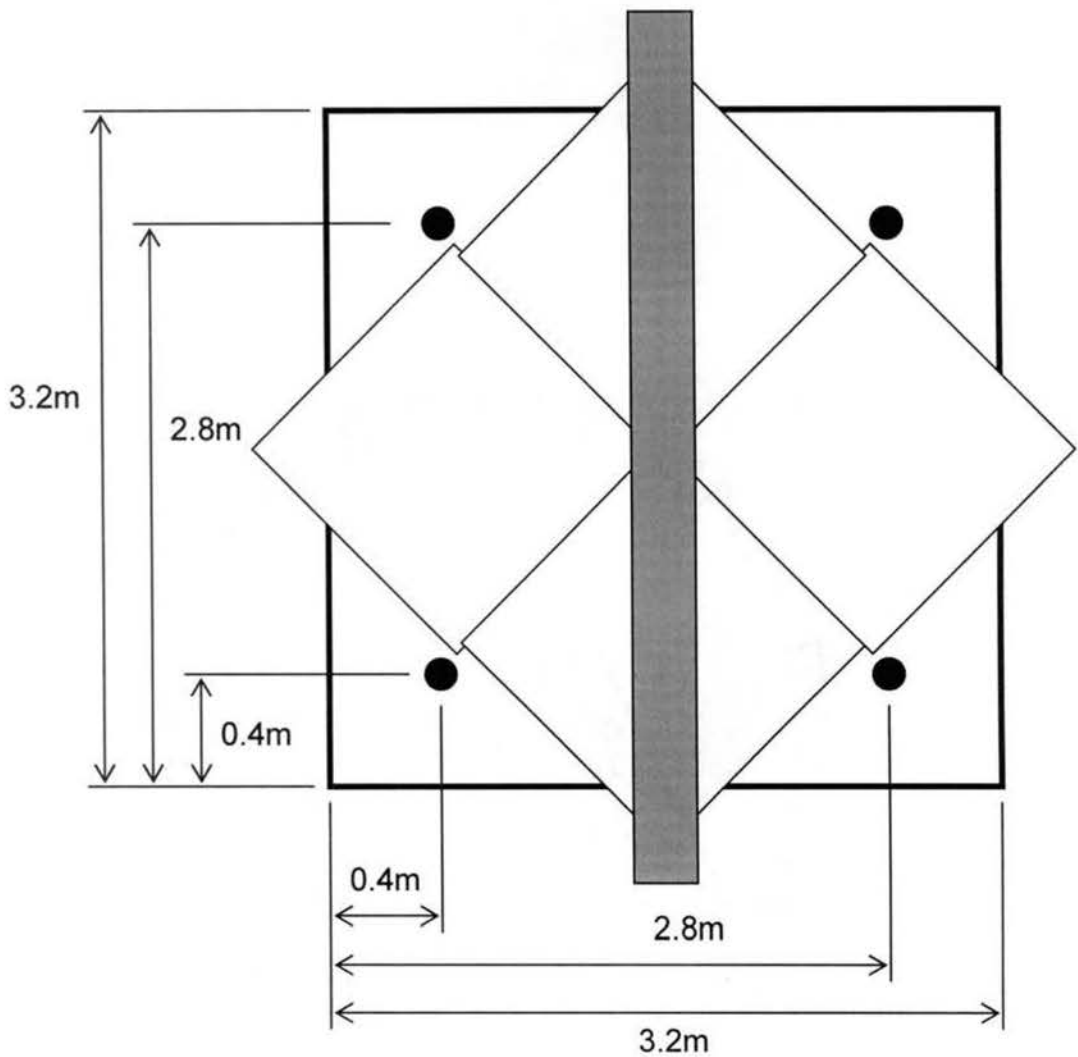


Figure 19. Configuration of 16-gage steel calibration sheets

The antennas were turned 20 degrees from vertical downward as shown in Figure 4. The network analyzer transmitted a voltage wave and the magnitude and phase of the reflection were recorded ($\Gamma_s = -1$, $\Gamma_{in} = \Gamma_1 - F_1$) as the frequency was swept from 80 MHz to 1 GHz. By detecting the reflections of the waves with the “radio wave mirror” in place, a reference of maximum reflection was established. The reference indicated antenna and network analyzer frequency response errors (F_1).

4. Maximum transmission: The downward turned antennas were aimed 20 degrees from vertical at the metal target. A voltage wave was transmitted from port 1 of

the network analyzer. The magnitude and phase of the transmission were recorded ($\Gamma_s = -1$, $\tau_{in} = \tau_1 - F_2$) as the frequency was swept from 80 MHz to 1 GHz. The measurements that resulted from the “radio wave mirror” reflection indicated a reference of maximum transmission and element frequency response errors (F_2).

The calibration was checked using the 16-gage steel sheets elevated 19.69 cm above the soil surface. The network analyzer reflection and transmission measurements of the offset steel plates were used with the calibration measurements in a MATLAB program to calculate the apparent reflection coefficient from the target as if it existed at the soil surface. An analytical reflection coefficient based on assumptions of complete detection of the reflected pattern and electromagnetic propagation through air was calculated and compared with the measured apparent reflection coefficient. The MATLAB code is in Appendix E and the calibration data is in Appendix F.

Field Apparatus Calibration Results

Recall that four static calibrations were needed to isolate soil reflection from the effects of the other network components. In the first measurement, the antennas were aimed at the sky and reflection measurements were made. In the upward configuration, the reflection was entirely due to impedance mismatch at the transmitting antenna. Figure 20 displays a sample measurement of a skyward reflection (Γ_1).

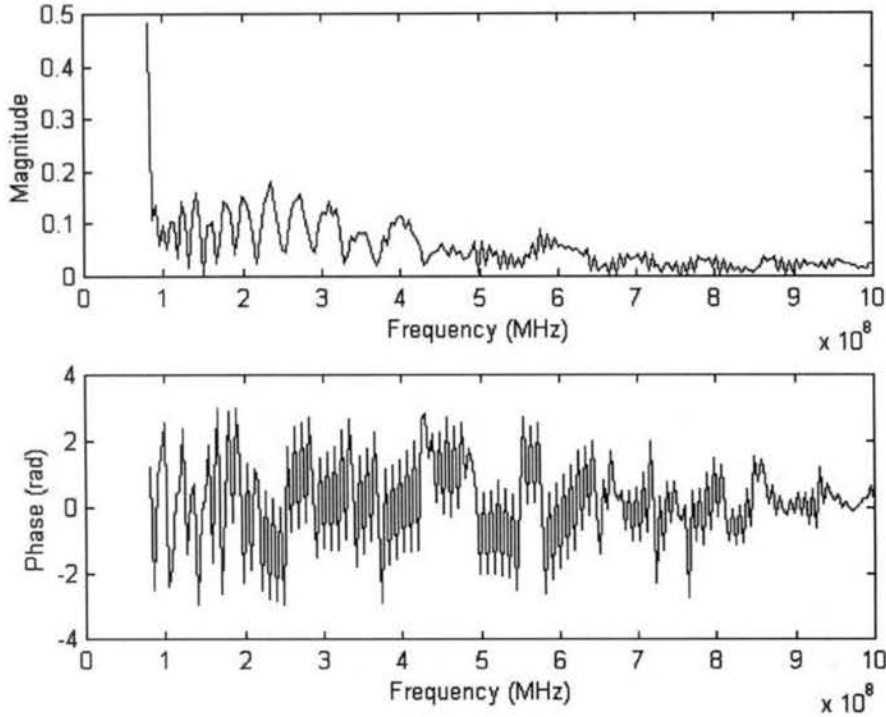


Figure 20. Reflection from sky (impedance mismatch at antenna)

The magnitude of the skyward reflection (Γ_1) shows that the impedance mismatch of the antenna was greatest at 80 MHz. Note that this calibration measurement of reflection (Γ_1) must be subtracted from all other network analyzer reflection measurements. An ideal antenna would result with magnitudes of zero at every frequency.

In the skyward configuration, a transmission measurement was also recorded by the network analyzer. The transmission resulted from the crosstalk between the antennas (τ_1). Figure 21 displays the skyward transmission measurement.

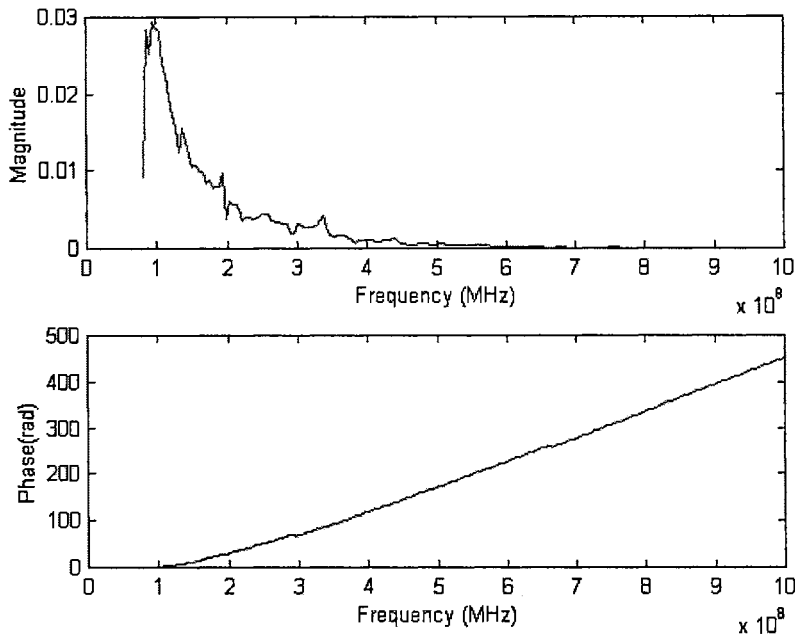


Figure 21. Transmission via the sky (antenna crosstalk)

The magnitude of the transmission measurement of antenna crosstalk (τ_1) was greatest at the lower frequencies. This calibration measurement must be subtracted from all other transmission measurements. An ideal configuration of antennas would yield a magnitude of zero at every frequency.

A reflection with the antennas aimed downward toward steel sheets on the surface of the ground was conducted to calibrate the reflection measurement for frequency response errors. The skyward reflection (Γ_1) was subtracted from the steel sheet measurement and the difference was multiplied by -1 to yield the reflection frequency response term, F_1 . Figure 22. displays the magnitude and phase of the frequency response term (F_1).

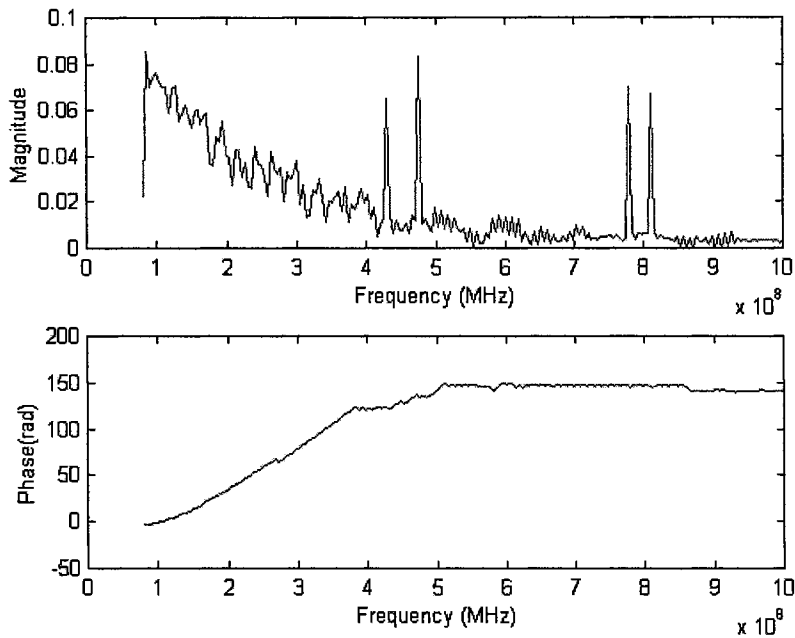


Figure 22. Reflection frequency response (F_1)

As Figure 22 shows, the magnitude of the frequency response term (F_1) is greatest at the lower frequencies. All measurements of soil reflection were divided by the frequency response. An ideal frequency response would have large magnitudes at every frequency.

A transmission measurement was made with the antennas aimed at the steel sheets. The skyward transmission was subtracted and the difference was multiplied by -1 to yield the transmission frequency response (F_2). Figure 23 shows the magnitude and phase of the transmission frequency response.

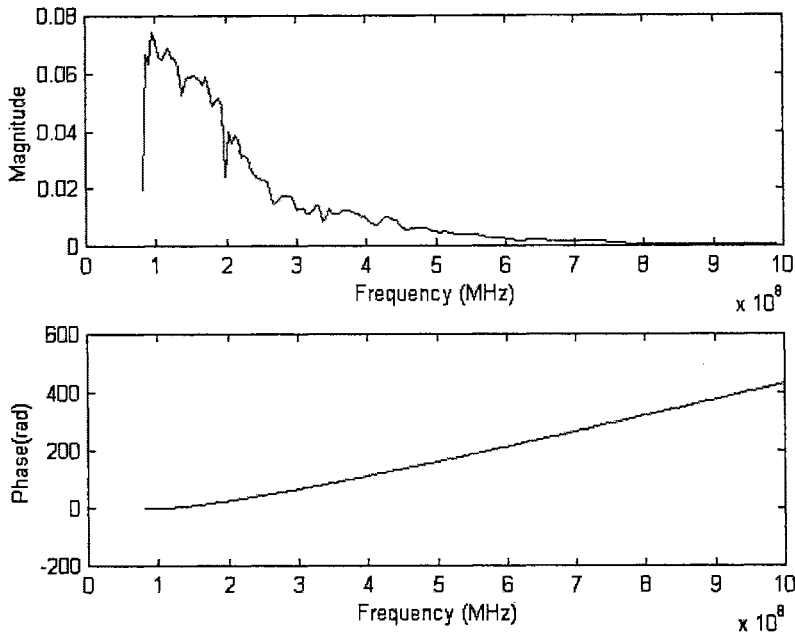


Figure 23. Transmission frequency response (F_2)

The figure shows that the transmission frequency response was greatest at the lower frequencies. All soil transmission measurements were divided by the transmission frequency response (F_2). Ideally, the magnitude of the frequency response would be large at all frequencies.

A calibration check was conducted measuring reflection and transmission from the 16-gage steel sheets, elevated 19.69 cm above the soil surface. Three calibration check reflection coefficients were averaged at each frequency and compared to analytical reflection coefficients to determine bias errors in the measurements. The standard deviations of the three measurements at each frequency were used as a measure of random error. Table 4 lists the averages of the bias and random errors.

Table 4. Reflection coefficient error of offset steel plates

As measured with network analyzer reflection		As measured with network analyzer transmission	
Average magnitude bias error	0.597	Average magnitude bias error	0.109
Average magnitude random error	0.348	Average magnitude random error	0.016
Average phase bias error (rad)	0.787	Average phase bias error (rad)	0.255
Average phase random error (rad)	0.611	Average phase random error (rad)	0.030

The table shows that the bias and random errors of the reflection coefficient as measured by network analyzer reflection are quite large. The average magnitude bias error was 59.7% and average random magnitude error was 34.8%. Errors this large indicate that the network analyzer reflection measurements are not suitable to calculate the reflection coefficient of the ground. Reflection coefficients as calculated from the network analyzer transmission measurements had average magnitude bias error of 10.9% and phase bias errors of 0.255 radians or 4.1%. Figures 24 and 25 display the measured reflection coefficients' magnitudes and phases and the analytical values.

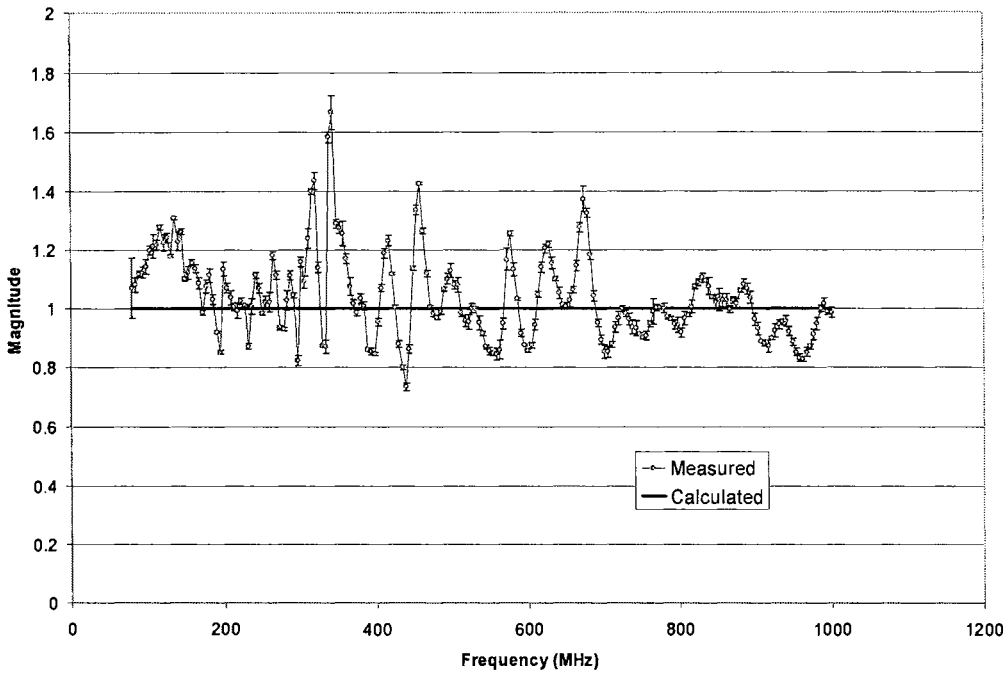


Figure 24. Reflection coefficient magnitude as measured by network analyzer transmission

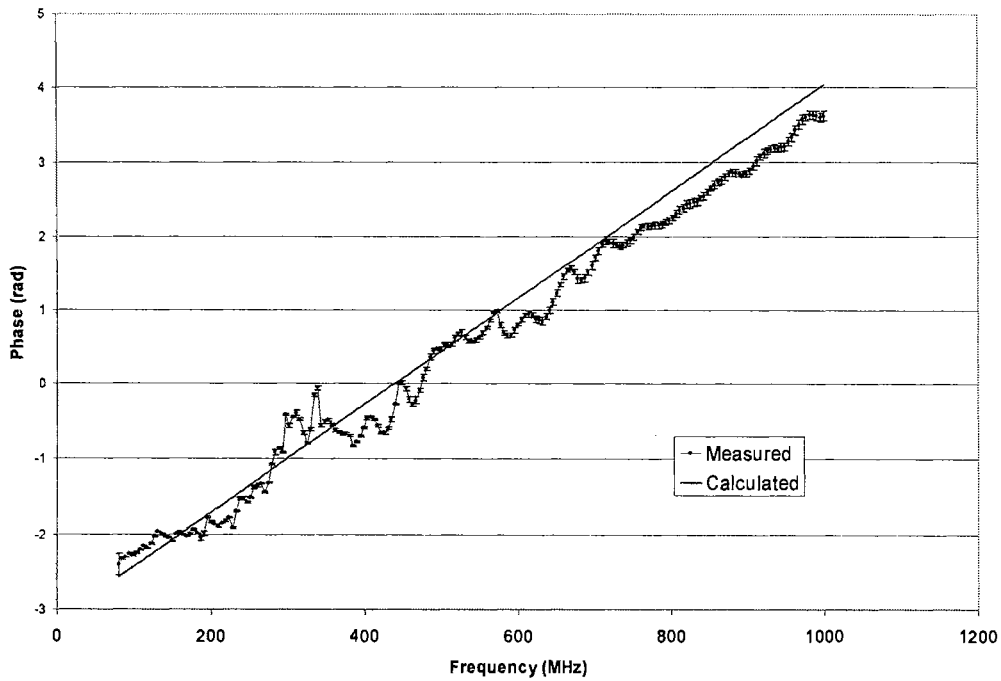


Figure 25. Reflection coefficient phase of offset steel plates as measured by network analyzer transmission

The large fluctuations in the magnitude measurements are likely attributed to interference patterns resulting from a reflection that is not truly in the far field of the antenna pattern. In other words, the assumption of plane wave reflection may not be valid for this specific configuration. The large magnitude fluctuations were also witnessed in the soil reflection coefficients and may partially result from this phenomenon.

CHAPTER V

SOIL DIELECTRIC VARIABILITY

Introduction

The prediction of soil moisture profiles using radio wave reflections required knowledge about the dielectric properties of the soil as it related to moisture. The prediction model utilized layers of dielectric material to simulate a moisture profile. The analysis depended on the assumption that there existed horizontal homogeneity within each of the soil layers and vertical homogeneity within each layer. Admittedly, soil properties are rarely homogeneous. Thus, a soil variability analysis was conducted on the soil properties known to affect the electrical characteristics. Soil density and particle size, which have been shown to affect soil dielectric properties, were measured. In addition, variability of permittivity and conductivity was tested.

Four soil cores with 4.45 cm diameters were collected within each of four plots to depths of 2.59 meters. The soil cores were divided into seventeen 15.2 cm samples. To remove density bias resulting from compaction within some of the cores, the 2 least compacted cores from each plot were used for homogeneity comparisons.

Soil Density

The dry soil densities were analyzed using an analysis of variance test (ANOVA) with alpha equal to 0.1 (Steel et al., 1997). Each sample was classified by plot number and by depth. Sub-samples were classified by hole number. The sub-samples were

averaged within each sample and the mean was used in the experiment in which depth was the treatment, and plot number was the replication. Essentially the test was used to determine if the average density varied between plots, or between depths. Table 5 contains the ANOVA results.

Table 5. Analysis of variance of density in plots and at depth

Source	df	SS	MS	F	P
Plot	3	0.1053	0.0351	2.17	0.1032
Depth	16	0.8381	0.0524	3.24	0.0008
Error	48	0.7751	0.0161		
Total	67	1.7185			

The test found that average densities were not significantly different between plots. However, average density was different at different depths. Tukey's procedure was used to conduct individual density comparisons between pairs of depths. The procedure identified at which depths the densities were significantly different. The layer with the highest average density, 2.44 meters deep, had a significantly higher average density than the depths of 0.15 m, 1.52 m, and 1.68 m. The top layer had the lowest average density. Table 6 lists the average densities by depth and Figure 26 shows a depth profile of average density in the field.

Table 6. Depth profile of average soil density

Depth (meters)	Average Density (g/cc)	Std. Dev. Density (g/cc)
-0.152	1.455	0.128
-0.305	1.509	0.180
-0.457	1.606	0.126
-0.610	1.701	0.165
-0.762	1.692	0.357
-0.914	1.765	0.142
-1.067	1.630	0.070
-1.219	1.596	0.078
-1.372	1.523	0.149
-1.524	1.503	0.161
-1.676	1.502	0.158
-1.829	1.568	0.269
-1.981	1.545	0.243
-2.134	1.697	0.108
-2.286	1.742	0.076
-2.438	1.804	0.072
-2.591	1.799	0.021

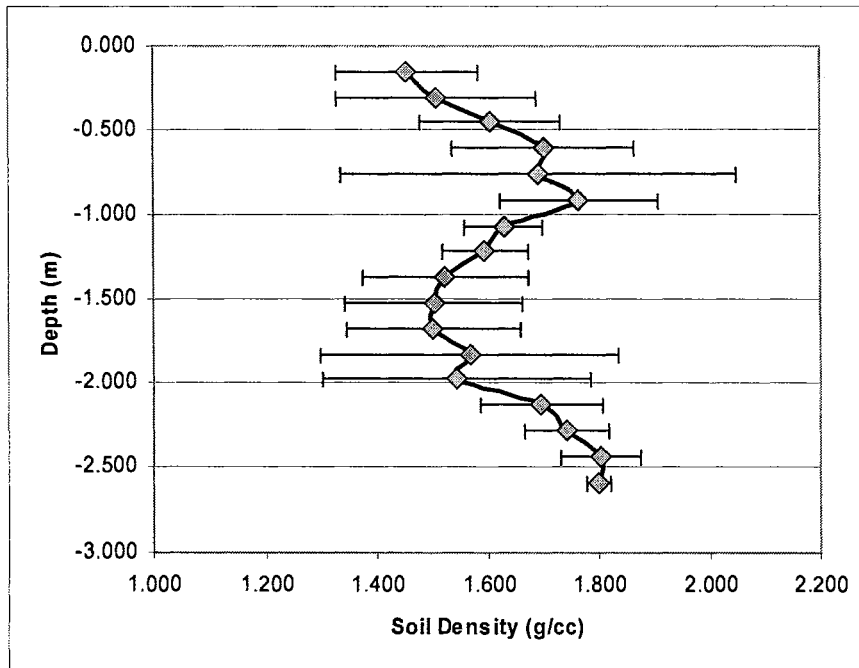


Figure 26. Depth profile of average soil density

Soil Particle Size

Particle size analyses were conducted on each 15.2-cm sample from the eight non-compacted cores with a hydrometer and utilizing Stokes Law. The diameters of the particles were divided into 3 categories: sand, silt, and clay. Upon completion of the hydrometer tests, the samples were also sieved to verify the particle size analyses. The percentage of each category of particle size was analyzed using three analysis of variance tests. Each test classified the samples by plot and by depth. Hole number was a sub-sample. The average percent value of each sample was used in the experiment in which depth was the treatment and plot number was the replication. The ANOVA results for the percentage of sand are displayed in Table 7.

Table 7. Analysis of variance of percent sand by plot and by depth

Source	df	SS	MS	F	p
Plot	3	213	71.01	1.2	0.3186
Depth	16	19926	1245	21.11	< 0.0001
Error	48	2832	59		
Total	67	22971			

All three of the ANOVA tests indicated that percentages of sand, silt, and clay were not different between plots but were different between depths. Further analysis indicated that none of the percentages of the three particle sizes were significantly different within the top 0.76 meters. The percentages of each category (sand, silt, and clay) in each plot and at each depth are displayed in Appendix G.

Dielectric properties

In addition to the measurements of density and particle size, the homogeneities of permittivity and conductivity were tested. Dielectric properties were measured on each

soil sample consisting of 21% volumetric moisture and soil densities that existed in the field. In order to measure the dielectric properties, radio wave reflection measurements were recorded with the 8712ET network analyzer connected to the coaxial cell filled with soil at the specified density and moisture. The reflection measurements were used to calculate the input impedance of the cell. With the calculated impedance, the dielectric property iterative algorithm was used to solve for permittivity and conductivity. Because the frequency was swept from 80 MHz to 1 GHz, there were 201 permittivity and conductivity values for each of the numerous soil samples. To reduce the data to a manageable number of dielectric property values, permittivities and conductivities were averaged within ten 92-MHz frequency ranges.

The measured properties were tested for homogeneity each using a two-factor ANOVA experiment in which the samples were classified by plot, depth, and frequency. Sub-samples were divided by hole number. The means of each sample were compared in the ANOVA analyses with depth and frequency as the factors and plot number as the replications. Interactions between depth and frequency were determined along with the individual tests on the factors. Table 8 and Table 9 display the ANOVA results.

Table 8. Analysis of variance of soil permittivity with frequency, in plots, and at depth

Source	df	SS	MS	F	P
Plot	3	138.95	46.32	25.4	< 0.0001
Depth	16	247.09	15.44	8.47	< 0.0001
Freq	9	2176.04	241.78	132.59	< 0.0001
Plot*Depth	48	287.33	5.99	3.28	< 0.0001
Plot*Freq	27	109.64	4.06	2.23	0.0005
Depth*Freq	144	1456.23	10.11	5.55	< 0.0001
<u>Error</u>	<u>432</u>	<u>787.77</u>	1.82		
Total	679	5203.05			

Table 9. Analysis of variance of soil conductivity with frequency, in plots, and at depth

Source	df	SS	MS	F	P
Plot	3	0.308	0.103	44.19	< 0.0001
Depth	16	2.07	0.129	55.76	< 0.0001
Freq	9	3.656	0.406	174.98	< 0.0001
Plot*Depth	48	0.647	0.013	5.81	< 0.0001
Plot*Freq	27	0.261	0.01	4.17	< 0.0001
Depth*Freq	144	1.01	0.007	3.03	< 0.0001
Error	432	1.003	0.002		
Total	679	8.959			

Significant interactions existed between plot, depth, and frequency in both the permittivity and conductivity analyses. The average values were also found to have significant differences between plots, between frequencies, and between depths. The tests revealed that the soil contained a complete lack of homogeneity.

Although the soil was shown to lack dielectric homogeneity, the quantity of difference between the mean dielectric values gave an indication as to how the soil could be divided in order to create a model for simulation. The largest difference of average relative permittivity between plots was 1.172. The largest average permittivity difference between depths was 2.45. The plots had a distance of 15 meters between them and the depths were within 1 meter of each other. The assumption was made that more variability existed vertically than horizontally. Maximum average conductivity differences showed similar results: 0.045 between plots and 0.16 between depths.

CHAPTER VI

SOIL MOISTURE AND DIELECTRIC PROPERTY RELATIONSHIPS

Procedure

In order to create a model for the average dielectric property—moisture content relationship at the field site, permittivity and conductivity values of soil samples were analyzed so that the effect of depth within each 92 MHz frequency range could be observed. Individual ANOVA tests were conducted on permittivity and conductivity for each frequency range in which depth was the treatment with 4 replications. Tukey's procedure comparing dielectric properties by depth was used to determine what depths had significantly different permittivity and conductivity values. The dielectric properties were found to be statistically similar in the top 0.76 meters, in the next 0.91 meters, and in the bottom 0.76 meters. The soils that were determined to have the similar dielectric properties were mixed, with equal masses from each soil sample. The mixtures were used in dielectric property measurements that related permittivity and conductivity to moisture content.

The mixtures of soil samples were dried. Reflection measurements were made with the network analyzer connected to the soil-filled coaxial cell with volumetric moisture contents ranging from 0% to 40% in 5% increments. An average field soil density of 1.64g/cc was targeted for the dielectric measurements. Input impedances were calculated. Permittivities and conductivities were determined with the calculated impedances and the iterative algorithm. The volumetric moisture content and average

dielectric property values were related with simple correlations within ten 92-MHz frequency increments for each mixture. The relationships were later used in the simulation of soil radio wave reflection and the reconstruction algorithm that determined volumetric moisture contents from soil reflection coefficients.

Soil Moisture—Dielectric Relationship

The dielectric properties of the soil samples that had been mixed based on dielectric homogeneity with depth were measured in the coaxial cell with varied moistures. Permittivities of the top layer exhibited a nearly constant increase with added moisture at every frequency used. Figure 27 shows the measured permittivities of the mixture of topsoil with several volumetric moistures as a function of frequency. Conductivity values varied as functions of frequency and moisture content as shown in Figure 28.

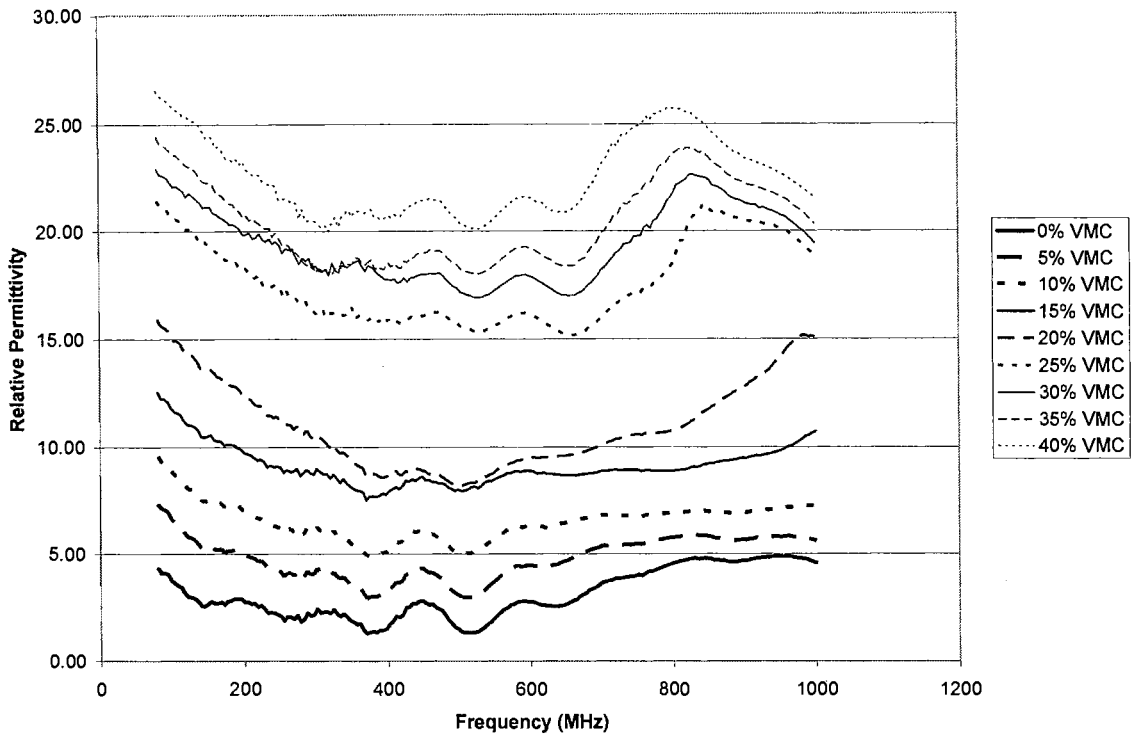


Figure 27. Permittivities of topsoil with various moisture contents

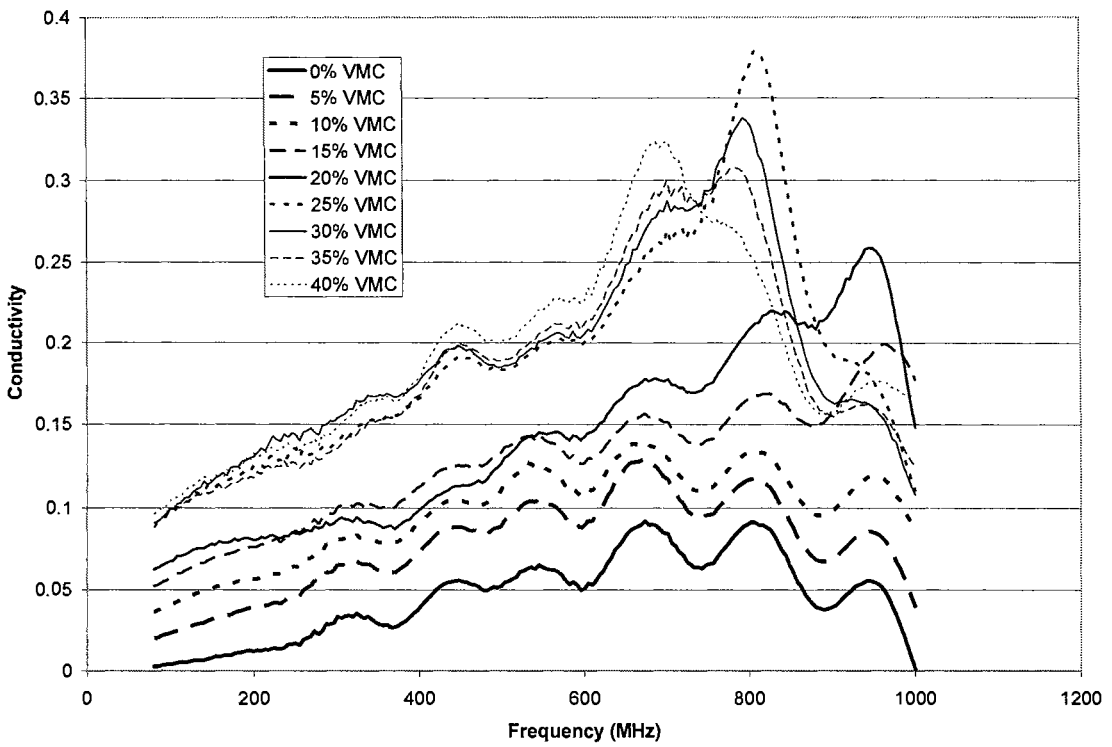


Figure 28. Conductivities of topsoil with various moisture contents

Note that the permittivity and conductivity values in Figures 27 and 28 contain some systematic error (ripple) from the coaxial cell measurements. The ripple originated from the impedance mismatch between the coaxial cable and the network analyzer. The measurements also appear to reveal specific resonant frequencies at which the soil's ability to store electric charge increases. The resonant frequencies appear as peaks on the permittivity plot in Figure 27.

The permittivity and conductivity values were averaged within ten 92-MHz increments. The dielectric property values were correlated to moisture content at each frequency increment and for each soil mixture. The values of each moisture, frequency range, and average dielectric property are displayed in Table 10 and Table 11.

Table 10. Soil permittivity at specific moistures, in depth layers and within each frequency range

		Permittivity of Top Layer (0 to 0.762 meter depth)									
Frequency		124	216	308	400	492	584	676	768	860	952
VMC (%)											
0		3.21	2.50	2.11	1.87	1.89	2.48	3.14	4.20	4.71	4.81
5		5.99	4.68	3.97	3.49	3.48	4.21	5.03	5.59	5.75	5.77
10		8.23	6.72	5.95	5.38	5.42	6.12	6.63	6.85	6.96	7.13
15		11.19	9.51	8.65	8.02	8.21	8.74	8.77	8.91	9.26	9.96
20		14.39	12.03	10.26	8.81	8.49	9.26	9.86	10.63	11.95	14.17
25		20.12	17.92	16.37	15.90	15.79	15.87	15.62	17.62	20.67	19.97
30		21.73	19.80	18.46	17.98	17.49	17.59	17.57	20.41	22.07	20.64
35		23.05	20.46	18.43	18.51	18.56	18.86	19.10	22.33	23.15	21.51
40		25.26	22.63	20.63	20.86	20.82	21.15	21.95	25.15	24.56	22.64

		Permittivity of Middle Layer (0.762 to 1.68 meter depth)									
Frequency		124	216	308	400	492	584	676	768	860	952
VMC (%)											
0		3.30	2.58	2.17	1.92	1.94	2.53	3.21	4.22	4.72	4.81
5		5.88	4.56	3.89	3.45	3.44	4.13	4.95	5.54	5.71	5.72
10		8.01	6.36	5.54	4.96	5.02	5.79	6.39	6.60	6.66	6.74
15		10.64	8.72	7.67	6.86	6.88	7.51	7.79	7.92	8.15	8.58
20		15.55	13.02	11.45	10.38	10.72	11.14	10.84	11.10	12.15	15.53
25		20.43	17.72	15.70	14.51	14.56	14.78	14.30	15.43	20.85	20.10
30		23.49	20.35	17.93	17.76	17.85	17.89	17.51	21.49	23.32	21.22
35		25.75	22.74	20.18	20.33	20.27	20.29	20.46	24.90	24.43	22.13
40		27.55	24.49	21.53	21.77	21.76	21.82	22.34	26.16	25.18	22.94

		Permittivity of Lower Layer (below 0.762 meter depth)									
Frequency		124	216	308	400	492	584	676	768	860	952
VMC (%)											
0		3.50	2.77	2.37	2.10	2.11	2.69	3.37	4.40	4.86	4.95
5		7.26	5.65	4.85	4.28	4.26	4.96	5.69	6.08	6.18	6.20
10		9.53	7.49	6.51	5.81	5.87	6.60	6.98	7.01	7.01	7.08
15		12.33	10.00	8.92	8.12	8.46	8.77	8.45	8.25	8.22	8.39
20		15.74	12.85	11.13	9.51	9.47	10.12	9.90	9.90	10.21	9.81
25		20.32	16.76	13.82	11.12	10.50	11.53	11.38	11.58	10.89	4.06
30		22.78	19.86	19.12	18.08	16.02	14.91	13.39	12.35	7.77	4.16
35		27.47	22.85	18.47	18.54	19.36	19.38	18.40	11.83	2.61	3.58
40		29.34	25.40	22.14	21.84	20.80	20.41	19.45	9.23	2.20	4.30

Table 11. Soil conductivity at specific moistures, in depth layers and within each frequency range

		Conductivity of Top Layer (0 to 0.762 meter depth)									
Frequency		124	216	308	400	492	584	676	768	860	952
VMC (%)	0	0.006	0.014	0.030	0.040	0.055	0.058	0.083	0.076	0.059	0.043
	5	0.027	0.041	0.062	0.074	0.092	0.097	0.120	0.105	0.086	0.074
	10	0.046	0.059	0.078	0.091	0.112	0.116	0.132	0.121	0.110	0.110
	15	0.063	0.079	0.098	0.112	0.132	0.134	0.150	0.151	0.158	0.187
	20	0.073	0.082	0.091	0.099	0.125	0.145	0.173	0.188	0.216	0.232
	25	0.104	0.126	0.143	0.169	0.188	0.202	0.249	0.316	0.269	0.167
	30	0.107	0.136	0.157	0.179	0.191	0.207	0.265	0.310	0.219	0.151
	35	0.104	0.122	0.139	0.172	0.194	0.213	0.276	0.295	0.198	0.153
	40	0.111	0.132	0.152	0.184	0.206	0.229	0.303	0.272	0.184	0.171
		Conductivity of Middle Layer (0.762 to 1.68 meter depth)									
Frequency		124	216	308	400	492	584	676	768	860	952
VMC (%)	0	0.006	0.014	0.030	0.041	0.056	0.059	0.083	0.076	0.059	0.043
	5	0.023	0.035	0.055	0.067	0.087	0.096	0.120	0.105	0.085	0.072
	10	0.043	0.057	0.077	0.091	0.114	0.121	0.136	0.123	0.109	0.106
	15	0.067	0.081	0.099	0.112	0.136	0.142	0.157	0.154	0.157	0.178
	20	0.105	0.119	0.132	0.156	0.185	0.192	0.215	0.245	0.307	0.345
	25	0.139	0.159	0.169	0.200	0.228	0.246	0.293	0.393	0.390	0.198
	30	0.150	0.169	0.186	0.233	0.255	0.274	0.345	0.430	0.267	0.194
	35	0.154	0.178	0.197	0.242	0.265	0.289	0.378	0.364	0.228	0.196
	40	0.157	0.179	0.197	0.244	0.269	0.292	0.382	0.334	0.227	0.223
		Conductivity of Lower Layer (below 0.762 meter depth)									
Frequency		124	216	308	400	492	584	676	768	860	952
VMC (%)	0	0.006	0.014	0.031	0.041	0.056	0.060	0.084	0.078	0.060	0.045
	5	0.030	0.044	0.065	0.078	0.100	0.109	0.129	0.115	0.098	0.089
	10	0.054	0.072	0.094	0.110	0.137	0.142	0.152	0.141	0.133	0.138
	15	0.092	0.113	0.137	0.158	0.181	0.175	0.184	0.187	0.200	0.239
	20	0.126	0.143	0.155	0.176	0.217	0.234	0.253	0.283	0.352	0.563
	25	0.163	0.173	0.167	0.187	0.246	0.285	0.320	0.393	0.622	0.726
	30	0.196	0.241	0.254	0.256	0.265	0.286	0.344	0.459	0.605	0.484
	35	0.209	0.228	0.246	0.349	0.377	0.414	0.570	0.921	0.697	0.477
	40	0.220	0.258	0.274	0.321	0.353	0.407	0.624	0.958	0.620	0.438

28

The permittivities of the top two soil layers exhibited very linear relationships with volumetric moisture content. The bottom layer also exhibited linear relationships between permittivity and moisture at low frequencies, but permittivity measurements at the higher frequencies tested exhibited what appeared to be dielectric relaxations (Figure 29).

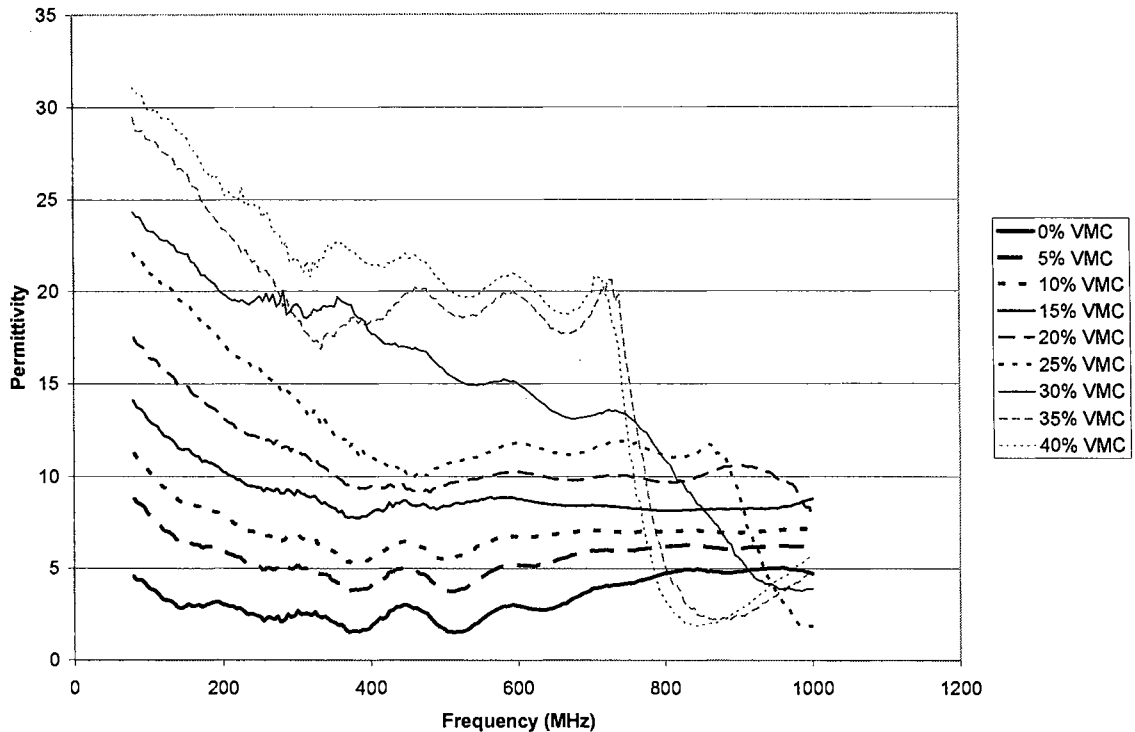


Figure 29. Moisture content—permittivity relationship of bottom layer

Linear equations relating permittivity to moisture were computed for the top two layers within each frequency range. The equations had simple correlation coefficients ranging from 0.923 to 0.985. The permittivity values from the top layer are displayed as functions of volumetric moisture in Figure 30. Along with the permittivity values, an example linear equation and the corresponding simple correlation coefficient is shown in Figure 30.

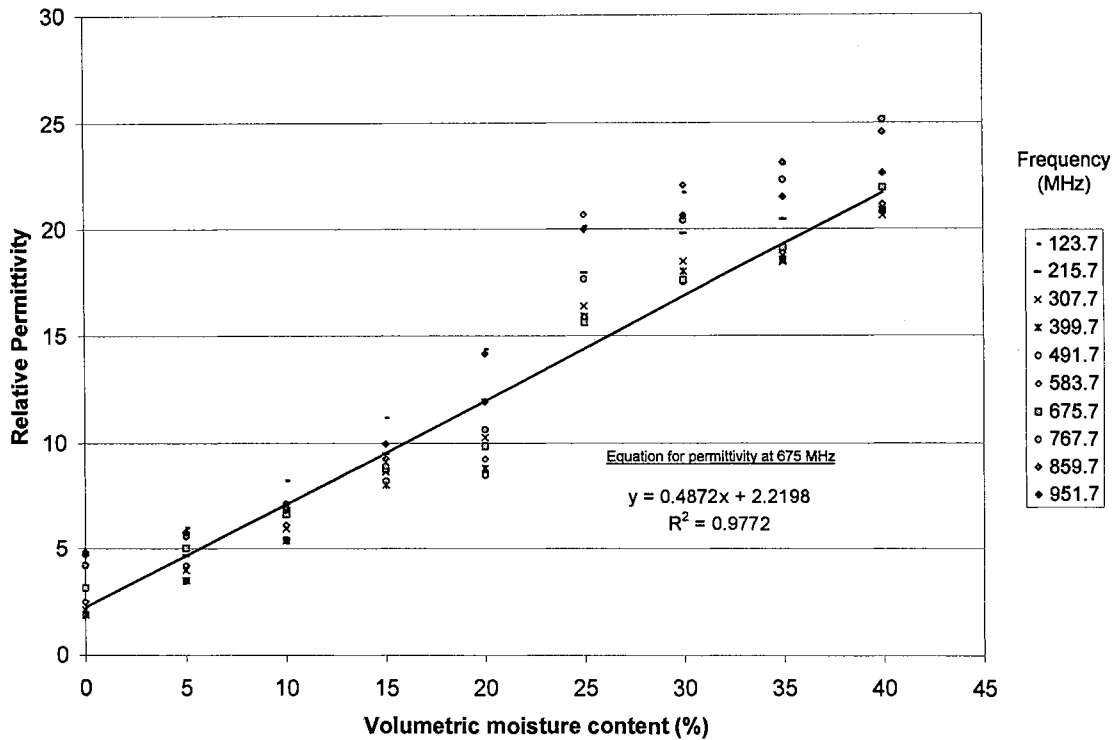


Figure 30. Moisture content / permittivity relationship of topsoil

Conductivity values that had been averaged within each 92 MHz frequency range were also related to volumetric moisture. The relationships were expressed as second and third-order polynomial equations. The conductivity values of the top layer are plotted as functions of moisture content in Figure 31 and the equations relating volumetric moisture content to permittivity and conductivity are shown in Table 12.

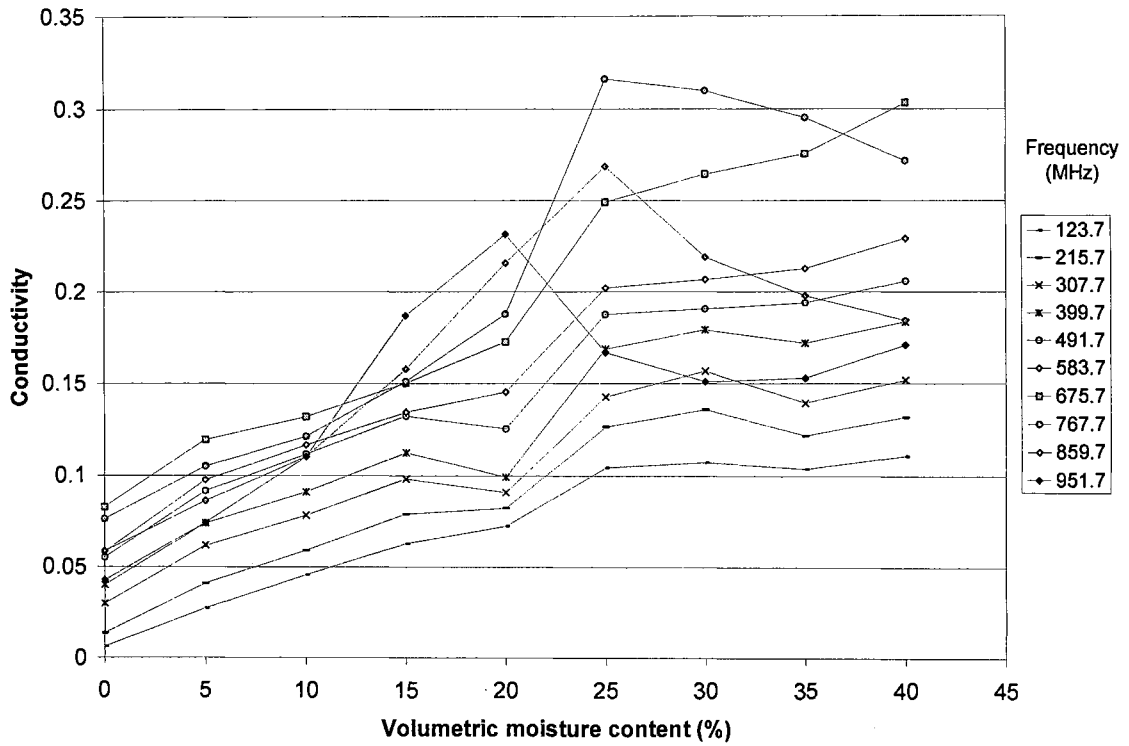


Figure 31. Moisture content / conductivity relationship of topsoil

Table 12. Characteristic equations relating moisture content to dielectric properties

Frequency range (MHz)	Permittivity of topsoil	Permittivity of middle layer	Conductivity of topsoil	Conductivity of middle layer
80 - 170	$y = 0.5844x + 3.1069$ R2 = 0.981	$y = 0.6579x + 2.4643$ R2 = 0.9845	$y = -6E-05x^2 + 0.005x + 0.0036$ R2 = 0.9775	$y = -6E-05x^2 + 0.0066x - 0.0049$ R2 = 0.9701
170 - 262	$y = 0.5415x + 2.0854$ R2 = 0.9754	$y = 0.5971x + 1.451$ R2 = 0.9833	$y = -6E-05x^2 + 0.0056x + 0.0118$ R2 = 0.9528	$y = -6E-05x^2 + 0.007x + 0.0037$ R2 = 0.9737
262 - 354	$y = 0.5006x + 1.6343$ R2 = 0.9674	$y = 0.5305x + 1.1751$ R2 = 0.9828	$y = -6E-05x^2 + 0.0053x + 0.0309$ R2 = 0.9272	$y = -5E-05x^2 + 0.0066x + 0.023$ R2 = 0.9818
354 - 446	$y = 0.5137x + 0.9284$ R2 = 0.963	$y = 0.5444x + 0.4373$ R2 = 0.9798	$y = -4E-05x^2 + 0.0053x + 0.0416$ R2 = 0.9209	$y = -4E-05x^2 + 0.0072x + 0.0313$ R2 = 0.9741
446 - 538	$y = 0.5089x + 0.951$ R2 = 0.9635	$y = 0.5436x + 0.5105$ R2 = 0.9809	$y = -5E-05x^2 + 0.0056x + 0.0582$ R2 = 0.9494	$y = -6E-05x^2 + 0.0081x + 0.0469$ R2 = 0.9789
538 - 630	$y = 0.4958x + 1.6695$ R2 = 0.9712	$y = 0.5237x + 1.2922$ R2 = 0.98	$y = -4E-05x^2 + 0.006x + 0.0607$ R2 = 0.9707	$y = -5E-05x^2 + 0.0083x + 0.0511$ R2 = 0.9761
630 - 722	$y = 0.4872x + 2.2198$ R2 = 0.9772	$y = 0.5061x + 1.8548$ R2 = 0.9806	$y = 7E-06x^2 + 0.0054x + 0.0817$ R2 = 0.965	$y = 3E-05x^2 + 0.0072x + 0.0733$ R2 = 0.9654
722 - 814	$y = 0.5661x + 2.1967$ R2 = 0.9598	$y = 0.6105x + 1.4982$ R2 = 0.945	$y = -2E-05x^3 + 0.0009x^2 - 0.0046x + 0.087$ R2 = 0.9456	$y = -3E-05x^3 + 0.0016x^2 - 0.0109x + 0.0923$ R2 = 0.9535
814 - 906	$y = 0.5774x + 2.793$ R2 = 0.9359	$y = 0.6134x + 2.3046$ R2 = 0.9237	$y = -1E-05x^3 + 0.0003x^2 + 0.0045x + 0.0543$ R2 = 0.9226	$y = -2E-05x^3 + 0.0008x^2 + 0.0028x + 0.0493$ R2 = 0.8058
906 - 1000	$y = 0.5186x + 3.6953$ R2 = 0.9458	$y = 0.5408x + 3.3829$ R2 = 0.9286	$y = 6E-06x^3 - 0.0006x^2 + 0.0171x + 0.0242$ R2 = 0.787	$y = 2E-06x^3 - 0.0004x^2 + 0.0173x + 0.0181$ R2 = 0.6498

x = Volumetric moisture content

y = Permittivity or conductivity

Measurement of the permittivity and conductivity values of the topsoil allowed calculation of the skin depth of the topsoil at each frequency. Recall that the skin depth was the depth at which the intensities of the fields were e^{-1} of the intensities at the surface. Table 13 lists the average skin depths and skin depths at specific frequencies of the topsoil at several moistures. Figure 32 displays the skin depths of the topsoil as functions of frequency.

Table 13 Calculated skin depths of topsoil at various moistures

Volumetric moisture (%)	Average Skin depth (m)	84.6 MHz Skin depth (m)	793 MHz Skin depth (m)
5	0.20	0.72	0.11
10	0.17	0.47	0.11
15	0.15	0.38	0.10
20	0.15	0.35	0.09
25	0.13	0.29	0.06
30	0.14	0.30	0.07
35	0.15	0.30	0.08
40	0.15	0.30	0.10

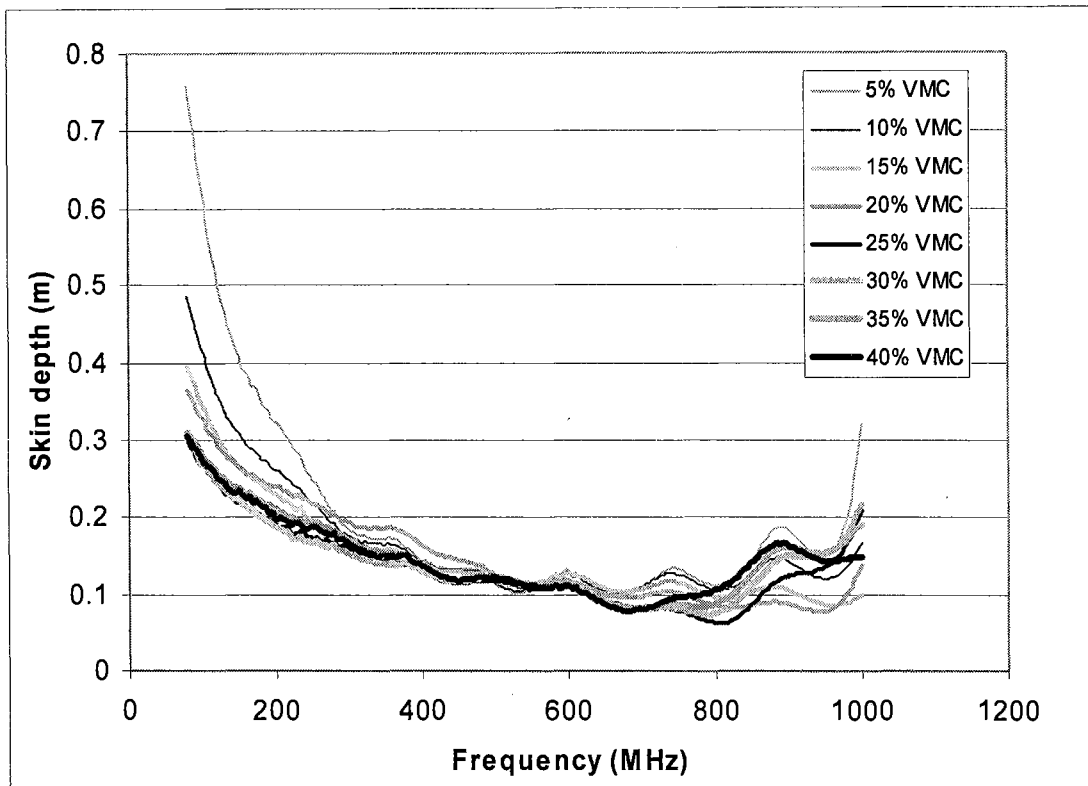


Figure 32. Calculated skin depths of topsoil at various moistures

Within the frequency range tested, the average skin depth was minimized at 9.2 cm at a frequency of 793 MHz. The average skin depth was maximized at 40.2 cm at a frequency of 80 MHz.

Recall that data from the literature was used to make preliminary calculations of skin depths and reflection coefficients so that an adequate frequency range could be predicted for the measurement of moisture at depth. But, the preliminary calculation of skin depths was slightly misleading as to the optimum frequency range for use. The permittivity values found in the literature (Curtis, 1998; Topp et al., 1980; Wang, 1980) were very similar to the ones calculated in this experiment. However, the conductivity values were much lower in the literature (Curtis, 1998) than the conductivity values

measured from the soil from the Oklahoma State Agronomy Research Station. The impact was that the preliminary calculations predicted much deeper penetration into soil than the measurements of soil in this experiment.

CHAPTER VII

SIMULATION OF REFLECTION COEFFICIENTS

Procedure

In order to predict the EM fields reflected by soil from the test site with various moisture layers, calculations were conducted in a MATLAB program (Appendix I). The program simulated plane waves that propagated through media with dielectric properties equal to those acquired from the coaxial cell measurements of the soil mixtures at various moistures. The simulation predicted reflections that would result from three types of moisture profiles in the soil.

1. Reflections were predicted from soil with constant volumetric moisture content throughout the profile. The reflection coefficients of soil with 0% to 40% volumetric moisture content in 5% increments were simulated at each selected frequency.
2. Reflections from a two layered dielectric model were predicted. The depth of an interface between soil at 15% volumetric moisture and soil at 30% volumetric moisture was varied, and the reflection coefficients at selected frequencies were recorded. The influence of depth on attenuation of signals was observed. In addition, because the sinusoidal waves reflecting from the subsurface interface interfered with the pattern reflected from the air/soil interface, the harmonic impact of the top layer thickness was observed.

3. The moisture profiles measured with the neutron probe during the field tests were simulated and the resulting reflection coefficients were recorded. The calculated reflection coefficients were compared with the reflection coefficients measured with the network analyzer and correlated to surface moisture.

The simulation consisted of a basic calculation of electrical properties of the soil. The relationships between soil depth, volumetric moisture content, and soil dielectric properties, which were developed with the coaxial cell measurements, were used to calculate permittivity and conductivity profiles. The dielectric profiles were used to calculate profiles of propagation constants:

$$\gamma_i = \sqrt{j\omega\mu(\sigma_i + j\omega\varepsilon_i)} \quad (53)$$

and intrinsic impedances:

$$Z_i = \sqrt{\frac{j\omega\mu}{\sigma_i + j\omega\varepsilon_i}} \quad (54)$$

The intrinsic impedances of the layers were used to calculate the reflection coefficient of each moisture boundary:

$$\Gamma_{i,i+1} = \frac{Z_{i+1} - Z_i}{Z_{i+1} + Z_i} \quad (55)$$

The reflection coefficients and propagation constants of each layer were used to calculate the total reflection coefficient of the ground:

$$\Gamma_s = \Gamma_{0,1} + \tau_{0,1}\tau_{1,0} \left[\Gamma_{1,2}e^{-2\gamma_1 d} + \Gamma_{2,3}e^{-2d(\gamma_1+\gamma_2)} + \Gamma_{3,4}e^{-2d(\gamma_1+\gamma_2+\gamma_3)} \dots \right] \quad (56)$$

where:

$$\Gamma_{0,1} = \frac{Z_1 \cos \theta_i - Z_0 \cos \theta_i}{Z_1 \cos \theta_i + Z_0 \cos \theta_i} \quad (57)$$

and $\tau_{0,1}$ was the forward transmission coefficient of the surface boundary, $\tau_{1,0}$ was the reverse transmission coefficient of the surface boundary, d was the thickness of each boundary, θ_i was the angle of incidence, θ_t was the transmitted angle, and Z_0 was the intrinsic impedance of air.

Profiles of Constant Moisture

The magnitudes and phases of the simulated reflection coefficients from soil with constant volumetric moisture content throughout the profile were compared using an analysis of variance test in which the profile moisture contents were analyzed as factors and the 201 frequencies were replications of each treatment. The resulting ANOVA of the magnitude of the reflection coefficient is shown in Table 14.

Table 14. ANOVA of magnitude of reflection from simulated profiles with constant moisture

Source	df	SS	MS	F	p
Moisture	8	21.57	2.7	3926	< 0.0001
Error	1800	1.24	0.00069		
Total	1808	22.81			

The test found that average reflection coefficient magnitude was different between profiles with different moistures. Magnitudes between profiles within a frequency range of 784 to 802 MHz were analyzed using Tukey's procedure. The procedure revealed that, within the frequency range of 784 to 802 MHz, significant differences existed between mean reflection coefficient magnitudes from every profile. The significant

differences showed that moisture content changes of 5% could be distinguished from reflection coefficient magnitudes at frequencies near 793 MHz.

The phase of the reflection coefficient was also tested with the same model. The resulting ANOVA is shown in Table 15.

Table 15. ANOVA of phase of simulated reflection from constant moisture profiles

Source	df	SS	MS	F	p
Moisture	8	21.09	2.64	318.4	< 0.0001
Error	1800	14.91	0.0083		
Total	1808	36			

The phase analysis of variance revealed that average reflection differed between moisture profiles. Tukey's procedure, used on the frequency range of 784 to 802 MHz, showed significant differences between average phases between all of the profiles. Thus, moisture content changes of 5% could be distinguished from reflection coefficient phase at frequencies near 793 MHz.

The magnitudes and phases of the reflection coefficients at a frequency of 793 MHz are plotted as functions of volumetric moisture content in Figure 33 and are listed in Table 16.

Table 16. Magnitude and phase of simulated reflection coefficients from simulated profiles with constant moisture at a frequency of 793 MHz

Moisture Content %	Magnitude	Phase (rad)
0	0.326	3.038
5	0.484	2.923
10	0.5627	2.916
15	0.6127	2.943
20	0.6437	2.971
25	0.6899	2.993
30	0.6932	3.002
35	0.6966	3.010
40	0.7054	3.018

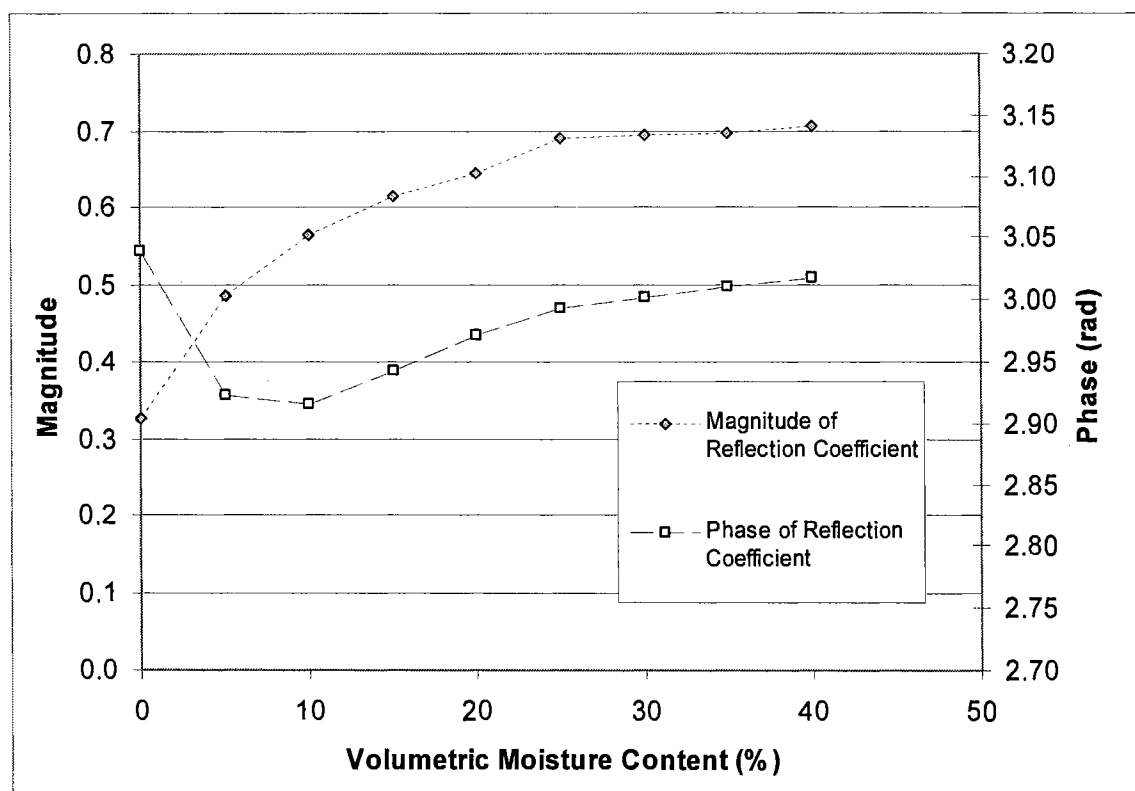


Figure 33. Magnitude and phase of reflection coefficients from simulated profiles with constant moisture at a frequency of 793 MHz

Two-Layer Moisture Profiles

The two-layer profiles consisted of two types, each containing a layer of 15% volumetric moisture and a layer of 30% volumetric moisture. The first type of profile contained 15% moisture in the top soil and 30% in the lower soil. The depth of the boundary between the two layers was varied to establish different profiles. The second type of two-layer profile consisted of 30% moisture in the top layer and 15% moisture in the lower layer. Depth of the boundary between layers was varied to establish different profiles.

Reflection coefficients from the two-layer profiles contained a sum of two large reflections, one from the air soil boundary and one from the boundary between moisture layers. The sum of reflections from the boundaries between moisture layers created interference patterns that were observed in the simulated reflection coefficient magnitudes and phases. Figure 34 displays reflection coefficient magnitudes from the profiles with a 15% moisture layer on top of a 30% moisture layer.

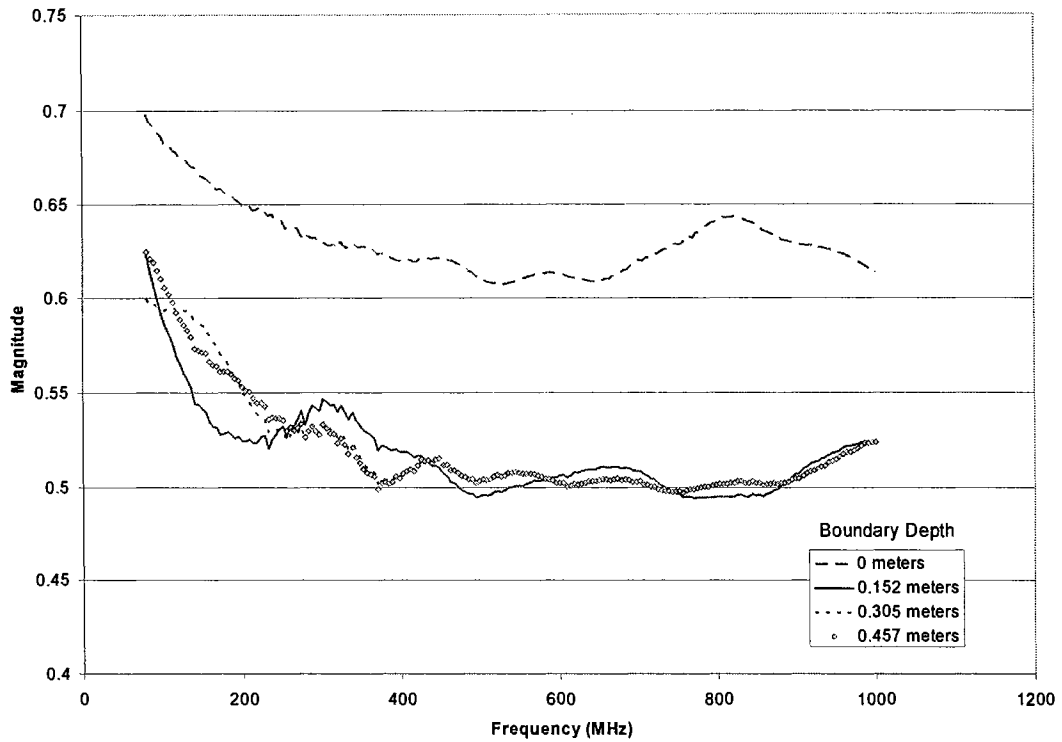


Figure 34. Magnitude of simulated reflection from two-layer (dry over wet) profiles with several boundary depths

Recall that the simulation of moisture profiles utilized dielectric-moisture relationships measured with the coaxial cell. The reflection magnitudes in Figure 34 contain a ripple which resulted from systematic error from the coaxial cell measurement. However, additional ripples exist in the reflection coefficient patterns with boundary depths of 0.152 meters and 0.305 meters. The additional ripples resulted from interference between the surface and subsurface reflections.

Figure 35 shows the phase of reflection coefficients from the profiles with dry soil over wet soil.

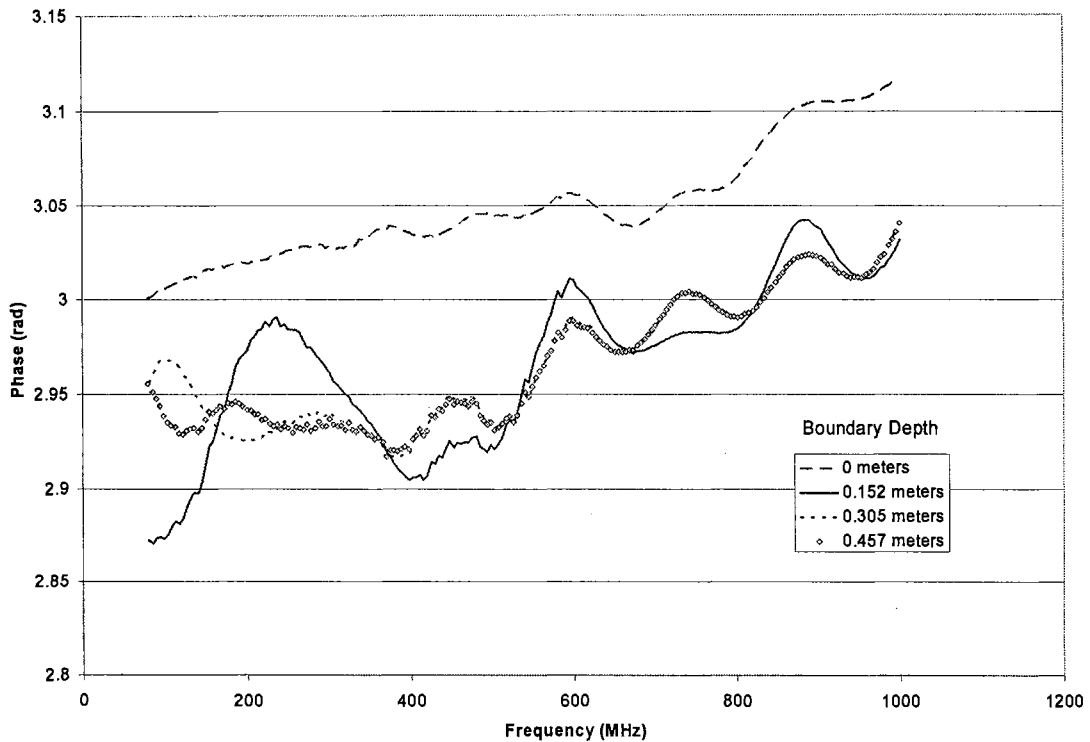


Figure 35. Phase of simulated reflection from two-layer (dry over wet) profiles with several boundary depths

The phase of the reflection coefficients also contain systematic error (ripples) originating from the coaxial cell measurements. Interference patterns were primarily observed in reflection coefficient phase with boundary depths of 0.152 meters and 0.305 meters.

Interference patterns also existed in the simulated reflection coefficients from the profiles in which the 30% moisture layer was on top of the 15% moisture layer. Figures 36 and 37 display the magnitudes and phases of the reflection coefficients from several profiles with wet soil above dry soil.

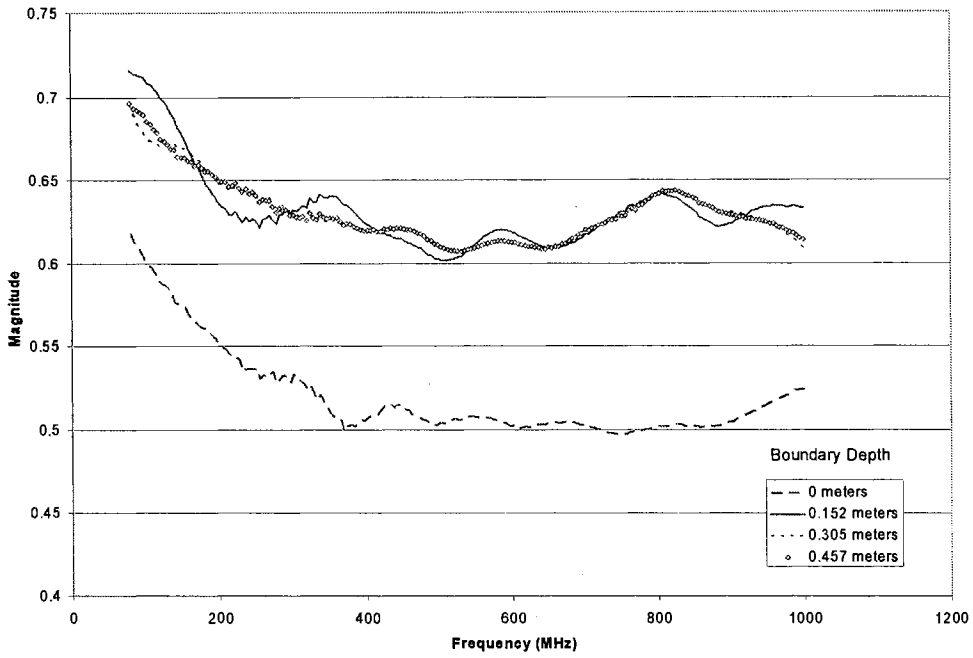


Figure 36. Magnitude of simulated reflection from two-layer (wet over dry) profiles with several boundary depths

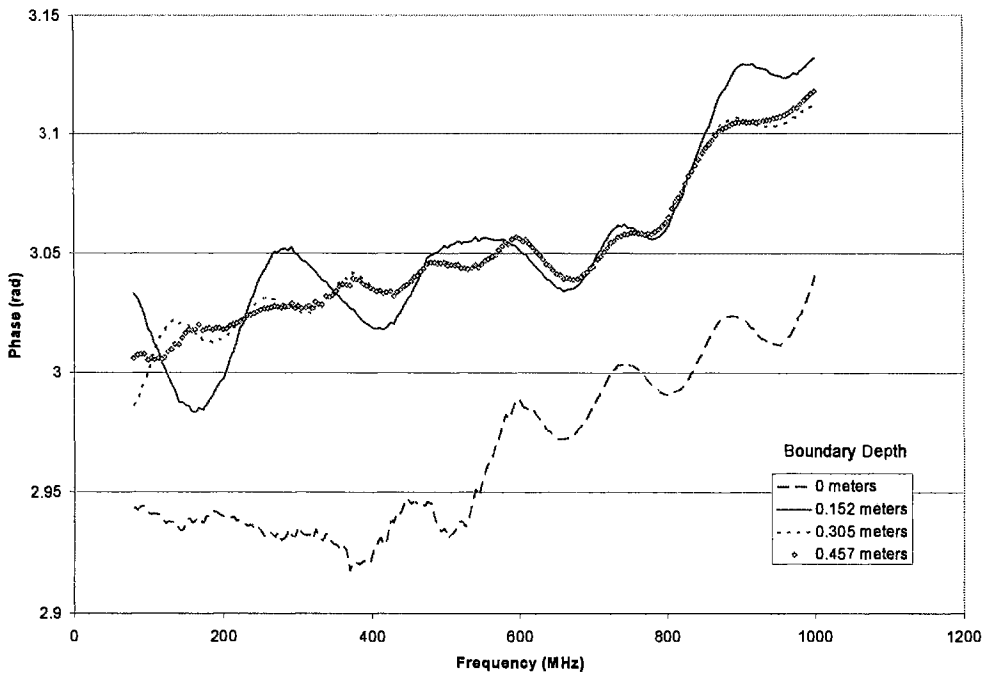


Figure 37. Phase of simulated reflection from two-layer (wet over dry) profiles with several boundary depths

The plots of magnitude and phase from Figures 36 and 37 contain ripples from systematic error in the coaxial cell measurements. Interference patterns also exist in the reflections with boundary depths of 0.152 meters and 0.305 meters.

Reflection coefficients from the two-layer moisture profiles with dry soil over wet soil were compared with an analysis of variance within the frequency ranges of 80 to 98 MHz and 784 to 802 MHz. Tukey’s procedure was used to conduct individual pair-wise comparisons between average reflection coefficient magnitudes and phases between the profiles. The objective of the test was to discover which frequency ranges could detect moisture changes at depth. Figure 38 contains line diagrams that display the results of the test.

Category	Boundary Depths (cm)									
84.6 MHz Magnitude	30.48	15.24	76.2	60.96	121.92	152.4	182.88	91.44	45.72	0
84.6 MHz Phase	15.24	60.96	152.4	182.88	121.92	91.44	76.2	45.72	30.48	0
793 MHz Magnitude	15.24	152.4	121.92	91.44	76.2	60.96	182.88	45.72	30.48	0
793 MHz Phase	15.24	152.4	121.92	91.44	76.2	60.96	45.72	182.88	30.48	0

Figure 38. Line diagrams of Tukey’s comparisons of simulated profiles with dry soil on top of wet soil

The line diagrams in Figure 38 list the profile boundary depths from left to right representing lowest average magnitude or phase to highest average magnitude or phase. The lines under the profile boundary depths connect the profiles that lacked significant differences between magnitudes or phases.

The line diagrams in Figure 38 indicate that frequencies near 84.6 MHz could detect differences in the reflection coefficient between boundary depths of 0, 15.2, 30.5, and 45.7 cm. Reflections from profiles with boundary depths below 45.7 cm were not significantly different than reflections from the profile with a boundary depth at 45.7 cm. Frequencies near 793 MHz could detect differences in reflection coefficients between 0, 15.2, and 30.5 cm boundary depths. Reflections from profiles with boundary depths below 30.5 cm could not be distinguished.

Tukey’s procedure was also used to analyze simulated reflection magnitudes and phases from the two layer profiles in which soil with 30% volumetric moisture was on top of soil with 15% volumetric moisture. Figure 39 displays the line diagrams resulting from the test.

Category		Boundary Depths (cm)									
84.6 MHz Magnitude	0	30.48	76.2	60.96	91.44	121.92	182.88	152.4	45.72	15.24	
84.6 MHz Phase	0	30.48	60.96	91.44	182.88	121.92	152.4	76.2	45.72	15.24	
793 MHz Magnitude	0	182.88	121.92	91.44	76.2	60.96	45.72	152.4	30.48	15.24	
793 MHz Phase	0	15.24	30.48	121.92	76.2	60.96	45.72	91.44	182.88	152.4	

Figure 39. Line diagrams of Tukey’s comparisons of simulated profiles with wet soil on top of dry soil

The line diagrams indicated that reflections of frequencies near 84.6 MHz, resulting from profiles with boundary depths of 0, 15.2, 30.5, and 45.7 cm, were significantly different. Reflections from profiles with boundary depths below 45.7 cm could not be

distinguished. Reflections from frequencies near 793 MHz were significantly different only in the profile with the dry soil boundary at the surface. When a layer with 30% moisture existed on the surface, the dry soil underneath could not be detected by frequencies near 793 MHz.

Profiles Acquired via Neutron Probe Measurements

In addition to the calculation of reflection coefficients from hypothetical profiles, the MATLAB simulation was used to predict reflection coefficients from the moisture profiles that existed in the field trials. Neutron probe measurements were collected at 15.2-cm increments to depths of 1.98 meters in each of four access tubes in each plot. The neutron counts were used to calculate volumetric moisture at each depth around each access hole. The four moisture profiles within each plot were averaged to calculate the plot volumetric moisture at each depth.

Selected moisture profiles were used with the coaxial cell dielectric property results to calculate profiles of dielectric layers. The layers were inputs to the MATLAB program that simulated radio wave reflection coefficients. Analysis of simulated reflection coefficients is presented in the next chapter along with the analysis of reflection coefficients measured in the field trials.

CHAPTER VIII

FIELD MEASUREMENTS

Procedure

Measurements of radio wave reflection coefficients from soil with various moisture profiles were collected with the network analyzer/antenna apparatus. Prior to each instance of soil reflection coefficient measurement, the wooden structure was centered directly over the plot. The apparatus was always placed so that the antennas were in an east-west plane. The instrument was calibrated immediately before each scheduled data collection to avoid drift errors from instrument temperature changes, antenna height changes, and other environmental characteristics that could have affected the measurements. The antennas were aimed at the sky, the metal sheets were placed on the plot, and reflection and transmission measurements were recorded. The antennas were then turned downward, and reflection and transmission measurements were recorded. After the calibration data were collected, the steel sheets were removed from the plot and reflection and transmission measurements of the soil were made.

The reflection coefficient of the ground was measured at each selected frequency with two different methods. The first method implemented transmission and reception of the EM waves with the antenna that was connected to port 1 of the network analyzer. The second method implemented transmission with the antenna connected to port 1 and detection with antenna connected to port 2. In each case, the magnitude and phase of the transmitted and received waves were used to calculate the reflection coefficient of the

ground. Systematic errors of the reflection coefficients resulting from network analyzer reflection measurements were found to be quite large. Thus, the analysis of measured soil reflection coefficients presented in this chapter resulted entirely from network analyzer transmission measurements.

Neutron probe measurements were collected at 15.2-cm increments to depths of 1.98 meters in each of four access tubes in each plot. A standard neutron count was made on the slow data collection speed at the beginning of each use of the neutron probe. Counts at each soil depth were made with the instrument set on the fast data collection speed. The neutron counts were used to calculate volumetric moisture at each depth around each access hole. Moistures at each depth were averaged to yield quantities of volumetric moisture per 15.2 cm depth.

Moisture profiles in the plots were artificially created using irrigation and tarps. Preparation of the four 3.2 meter x 3.2 meter x 2 meter test plots included covering with 6 meter x 9.1 meter tarps to prevent rain from adding unwanted moisture to the plot. The tarps also sterilized the surface so that no vegetation grew on the plot. The irrigation system consisted of 3.18-cm (1.25-inch) thin wall PVC tubes with garden sprinklers attached in the configuration shown in Figure 40.

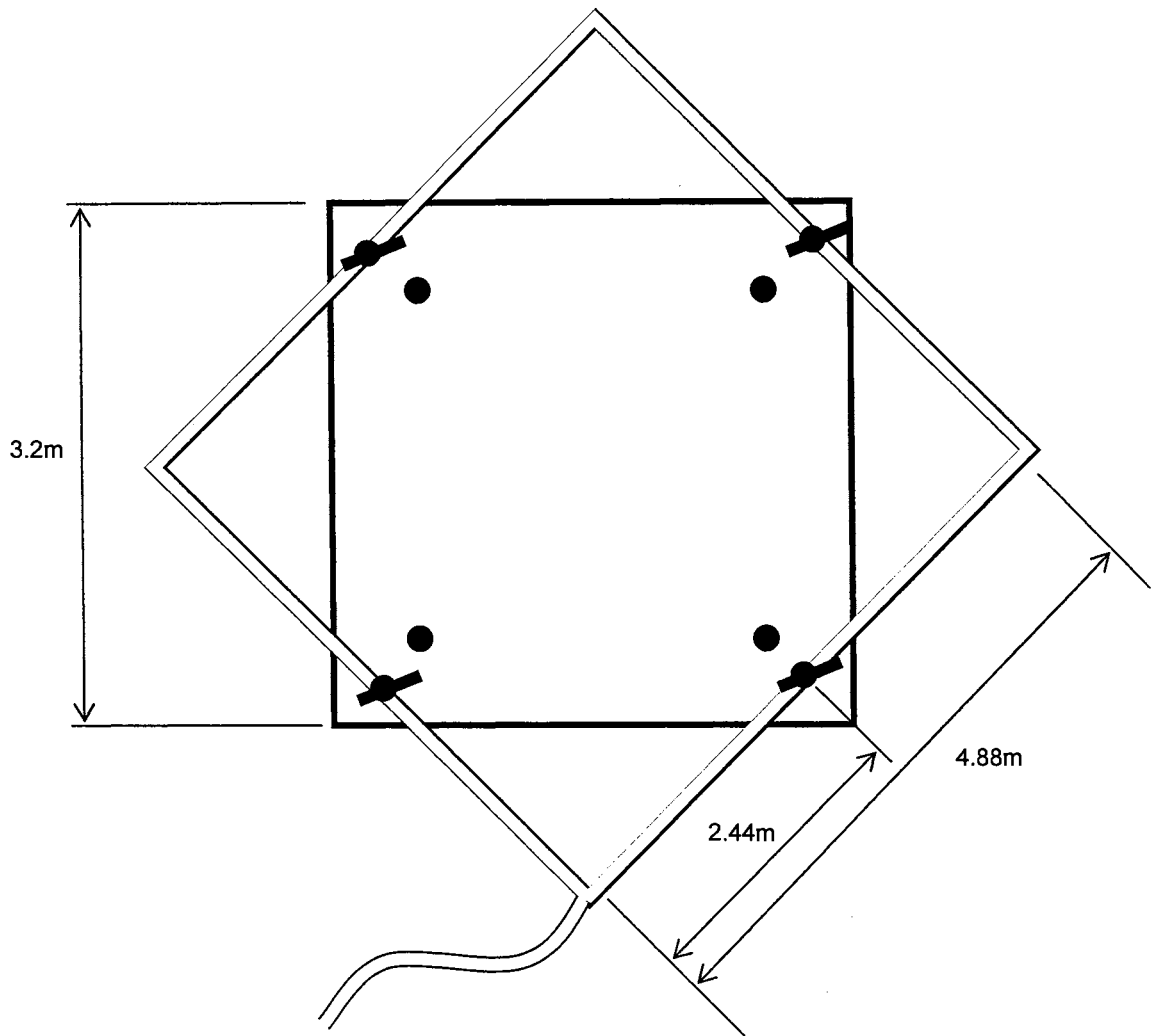


Figure 40. Geometry of irrigation sprinkler system

Each of the 4 sprinklers contained nozzles that applied water at a rate of 7.19 liters per minute within a diameter of 6 meters at an operating pressure of 172 kPa (25 psi.). Four rain gages were placed in the plot to verify the uniformity of the application rate. The application rate of the system exceeded the infiltration rate of the soil. The system was turned off periodically to allow infiltration to occur.

Upon completion of neutron counts and reflection coefficient measurements on each dry plot, irrigation added 3.8 cm of water to the plot's surface. Neutron counts and reflection coefficients were measured shortly after irrigation. Five additional centimeters

of water were added to the plot and allowed to sit for several hours before data collection. Finally, twelve additional centimeters were added and redistribution was allowed to occur prior to measurement. Although identical irrigation cycles were executed on the four plots, the moisture profiles that resulted were different.

Field Trial Measurement Results

Eight moisture profiles were selected from the field trials for analysis. Table 17 and Figures 41 and 42 display the average moisture at each depth for the eight profiles selected.

Table 17. Average soil moisture at each depth for eight selected profiles as measured by the neutron probe

Depth (meters)	Volumetric Moisture Content							
	Profile 1	Profile 2	Profile 3	Profile 4	Profile 5	Profile 6	Profile 7	Profile 8
-0.152	0.206	0.178	0.233	0.302	0.274	0.328	0.286	0.307
-0.305	0.249	0.226	0.273	0.303	0.297	0.338	0.293	0.316
-0.457	0.240	0.206	0.259	0.318	0.251	0.285	0.231	0.328
-0.610	0.246	0.239	0.270	0.287	0.265	0.293	0.283	0.326
-0.762	0.282	0.305	0.291	0.325	0.327	0.311	0.320	0.303
-0.914	0.311	0.336	0.298	0.305	0.342	0.319	0.335	0.326
-1.067	0.321	0.343	0.299	0.307	0.348	0.316	0.336	0.302
-1.219	0.291	0.309	0.303	0.299	0.303	0.301	0.321	0.326
-1.372	0.304	0.321	0.327	0.321	0.323	0.308	0.319	0.323
-1.524	0.312	0.337	0.320	0.319	0.335	0.311	0.346	0.330
-1.676	0.322	0.339	0.336	0.316	0.337	0.308	0.344	0.332
-1.829	0.318	0.338	0.330	0.305	0.333	0.310	0.335	0.320
-1.981	0.298	0.335	0.323	0.313	0.326	0.289	0.330	0.309
-2.134	0.278	0.342	0.320	0.312	0.337	0.278	0.338	0.314

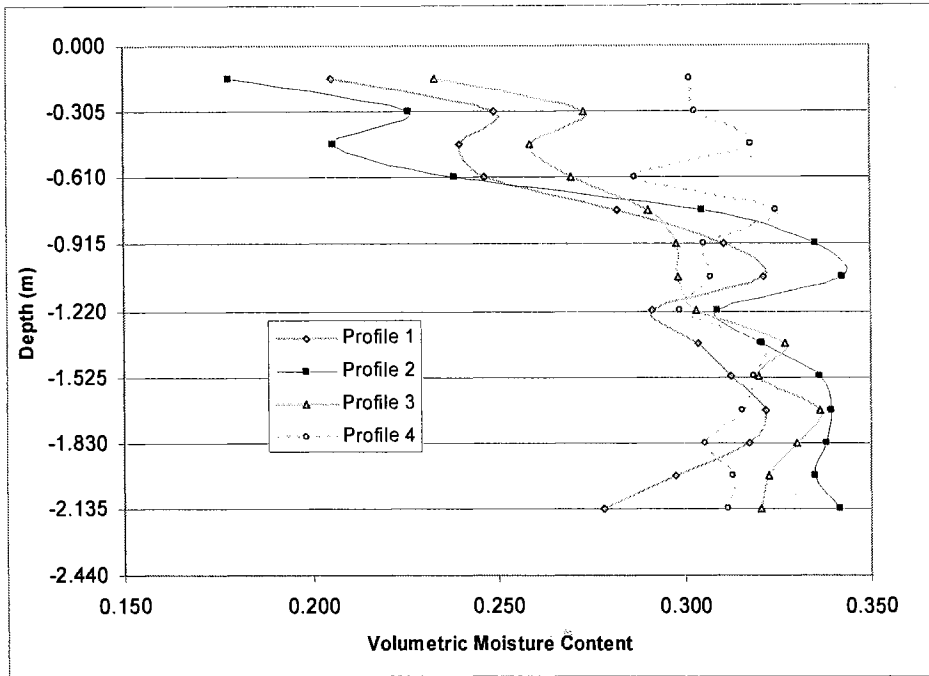


Figure 41. Average absolute volumetric moisture at depth (Profiles 1-4 measured with the neutron probe)

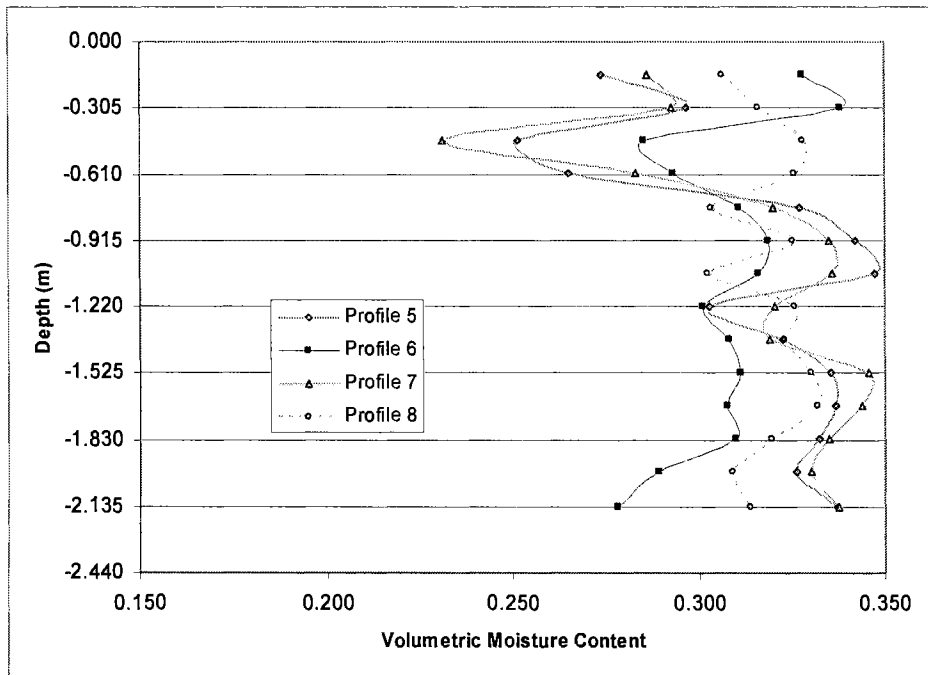


Figure 42. Average absolute volumetric moisture at depth (Profiles 5-8 measured with the neutron probe)

The average moisture profiles calculated from the neutron probe measurements were used to determine the dielectric profiles of the soil. Given the layered dielectric profiles, reflection coefficients were simulated in a MATLAB program. Figure 43 shows the simulated reflection coefficient from moisture profile number 2.

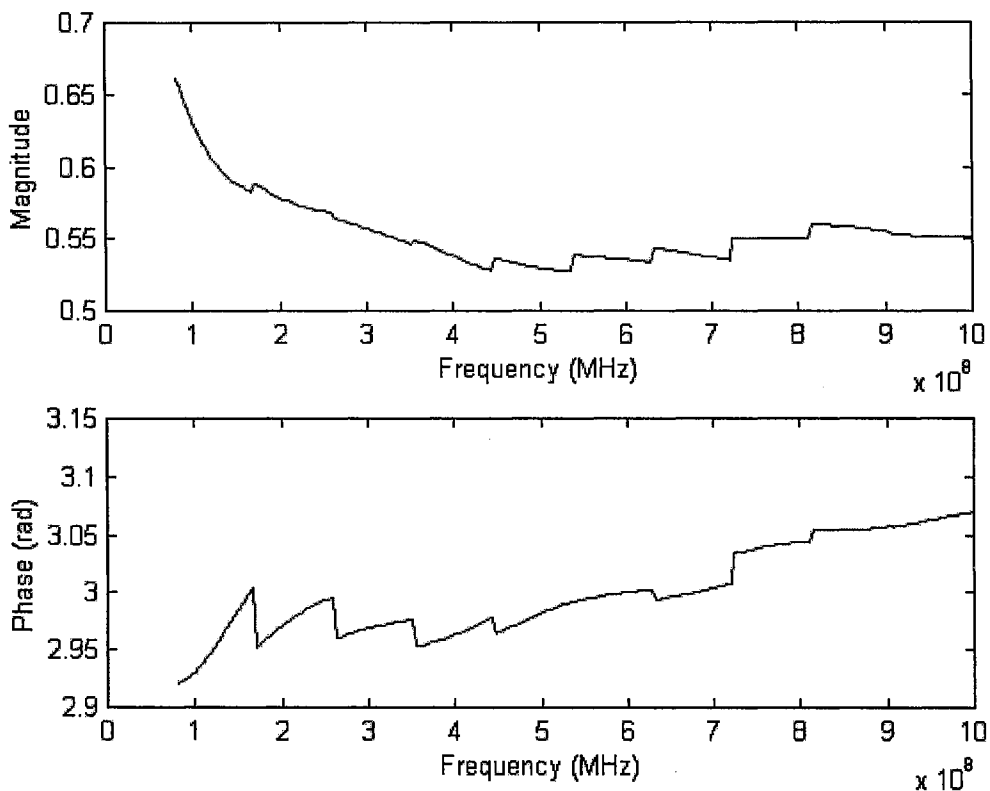


Figure 43. MATLAB simulated reflection coefficient of moisture profile number 2

The magnitude of the simulated reflection coefficient was greater at lower frequencies. Most of this effect can be attributed simply to the dielectric characteristics of the topsoil with volumetric moisture at 17.8%. However, a small amount of the effect is likely due to moisture beneath the surface, which would have a greater impact on magnitudes of the lower frequencies. The discontinuities were simply an artifact of the model resulting

from boundaries between the frequency ranges used to relate moisture to dielectric properties.

Figure 44 shows the reflection coefficient resulting from transmission measurements of the network analyzer on moisture profile number 2.

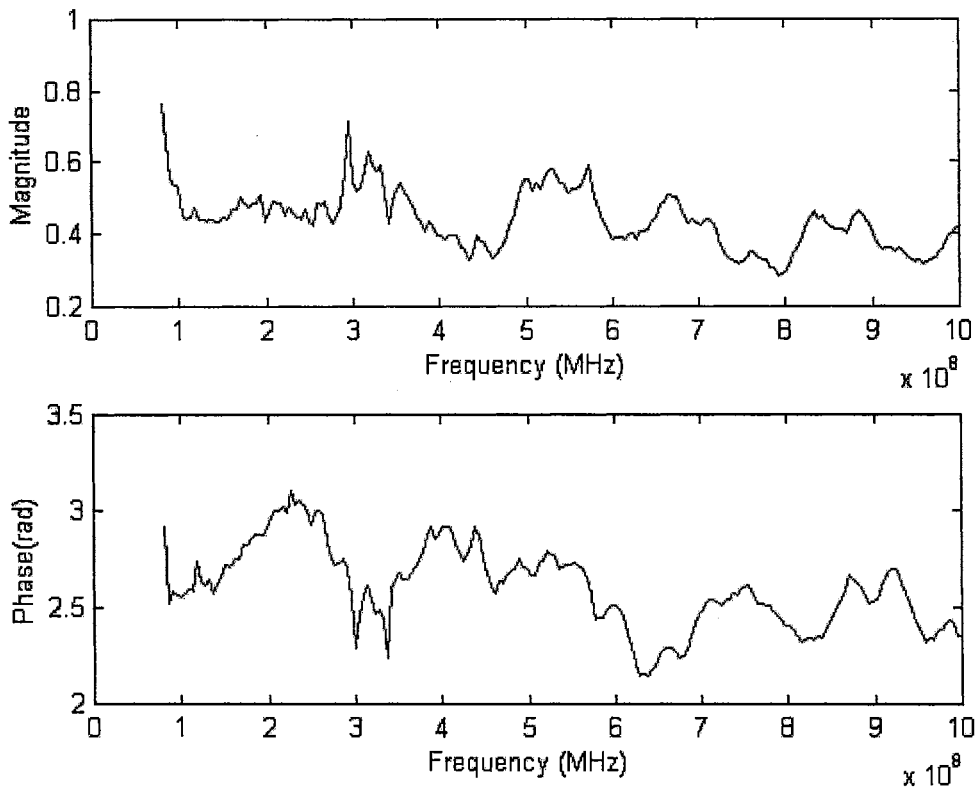


Figure 44. Measured soil reflection coefficient of moisture profile number 2

The average magnitude and phase of the measured reflection coefficient shown in Figure 44 appear substantially lower than the values from the simulated reflection coefficient (see Figure 43). The difference in magnitude could result from slightly different surface moisture in the center of the plot than the moistures measured with the neutron probe in the corners of the plot. However, the difference in phase cannot be explained simply by an error in the moisture measurement. The shift indicates systematic

error from the field apparatus measurement of reflection coefficients, the coaxial cell measurement of soil dielectric properties, or the assumption of soil homogeneity horizontally within the plot.

The ripples in the measured reflection (Figure 44) could partially result from systematic error of the antenna detection as witnessed in the calibration check (see Figure 24). In addition, profile number 2 had large changes in volumetric moisture content in the top 30.5 cm of soil. The reflection interference patterns from boundaries between layers of different moistures could add to the ripples resulting from systematic error.

Comparisons of Reflection Coefficients

A comparison of the magnitudes of the two methods was conducted with a two factor analysis of variance. The ANOVA was modeled in which the profile number (1 through 8) and calculation method (simulation or field measurement) were the factors and the 201 individual frequencies were the replications. The resulting ANOVA data is shown in Table 18.

Table 18. ANOVA of simulated reflection magnitude from field profile measurements

Source	df	SS	MS	F	p
Method	1	1.73	1.73	794	< 0.0001
Profile	7	7.28	1.04	476	< 0.0001
Method*Profile	7	1.94	0.28	127	< 0.0001
Error	3200	6.99	0.0022		
Total	3215	17.94			

The test revealed that the profile and the calculation method interacted to affect the magnitude of the reflection coefficient. Tukey's procedure was used to compare the

average profile reflection magnitudes within each calculation method (simulation of field measurement) and within two frequency ranges, 80 to 98 MHz and 784 to 802 MHz. Figure 45 displays the results of the Tukey's procedures in the form of line diagrams.

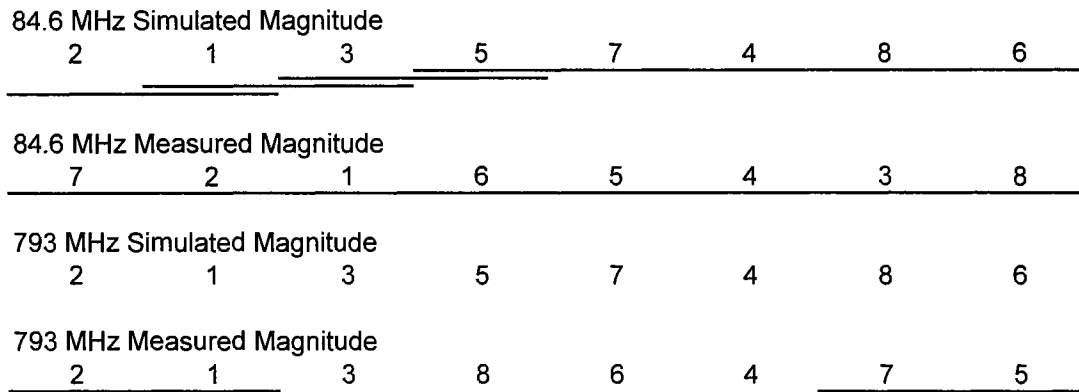


Figure 45. Line diagrams of Tukey's comparisons of reflection magnitude (field trials)

The line diagrams in Figure 45 list, from left to right, the profile numbers from lowest reflection coefficient magnitude to highest reflection coefficient magnitude. The lines connecting the profile numbers indicate differences too small to be considered significant.

Within the frequency range of 80 to 98 MHz, the simulated magnitude had few significant differences between profiles, and the measured magnitude had no significant differences between profiles. Within the frequency range of 784 to 802 MHz, all simulated magnitudes were different between profiles, and many significant differences of measured reflection coefficient magnitudes existed between profiles.

The phase of the reflection coefficient was compared in a manner similar to the magnitude. The ANOVA test (Table 19) showed significant interaction between all of the factors.

Table 19. ANOVA of simulated reflection phase from field profile measurements

Source	df	SS	MS	F	p
Method	1	54.61	54.61	3619	< 0.0001
Profile	7	35.62	5.09	337	< 0.0001
Method*Profile	7	26.3	3.76	249	< 0.0001
Error	3200	48.28	0.015		
Total	3215	164.82			

Tukey’s procedure was used to make comparisons to find significant differences in average reflection phases between the profiles within the two frequency ranges: 80 to 98 MHz and 784 to 802 MHz. Figure 46 displays the resulting line diagrams.

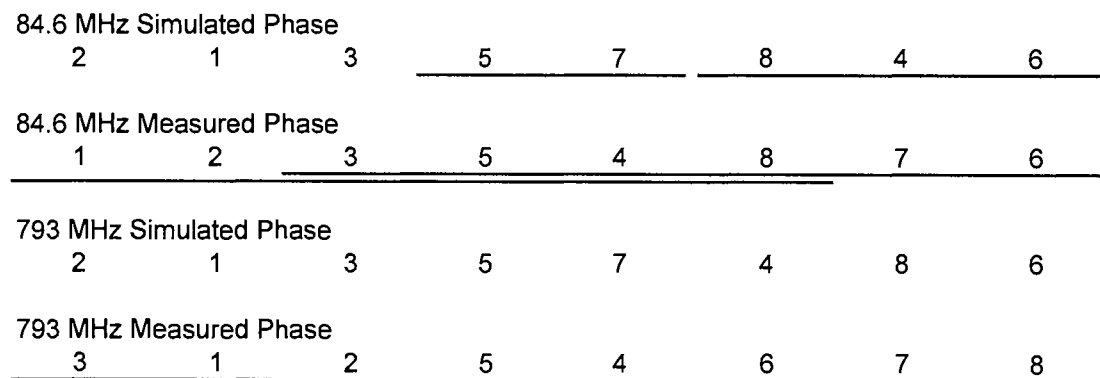


Figure 46. Line diagrams of Tukey’s comparisons of reflection phase (field trials)

Within the frequency range of 80 to 98 MHz, the simulated phases had significant differences between profiles 2, 1, and 3. Profiles 5 and 7 were not significantly different, nor were 8, 4, and 6. The measured phases had few significant differences between profiles; profiles 1 and 2 were significantly different than profiles 6 and 7. Within the frequency range of 784 to 802 MHz, all simulated phases were different between profiles, and nearly all measured reflection phases were significantly different between profiles.

The results in the line diagrams indicate that the higher frequency range, near 793 MHz, was more sensitive to the differences in surface moisture than the lower frequencies near 84.6 MHz. In addition, the lack of sensitivity of the lower frequencies may be attributed to the similar subsoil moisture in all of the profiles.

Correlation of Reflection Coefficients to Moisture

The magnitudes of the simulated reflection coefficients were averaged over the entire frequency range of 80 MHz to 1 GHz and the mean was correlated to volumetric moisture in the surface layer of soil. The magnitudes of the measured reflection coefficients were also averaged over the frequency range and were correlated to moisture in the surface layer. Table 20 lists the values of volumetric moisture in the surface layer and the reflection coefficient magnitude averages. Figure 47 displays the magnitude averages as functions of moisture. Equations with simple correlation coefficients are also displayed.

Table 20. Volumetric moisture content vs. average reflection magnitudes

Average Magnitude of Reflection Coefficient			
Profile	VMC in top 15.2 cm of soil	Simulated Reflection	Measured Reflection
1	0.21	0.57	0.46
2	0.18	0.55	0.44
3	0.23	0.59	0.50
4	0.30	0.62	0.62
5	0.27	0.61	0.63
6	0.33	0.63	0.60
7	0.29	0.61	0.60
8	0.31	0.62	0.59

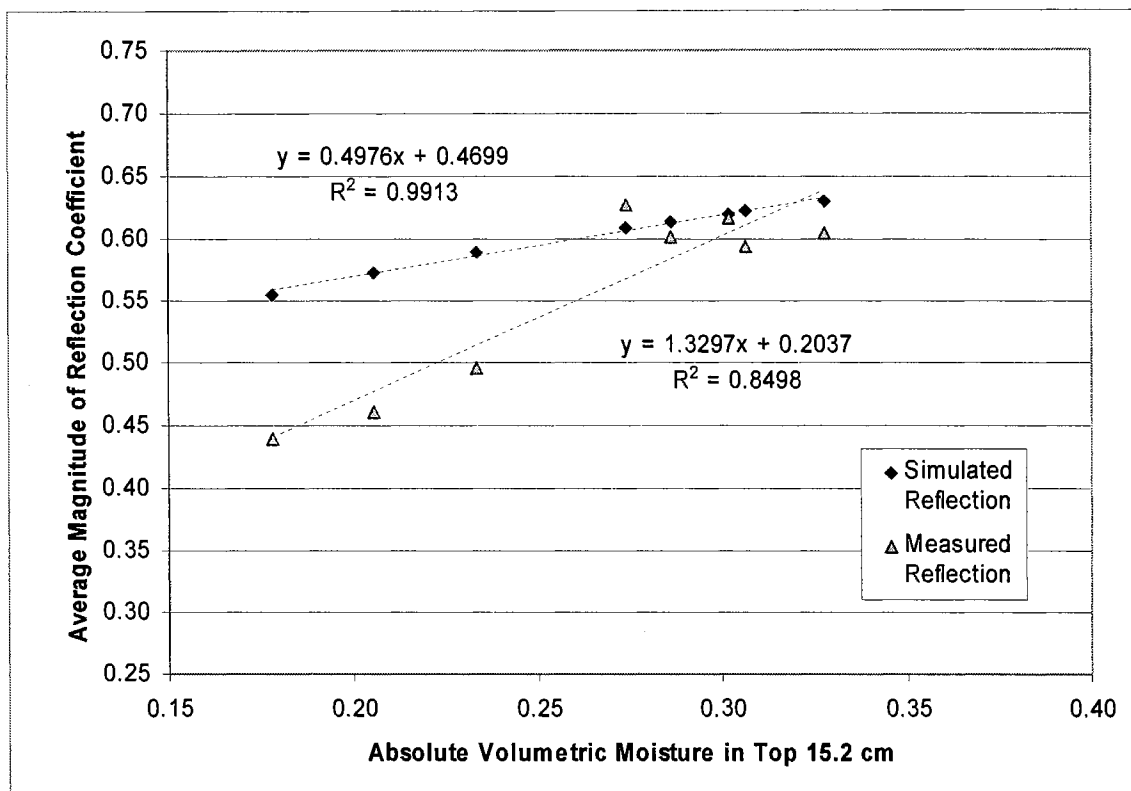


Figure 47. Volumetric moisture content vs. average reflection magnitudes

As Figure 47 indicates, the simple correlation coefficients relating volumetric moisture to average reflection magnitudes are 0.991 for the simulated reflection and 0.850 for the measured reflection. Although the simulated and measured magnitudes are different, the results indicate that average reflection coefficient magnitude within a frequency range of 80 MHz to 1 GHz gives a good indication of surface moisture in the top 15 cm, regardless of the method of calculation.

The phases of the simulated and measured reflection coefficients were also averaged over the frequency range and were correlated to moisture in the surface layer. Table 21 lists the values of volumetric moisture in the surface layer and the reflection

coefficient phase averages. Figure 48 displays the phase averages as functions of moisture. Equations with simple correlation coefficients are also displayed

Table 21. Volumetric moisture content vs. average reflection phase

Average Phase of Reflection Coefficient			
Profile	VMC in top 15.2 cm of soil	Simulated Reflection	Measured Reflection
1	0.21	3.01	2.51
2	0.18	3.00	2.60
3	0.23	3.03	2.50
4	0.30	3.05	2.84
5	0.27	3.04	2.83
6	0.33	3.06	2.92
7	0.29	3.04	3.03
8	0.31	3.05	2.96

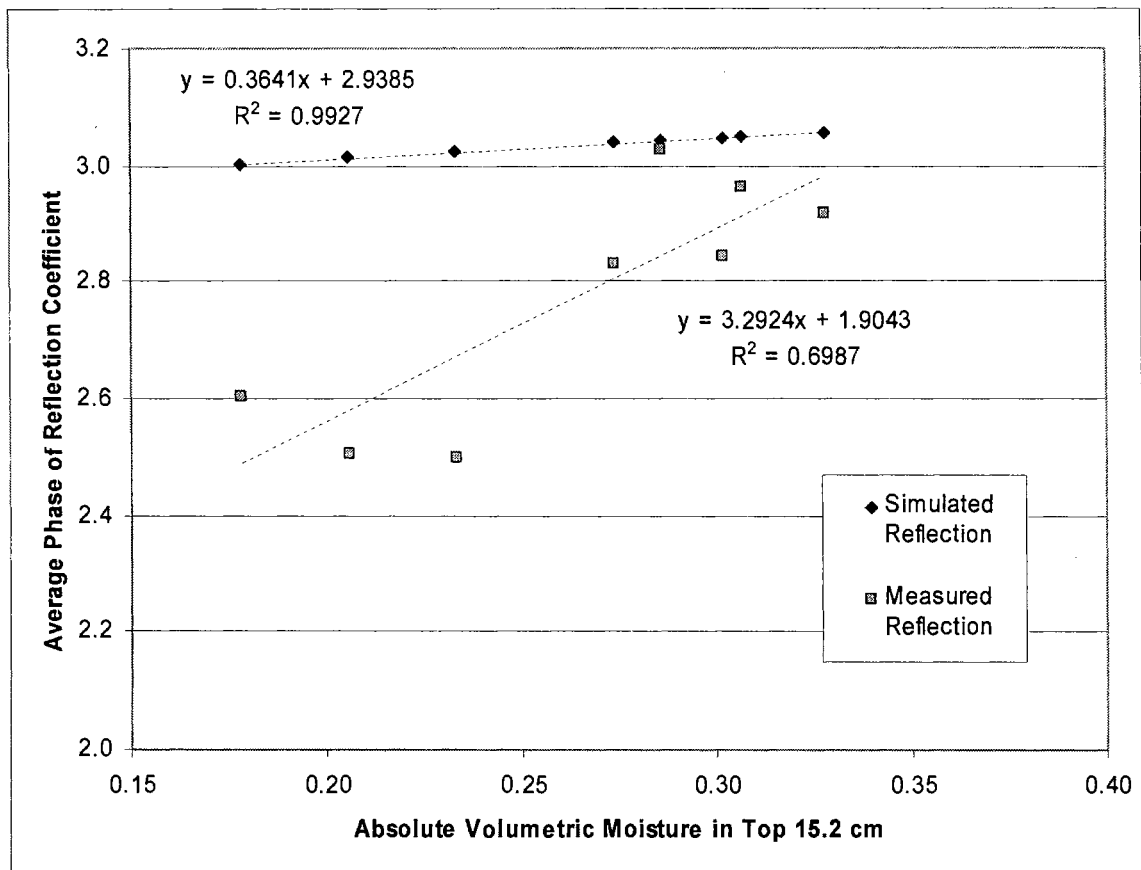


Figure 48. Volumetric moisture content vs. average reflection phases

The correlation coefficients of 0.992 and 0.699 relating volumetric moisture in the surface layer to the respective simulated and measured reflection coefficient phases indicate that average phase can also be used to predict moisture.

Simulated and measured reflection coefficients at specific frequencies (84.6 MHz and 793 MHz) were also correlated to the moisture that existed in the top 15.2 cm of soil. Table 22 and Figure 49 display the magnitudes of the reflection coefficients at the specific frequencies as they relate to surface moisture.

Table 22. Volumetric moisture content vs. reflection magnitude at specific frequencies

Magnitude of Reflection Coefficient (single frequencies)					
Profile	VMC in top 15.2 cm of soil	Simulated		Measured	
		84.6 MHz	793 MHz	84.6 MHz	793 MHz
1	0.21	0.67	0.57	0.63	0.30
2	0.18	0.65	0.55	0.66	0.29
3	0.23	0.68	0.59	0.67	0.40
4	0.30	0.70	0.62	0.65	0.60
5	0.27	0.69	0.61	0.65	0.64
6	0.33	0.70	0.63	0.63	0.54
7	0.29	0.69	0.61	0.64	0.63
8	0.31	0.70	0.62	0.66	0.50

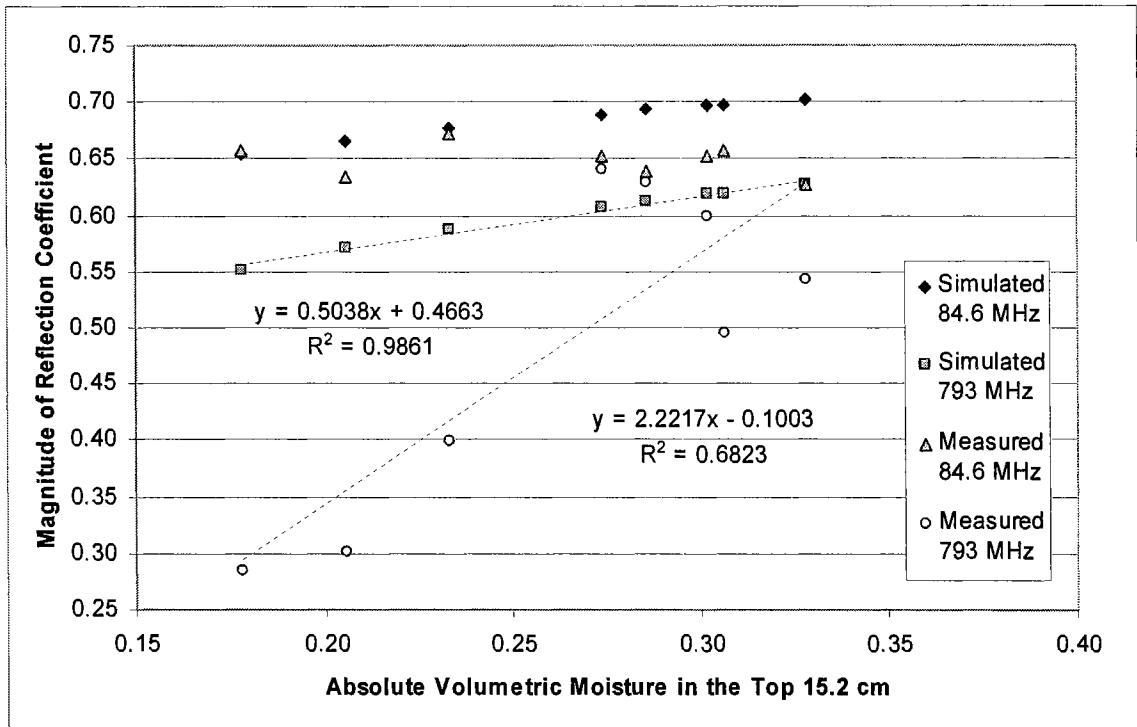


Figure 49. Volumetric moisture content vs. reflection magnitude at specific frequencies

The relationships in Figure 49 indicate that the reflection coefficient magnitudes of the higher frequencies, both simulated and measured, were more sensitive to moisture than the lower frequencies as indicated by the slopes of the trends. These conclusions agree with the line diagram conclusions from the Tukey's statistical procedures.

Table 23 and Figure 50 display the phases of the reflection coefficients at the specific frequencies as they relate to moisture.

Table 23. Volumetric moisture content vs. reflection phase at specific frequencies

Phase of Reflection Coefficient (single frequencies)					
Profile	VMC in top 15.2 cm of soil	Simulated		Measured	
		84.6 MHz	793 MHz	84.6 MHz	793 MHz
1	0.21	2.94	3.05	2.62	2.29
2	0.18	2.92	3.04	2.52	2.43
3	0.23	2.95	3.05	2.67	2.23
4	0.30	2.99	3.08	2.80	2.81
5	0.27	2.97	3.07	2.85	2.75
6	0.33	2.99	3.09	2.86	2.92
7	0.29	2.98	3.07	2.83	2.98
8	0.31	2.99	3.08	2.87	3.02

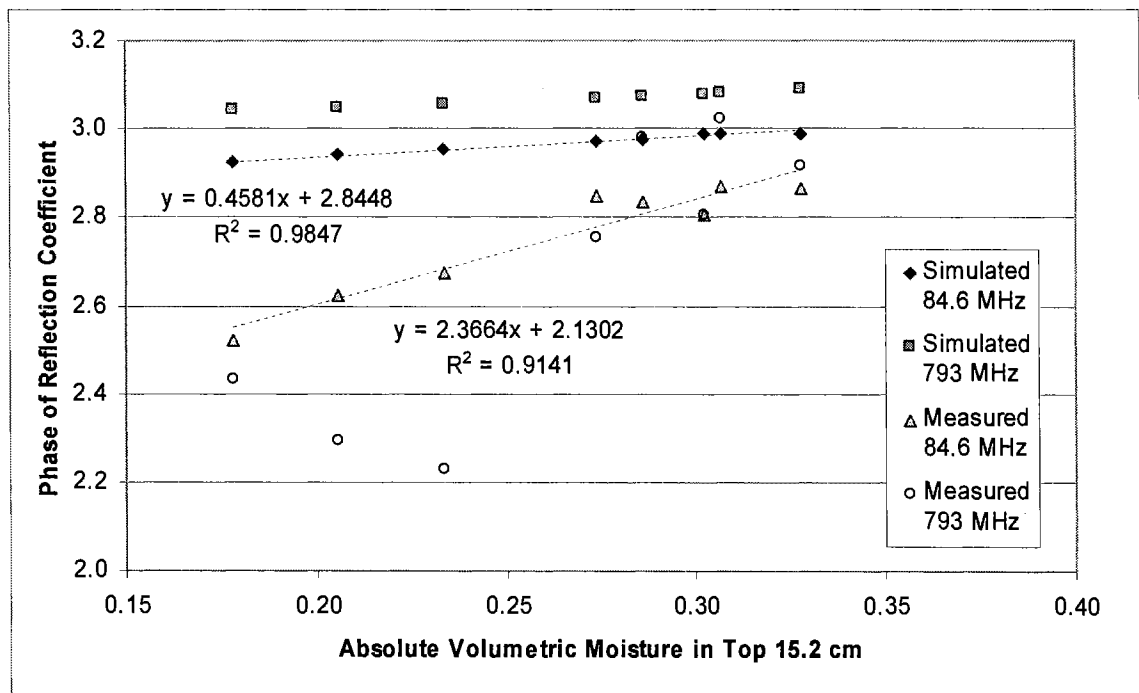


Figure 50. Volumetric moisture content vs. reflection phase at specific frequencies

The measured reflection coefficient phase of the lower frequency (84.6 MHz) exhibited a very high correlation coefficient (0.914) to moisture in the surface layer. This correlation

indicates a very promising method for the detection of surface moisture in a very simple way.

CHAPTER IX

PROFILE RESTORATION ALGORITHM

Procedure

The calculation of the reflection coefficients at the soil surface using known dielectric profiles was relatively simple. The opposite problem was not as straightforward. However, utilizing the assumptions that the soil caused random scattering of radio waves and the moisture content didn't change suddenly with depth, a simplified moisture profile was estimated. The magnitude and phase of each reflection estimated moisture and the skin depth of each frequency limited the depth of measurement. The profile restoration algorithm followed six basic steps.

1. The reflection coefficient of the surface layer (approx 30 cm) was measured using the highest frequency (1GHz). The skin depth of 1 GHz was estimated at 30 cm in wet soil and 60 cm in dry soil. A wave reflected below the skin depth would travel through the surface layer twice attenuating the signal to less than 13.5% of its original intensity. Thus, a moisture gradient reflection below the skin depth of the wave would exhibit little interference with the reflection from the air-soil interface.
2. The measured reflection coefficient was used to calculate the dielectric properties of soil in the surface layer. This step involved the calculation of the intrinsic impedance of the top layer:

$$Z_1 = Z_0 \frac{1 + \Gamma_{0,1}}{1 - \Gamma_{0,1}} \quad (58)$$

where Z_0 was the impedance of air, and $\Gamma_{0,1}$ was the forward reflection coefficient of the soil at the highest frequency. The dielectric properties were calculated using an initial guess of permittivity and conductivity values of soil at 20% volumetric moisture content. The values were used to calculate a predicted intrinsic impedance of the top layer:

$$Z_1' = \sqrt{\frac{j\omega\mu}{\sigma_1 + j\omega\epsilon_1}} \quad (59)$$

The distance of the predicted impedance from the measured impedance was found using:

$$dist = \sqrt{(real(Z_1') - real(Z_1))^2 + (imag(Z_1') - imag(Z_1))^2} \quad (60)$$

Small increments were added to and subtracted from the permittivity and conductivity values and respective impedance values were calculated in a fashion similar to the calibration method of the coaxial cell. The permittivity and conductivity values that resulted in the smallest distance from the measured impedance were selected as the new guess. The iteration was repeated until the predicted intrinsic impedance of the top layer converged to the measured value. Once calculated, the permittivity was related to moisture content using the relationships obtained from the coaxial cell measurements, and the permittivity and conductivity were used to calculate the propagation constant that attenuated reflections from lower layers.

3. The reflection coefficient was measured using the second highest frequency.

4. The air-soil surface reflection of the second frequency was estimated using the moisture content of the top layer. The volumetric moisture was used to calculate permittivity and conductivity at the second frequency using the equations acquired from the coaxial cell measurements. The dielectric values were used to calculate the surface layer's contribution to the total reflection coefficient. The dielectric values were also used to calculate the attenuation through the top layer. The contribution of the surface reflection was subtracted from the total measured reflection of the second frequency to yield the reflection from the first sub-surface interface attenuated by propagation through the top layer.

$$\Gamma_{1,2}e^{-2\gamma_1d_1} = \frac{\Gamma_s}{\tau_{0,1}\tau_{1,0}} - \Gamma_{0,1} \quad (61)$$

where $\Gamma_{1,2}$ was the forward reflection coefficient of the first subsurface boundary, γ_1 was the propagation constant of the top layer, d_1 was the thickness of the top layer, Γ_s was the total reflection coefficient of the soil, $\tau_{0,1}$ was the forward transmission coefficient of the surface boundary, and $\tau_{1,0}$ was the reverse transmission coefficient of the surface boundary.

5. The reflection from the sub-surface layer ($\Gamma_{1,2}$) was then used to calculate the dielectric properties of the second layer using the impedance calculation and the iterative algorithm. Knowledge of the dielectric properties yielded the moisture content of the second layer and the propagation constant that affected the lower frequencies.
6. Repeated steps 3, 4, and 5 for all subsequent layers.

Two primary layers were predicted: the top 30.5 cm and the next 30.5 cm. The frequencies used were 793 MHz and 84.6 MHz. The algorithm was used to test the simulated constant moisture reflections, the simulated two layer profile reflections, the simulated profile reflections based on neutron probe measurements from the field, and the measured reflections from the network analyzer/antenna instrument.

The error analyses of the profile restoration algorithm's predictions of moisture for the hypothetical moisture profiles involved comparisons of each predicted profile to the analytical volumetric moisture content in the in the top two 30.5-cm layers. Error analyses of the algorithm's predictions of the profiles that existed in the field were evaluated with moisture averages calculated from moistures in the four neutron probe access tubes. Average neutron probe measurements of moisture were compared to the restoration algorithm's predictions of moisture from simulated reflection coefficients and measured reflection coefficients.

Results of Profile Restoration Algorithm

The simulated reflection coefficients of the hypothetical moisture profiles were used to test the profile restoration algorithm. The same equations that were used in the simulation relating moisture to dielectric properties and relating dielectric properties to reflection coefficients were also used in the restoration algorithm. The primary differences between the forward problem, and the reverse problem were that in the reverse problem, the skin depth of the high frequency was assumed to limit the effects of subsurface boundaries and the non-linear equations relating dielectric properties to impedance required an iterative solution.

The simulated reflection coefficients from profiles of constant moisture were tested. Predicted and actual moisture values from the simulated constant profiles are shown in Table 24.

Table 24. Algorithm predicted moisture from simulated reflections of profiles with constant moisture

	Profiles of Constant Moisture		
	Actual	Predicted	
	Moisture	Moisture	
	Content (%)	Content (%)	Difference
Top 30.5 cm:	0.00	4.21	4.21
	5.00	6.44	1.44
	10.00	8.48	-1.52
	15.00	11.98	-3.02
	20.00	15.20	-4.80
	25.00	28.38	3.38
	30.00	34.06	4.06
	35.00	37.28	2.28
	40.00	41.62	1.62
Next 30.5 cm:	0.00	-6.80	-6.80
	5.00	-3.89	-8.89
	10.00	-3.86	-13.86
	15.00	-4.01	-19.01
	20.00	-4.40	-24.40
	25.00	26.71	1.71
	30.00	32.74	2.74
	35.00	35.72	0.72
	40.00	39.79	-0.21

The algorithm approximated moisture in the top layer with an average difference of 2.92% from the actual moisture in the profile. In the next 30.5 cm layer, the algorithm predicted moisture very well when the moisture contents were high, with an average difference of 1.34%. However, on the profiles with lower moisture, the dielectric properties failed to converge in the iterative algorithm. It is believed that small differences in the predicted dielectric properties of the top layer resulted as calculated lower-layer impedances that did not allow convergence of realistic dielectric properties.

Moisture profiles were also predicted on the simulated models that contained two-layer moisture profiles. The two-layer profiles each contained layers with 15% and 30% volumetric moisture. The two-layer profiles were divided into two groups: one with dry soil on top of wet soil, and one with wet soil on top of dry soil. Within the groups, the depth of the boundary was varied to yield different layering effects in the profile. The predicted and actual moistures of the top 61.0 cm of the two-layer profiles are listed in Table 25.

Table 25. Predicted and actual moisture from simulated reflection of 2-layer moisture profiles

	Depth of Boundary	Profiles of dry soil over wet soil			Profiles of wet soil over dry soil		
		Actual Moisture Content (%)	Predicted Moisture Content (%)	Difference	Actual Moisture Content (%)	Predicted Moisture Content (%)	Difference
Top 30.5 cm:	0.00	30.00	34.06	4.06	15.00	11.98	-3.02
	15.24	22.50	11.35	-11.15	22.50	33.78	11.28
	30.48	15.00	12.02	-2.98	30.00	34.06	4.06
	45.72	15.00	11.98	-3.02	30.00	34.06	4.06
	60.96	15.00	11.98	-3.02	30.00	34.06	4.06
	76.20	15.00	11.98	-3.02	30.00	34.06	4.06
	91.44	15.00	11.98	-3.02	30.00	34.06	4.06
	106.68	15.00	11.98	-3.02	30.00	34.06	4.06
	121.92	15.00	11.98	-3.02	30.00	34.06	4.06
	137.16	15.00	11.98	-3.02	30.00	34.06	4.06
Next 30.5 cm:	0.00	30.00	32.74	2.74	15.00	-4.01	-19.01
	15.24	30.00	10.74	-19.26	15.00	32.87	17.87
	30.48	30.00	-3.37	-33.37	15.00	32.43	17.43
	45.72	22.50	-4.54	-27.04	22.50	33.12	10.62
	60.96	15.00	-3.94	-18.94	30.00	32.60	2.60
	76.20	15.00	-3.92	-18.92	30.00	32.84	2.84
	91.44	15.00	-4.06	-19.06	30.00	32.74	2.74
	106.68	15.00	-3.99	-18.99	30.00	32.74	2.74
	121.92	15.00	-4.02	-19.02	30.00	32.74	2.74
	137.16	15.00	-4.01	-19.01	30.00	32.74	2.74

The prediction of the top layer was quite effective. An average difference of 4.31% volumetric moisture content existed between the predicted moistures and the actual

values. The lower layers were estimated closely in the profiles with wet soil on top of dry soil with deep boundaries. Of the profiles that exhibited dielectric calculations that did not converge, vary large errors including some negative values occurred in predicted volumetric moisture content.

The profiles originating in the field trials were also tested with the algorithm. The moisture that had been measured with the neutron probe in the four access tubes in each plot were averaged for the top two 30.5-cm layers. The average moistures were compared to the restoration algorithm's predictions of moisture from simulated reflection coefficients and measured reflection coefficients. The values of average actual moisture, the standard deviations of actual moisture (from the four tubes), the predicted moisture from simulated radio wave reflections, and the predicted moisture from measured radio wave reflections are displayed in Table 26 and are graphed in Figures 51 and 52.

Table 26. Moisture profiles from simulated and measured reflections from field trials

Moisture Profiles From Field Trials				
Profile	Average	Std Dev	Simulated	Measured
Number	Actual	Actual	Moisture	Moisture
	Moisture (%)	Moisture (%)	Content	Content
1	22.73	0.76	20.92	-1.30
2	20.20	1.15	18.20	-0.52
3	25.33	2.15	23.54	-2.50
4	30.28	1.73	30.39	6.08
5	28.52	0.89	27.46	0.68
6	33.30	2.05	32.97	11.91
7	28.93	2.17	28.73	23.31
8	31.13	4.84	30.78	12.37
1	24.31	1.65	19.53	-52.15
2	22.24	1.82	17.08	8.59
3	26.43	0.79	22.04	-53.72
4	30.26	2.30	-14.06	6.30
5	25.81	2.85	-17.74	1.17
6	28.93	2.96	-3.84	11.41
7	25.70	1.66	-21.02	74.65
8	32.68	5.10	-13.77	11.53

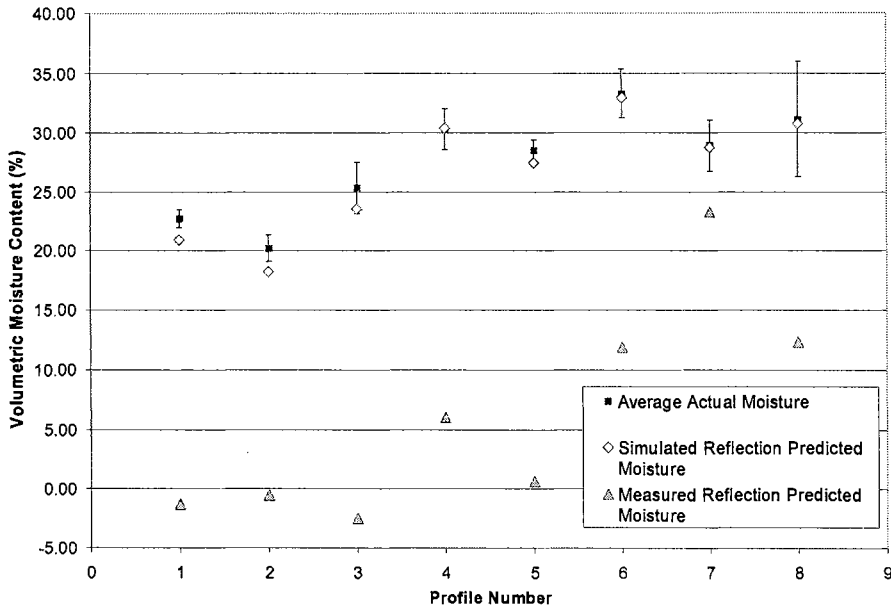


Figure 49. Soil moisture predictions in top 30.5 cm from simulated and measured reflection coefficients

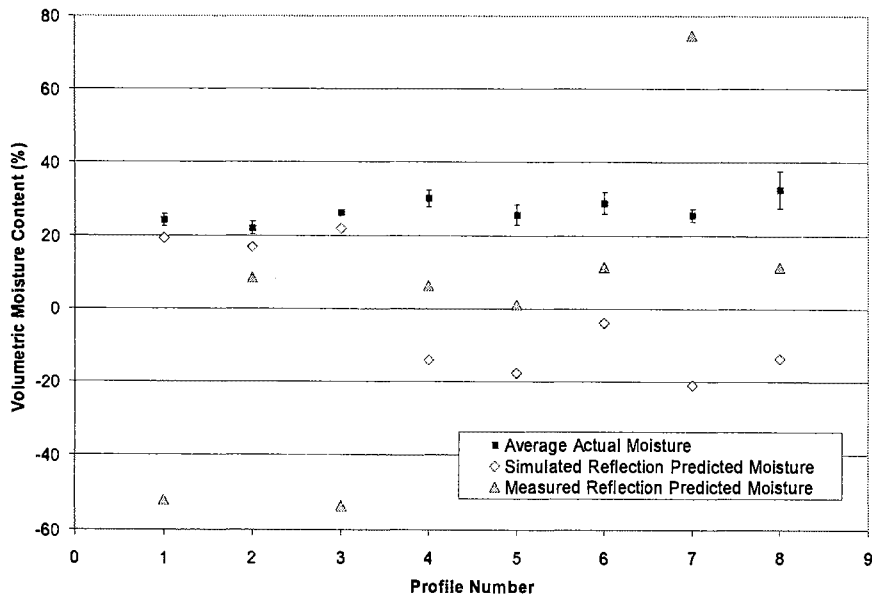


Figure 50. Soil moisture predictions in lower 30.5 cm from simulated and measured reflection coefficients

In the top layer, the restoration algorithm utilized simulated radio wave reflections to predict volumetric moisture within 0.96% of the actual volumetric moisture. In the bottom layer, only 3 of the moisture predictions from simulated reflection coefficients were close to the actual values.

The divergence problem existed in nearly all of the predictions of moisture that were based on measured reflection values. Of the 8 moisture values in the top 30.5 cm, and the 8 moistures in the lower 30.5 cm, only one prediction of volumetric moisture was within 10% of the actual value. The reason for the failure was that the measured reflection magnitudes and phases differed from the predicted values. Those differences were multiplied in the nonlinear equations relating impedance to dielectric properties which caused the iterative algorithm to diverge.

The results of the profile restoration tests indicated that the algorithm was very sensitive to small errors in reflection coefficients. The prediction of the lower layers was also extremely sensitive to error in the prediction of the top layer.

CHAPTER X

CONCLUSIONS AND RECOMENDATIONS

Summary

A technique was developed to measure moisture profiles in soil using reflection measurements of UHF and VHF radio waves. The development included the testing of soil dielectric homogeneity, the calibration of equipment, the measurement of dielectric properties of soil with various moisture contents, the writing of an electromagnetic reflection coefficient simulation algorithm, the measurement of electromagnetic reflections from soil containing various moisture profiles, and the testing of a moisture profile restoration algorithm.

The first simulation algorithm predicted electromagnetic reflection coefficients of Oklahoma soil containing hypothetical and naturally occurring moisture profiles within a frequency range of 80 MHz to 1 GHz. Spatial variability of soil dielectric properties was tested and the resulting variability was implemented in the model. The simulation of soil reflection coefficients was executed in a MATLAB program that utilized homogeneous dielectric layers. The layers in the model were determined directly from moisture-dielectric relationships measured in a coaxial cell.

The moisture detection technique in the field experiment included the measurement of electromagnetic reflection coefficients from Oklahoma soil containing profiles of varied moistures. Radio waves were transmitted by a log-periodic antenna, reflected by the air-soil surface and subsurface layers of dissimilar moisture, and detected

by a receiving log-periodic antenna. Frequencies ranging from 80 MHz to 1 GHz were used to penetrate through the soil to various depths. The magnitude and phase of the reflections were recorded and analyzed.

The technique for the detection of soil moisture profiles also required the formulation of a moisture profile restoration algorithm that estimated soil volumetric moisture within layered depths from electromagnetic reflection coefficients. The algorithm used a high frequency reflection coefficient to predict the surface moisture of the soil. The effect of the surface moisture was subtracted from the reflection coefficient of a lower frequency. The difference was used to predict the moisture content of the next lower layer. The process was repeated until all desired layers had been predicted.

Performance of the profile restoration algorithm was tested with modeled and measured reflection coefficients were used. Electromagnetic reflection coefficients were predicted from profiles of constant moisture, profiles containing two layers of moisture, and profiles of moisture that were measured in the field. The predicted electromagnetic reflection coefficients and reflection coefficients that were measured in the field were used as inputs to the profile restoration algorithm. The algorithm's predictions of moisture at depth were compared to the analytical and actual values.

Conclusions

Analytical Prediction of Soil Reflection Coefficients

The model that simulated reflection coefficients in the frequency range of 80 MHz to 1 GHz was tested using hypothetical and existent moisture profiles. Results of simulated profiles with constant moisture indicated that reflection coefficients in the upper frequency range (near 793 MHz) could be used to distinguish between volumetric surface moisture differences of 5%. Results of simulated two layer profiles indicated that reflection coefficients at frequencies in the lower range (near 84.6 MHz) could detect a subsurface boundary to a depth of 45.7 cm. Reflection coefficients at higher frequencies (near 793 MHz) could detect a subsurface boundary through a 15% moisture layer to a depth of 30.5 cm and could not detect a subsurface boundary through a 15.2 cm layer of 30% moisture.

Field Measurement of Soil Reflection Coefficients

Reflection measurements made with the network analyzer/antenna instrument indicated that linear correlation could be made with volumetric moisture in the top 15.2 cm. Although the measured reflections differed from theoretical predictions of reflectance, the linear relationship of average reflection magnitude to moisture had a simple correlation coefficient of 0.850. The linear relationship of moisture and reflection phase at a frequency of 84.6 MHz had a simple correlation coefficient of 0.914.

Moisture Profile Restoration from Soil Reflection Coefficients

The profile restoration algorithm closely predicted volumetric moisture (error = 3.88% volumetric moisture content) for the top layer of all simulated profiles tested. The prediction of moisture for the bottom layer had a high failure rate. The failures were attributed to the iterative portion of the algorithm, which had a tendency to diverge from the correct values due to small errors in the calculation of the top layer. The field measurements of the reflection coefficient differed from the simulated values. Because the same equations were used to predict reflection coefficients and restore profiles, the differences between the simulated and measured reflections were attributed with the 100% failure rate on the measured profiles. The high failure rate of the lower layers of simulated profiles and the high failure rate of all layers of the measured profiles indicated that the restoration algorithm did not effectively resolve layers of moisture in soil.

Recommendations for Further Research

The technique for the detection of soil moisture profiles using radio wave reflection has been outlined, and strengths and weaknesses of the procedure have been determined. Simulated and measured reflection coefficients of significant difference resulted from profiles of different volumetric moistures, but the profile restoration algorithm failed to accurately predict moisture in layers. The following is a list of suggestions for areas of further study.

1. Further modeling of the dielectric properties of the soil.

The measurements of conductivity in this study greatly exceeded the values expected based on the literature. Further dielectric characterization of Oklahoma soil is needed so that the moisture-permittivity and moisture-conductivity relationships are better understood. If the soil is more accurately characterized, future algorithms that resolve moisture layers will likely have a greater success rate.

2. Use of lower frequencies.

Larger skin depths are needed in order to detect the entire root zone of most crops. Lower frequencies will also have the added benefit of small phase errors from sensor height changes.

3. Correlation studies relating average magnitude from a band of frequencies to the volumetric moisture content in the topsoil

The profile restoration algorithm utilized nonlinear equations to manipulate values that were already closely correlated with moisture content. Simply using a broadband measurement of magnitude to detect moisture directly eliminates interference patterns associated with reflections at multiple boundaries. Several broadband measurements in different frequency ranges could potentially detect moisture at depth.

4. Correlation studies relating phase from a single frequency to surface volumetric moisture.

The phase of the reflection coefficient at a frequency of 84.6 MHz was highly correlated ($R^2 = 0.91$) to moisture in the topsoil. A sensor that measures phase at a single frequency in the VHF range could be potentially easy and inexpensive to build for widespread agricultural applications.

5. Potential use of conductivity or dielectric relaxations to predict soil type.

One of the limitations of electromagnetic detection of moisture is that it typically detects volumetric moisture. But, volumetric moisture does not indicate the water that can be used by crops. The matric potential is highly dependent on particle size. Both conductivity and dielectric relaxations are greatly affected by particle size. Characterizations of conductivity or dielectric relaxations may allow multi-frequency measurements to predict average particle size.

BIBLIOGRAPHY

- Arnold, G.J. The development of a dielectric based soil moisture sensor. Master's Thesis, Oklahoma State University, 1992.
- Arulandan, K., S.S. Smith. "Electrical Dispersion in Relation to Soil Structure." *Journal of the Soil Mechanics and Foundations Division, ASCE*, Vol. 99, SM12, Proceedings Paper 10235, Dec. 1973, pp. 1113-1133.
- Assal, H.M., S.F. Mahmoud. 1986. "Determination of resistivity and permittivity profiles of layered earth". *IGARSS '86 Symposium: Zurich, 8-11 September 1986, IEEE Cat.no.86CM2268-1*, pp. 205-209.
- Babb, A.T.S. 1951. "A radio-frequency electronic moisture meter". *Analyst*. 76, pp. 12-18.
- Balanis, C.A. Advanced Engineering Electromagnetics. John Wiley & Sons, New York. 1989.
- Batlivala, P., F.T. Ulaby. "Estimation of soil Moisture with Radar Remote Sensing," *Proceedings of the 11th International Symposium, Remote Sensing of the Environment, Environmental Research Institute of Michigan, 1977*, pp. 1557-1566.
- Boisvert J.B., Q.H.J. Gwyn, A. Chanzy, D.J. Major, B. Brisco, R.J. Brown. 1997. "Effect of Surface Soil Moisture Gradients on Modeling Radar Backscattering from Bare Fields". *Int. J. Remote Sens.* 18:153-170.
- Bowers, C.G., H.D. Bowen. 1975. "Drying front sensing and signal evaluation for planter depth control". *Transactions of the ASAE*. 18(6): 1051-1056.
- Buckley, F., A.A. Maryott. 1958. "Tables of dielectric dispersion data for pure liquids and dilute solutions". *National Bureau of Standards Circular* 589.
- Chanzy, A., A. Tarussov, A. Judge, F Bonn. "Soil water content determination using a digital ground-penetrating radar." *Soil Science Society of America Journal*. Sept/Oct 1996. Vol. 60 pp 1318-1326.
- Cheng, D.K. Field and Wave Electromagnetics. Addison-Wesley Publishing Co. Reading, Mass. 1983.
- Chudobiak, W.J., B.A. Syrett, H.M. Hafez. "Recent Advances in Broad-band VHF and UHF Transmission Line Methods for Moisture Content and Dielectric Constant

Measurement." IEEE Transactions on Instrumentation and Measurement, Institute of Electrical and Electronic Engineers, Vol.28, 1979, pp. 284-289.

Curtis, John. "Data Report: Dielectric Properties of Soils. JUXOCO Pilot Site, Fort A.P. Hill". U.S. Army Corps of Engineers. 8 September 1998.

Debye, P. 1829. Polar molecules. New York: The Chemical Catalog Co.

Entekhabi, D., H. Nakamura, E.G. Njoku. 1994. "Solving the inverse problem for soil moisture and temperature profiles by sequential assimilation of multifrequency remotely sensed observations". IEEE Transactions on Geoscience and Remote Sensing, Vol. 32, No. 2, pp. 438-448.

Hallikainen, M.T., F.T. Ulaby, M.C. Dobson, M.A. El-Rayes, L. Wu. 1985. "Microwave dielectric behavior of wet soil—Part 1: Empirical models and experimental observations". IEEE Transactions on Geoscience and Remote Sensing, Vol. 23, No.1, pp. 25-34.

Hanks, R.J., G.L. Ashcroft. Applied Soil Physics: Soil Water and Temperature Applications. Springer-Verlag, Berlin. 1980.

Hipp, J.E. "Soil Electromagnetic Parameters as a Function of Frequency, Soil Density and Soil Moisture," Proceedings of the IEEE, Institute of Electrical and Electronic Engineers, Vol 62, Jan. 1974, pp. 98-103.

Hoekstra, P., A. Delaney. "Dielectric Properties of Soils at UHF and Microwave Frequencies," Journal of Geophysical Research, Vol. 79, 1974, pp. 1699-1708.

Holdem, J.R., R.B. Keam, J.A. Schoones. 2000. "Estimation of the Number of Frequencies and Bandwidth for the Surface Measurement of Soil Moisture as a Function of Depth". IEEE Transactions on Instrumentation and Measurement. Vol. 49, No. 5, pp. 964-970.

Jackson, T.J. 1980. "Profile soil moisture from surface measurements". J. Irrigation and Drainage Engineering. 106(IR2):81-92.

Jorgensen, J.L., A.R. Edison, S.O. Nelson, L.E. Stetson. 1970. "A bridge method for dielectric measurements of grain and seed in the 50- to 250-MHz range." Transactions of the ASAE. Vol. 13, No. 1, pp. 18-24.

Josephson, B., A. Blomquist. "The Influence of Moisture in the Ground, Temperature, and Terrain on Ground-Wave Propagation in the VHF Band," IRE Transactions on Antennas and Propagation, Institute of Radio Engineers, Vol. 6, No. 2, 1958, pp. 169-172.

- Lager, D.L., R.J. Lytle. "Determining a Subsurface Electromagnetic Profile From High-Frequency Measurements by Applying Reconstruction-technique Algorithms," *Radio Science*, Vol. 12, No. 2, Mar-Apr., 1977, pp. 249-260.
- Lawrence, K.C., S.O. Nelson, A.W. Kraszewski. 1989. "Automatic System for Dielectric Properties Measurements from 100 kHz to 1 GHz." *Transactions of the ASAE*, 32(1):304-308.
- Lundien, J.R. "Determining Presence, Thickness, and Electrical Properties of Stratified Media Using Swept-Frequency Radar," Technical Report M-72-4, Nov 1972, US Army Engineer Waterways Experiment Station, CE, Vicksburg, Miss.
- Lundien, J.R. "Terrain Analysis by Electromagnetic Means; Radar Responses to Laboratory Prepared Soil Samples," Technical Report No. 3-693, Report 2, Sep 1966, US Army Engineer Waterways Experiment Station, CE, Vicksburg, Miss.
- Maley, S.W. "A Method for the Measurement of the Parameters of a Two-Layer Stratified Earth," *IEEE Transactions on Antennas and Propagation*, Vol. AP-11, May 1963, pp.366-369.
- McNeill, J.D. 1980. "Electrical Conductivity of Soils and Rocks." Technical Note TN-5. Geonics Limited, #8, Mississauga, Ont.
- Moghaddam, M., Y. Rahmat-Samii, E. Rodriguez, D. Moller. 2002. "Dual-Low-Frequency Radar for Soil Moisture under Vegetation and At-Depth". NASA Earth Science Technology Conference. Pasadena, CA. Paper no. B2P6.
- Nelson, S.O. 1983. "Density dependence of the dielectric properties of particulate materials". *Transactions of the ASAE*, 26(6):1823-1825, 1829.
- Nikodem, H.J. "Effects of Soil Layering on the Use of VHF Radio Waves for Remote Terrain Analyses," *Proceedings of 4th Symposium on Remote Sensing of Environment*, University of Michigan, Ann Arbor, 1966, pp.691-703.
- Rao, R.G., F.T. Ulaby. 1977. "Optimal spatial sampling techniques for ground truth data in microwave remote sensing of soil moisture". *Remote Sensing of Environment* 6, pp. 289-301.
- Ratcliffe and Shaw. "A determination of the dielectric constant of the ground". *Nature*, Vol. 124, pp. 617, October 19, 1929.
- Scott, W.R., G.S. Smith. 1986. "Error Analysis for Dielectric Spectroscopy using Shielded Open-Circuited Coaxial Lines of General Length" *IEEE Transactions on Instrumentation and Measurement*. IM-35(2):130-137.

Smith-Rose, R.L. 1935. "The electrical properties of soil at frequencies up to 100 megacycles per second; With a note on the resistivity of ground in the United Kingdom". Proceedings of the Physics Society (London), Vol. 47, pp. 923-931.

Steel, R.G.D., J.H. Torrie, D.A. Dickey. Principles and Procedures of Statistics: a Biometrical Approach. Third Ed. McGraw-Hill, Boston, Mass. 1997.

Topp, G.C., J.L. Davis, A.P. Annan. (1980). "Electromagnetic determination of soil water content: Measurements in coaxial transmission lines". Water Resources Research 16, 574-582.

Ulaby, F.T. 1974. "Radar measurement of soil moisture content". IEEE Transactions on Antennas and Propagation, Vol. 22, No. 2, pp. 257-265.

Vellidis, G., M.C. Smith, D.L. Thomas, L.E. Asmussen. "Detecting wetting front movement in a sandy soil with ground-penetrating radar." Transactions of the ASAE. St. Joseph, Mich. v 33. pp 1867-1874. 1990.

Vlotman, W.F. "Soil Moisture Measurement with VHF Radio Waves." PhD Dissertation, Utah State University, 1985.

Wang, J.R. (1980). "The dielectric properties of soil-water mixtures at microwave frequencies". Radio Science 15, 977-85.

Zur B., U. Ben-Hannan, A. Rimmer, A. Yardeni. 1994. "Control of irrigation amounts using velocity and position of wetting front". Irrigation Science 14:207-12.

APPENDICES

APPENDIX A

INTERFERING ELECTROMAGNETIC ENERGY MEASURED BY THE DISCONE ANTENNA

Frequency (MHz)	Measured Spectrum Analyzer Power (dBm)	Measured Antenna Reflection (Mag)	Calculated Air EM Power (dBm)
90.30	-71	0.753	-58.5
92.25	-32	0.732	-20.2
94.20	-50	0.701	-37.8
95.25	-71	0.662	-59.6
96.65	-66	0.612	-55.1
97.45	-63	0.583	-52.4
98.65	-47	0.546	-36.6
102.59	-64	0.516	-53.8
103.34	-62	0.510	-51.8
103.69	-67	0.507	-56.9
104.69	-72	0.499	-61.9
105.74	-68	0.490	-58.0
106.19	-49	0.486	-39.0
107.39	-63	0.476	-53.0
149.38	-51	0.206	-42.0
152.80	-51	0.208	-42.0
153.48	-57	0.209	-48.0
154.78	-65	0.207	-56.0
158.38	-62	0.201	-53.0
169.58	-69	0.247	-59.9
444.16	-69	0.160	-60.0
459.66	-61	0.264	-51.8
512.44	-69	0.456	-59.1
850.06	-68	0.345	-58.6
853.06	-72	0.253	-62.9
854.56	-64	0.233	-54.9
854.96	-68	0.228	-58.9
855.56	-64	0.220	-54.9
860.75	-63	0.262	-53.8
865.25	-58	0.332	-48.7
866.35	-38	0.347	-28.6
868.15	-41	0.344	-31.6
869.60	-47	0.337	-37.6
871.10	-47	0.331	-37.7
871.45	-41	0.326	-31.7
872.15	-40	0.312	-30.7
872.85	-44	0.298	-34.8
874.85	-38	0.258	-28.9
875.45	-37	0.246	-27.9
876.95	-51	0.223	-41.9
877.95	-76	0.210	-67.0
879.55	-75	0.188	-66.0
882.70	-65	0.214	-56.0
884.20	-72	0.239	-62.9
884.70	-71	0.247	-61.9
885.30	-67	0.256	-57.9
887.80	-51	0.290	-41.8
919.89	-49	0.296	-39.8
922.39	-36	0.266	-26.8
924.49	-69	0.235	-59.9
924.99	-34	0.228	-24.9
926.39	-74	0.208	-65.0
926.99	-74	0.199	-65.0
932.49	-36	0.240	-26.9

APPENDIX B

NEUTRON PROBE CALIBRATION DATA

Measurements in Soil				
Corrected Neutron Counts	Volumetric Moisture	Corrected Neutron Counts	Volumetric Moisture	
434	0.206	422	0.233	PVC in water
406	0.239	388	0.166	1131
454	0.319	425	0.260	1121
485	0.276	518	0.219	1126
524	0.320	561	0.347	1126
533	0.281	572	0.317	Steel in water
514	0.301	522	0.290	1321
538	0.101	541	0.320	
524	0.363	555	0.316	
529	0.410	558	0.317	PVC in air
512	0.350	555	0.324	11
414	0.230	551	0.290	12
429	0.218	563	0.313	
455	0.232	479	0.252	
438	0.234	471	0.280	
459	0.254	489	0.286	
504	0.312	496	0.274	
540	0.319	507	0.311	
542	0.295	521	0.286	
509	0.285	529	0.304	
529	0.329	526	0.323	
543	0.366	534	0.303	
539	0.366	542	0.329	
561	0.323	533	0.306	
497	0.210	473	0.213	
445	0.257	432	0.232	
462	0.285	223	0.206	
478	0.287	469	0.171	
480	0.260	462	0.196	
486	0.279	491	0.258	
505	0.282	483	0.399	
501	0.290	509	0.370	
475	0.251	519	0.282	
510	0.318	518	0.357	
481	0.285	530	0.363	
283	0.139	540	0.334	
307	0.148	531	0.232	
444	0.211	534	0.246	
505	0.318	516	0.262	
478	0.272	427	0.285	
460	0.252	436	0.246	
508	0.302	397	0.207	
508	0.319	432	0.299	
504	0.292	505	0.317	
514	0.290	529	0.326	
534	0.308	565	0.274	
551	0.319	510	0.318	
464	0.297	534	0.306	
321	0.102	545	0.307	
417	0.133	545	0.334	
454	0.225	545	0.326	
561	0.298	550	0.296	

APPENDIX C

MATLAB CODE: COAXIAL CELL DIELECTRIC ITERATION ALGORITHM

```
% Soil Dielectric Calculator

% This program calculates the dielectric properties of soil from the
% reflection coefficients of the coaxial cell.
% Written by Duane Needham
% June 11, 2003

%*****
% EM numeric constants
e = 8.854*10^-12;
u = 4*pi*10^-7;
Zo = 50;

% Cell dimensions
a = 0.0233;
b = 0.054;
l = 0.064;

% initial conditions
r1 = 0;

%*****
% This portion determines the propagation term of the cable and the
% terminating impedance (Zcap)

calib      %recalls calibrating freq, mag, phase stored in "calib.m"
f = 1000000*A(:,1);
w = 2*pi*f;

for x = 1:10,          % 10 samples of reflection, sample impedance = 0
    M = A(:,2*x);
    p = A(:,2*x+1);
    r = ((M.*cos(pi/180*p))+(j*M.*sin(pi/180*p)));
    r1 = r1+r;
end
r1 = r1./10;
Prop = -r1;           % propagation constant of the cable

r1 = 0;
for x = 11:20,        %10 samples of reflection, cell with air, Zcap = 0
    M = A(:,2*x);
    p = A(:,2*x+1);
    r = ((M.*cos(pi/180*p))+(j*M.*sin(pi/180*p)));
    r1 = r1+r;
end
r1 = r1./10;
Prop2 = -r1./Prop;
```

```

r1 = 0;
Bfree = w*(u*e)^0.5; % free space propagation constant
for x = 21:30, %10 samples of reflection, cell with air
    M = A(:,2*x);
    p = A(:,2*x+1);
    r = ((M.*cos(pi/180*p))+(j*M.*sin(pi/180*p)));
    r1 = r1+r;
end
r1 = r1./10;
r1 = r1./Prop./Prop2;
Zcap = Zo*(1+r1)./(1-r1);

%*****
soil43 % recalls measured mag and phase measurements stored in the
        %file: soil plot# hole#

for x = 1:17,
    M = A(:,2*x);
    p = A(:,2*x+1);
    r = ((M.*cos(pi/180*p))+(j*M.*sin(pi/180*p)));
    r = r./Prop;
    Zin = Zo*(1+r)./(1-r);

    % Start with permittivity and conductivity values for soil @ 20%
        %moisture (from literature: Curtis)
    k = 11*ones(size(w));
    s = 0.07*ones(size(w));

    gamma = zeros(201,9);
    Zs = zeros(201,9);
    ZL = zeros(201,9);
    d = zeros(201,9);

    for x1 = 1:1000,
        gamma(:,1) = ((j*w*u).*(s+j*w.*k*e)).^0.5;
        gamma(:,2) = ((j*w*u).*(s+j*w.*(k-0.01)*e)).^0.5;
        gamma(:,3) = ((j*w*u).*(s+j*w.*(k+0.01)*e)).^0.5;
        gamma(:,4) = ((j*w*u).*((s-0.001)+j*w.*k*e)).^0.5;
        gamma(:,5) = ((j*w*u).*((s+0.001)+j*w.*k*e)).^0.5;
        gamma(:,6) = ((j*w*u).*((s-0.001)+j*w.*(k-0.01)*e)).^0.5;
        gamma(:,7) = ((j*w*u).*((s-0.001)+j*w.*(k+0.01)*e)).^0.5;
        gamma(:,8) = ((j*w*u).*((s+0.001)+j*w.*(k-0.01)*e)).^0.5;
        gamma(:,9) = ((j*w*u).*((s+0.001)+j*w.*(k+0.01)*e)).^0.5;

        for x2 = 1:9,
            Zs(:,x2) = (j*w*u)./(gamma(:,x2)*2*pi)*log(b/a);
            ZL(:,x2) =
Zs(:,x2).*(Zcap+Zs(:,x2).*tanh(gamma(:,x2)*1))./(Zs(:,x2)+Zcap.*tanh(ga
mma(:,x2)*1));
            d(:,x2) = abs(ZL(:,x2)-Zin);
        end

        d1 = min(d');
        for x2 = 1:201,

```

```

    for x3 = 1:9,
        if d1(x2) == d(x2,x3)
            adj(x2) = x3;
        end
    end
    if adj(x2) == 2
        k(x2) = k(x2)-0.01;
    end
    if adj(x2) == 3
        k(x2) = k(x2)+0.01;
    end
    if adj(x2) == 4
        s(x2) = s(x2)-0.001;
    end
    if adj(x2) == 5
        s(x2) = s(x2)+0.001;
    end
    if adj(x2) == 6
        s(x2) = s(x2)-0.001;
        k(x2) = k(x2)-0.01;
    end
    if adj(x2) == 7
        s(x2) = s(x2)-0.001;
        k(x2) = k(x2)+0.01;
    end
    if adj(x2) == 8
        s(x2) = s(x2)+0.001;
        k(x2) = k(x2)-0.01;
    end
    if adj(x2) == 9
        s(x2) = s(x2)+0.001;
        k(x2) = k(x2)+0.01;
    end
end
end

Zin
plot (real(Zin),imag(Zin))
Title('Measured Load Impedance of Soil')
xlabel('Real Impedance (Ohms)')
ylabel('Imaginary Impedance (Ohms)')
pause

plot (real(ZL(:,1)),imag(ZL(:,1)))
Title('Calculated Load Impedance of Soil')
xlabel('Real Impedance (Ohms)')
ylabel('Imaginary Impedance (Ohms)')
pause

k
plot (f,k)
Title('Measured Permittivity of Soil')
xlabel('Frequency (Hz)')
ylabel('Permittivity')
pause

s

```

```
plot (f, (s)) Title('Measured Conductivity of Soil')
xlabel('Frequency (Hz)')
ylabel('Conductivity')
pause end
```

APPENDIX D

COAXIAL CELL CALIBRATION DATA

Frequency (MHz)	Cable & lower cell			Upper Cell			Impedance		
	Propagation Term	Prop =	Zcap (ohms)	Propagation Term	Prop2 =	Zcap (ohms)	Propagation Term	Prop =	Zcap (ohms)
80	-0.8688 + 0.4367i	0.9686 - 0.2329i	4.6838 + 6.6139i	544.6	0.5033 + 0.7818i	-0.0985 - 0.9716i	-0.0157 - 0.2477i		
84.6	-0.7583 + 0.6082i	0.9644 - 0.2485i	1.1415 + 3.5735i	549.2	0.6527 + 0.6612i	-0.1023 - 0.9714i	-0.0150 - 0.2405i		
89.2	-0.6132 + 0.7556i	0.9615 - 0.2593i	0.8621 + 2.6584i	553.8	0.7719 + 0.5140i	-0.1099 - 0.9723i	-0.0142 - 0.2322i		
93.8	-0.4398 + 0.8681i	0.9572 - 0.2722i	0.5905 + 2.1619i	558.4	0.8589 + 0.3491i	-0.1179 - 0.9712i	-0.0133 - 0.2232i		
98.4	-0.2507 + 0.9412i	0.9542 - 0.2824i	0.7039 + 2.1924i	563	0.9096 + 0.1732i	-0.1319 - 0.9706i	-0.0117 - 0.2160i		
103	-0.0477 + 0.9733i	0.9492 - 0.2936i	0.6715 + 2.1528i	567.6	0.9264 - 0.0160i	-0.1418 - 0.9691i	-0.0114 - 0.2146i		
107.6	0.1551 + 0.9604i	0.9467 - 0.3022i	0.6895 + 2.2403i	572.2	0.9030 - 0.1999i	-0.1560 - 0.9671i	-0.0112 - 0.2110i		
112.2	0.3498 + 0.9061i	0.9439 - 0.3100i	0.8082 + 2.5677i	576.8	0.8457 - 0.3746i	-0.1752 - 0.9640i	-0.0107 - 0.2085i		
116.8	0.5237 + 0.8168i	0.9393 - 0.3209i	1.4198 + 3.5518i	581.4	0.7533 - 0.5346i	-0.1898 - 0.9612i	-0.0105 - 0.2057i		
121.4	0.6775 + 0.6932i	0.9363 - 0.3297i	4.2029 + 5.8157i	586	0.6354 - 0.6703i	-0.2113 - 0.9565i	-0.0098 - 0.2060i		
126	0.7999 + 0.5430i	0.9343 - 0.3364i	3.5011 - 6.5769i	590.6	0.4924 - 0.7813i	-0.2350 - 0.9516i	-0.0099 - 0.2076i		
130.6	0.8898 + 0.3742i	0.9293 - 0.3476i	0.2293 - 3.2688i	595.2	0.3292 - 0.8608i	-0.2584 - 0.9459i	-0.0106 - 0.2113i		
135.2	0.9447 + 0.1884i	0.9257 - 0.3555i	-0.0422 - 2.0334i	599.8	0.1597 - 0.9084i	-0.2871 - 0.9371i	-0.0106 - 0.2172i		
139.8	0.9620 + 0.0000i	0.9211 - 0.3669i	-0.0783 - 1.4007i	604.4	-0.0158 - 0.9221i	-0.3194 - 0.9265i	-0.0114 - 0.2253i		
144.4	0.9410 - 0.1894i	0.9196 - 0.3745i	-0.0565 - 1.0101i	609	-0.1941 - 0.9003i	-0.3471 - 0.9166i	-0.0123 - 0.2357i		
149	0.8837 - 0.3707i	0.9138 - 0.3873i	-0.0662 - 0.8803i	613.6	-0.3662 - 0.8463i	-0.3796 - 0.9022i	-0.0144 - 0.2487i		
153.6	0.7910 - 0.5379i	0.9112 - 0.3951i	-0.0506 - 0.7074i	618.2	-0.5246 - 0.7575i	-0.4115 - 0.8878i	-0.0162 - 0.2624i		
158.2	0.6712 - 0.6800i	0.9024 - 0.4128i	-0.0546 - 0.6529i	622.8	-0.6646 - 0.6399i	-0.4397 - 0.8717i	-0.0187 - 0.2773i		
162.8	0.5224 - 0.7974i	0.8992 - 0.4237i	-0.0416 - 0.5808i	627.4	-0.7781 - 0.4955i	-0.4688 - 0.8552i	-0.0226 - 0.2959i		
167.4	0.3537 - 0.8844i	0.8934 - 0.4364i	-0.0312 - 0.5406i	632	-0.8615 - 0.3262i	-0.4930 - 0.8406i	-0.0262 - 0.3174i		
172	0.1743 - 0.9351i	0.8857 - 0.4531i	-0.0234 - 0.5151i	636.6	-0.9112 - 0.1448i	-0.5126 - 0.8262i	-0.0316 - 0.3347i		
176.6	-0.0180 - 0.9509i	0.8803 - 0.4645i	-0.0184 - 0.5103i	641.2	-0.9210 + 0.0411i	-0.5330 - 0.8126i	-0.0391 - 0.3551i		
181.2	-0.2077 - 0.9285i	0.8731 - 0.4790i	-0.0101 - 0.5094i	645.8	-0.8932 + 0.2284i	-0.5465 - 0.8015i	-0.0436 - 0.3664i		
185.8	-0.3911 - 0.8677i	0.8679 - 0.4899i	-0.0034 - 0.4981i	650.4	-0.8269 + 0.4085i	-0.5580 - 0.7936i	-0.0450 - 0.3702i		
190.4	-0.5591 - 0.7708i	0.8588 - 0.5059i	0.0026 - 0.5031i	655	-0.7235 + 0.5701i	-0.5689 - 0.7865i	-0.0471 - 0.3695i		
195	-0.7061 - 0.6400i	0.8494 - 0.5222i	0.0106 - 0.5179i	659.6	-0.5867 + 0.7102i	-0.5775 - 0.7788i	-0.0484 - 0.3724i		
199.6	-0.8242 - 0.4819i	0.8410 - 0.5338i	0.0156 - 0.5356i	664.2	-0.4196 + 0.8191i	-0.5741 - 0.7828i	-0.0430 - 0.3549i		
204.2	-0.9066 - 0.2977i	0.8340 - 0.5455i	0.0226 - 0.5650i	668.8	-0.2379 + 0.8872i	-0.5784 - 0.7815i	-0.0393 - 0.3374i		
208.8	-0.9490 - 0.1053i	0.8237 - 0.5594i	0.0300 - 0.5837i	673.4	-0.0439 + 0.9174i	-0.5837 - 0.7780i	-0.0361 - 0.3250i		
213.4	-0.9494 + 0.0994i	0.8201 - 0.5651i	0.0366 - 0.6150i	678	0.1526 + 0.9041i	-0.5818 - 0.7819i	-0.0304 - 0.3060i		
218	-0.9093 + 0.2933i	0.8126 - 0.5753i	0.0438 - 0.6283i	682.6	0.3359 + 0.8511i	-0.5833 - 0.7834i	-0.0261 - 0.2880i		
222.6	-0.8282 + 0.4767i	0.8027 - 0.5883i	0.0539 - 0.6774i	687.2	0.5069 + 0.7609i	-0.5822 - 0.7853i	-0.0220 - 0.2704i		
227.2	-0.7110 + 0.6399i	0.7947 - 0.5980i	0.0653 - 0.7046i	691.8	0.6530 + 0.6388i	-0.5826 - 0.7860i	-0.0185 - 0.2554i		
231.8	-0.5601 + 0.7748i	0.7906 - 0.6035i	0.0590 - 0.6965i	696.4	0.7701 + 0.4910i	-0.5828 - 0.7869i	-0.0159 - 0.2426i		
236.4	-0.3848 + 0.8758i	0.7856 - 0.6085i	0.0572 - 0.6819i	701	0.8532 + 0.3263i	-0.5895 - 0.7811i	-0.0149 - 0.2334i		
241	-0.1921 + 0.9368i	0.7807 - 0.6133i	0.0508 - 0.6597i	705.6	0.9014 + 0.1368i	-0.5882 - 0.7857i	-0.0122 - 0.2234i		
245.6	0.0056 + 0.9557i	0.7741 - 0.6207i	0.0405 - 0.6302i	710.2	0.9105 - 0.0467i	-0.5940 - 0.7811i	-0.0104 - 0.2123i		
250.2	0.2040 + 0.9335i	0.7701 - 0.6238i	0.0252 - 0.5731i	714.8	0.8809 - 0.2331i	-0.6034 - 0.7731i	-0.0105 - 0.2090i		
254.8	0.3882 + 0.8707i	0.7673 - 0.6287i	0.0187 - 0.5206i	719.4	0.8157 - 0.4032i	-0.6121 - 0.7682i	-0.0091 - 0.2036i		
259.4	0.5564 + 0.7743i	0.7615 - 0.6338i	0.0122 - 0.4728i	724	0.7144 - 0.5616i	-0.6207 - 0.7617i	-0.0090 - 0.1993i		
264	0.7005 + 0.6455i	0.7555 - 0.6389i	0.0041 - 0.4269i	728.6	0.5917 - 0.6886i	-0.6384 - 0.7486i	-0.0077 - 0.1996i		
268.6	0.8114 + 0.4941i	0.7535 - 0.6429i	0.0012 - 0.3826i	733.2	0.4444 - 0.7913i	-0.6500 - 0.7404i	-0.0070 - 0.1962i		
273.2	0.8916 + 0.3235i	0.7491 - 0.6484i	-0.0011 - 0.3499i	737.8	0.2818 - 0.8631i	-0.6689 - 0.7247i	-0.0071 - 0.1992i		
277.8	0.9363 + 0.1453i	0.7408 - 0.6577i	-0.0030 - 0.3140i	742.4	0.1105 - 0.9007i	-0.6871 - 0.7060i	-0.0075 - 0.2023i		
282.4	0.9466 - 0.0397i	0.7320 - 0.6654i	-0.0044 - 0.2934i	747	-0.0667 - 0.9060i	-0.7065 - 0.6858i	-0.0076 - 0.2058i		
287	0.9181 - 0.2265i	0.7289 - 0.6714i	-0.0040 - 0.2697i	751.6	-0.2435 - 0.8740i	-0.7288 - 0.6656i	-0.0075 - 0.2094i		
291.6	0.8560 - 0.3992i	0.7201 - 0.6826i	-0.0031 - 0.2521i	756.2	-0.4143 - 0.8083i	-0.7420 - 0.6463i	-0.0082 - 0.2143i		
296.2	0.7622 - 0.5568i	0.7084 - 0.6941i	-0.0026 - 0.2412i	760.8	-0.5648 - 0.7109i	-0.7620 - 0.6224i	-0.0081 - 0.2199i		
300.8	0.6379 - 0.6939i	0.7002 - 0.7039i	-0.0017 - 0.2299i	765.4	-0.6938 - 0.5866i	-0.7789 - 0.5991i	-0.0093 - 0.2254i		
305.4	0.4931 - 0.8031i	0.6883 - 0.7156i	-0.0013 - 0.2223i	770	-0.7984 - 0.4327i	-0.7903 - 0.5818i	-0.0097 - 0.2266i		
310	0.3275 - 0.8826i	0.6780 - 0.7266i	-0.0005 - 0.2169i	774.6	-0.8686 - 0.2641i	-0.8026 - 0.5663i	-0.0096 - 0.2263i		
314.6	0.1528 - 0.9288i	0.6628 - 0.7418i	0.0007 - 0.2158i	779.2	-0.9047 - 0.0820i	-0.8102 - 0.5510i	-0.0107 - 0.2267i		
319.2	-0.0314 - 0.9404i	0.6500 - 0.7533i	0.0006 - 0.2119i	783.8	-0.9023 + 0.1047i	-0.8171 - 0.5406i	-0.0109 - 0.2234i		
323.8	-0.2128 - 0.9169i	0.6348 - 0.7683i	0.0023 - 0.2128i	788.4	-0.8614 + 0.2867i	-0.8209 - 0.5339i	-0.0104 - 0.2184i		
328.4	-0.3890 - 0.8589i	0.6158 - 0.7824i	0.0034 - 0.2138i	793	-0.7827 + 0.4599i	-0.8222 - 0.5310i	-0.0095 - 0.2072i		
333	-0.5539 - 0.7631i	0.5993 - 0.7952i	0.0039 - 0.2186i	797.6	-0.6669 + 0.6147i	-0.8251 - 0.5297i	-0.0083 - 0.2006i		
337.6	-0.6989 - 0.6339i	0.5855 - 0.8058i	0.0045 - 0.2231i	802.2	-0.5184 + 0.7429i	-0.8224 - 0.5347i	-0.0074 - 0.1895i		
342.2	-0.8116 - 0.4801i	0.5660 - 0.8198i	0.0048 - 0.2286i	806.8	-0.3465 + 0.8359i	-0.8221 - 0.5364i	-0.0067 - 0.1796i		
346.8	-0.8927 - 0.3075i	0.5476 - 0.8312i	0.0054 - 0.2353i	811.4	-0.1602 + 0.8878i	-0.8193 - 0.5474i	-0.0053 - 0.1696i		
351.4	-0.9374 - 0.1177i	0.5348 - 0.8377i	0.0048 - 0.2399i	816	0.0317 + 0.9023i	-0.8157 - 0.5517i	-0.0043 - 0.1607i		
356	-0.9411 + 0.0766i	0.5187 - 0.8482i	0.0058 - 0.2465i	820.6	0.2251 + 0.8734i	-0.8111 - 0.5616i	-0.0033 - 0.1516i		
360.6	-0.9049 + 0.2706i	0.5038 - 0.8551i	0.0046 - 0.2568i	825.2	0.4022 + 0.8070i	-0.8058 - 0.5690i	-0.0029 - 0.1433i		
365.2	-0.8311 + 0.4497i	0.4844 - 0.8648i	0.0045 - 0.2642i	829.8	0.5818 + 0.7025i	-0.8052 - 0.5759i	-0.0018 - 0.1370i		
369.8	-0.7190 + 0.6125i	0.4775 - 0.8691i	0.0042 - 0.2671i	834.4	0.6967 + 0.5684i	-0.8020 - 0.5816i	-0.0015 - 0.1315i		
374.4	-0.5756 + 0.7488i	0.4644 - 0.8738i	0.0021 - 0.2724i	839	0.7991 + 0.4084i	-0.7970 - 0.5932i	-0.0009 - 0.1256i		
379	-0.4062 + 0.8527i	0.4560 - 0.8780i	0.0021 - 0.2681i	843.6	0.8666 + 0.2325i	-0.7980 - 0.5941i	-0.0005 - 0.1211i		
383.6	-0.2144 + 0.9187i	0.4507 - 0.8797i	-0.0003 - 0.2643i	848.2	0.8949 + 0.0450i	-0.7956 - 0.5983i	-0.0004 - 0.1165i		
388.2	-0.0171 + 0.9428i	0.4430 - 0.8834i	-0.0010 - 0.2602i	852.8	0.8840 - 0.1422i	-0.7961 - 0.6001i	-0.0002 - 0.1139i		
392.8	0.1766 + 0.9259i	0.4378 - 0.8855i	-0.0012 - 0.2510i	857.4	0.8342 - 0.3234i	-0.7949 - 0.6037i	-0.0001 - 0.1107i		
397.4	0.3616 + 0.8689i	0.4279 - 0.8883i	-0.0038 - 0.2428i	862	0.7524 - 0.4844i	-0.7982 - 0.5996i	0.0000 - 0.1083i		
402	0.5317 + 0.7762i	0.4246 - 0.8906i	-0.0035 - 0.2347i	866.6	0.6427 - 0.6239i	-0.8062 - 0.5861i	0.0002 - 0.1072i		

Frequency (MHz)	Reagent grade n-prop anol						Frequency (MHz)	Reagent grade n-propa nol					
	Average		Std. Dev	Average		Std. Dev		Average		Std. Dev	Average		Std. Dev
	Theoretical Permittivity	Measured Permittivity	Permittivity	Theoretical Conductivity	Measured Conductivity	Conductivity		Theoretical Permittivity	Measured Permittivity	Permittivity	Theoretical Conductivity	Measured Conductivity	Conductivity
80	19.498	18.339	0.146	0.0139	0.0118	0.00074	544.6	9.472	11.098	0.683	0.2454	0.1844	0.01278
84.6	19.430	18.512	0.148	0.0155	0.0134	0.00074	549.2	9.406	10.864	0.697	0.2469	0.1876	0.01277
89.2	19.358	18.430	0.115	0.0171	0.0144	0.00067	553.8	9.342	10.644	0.701	0.2484	0.1900	0.01437
93.8	19.284	18.458	0.107	0.0189	0.0159	0.00115	558.4	9.278	10.440	0.698	0.2496	0.1922	0.01646
98.4	19.206	18.636	0.117	0.0206	0.0175	0.00089	563	9.215	10.254	0.661	0.2513	0.1935	0.01510
103	19.125	18.713	0.154	0.0225	0.0192	0.00082	567.6	9.152	10.104	0.652	0.2527	0.1962	0.01556
107.6	19.042	18.716	0.142	0.0244	0.0204	0.00115	572.2	9.091	9.940	0.644	0.2542	0.1989	0.01737
112.2	18.965	18.747	0.084	0.0264	0.0219	0.00135	576.8	9.030	9.793	0.643	0.2556	0.2044	0.01951
116.8	18.867	18.952	0.097	0.0285	0.0241	0.00126	581.4	8.971	9.659	0.649	0.2569	0.2085	0.02162
121.4	18.776	19.014	0.159	0.0306	0.0259	0.00142	586	8.911	9.615	0.621	0.2583	0.2083	0.02145
126	18.682	18.914	0.224	0.0327	0.0273	0.00135	590.6	8.853	9.557	0.589	0.2597	0.2116	0.02277
130.5	18.586	18.906	0.203	0.0350	0.0294	0.00126	595.2	8.796	9.516	0.568	0.2610	0.2159	0.02254
135.2	18.488	18.943	0.161	0.0372	0.0314	0.00169	599.8	8.739	9.530	0.547	0.2623	0.2163	0.02452
139.8	18.389	19.057	0.171	0.0395	0.0339	0.00171	604.4	8.683	9.548	0.512	0.2636	0.2144	0.02358
144.4	18.286	18.954	0.291	0.0419	0.0355	0.00171	609	8.628	9.593	0.471	0.2649	0.2168	0.02568
149	18.182	18.761	0.205	0.0443	0.0373	0.00183	613.6	8.573	9.641	0.455	0.2661	0.2154	0.02567
153.6	18.076	18.503	0.091	0.0467	0.0398	0.00264	618.2	8.519	9.691	0.413	0.2674	0.2137	0.02427
158.2	17.968	18.540	0.221	0.0492	0.0418	0.00299	622.8	8.465	9.720	0.375	0.2686	0.2126	0.02477
162.8	17.859	18.398	0.278	0.0517	0.0436	0.00191	627.4	8.413	9.741	0.343	0.2698	0.2093	0.02472
167.4	17.749	18.165	0.247	0.0543	0.0457	0.00227	632	8.362	9.743	0.321	0.2710	0.2073	0.02412
172	17.637	18.214	0.239	0.0569	0.0489	0.00245	636.6	8.310	9.754	0.287	0.2722	0.2040	0.02371
176.6	17.524	17.945	0.180	0.0595	0.0501	0.00291	641.2	8.260	9.743	0.281	0.2734	0.2028	0.02482
181.2	17.410	17.789	0.261	0.0621	0.0522	0.00218	645.8	8.210	9.718	0.256	0.2745	0.2013	0.02467
185.8	17.295	17.570	0.196	0.0648	0.0546	0.00333	650.4	8.161	9.641	0.242	0.2756	0.1990	0.02346
190.4	17.179	17.435	0.289	0.0674	0.0564	0.00302	655	8.112	9.561	0.223	0.2768	0.1976	0.02411
195	17.062	17.335	0.214	0.0701	0.0588	0.00390	659.6	8.064	9.486	0.219	0.2779	0.1975	0.02467
199.6	16.944	17.361	0.311	0.0729	0.0623	0.00267	664.2	8.017	9.378	0.204	0.2790	0.1980	0.02461
204.2	16.825	17.227	0.290	0.0756	0.0644	0.00402	668.8	7.970	9.238	0.198	0.2800	0.1974	0.02547
208.8	16.706	17.189	0.316	0.0784	0.0674	0.00320	673.4	7.924	9.096	0.192	0.2811	0.1966	0.02496
213.4	16.587	17.047	0.243	0.0811	0.0693	0.00457	678	7.879	8.958	0.181	0.2822	0.1959	0.02667
218	16.467	17.080	0.277	0.0839	0.0724	0.00403	682.6	7.834	8.796	0.174	0.2832	0.2007	0.02629
222.6	16.346	16.931	0.151	0.0867	0.0745	0.00537	687.2	7.790	8.652	0.178	0.2842	0.2026	0.02798
227.2	16.226	16.951	0.251	0.0894	0.0771	0.00462	691.8	7.746	8.508	0.181	0.2852	0.2059	0.02865
231.8	16.105	17.008	0.288	0.0922	0.0805	0.00416	696.4	7.703	8.359	0.177	0.2862	0.2089	0.02910
236.4	15.984	16.877	0.316	0.0950	0.0824	0.00506	701	7.660	8.195	0.169	0.2872	0.2104	0.02912
241	15.863	16.780	0.332	0.0978	0.0831	0.00562	705.6	7.618	8.034	0.161	0.2882	0.2165	0.03093
245.6	15.742	16.751	0.232	0.1006	0.0858	0.00573	710.2	7.576	7.962	0.167	0.2891	0.2191	0.03207
250.2	15.621	16.705	0.364	0.1034	0.0880	0.00650	714.8	7.535	7.884	0.206	0.2901	0.2239	0.03303
254.8	15.501	16.814	0.286	0.1062	0.0919	0.00691	719.4	7.495	7.757	0.195	0.2910	0.2262	0.03331
259.4	15.380	16.481	0.247	0.1090	0.0914	0.00633	724	7.455	7.717	0.206	0.2919	0.2315	0.03415
264	15.260	16.392	0.202	0.1117	0.0931	0.00667	728.6	7.415	7.662	0.232	0.2929	0.2338	0.03596
268.6	15.140	16.382	0.231	0.1145	0.0948	0.00797	733.2	7.376	7.587	0.234	0.2938	0.2364	0.03651
273.2	15.021	16.092	0.407	0.1173	0.0943	0.00723	737.8	7.338	7.559	0.243	0.2946	0.2372	0.03832
277.8	14.902	16.259	0.293	0.1200	0.0991	0.00810	742.4	7.300	7.531	0.270	0.2955	0.2386	0.03639
282.4	14.783	16.049	0.348	0.1228	0.1001	0.00658	747	7.262	7.487	0.244	0.2964	0.2375	0.03633
287	14.665	15.622	0.196	0.1255	0.0985	0.00855	751.6	7.225	7.461	0.270	0.2972	0.2377	0.03642
291.6	14.547	15.620	0.294	0.1282	0.1015	0.00706	756.2	7.189	7.487	0.296	0.2981	0.2383	0.03671
296.2	14.430	15.448	0.300	0.1309	0.1034	0.00897	760.8	7.153	7.410	0.263	0.2989	0.2352	0.03615
300.8	14.314	15.037	0.294	0.1336	0.1021	0.00987	765.4	7.117	7.361	0.262	0.2997	0.2331	0.03553
305.4	14.198	15.113	0.300	0.1363	0.1058	0.00982	770	7.082	7.344	0.283	0.3006	0.2317	0.03550
310	14.083	14.938	0.341	0.1389	0.1072	0.00997	774.6	7.047	7.288	0.280	0.3014	0.2294	0.03555
314.6	13.969	14.853	0.353	0.1415	0.1094	0.01020	779.2	7.012	7.238	0.292	0.3022	0.2272	0.03480
319.2	13.855	14.801	0.450	0.1442	0.1129	0.01188	783.8	6.979	7.157	0.267	0.3028	0.2253	0.03478
323.8	13.743	14.506	0.274	0.1468	0.1134	0.01131	788.4	6.945	7.082	0.264	0.3037	0.2237	0.03419
328.4	13.631	14.613	0.330	0.1494	0.1178	0.01177	793	6.912	6.991	0.289	0.3045	0.2226	0.03412
333	13.520	14.591	0.388	0.1519	0.1215	0.01371	797.6	6.879	6.885	0.280	0.3052	0.2216	0.03456
337.6	13.410	14.373	0.438	0.1545	0.1231	0.01275	802.2	6.847	6.780	0.285	0.3060	0.2214	0.03449
342.2	13.300	14.425	0.523	0.1570	0.1273	0.01509	806.8	6.815	6.858	0.284	0.3067	0.2219	0.03438
346.8	13.192	14.474	0.481	0.1595	0.1316	0.01563	811.4	6.784	6.546	0.296	0.3074	0.2238	0.03538
351.4	13.085	14.427	0.385	0.1620	0.1354	0.01571	816	6.752	6.424	0.319	0.3082	0.2247	0.03512
356	12.978	14.451	0.653	0.1644	0.1388	0.01730	820.6	6.722	6.304	0.333	0.3089	0.2267	0.03617
360.6	12.873	14.321	0.566	0.1669	0.1407	0.01769	825.2	6.691	6.145	0.314	0.3096	0.2290	0.03646
365.2	12.768	14.469	0.633	0.1693	0.1447	0.01812	829.8	6.661	6.023	0.335	0.3103	0.2327	0.03692
369.8	12.664	14.551	0.759	0.1717	0.1471	0.01833	834.4	6.632	5.956	0.391	0.3109	0.2375	0.03810
374.4	12.562	14.402	0.644	0.1740	0.1484	0.01778	839	6.602	5.844	0.402	0.3116	0.2425	0.03865
379	12.460	14.280	0.656	0.1764	0.1492	0.01731	843.6	6.574	5.710	0.410	0.3123	0.2458	0.03977
383.6	12.360	14.198	0.794	0.1787	0.1503	0.01821	848.2	6.546	5.644	0.456	0.3129	0.2520	0.04011
388.2	12.260	14.002	0.772	0.1810	0.1503	0.01762	852.8	6.517	5.572	0.483	0.3136	0.2569	0.04189
392.8	12.161	13.903	0.681	0.1833	0.1502	0.01688	857.4	6.488	5.567	0.537	0.3142	0.2634	0.04123
397.4	12.064	13.755	0.878	0.1855	0.1507	0.01640	862	6.461	5.460	0.593	0.3149	0.2673	0.04241
402	11.967	13.437	0.812	0.1878	0.1502	0.01618	866.6	6.434	5.438	0.573	0.3155	0.2719	0.04167

APPENDIX E

MATLAB CODE: FIELD INSTRUMENT REFLECTION CALCULATIONS

```
% Reflection Calculator

% This program calculates soil reflection coefficients from the outdoor
% network analyzer measurements.
% Written by Duane Needham
% May 21, 2003

% numeric constants
e = 8.854*10^-12;
u = 4*pi*10^-7;
Zo = 50;
Zfree = (u/e)^0.5;

% This portion determines the characteristics of the coaxial line and
% cell with air

plot14      %recalls calibrating freq, mag, and
            %phase measurements stored in the file "plot14.m"

f = 1000000*A(:,1);
w = 2*pi*f;

% Reflection of antenna 1 from sky
M = A(:,2);
p = A(:,3);
r1 = (M.*cos(pi/180*p))+(j*M.*sin(pi/180*p));

% Transmission -- sky
M = A(:,4);
p = A(:,5);
t1 = (M.*cos(pi/180*p))+(j*M.*sin(pi/180*p));

% Reflection -- metal
M = A(:,6);
p = A(:,7);
r2 = (M.*cos(pi/180*p))+(j*M.*sin(pi/180*p));
Const1 = -(r2-r1);

% Transmission -- metal
M = A(:,8);
p = A(:,9);
t2 = (M.*cos(pi/180*p))+(j*M.*sin(pi/180*p));
Const2 = -(t2-t1);

% Reflection from soil
```

```

M = A(:,10);
p = A(:,11);
r3 = (M.*cos(pi/180*p))+(j*M.*sin(pi/180*p));
rs1 = (r3-r1)./Const1;

% Transmission from soil
M = A(:,12);
p = A(:,13);
t3 = (M.*cos(pi/180*p))+(j*M.*sin(pi/180*p));
rs2 = (t3-t1)./Const2;

plot (real(r1),imag(r1))
    xlabel('Real Part of Reflection Coefficient')
    ylabel('Imaginary Part of Reflection Coefficient')
pause
plot (real(r2),imag(r2))
    xlabel('Real Part of Reflection Coefficient')
    ylabel('Imaginary Part of Reflection Coefficient')
pause
plot (real(Const1),imag(Const1))
pause
plot (real(r3),imag(r3))
pause
plot (real(r3-r1),imag(r3-r1))
pause
plot (real(rs1),imag(rs1))
pause
plot (real(t1),imag(t1))
    xlabel('Real Part of Transmission Coefficient')
    ylabel('Imaginary Part of Transmission Coefficient')
pause
plot (real(t2),imag(t2))
    xlabel('Real Part of Transmission Coefficient')
    ylabel('Imaginary Part of Transmission Coefficient')
pause
plot (real(Const2),imag(Const2))
pause
plot (real(t3),imag(t3))
pause
plot (real(t3-t1),imag(t3-t1))
pause
plot (real(rs2),imag(rs2))
    xlabel('Real Part of Reflection Coefficient')
    ylabel('Imaginary Part of Reflection Coefficient')
real(rs2)
pause
imag(rs2)

```

APPENDIX F

FIELD INSTRUMENT CALIBRATION DATA

Average Complex Components of Calibration Measurements								
Freq(MHz)	Sky reflection		Sky transmission		Metal reflection		Metal transmission	
	Real	Imaginary	Real	Imaginary	Real	Imaginary	Real	Imaginary
80	0.2059	0.4354	0.0051	0.0080	0.2195	0.4450	-0.0127	0.0026
84.6	-0.0875	-0.0630	0.0284	0.0009	-0.0208	-0.0404	-0.0147	0.0491
89.2	0.0898	0.0990	0.0261	-0.0066	0.1446	0.1510	0.0012	0.0589
93.8	-0.0034	0.0558	0.0290	0.0055	0.0164	0.1346	-0.0109	0.0685
98.4	-0.0803	0.6603	0.0234	0.0159	-0.1160	0.1324	-0.0304	0.0643
103	-0.0451	-0.0311	0.0092	0.0257	-0.1187	-0.0133	-0.0535	0.0411
107.6	-0.0228	-0.1002	-0.0056	0.0231	-0.0777	-0.1481	-0.0681	0.0080
112.2	0.0927	0.0262	-0.0192	0.0106	0.1102	-0.0464	-0.0600	-0.0394
116.8	0.0348	0.0156	-0.0209	-0.0053	0.1021	0.0011	-0.0182	-0.0730
121.4	-0.0981	0.1047	-0.0052	-0.0172	-0.0628	0.1619	0.0422	-0.0622
126	0.0084	-0.1215	0.0124	-0.0105	-0.0361	-0.0759	0.0779	-0.0039
130.6	0.0247	0.0080	0.0119	0.0068	-0.0235	-0.0280	0.0510	0.0557
135.2	0.0801	0.0750	-0.0018	0.0158	0.1105	0.0228	-0.0247	0.0656
139.8	-0.1514	-0.0442	-0.0131	0.0031	-0.1036	-0.0173	-0.0704	0.0049
144.4	0.1196	0.0037	-0.0057	-0.0105	0.0906	0.0470	-0.0305	-0.0617
149	-0.0201	-0.0078	0.0079	-0.0073	-0.0585	-0.0409	0.0497	-0.0492
153.6	-0.0034	0.0750	0.0072	0.0069	0.0337	0.0388	0.0629	0.0326
158.2	-0.0245	-0.0859	-0.0066	0.0077	0.0039	-0.0406	-0.0138	0.0687
162.8	0.0812	0.0512	-0.0079	-0.0060	0.0331	0.0695	-0.0671	0.0021
167.4	-0.0237	0.0089	0.0055	-0.0079	-0.0283	-0.0428	-0.0142	-0.0645
172	-0.0637	-0.0383	0.0064	0.0059	-0.0080	-0.0255	0.0600	-0.0259
176.6	0.1493	0.0011	-0.0053	0.0074	0.1273	0.0424	0.0322	0.0500
181.2	-0.1357	0.0459	-0.0060	-0.0050	-0.1656	0.0125	-0.0418	0.0310
185.8	0.1065	-0.0667	0.0060	-0.0052	0.1552	-0.0821	-0.0303	-0.0427
190.4	-0.0423	0.0133	0.0048	0.0068	-0.0409	0.0624	0.0395	-0.0337
195	0.0380	0.0698	-0.0080	0.0064	-0.0078	0.0434	0.0371	0.0294
199.6	-0.1107	-0.1125	-0.0026	-0.0031	-0.0904	-0.1296	-0.0198	0.0157
204.2	0.0458	0.1296	0.0060	-0.0005	0.0439	0.1706	-0.0204	-0.0323
208.8	-0.0565	-0.1094	-0.0010	0.0056	-0.0886	-0.1289	0.0303	-0.0153
213.4	0.0386	0.0612	-0.0051	-0.0027	0.0798	0.0444	0.0117	0.0334
218	0.0188	0.0071	0.0033	-0.0038	0.0178	0.0619	-0.0322	0.0086
222.6	-0.0708	-0.0433	0.0021	0.0028	-0.1029	-0.0630	-0.0024	-0.0288
227.2	0.1330	0.0538	-0.0039	-0.0019	0.1684	0.0452	0.0278	0.0044
231.8	-0.1572	-0.0378	0.0024	-0.0034	-0.1704	-0.0076	-0.0090	0.0254
236.4	0.1803	0.0218	0.0019	0.0034	0.1708	-0.0085	-0.0208	-0.0120
241	-0.1357	-0.0221	-0.0041	0.0000	-0.0986	-0.0089	0.0160	-0.0157
245.6	0.0969	-0.0181	0.0017	-0.0038	0.0663	0.0026	0.0096	0.0182
250.2	-0.0552	-0.0026	0.0031	0.0035	-0.0500	-0.0340	-0.0206	0.0037
254.8	-0.0047	0.0391	-0.0046	0.0017	0.0131	0.0652	0.0018	-0.0211
259.4	0.0644	-0.0815	-0.0005	-0.0046	0.0340	-0.0844	0.0203	0.0063
264	-0.0940	0.0962	0.0033	0.0017	-0.0682	0.0769	-0.0093	0.0140
268.6	0.1005	-0.1092	-0.0031	0.0015	0.0997	-0.0791	-0.0060	-0.0132
273.2	-0.1122	0.1033	0.0006	-0.0034	-0.1261	0.0817	0.0159	0.0017
277.8	0.0989	-0.0709	0.0025	0.0023	0.1233	-0.0594	-0.0087	0.0156
282.4	-0.0758	0.0435	-0.0031	0.0010	-0.1013	0.0496	-0.0123	-0.0143
287	0.0520	0.0214	0.0004	-0.0030	0.0679	-0.0037	0.0176	-0.0057
291.6	-0.0091	-0.0498	0.0019	0.0009	-0.0002	-0.0181	-0.0008	0.0184
296.2	0.0232	0.0919	-0.0004	-0.0016	-0.0034	0.0773	-0.0159	-0.0056
300.8	0.0156	-0.1256	0.0027	-0.0017	0.0434	-0.1309	0.0131	-0.0088
305.4	0.0050	0.1182	0.0004	0.0029	-0.0091	0.1352	0.0024	0.0158
310	0.0105	-0.1432	-0.0025	-0.0012	0.0163	-0.1662	-0.0148	-0.0050
314.6	-0.0070	0.1159	0.0024	-0.0013	0.0014	0.1363	0.0108	-0.0092
319.2	0.0161	-0.1278	-0.0005	0.0026	-0.0039	-0.1378	0.0011	0.0136
323.8	-0.0437	0.0679	-0.0017	-0.0021	-0.0191	0.0627	-0.0128	-0.0075
328.4	0.0092	-0.0301	0.0030	0.0000	-0.0061	-0.0082	0.0140	-0.0089
333	-0.0342	0.0167	-0.0022	0.0030	-0.0116	-0.0031	0.0031	0.0155
337.6	0.0536	0.0437	-0.0029	-0.0031	0.0666	0.0641	-0.0118	-0.0045
342.2	-0.0317	-0.0609	0.0026	-0.0011	-0.0496	-0.0670	0.0117	-0.0058
346.8	0.0154	0.0784	-0.0008	0.0015	0.0374	0.0726	0.0007	0.0144
351.4	-0.0080	-0.0807	-0.0001	-0.0015	-0.0207	-0.0636	-0.0111	-0.0055
356	-0.0041	0.0830	0.0010	0.0012	-0.0021	0.0615	0.0106	-0.0053
360.6	0.0181	-0.0589	-0.0016	-0.0002	0.0276	-0.0405	-0.0019	0.0117
365.2	-0.0169	0.0331	0.0013	-0.0011	-0.0333	0.0233	-0.0090	-0.0064
369.8	0.0154	-0.0140	0.0001	0.0016	0.0358	-0.0147	0.0122	-0.0031
374.4	-0.0284	-0.0054	-0.0011	-0.0008	-0.0528	0.0058	-0.0038	0.0119
379	0.0389	0.0559	0.0010	-0.0003	0.0465	0.0396	-0.0075	-0.0092
383.6	-0.0276	-0.0589	-0.0004	0.0005	-0.0230	-0.0430	0.0114	-0.0010
388.2	0.0446	0.0842	0.0003	-0.0010	0.0353	0.0718	-0.0050	0.0094
392.8	-0.0262	-0.0956	0.0007	0.0008	-0.0107	-0.0909	-0.0042	-0.0087
397.4	0.0333	0.1047	-0.0010	-0.0001	0.0189	0.1049	0.0089	0.0017
402	-0.0028	-0.1139	0.0008	-0.0007	0.0100	-0.1198	-0.0061	0.0054
406.6	0.0078	0.0892	-0.0001	0.0010	-0.0001	0.0980	-0.0003	-0.0073
411.2	-0.0021	-0.1083	-0.0006	-0.0007	0.0014	-0.1200	0.0052	0.0045
415.8	-0.0154	0.0751	0.0009	0.0001	-0.0132	0.0987	-0.0089	0.0005
420.4	0.0024	-0.0796	-0.0008	0.0005	-0.0058	-0.0901	0.0049	-0.0062
425	-0.0447	0.0343	0.0002	-0.0009	-0.0315	0.0395	0.0026	0.0084
429.6	-0.0258	0.0063	0.0005	0.0009	-0.0080	-0.0017	-0.0092	-0.0025
434.2	0.0010	0.0235	-0.0011	-0.0002	0.0126	0.0157	0.0068	-0.0064
438.8	-0.0218	0.0391	0.0010	-0.0008	-0.0267	0.0495	0.0015	0.0086

Average Complex Components of Calibration Measurements								
Freq(MHz)	Sky reflection		Sky transmission		Metal reflection		Metal transmission	
	Real	Imaginary	Real	Imaginary	Real	Imaginary	Real	Imaginary
544.6	-0.0190	-0.0049	0.0003	0.0001	-0.0247	-0.0011	-0.0004	-0.0039
549.2	0.0294	0.0000	-0.0003	0.0001	0.0306	0.0017	0.0029	0.0026
553.8	-0.0173	0.0132	0.0002	-0.0002	-0.0191	0.0188	-0.0038	0.0001
558.4	0.0329	-0.0094	0.0000	0.0003	0.0324	-0.0156	0.0025	-0.0027
563	-0.0146	0.0256	-0.0002	-0.0003	-0.0208	0.0366	0.0001	0.0034
567.6	0.0556	-0.0106	0.0004	0.0001	0.0520	-0.0154	-0.0021	-0.0021
572.2	-0.0227	0.0285	-0.0003	0.0002	-0.0179	0.0289	0.0026	0.0003
576.8	0.0828	-0.0185	0.0000	-0.0003	0.0770	-0.0204	-0.0022	0.0012
581.4	-0.0459	-0.0057	0.0001	0.0002	-0.0413	-0.0076	0.0011	-0.0023
586	0.0760	0.0044	-0.0001	-0.0001	0.0707	0.0055	0.0007	0.0025
590.6	-0.0459	-0.0279	0.0001	0.0001	-0.0420	-0.0299	-0.0022	-0.0014
595.2	0.0628	0.0232	-0.0001	0.0000	0.0596	0.0247	0.0025	-0.0004
599.8	-0.0378	-0.0428	0.0001	0.0000	-0.0349	-0.0463	-0.0015	0.0019
604.4	0.0433	0.0370	-0.0001	0.0001	0.0411	0.0402	-0.0001	-0.0023
609	-0.0233	-0.0452	0.0001	-0.0001	-0.0210	-0.0495	0.0014	0.0015
613.6	0.0301	0.0429	0.0000	0.0002	0.0293	0.0452	-0.0019	-0.0004
618.2	-0.0103	-0.0489	-0.0001	-0.0001	-0.0102	-0.0539	0.0017	-0.0008
622.8	0.0081	0.0497	0.0001	0.0001	0.0089	0.0518	-0.0009	0.0016
627.4	0.0143	-0.0380	-0.0001	0.0000	0.0118	-0.0416	-0.0003	-0.0019
632	-0.0022	0.0392	0.0001	0.0000	0.0011	0.0405	0.0015	0.0014
636.6	0.0323	-0.0258	-0.0001	0.0001	0.0283	-0.0275	-0.0022	-0.0001
641.2	-0.0066	0.0137	0.0001	-0.0001	-0.0019	0.0131	0.0018	-0.0015
645.8	0.0299	0.0066	0.0000	0.0001	0.0248	-0.0114	-0.0002	0.0023
650.4	-0.0073	-0.0060	-0.0001	-0.0001	-0.0035	-0.0086	-0.0014	-0.0018
655	0.0103	0.0099	0.0001	0.0000	0.0075	0.0112	0.0021	0.0003
659.6	0.0153	-0.0074	-0.0001	0.0000	0.0170	-0.0119	-0.0016	0.0010
664.2	-0.0042	0.0069	0.0000	0.0000	-0.0050	0.0093	0.0005	-0.0017
668.8	0.0256	0.0039	-0.0001	0.0000	0.0248	-0.0003	0.0005	0.0015
673.4	-0.0020	0.0023	0.0001	-0.0001	-0.0012	0.0048	-0.0013	-0.0009
678	0.0358	0.0079	0.0001	0.0001	0.0343	0.0049	0.0016	-0.0001
682.6	0.0015	-0.0103	-0.0001	0.0000	0.0038	-0.0089	-0.0012	0.0011
687.2	0.0116	0.0083	0.0001	0.0000	0.0345	0.0044	0.0003	-0.0016
691.8	0.0008	-0.0244	-0.0001	0.0001	0.0038	-0.0239	0.0008	0.0014
696.4	0.0304	0.0097	0.0000	-0.0001	0.0193	0.0023	-0.0015	-0.0006
701	0.0028	-0.0365	0.0000	0.0001	0.0058	-0.0370	0.0015	-0.0004
705.6	0.0154	0.0149	-0.0001	-0.0001	0.0120	0.0145	-0.0009	0.0012
710.2	0.0136	-0.0387	0.0001	0.0000	0.0160	-0.0403	0.0000	-0.0015
714.8	-0.0030	0.0099	-0.0001	0.0000	-0.0051	0.0111	0.0009	0.0012
719.4	0.0228	-0.0303	0.0001	-0.0001	0.0221	-0.0100	-0.0014	-0.0004
724	-0.0206	-0.0067	0.0000	0.0001	-0.0202	-0.0044	0.0014	-0.0005
728.6	0.0124	-0.0029	0.0000	-0.0001	0.0149	0.0031	-0.0007	0.0013
733.2	-0.0104	-0.0057	0.0001	0.0001	-0.0090	-0.0038	-0.0003	-0.0014
737.8	0.0137	0.0097	-0.0001	0.0000	0.0122	0.0067	0.0011	0.0009
742.4	0.0062	-0.0150	0.0001	0.0000	0.0081	-0.0137	-0.0014	0.0000
747	0.0029	0.0070	0.0000	0.0001	0.0002	0.0047	0.0010	-0.0009
751.6	0.0142	-0.0139	0.0000	-0.0001	0.0185	-0.0133	-0.0001	0.0012
756.2	-0.0054	0.0013	0.0001	0.0001	-0.0080	0.0006	-0.0006	-0.0009
760.8	0.0142	-0.0005	-0.0001	0.0000	0.0161	-0.0098	0.0009	0.0003
765.4	-0.0137	0.0037	0.0001	-0.0001	-0.0152	0.0041	-0.0009	0.0003
770	0.0234	0.0044	0.0000	0.0001	0.0245	0.0033	0.0005	-0.0007
774.6	-0.0083	-0.0013	0.0000	-0.0001	-0.0087	-0.0007	0.0000	0.0008
779.2	0.0296	0.0158	0.0000	0.0000	0.0240	0.0034	-0.0005	-0.0006
783.8	-0.0068	-0.0240	0.0000	0.0000	-0.0068	-0.0229	0.0007	0.0003
788.4	0.0119	0.0109	0.0000	0.0000	0.0171	0.0164	-0.0007	0.0002
793	0.0079	-0.0272	0.0000	0.0000	0.0079	-0.0260	0.0005	-0.0006
797.6	0.0063	0.0175	0.0000	0.0000	0.0055	0.0152	0.0000	0.0008
802.2	0.0207	-0.0253	0.0000	0.0000	0.0214	-0.0238	-0.0005	-0.0007
806.8	-0.0037	0.0028	0.0000	0.0000	-0.0047	0.0008	0.0008	0.0002
811.4	0.0165	-0.0079	0.0000	0.0000	0.0010	-0.0032	-0.0007	0.0003
816	-0.0067	-0.0030	0.0000	0.0000	-0.0083	-0.0043	0.0004	-0.0007
820.6	0.0136	-0.0113	0.0000	0.0000	0.0148	-0.0107	0.0001	0.0007
825.2	-0.0074	-0.0067	0.0000	0.0000	-0.0091	-0.0071	-0.0005	-0.0005
829.8	0.0103	0.0016	0.0000	0.0000	0.0088	-0.0067	0.0007	0.0001
834.4	-0.0082	-0.0053	0.0000	0.0000	-0.0100	-0.0048	-0.0006	0.0003
839	0.0060	0.0008	0.0000	0.0000	0.0067	0.0000	0.0003	-0.0006
843.6	-0.0052	-0.0092	0.0000	0.0000	-0.0067	-0.0079	0.0002	0.0007
848.2	-0.0072	0.0064	0.0000	0.0000	-0.0066	0.0054	-0.0005	-0.0004
852.8	-0.0009	0.0048	0.0000	0.0000	-0.0017	0.0063	0.0007	0.0000
857.4	-0.0051	0.0160	0.0000	0.0000	-0.0050	0.0149	-0.0005	0.0004
862	0.0209	0.0179	0.0000	0.0000	0.0203	0.0192	0.0001	-0.0006
866.6	0.0120	-0.0024	0.0000	0.0000	0.0117	-0.0032	0.0003	0.0005
871.2	0.0191	0.0105	0.0000	0.0000	0.0188	0.0115	-0.0004	-0.0002
875.8	0.0163	-0.0165	-0.0001	0.0000	0.0155	-0.0170	0.0004	0.0000
880.4	0.0032	0.0052	0.0000	0.0000	0.0035	0.0059	-0.0003	0.0002
885	0.0163	-0.0127	0.0000	0.0000	0.0149	-0.0127	0.0002	-0.0004
889.6	-0.0049	0.0030	0.0000	0.0000	-0.0041	0.0035	0.0001	0.0004
894.2	0.0168	-0.0034	0.0000	0.0000	0.0153	-0.0032	-0.0002	-0.0003
898.8	-0.0036	0.0010	0.0000	0.0000	-0.0027	0.0013	0.0004	0.0001
903.4	0.0182	0.0013	0.0000	0.0000	0.0164	0.0016	-0.0004	0.0001

Standard Deviation of Complex Components of Calibration Measurements								
Freq(MHz)	Sky reflection		Sky transmission		Metal reflection		Metal transmission	
	Real	Imaginary	Real	Imaginary	Real	Imaginary	Real	Imaginary
80	0.0248	0.0119	0.0022	0.0015	0.0222	0.0083	0.0034	0.0020
84.6	0.0089	0.0044	0.0009	0.0018	0.0120	0.0067	0.0021	0.0039
89.2	0.0054	0.0073	0.0007	0.0015	0.0075	0.0077	0.0028	0.0027
93.8	0.0033	0.0026	0.0007	0.0009	0.0051	0.0046	0.0044	0.0031
98.4	0.0046	0.0036	0.0008	0.0009	0.0070	0.0083	0.0038	0.0051
103	0.0054	0.0038	0.0010	0.0005	0.0079	0.0080	0.0028	0.0053
107.6	0.0051	0.0047	0.0010	0.0004	0.0115	0.0076	0.0019	0.0045
112.2	0.0029	0.0129	0.0005	0.0009	0.0096	0.0137	0.0029	0.0037
116.8	0.0039	0.0065	0.0014	0.0009	0.0071	0.0107	0.0043	0.0020
121.4	0.0046	0.0046	0.0010	0.0003	0.0124	0.0060	0.0033	0.0035
126	0.0133	0.0082	0.0004	0.0009	0.0110	0.0076	0.0021	0.0047
130.6	0.0090	0.0087	0.0011	0.0011	0.0077	0.0090	0.0042	0.0033
135.2	0.0090	0.0082	0.0013	0.0008	0.0185	0.0121	0.0052	0.0030
139.8	0.0123	0.0221	0.0008	0.0009	0.0077	0.0264	0.0036	0.0051
144.4	0.0228	0.0290	0.0012	0.0009	0.0260	0.0240	0.0049	0.0048
149	0.0411	0.0068	0.0019	0.0021	0.0352	0.0052	0.0029	0.0060
153.6	0.0358	0.0219	0.0014	0.0010	0.0308	0.0186	0.0062	0.0055
158.2	0.0167	0.0253	0.0005	0.0006	0.0221	0.0228	0.0067	0.0033
162.8	0.0042	0.0242	0.0005	0.0005	0.0037	0.0264	0.0014	0.0065
167.4	0.0085	0.0129	0.0006	0.0004	0.0104	0.0147	0.0061	0.0016
172	0.0090	0.0082	0.0011	0.0002	0.0099	0.0081	0.0016	0.0073
176.6	0.0103	0.0164	0.0005	0.0007	0.0083	0.0152	0.0057	0.0029
181.2	0.0025	0.0122	0.0006	0.0005	0.0119	0.0134	0.0030	0.0053
185.8	0.0085	0.0159	0.0005	0.0006	0.0099	0.0194	0.0054	0.0035
190.4	0.0036	0.0040	0.0008	0.0003	0.0059	0.0062	0.0038	0.0049
195	0.0078	0.0116	0.0005	0.0012	0.0072	0.0187	0.0041	0.0042
199.6	0.0121	0.0100	0.0006	0.0004	0.0233	0.0093	0.0016	0.0031
204.2	0.0143	0.0102	0.0002	0.0007	0.0210	0.0085	0.0050	0.0020
208.8	0.0179	0.0048	0.0007	0.0002	0.0253	0.0089	0.0017	0.0048
213.4	0.0066	0.0099	0.0004	0.0007	0.0045	0.0155	0.0052	0.0012
218	0.0019	0.0189	0.0005	0.0005	0.0070	0.0061	0.0010	0.0051
222.6	0.0111	0.0067	0.0004	0.0003	0.0153	0.0109	0.0047	0.0007
227.2	0.0090	0.0187	0.0005	0.0006	0.0080	0.0258	0.0013	0.0045
231.8	0.0088	0.0184	0.0005	0.0004	0.0090	0.0206	0.0040	0.0020
236.4	0.0053	0.0299	0.0005	0.0002	0.0050	0.0307	0.0024	0.0035
241	0.0080	0.0165	0.0001	0.0006	0.0091	0.0118	0.0023	0.0030
245.6	0.0037	0.0194	0.0005	0.0004	0.0035	0.0173	0.0034	0.0015
250.2	0.0041	0.0055	0.0006	0.0003	0.0136	0.0048	0.0005	0.0037
254.8	0.0042	0.0046	0.0001	0.0007	0.0065	0.0055	0.0038	0.0011
259.4	0.0161	0.0137	0.0009	0.0002	0.0193	0.0116	0.0020	0.0034
264	0.0123	0.0117	0.0004	0.0005	0.0078	0.0082	0.0025	0.0022
268.6	0.0185	0.0206	0.0002	0.0006	0.0183	0.0222	0.0027	0.0011
273.2	0.0144	0.0155	0.0005	0.0002	0.0083	0.0191	0.0010	0.0030
277.8	0.0131	0.0215	0.0005	0.0004	0.0142	0.0269	0.0025	0.0023
282.4	0.0055	0.0089	0.0002	0.0006	0.0029	0.0166	0.0032	0.0021
287	0.0020	0.0139	0.0005	0.0002	0.0065	0.0174	0.0011	0.0036
291.6	0.0126	0.0039	0.0003	0.0003	0.0111	0.0053	0.0036	0.0012
296.2	0.0140	0.0081	0.0002	0.0002	0.0103	0.0059	0.0020	0.0033
300.8	0.0263	0.0079	0.0003	0.0005	0.0304	0.0122	0.0017	0.0031
305.4	0.0187	0.0047	0.0005	0.0001	0.0228	0.0070	0.0035	0.0009
310	0.0292	0.0063	0.0003	0.0005	0.0362	0.0079	0.0017	0.0032
314.6	0.0202	0.0053	0.0002	0.0005	0.0245	0.0072	0.0019	0.0027
319.2	0.0257	0.0077	0.0005	0.0002	0.0315	0.0057	0.0031	0.0009
323.8	0.0121	0.0052	0.0004	0.0003	0.0110	0.0048	0.0022	0.0028
328.4	0.0094	0.0102	0.0001	0.0006	0.0061	0.0083	0.0019	0.0033
333	0.0023	0.0040	0.0006	0.0005	0.0330	0.0104	0.0037	0.0009
337.6	0.0056	0.0152	0.0007	0.0005	0.0104	0.0183	0.0016	0.0026
342.2	0.0165	0.0039	0.0002	0.0006	0.0215	0.0066	0.0011	0.0030
346.8	0.0141	0.0088	0.0003	0.0002	0.0131	0.0134	0.0036	0.0006
351.4	0.0219	0.0050	0.0003	0.0000	0.0218	0.0047	0.0017	0.0026
356	0.0142	0.0057	0.0003	0.0002	0.0095	0.0088	0.0012	0.0029
360.6	0.0167	0.0088	0.0001	0.0003	0.0162	0.0121	0.0031	0.0008
365.2	0.0064	0.0049	0.0002	0.0003	0.0033	0.0057	0.0024	0.0022
369.8	0.0077	0.0112	0.0004	0.0000	0.0103	0.0162	0.0008	0.0034
374.4	0.0279	0.0050	0.0002	0.0003	0.0071	0.0091	0.0032	0.0012
379	0.0090	0.0151	0.0001	0.0003	0.0053	0.0177	0.0026	0.0021
383.6	0.0194	0.0035	0.0001	0.0001	0.0197	0.0053	0.0006	0.0031
388.2	0.0156	0.0153	0.0003	0.0001	0.0130	0.0144	0.0025	0.0015
392.8	0.0283	0.0036	0.0002	0.0002	0.0311	0.0051	0.0025	0.0011
397.4	0.0218	0.0119	0.0000	0.0003	0.0216	0.0099	0.0006	0.0025
402	0.0319	0.0049	0.0001	0.0002	0.0371	0.0091	0.0016	0.0018
406.6	0.0200	0.0088	0.0003	0.0000	0.0221	0.0089	0.0022	0.0005
411.2	0.0305	0.0052	0.0002	0.0001	0.0380	0.0070	0.0014	0.0015
415.8	0.0184	0.0056	0.0001	0.0002	0.0204	0.0075	0.0004	0.0021
420.4	0.0230	0.0084	0.0001	0.0002	0.0297	0.0071	0.0019	0.0014
425	0.0067	0.0045	0.0003	0.0001	0.0072	0.0043	0.0026	0.0008
429.6	0.0049	0.0031	0.0003	0.0001	0.0408	0.0180	0.0009	0.0027
434.2	0.0009	0.0089	0.0001	0.0003	0.0045	0.0120	0.0020	0.0021
438.8	0.0036	0.0043	0.0002	0.0003	0.0059	0.0065	0.0027	0.0007

Standard Deviation of Complex Components of Calibration Measurements								
Freq(MHz)	Sky reflection		Sky transmission		Metal reflection		Metal transmission	
	Real	Imaginary	Real	Imaginary	Real	Imaginary	Real	Imaginary
544.6	0.0075	0.0064	0.0001	0.0001	0.0099	0.0079	0.0015	0.0003
549.2	0.0088	0.0165	0.0000	0.0001	0.0165	0.0176	0.0011	0.0010
553.8	0.0033	0.0058	0.0001	0.0001	0.0044	0.0073	0.0003	0.0015
558.4	0.0122	0.0179	0.0001	0.0000	0.0166	0.0178	0.0010	0.0011
563	0.0222	0.0174	0.0001	0.0001	0.0048	0.0091	0.0014	0.0003
567.6	0.0137	0.0255	0.0001	0.0001	0.0185	0.0253	0.0010	0.0008
572.2	0.0037	0.0102	0.0001	0.0001	0.0044	0.0105	0.0003	0.0011
576.8	0.0149	0.0334	0.0001	0.0000	0.0185	0.0330	0.0005	0.0010
581.4	0.0086	0.0169	0.0001	0.0000	0.0119	0.0160	0.0009	0.0006
586	0.0070	0.0340	0.0001	0.0000	0.0092	0.0334	0.0011	0.0003
590.6	0.0177	0.0156	0.0000	0.0000	0.0218	0.0153	0.0007	0.0009
595.2	0.0059	0.0303	0.0000	0.0001	0.0087	0.0300	0.0002	0.0011
599.8	0.0245	0.0126	0.0000	0.0001	0.0287	0.0122	0.0008	0.0007
604.4	0.0095	0.0227	0.0000	0.0001	0.0096	0.0237	0.0010	0.0002
609	0.0259	0.0075	0.0001	0.0000	0.0315	0.0079	0.0008	0.0006
613.6	0.0113	0.0186	0.0001	0.0000	0.0122	0.0193	0.0003	0.0009
618.2	0.0287	0.0055	0.0001	0.0000	0.0345	0.0065	0.0004	0.0008
622.8	0.0126	0.0107	0.0000	0.0000	0.0131	0.0117	0.0008	0.0005
627.4	0.0258	0.0109	0.0000	0.0001	0.0309	0.0109	0.0010	0.0003
632	0.0093	0.0080	0.0000	0.0001	0.0099	0.0085	0.0008	0.0007
636.6	0.0203	0.0178	0.0000	0.0001	0.0242	0.0177	0.0003	0.0011
641.2	0.0049	0.0067	0.0001	0.0000	0.0070	0.0080	0.0008	0.0009
645.8	0.0125	0.0209	0.0001	0.0000	0.0171	0.0143	0.0012	0.0003
650.4	0.0107	0.0058	0.0000	0.0000	0.0151	0.0069	0.0009	0.0007
655	0.0062	0.0109	0.0000	0.0000	0.0083	0.0107	0.0003	0.0011
659.6	0.0130	0.0121	0.0000	0.0000	0.0179	0.0136	0.0006	0.0008
664.2	0.0075	0.0069	0.0000	0.0000	0.0088	0.0076	0.0009	0.0004
668.8	0.0094	0.0164	0.0000	0.0000	0.0141	0.0173	0.0008	0.0003
673.4	0.0100	0.0076	0.0001	0.0000	0.0114	0.0081	0.0005	0.0007
678	0.0085	0.0198	0.0001	0.0000	0.0121	0.0202	0.0002	0.0008
682.6	0.0155	0.0074	0.0000	0.0001	0.0177	0.0084	0.0006	0.0006
687.2	0.0305	0.0166	0.0000	0.0000	0.0116	0.0193	0.0008	0.0002
691.8	0.0196	0.0075	0.0000	0.0000	0.0224	0.0082	0.0007	0.0004
696.4	0.0050	0.0175	0.0000	0.0000	0.0191	0.0174	0.0003	0.0008
701	0.0251	0.0081	0.0000	0.0000	0.0297	0.0090	0.0003	0.0008
705.6	0.0058	0.0128	0.0000	0.0000	0.0084	0.0122	0.0007	0.0005
710.2	0.0265	0.0113	0.0000	0.0001	0.0316	0.0129	0.0008	0.0002
714.8	0.0068	0.0075	0.0000	0.0000	0.0090	0.0079	0.0006	0.0005
719.4	0.0226	0.0162	0.0000	0.0000	0.0314	0.0332	0.0003	0.0008
724	0.0122	0.0072	0.0000	0.0000	0.0142	0.0083	0.0003	0.0008
728.6	0.0120	0.0130	0.0000	0.0000	0.0141	0.0176	0.0007	0.0004
733.2	0.0142	0.0054	0.0000	0.0000	0.0162	0.0063	0.0008	0.0002
737.8	0.0076	0.0126	0.0000	0.0001	0.0115	0.0131	0.0005	0.0006
742.4	0.0188	0.0091	0.0000	0.0000	0.0210	0.0106	0.0002	0.0008
747	0.0080	0.0079	0.0000	0.0000	0.0119	0.0086	0.0005	0.0005
751.6	0.0180	0.0132	0.0001	0.0000	0.0210	0.0149	0.0007	0.0002
756.2	0.0103	0.0061	0.0000	0.0000	0.0138	0.0067	0.0005	0.0004
760.8	0.0167	0.0192	0.0000	0.0001	0.0205	0.0161	0.0002	0.0005
765.4	0.0111	0.0066	0.0000	0.0000	0.0138	0.0074	0.0002	0.0005
770	0.0123	0.0179	0.0000	0.0000	0.0160	0.0192	0.0004	0.0003
774.6	0.0142	0.0073	0.0000	0.0000	0.0169	0.0074	0.0005	0.0001
779.2	0.0176	0.0187	0.0000	0.0000	0.0283	0.0211	0.0004	0.0003
783.8	0.0245	0.0075	0.0000	0.0000	0.0280	0.0075	0.0002	0.0004
788.4	0.0116	0.0197	0.0000	0.0000	0.0081	0.0159	0.0002	0.0004
793	0.0269	0.0091	0.0000	0.0000	0.0302	0.0098	0.0004	0.0003
797.6	0.0068	0.0095	0.0000	0.0000	0.0095	0.0103	0.0005	0.0001
802.2	0.0254	0.0151	0.0000	0.0000	0.0289	0.0164	0.0004	0.0003
806.8	0.0099	0.0065	0.0000	0.0000	0.0143	0.0071	0.0002	0.0005
811.4	0.0222	0.0225	0.0000	0.0000	0.0301	0.0261	0.0002	0.0005
816	0.0134	0.0061	0.0000	0.0000	0.0183	0.0071	0.0004	0.0003
820.6	0.0189	0.0136	0.0000	0.0000	0.0229	0.0155	0.0005	0.0001
825.2	0.0159	0.0056	0.0000	0.0000	0.0205	0.0068	0.0003	0.0003
829.8	0.0137	0.0166	0.0000	0.0000	0.0209	0.0130	0.0001	0.0005
834.4	0.0159	0.0049	0.0000	0.0000	0.0200	0.0066	0.0002	0.0004
839	0.0137	0.0106	0.0000	0.0000	0.0183	0.0124	0.0004	0.0002
843.6	0.0190	0.0054	0.0000	0.0000	0.0229	0.0060	0.0005	0.0001
848.2	0.0116	0.0057	0.0000	0.0000	0.0160	0.0067	0.0003	0.0004
852.8	0.0144	0.0079	0.0000	0.0000	0.0175	0.0083	0.0001	0.0005
857.4	0.0096	0.0063	0.0000	0.0000	0.0138	0.0071	0.0003	0.0004
862	0.0098	0.0160	0.0000	0.0000	0.0126	0.0173	0.0004	0.0001
866.6	0.0185	0.0094	0.0000	0.0000	0.0237	0.0101	0.0004	0.0002
871.2	0.0104	0.0137	0.0000	0.0000	0.0132	0.0151	0.0002	0.0003
875.8	0.0248	0.0115	0.0000	0.0000	0.0303	0.0126	0.0001	0.0003
880.4	0.0112	0.0071	0.0000	0.0000	0.0148	0.0089	0.0002	0.0002
885	0.0218	0.0134	0.0000	0.0000	0.0270	0.0141	0.0003	0.0001
889.6	0.0125	0.0063	0.0000	0.0000	0.0167	0.0075	0.0003	0.0001
894.2	0.0179	0.0150	0.0000	0.0000	0.0229	0.0151	0.0002	0.0002
898.8	0.0152	0.0064	0.0000	0.0000	0.0195	0.0073	0.0001	0.0003
903.4	0.0163	0.0155	0.0000	0.0000	0.0211	0.0160	0.0001	0.0003

APPENDIX G

SOIL HOMOGENEITY DATA

Average Dielectric Property Values									
Depth	Frequency	Plot 1		Plot 2		Plot 3		Plot 4	
		Permittivity	Conductivity	Permittivity	Conductivity	Permittivity	Conductivity	Permittivity	Conductivity
0.152	123.7	13.69	0.0414	14.50	0.0517	14.21	0.0442	14.41	0.0497
0.152	215.7	12.06	0.0439	12.79	0.0542	12.62	0.0468	13.58	0.0603
0.152	307.7	10.75	0.0397	10.98	0.0469	11.44	0.0437	13.27	0.0627
0.152	399.7	9.67	0.0406	9.47	0.0454	10.60	0.0461	12.72	0.0586
0.152	491.7	9.79	0.0553	9.23	0.0561	10.65	0.0557	11.83	0.0543
0.152	583.7	10.90	0.0762	9.80	0.0753	11.20	0.0709	11.33	0.0598
0.152	675.7	12.01	0.0844	10.67	0.0742	11.73	0.0798	11.07	0.0529
0.152	767.7	12.47	0.1040	10.46	0.0852	12.04	0.1172	10.58	0.0789
0.152	859.7	13.07	0.1219	10.37	0.1177	13.75	0.1734	10.50	0.1082
0.152	951.7	13.76	0.1123	11.49	0.1592	15.48	0.1213	11.39	0.1369
0.305	123.7	14.61	0.0459	14.38	0.0564	14.43	0.0483	13.06	0.0407
0.305	215.7	13.59	0.0536	13.25	0.0658	13.19	0.0535	12.15	0.0468
0.305	307.7	12.88	0.0532	12.35	0.0656	12.21	0.0516	11.77	0.0488
0.305	399.7	12.02	0.0519	11.47	0.0640	11.50	0.0539	11.38	0.0481
0.305	491.7	11.47	0.0520	11.04	0.0636	11.30	0.0564	10.87	0.0451
0.305	583.7	11.20	0.0590	10.89	0.0719	11.20	0.0609	10.45	0.0519
0.305	675.7	11.19	0.0630	11.01	0.0718	11.16	0.0653	10.45	0.0556
0.305	767.7	10.90	0.0832	10.56	0.0864	10.93	0.0889	10.02	0.0668
0.305	859.7	11.14	0.1302	10.39	0.1280	11.53	0.1369	9.85	0.0878
0.305	951.7	13.44	0.1622	11.73	0.1796	13.47	0.1490	10.39	0.1100
0.457	123.7	16.83	0.0625	14.87	0.0709	14.95	0.0457	15.01	0.0517
0.457	215.7	14.89	0.0677	13.37	0.0819	14.23	0.0542	13.32	0.0566
0.457	307.7	13.26	0.0523	11.80	0.0777	13.52	0.0531	12.01	0.0535
0.457	399.7	12.07	0.0686	10.57	0.0870	12.59	0.0526	10.95	0.0562
0.457	491.7	11.97	0.0803	11.55	0.1059	12.08	0.0551	10.84	0.0665
0.457	583.7	12.33	0.0958	12.08	0.0993	11.88	0.0608	11.36	0.0796
0.457	675.7	12.59	0.1018	11.71	0.0825	11.80	0.0846	11.79	0.0845
0.457	767.7	12.60	0.1282	10.84	0.0888	11.55	0.0839	11.78	0.1029
0.457	859.7	13.25	0.1947	10.21	0.1156	11.91	0.1166	12.09	0.1308
0.457	951.7	14.54	0.1495	10.39	0.1822	13.08	0.1266	13.06	0.1375
0.610	123.7	15.99	0.0533	15.62	0.0676	16.59	0.0643	17.99	0.0884
0.610	215.7	14.46	0.0802	13.71	0.0715	15.36	0.0745	16.06	0.0980
0.610	307.7	13.29	0.0586	11.99	0.0664	14.57	0.0762	14.73	0.0961
0.610	399.7	12.35	0.0631	10.81	0.0749	14.24	0.0843	13.84	0.1054
0.610	491.7	12.39	0.0729	11.08	0.0942	14.13	0.0844	13.72	0.1135
0.610	583.7	12.68	0.0825	12.00	0.1161	13.69	0.0867	13.63	0.1261
0.610	675.7	12.76	0.0848	12.55	0.1081	13.13	0.0931	13.42	0.1374
0.610	767.7	12.60	0.1048	12.24	0.1227	12.85	0.1304	13.37	0.1876
0.610	859.7	12.98	0.1371	12.27	0.1515	13.89	0.1920	14.90	0.2501
0.610	951.7	14.24	0.1380	12.85	0.1394	15.84	0.1557	16.35	0.1744
0.762	123.7	15.77	0.0551	14.02	0.0528	14.86	0.0575	15.24	0.0676
0.762	215.7	14.20	0.0622	12.32	0.0527	13.89	0.0664	13.77	0.0778
0.762	307.7	13.01	0.0608	10.61	0.0450	13.39	0.0671	12.94	0.0813
0.762	399.7	12.30	0.0685	9.33	0.0496	12.66	0.0691	12.65	0.0970
0.762	491.7	12.53	0.0791	9.72	0.0795	12.14	0.0719	13.30	0.1091
0.762	583.7	12.87	0.0885	11.68	0.1084	11.76	0.0788	13.53	0.1126
0.762	675.7	12.96	0.0957	12.59	0.0939	11.64	0.0854	13.25	0.1132
0.762	767.7	13.06	0.1315	12.42	0.1042	11.56	0.1145	12.91	0.1379
0.762	859.7	14.28	0.1782	12.50	0.1261	12.20	0.1522	13.16	0.1738
0.762	951.7	15.67	0.1378	12.93	0.1139	13.01	0.1294	14.14	0.1672
0.914	123.7	18.48	0.0970	17.20	0.0990	17.89	0.1094	17.80	0.1201
0.914	215.7	16.31	0.1086	16.22	0.1236	15.95	0.1310	15.84	0.1488
0.914	307.7	14.84	0.1044	16.31	0.1256	15.81	0.1456	14.81	0.1772
0.914	399.7	13.75	0.1112	15.57	0.1117	16.19	0.1480	14.69	0.1966
0.914	491.7	13.42	0.1197	14.18	0.0978	15.09	0.1285	15.06	0.1664
0.914	583.7	13.27	0.1329	12.98	0.0994	13.72	0.1366	14.33	0.1623
0.914	675.7	13.00	0.1441	12.13	0.1064	12.77	0.1646	13.49	0.1662
0.914	767.7	12.75	0.1967	11.39	0.1439	12.21	0.2639	12.87	0.2063
0.914	859.7	14.26	0.2934	11.41	0.2381	9.72	0.5708	13.17	0.2670
0.914	951.7	16.71	0.1917	15.37	0.2937	2.99	0.7003	14.92	0.2458
1.067	123.7	19.70	0.1329	16.67	0.0906	17.56	0.1032	16.85	0.1125
1.067	215.7	17.43	0.1541	15.04	0.0999	14.95	0.1184	15.81	0.1486
1.067	307.7	16.22	0.1496	13.80	0.0905	14.21	0.1341	16.78	0.1674
1.067	399.7	15.02	0.1559	12.34	0.0822	14.55	0.1302	17.17	0.1486
1.067	491.7	14.28	0.1625	11.30	0.0838	13.18	0.1172	15.42	0.1201
1.067	583.7	13.70	0.1828	10.95	0.0888	12.16	0.1340	13.84	0.1188
1.067	675.7	12.99	0.2084	11.02	0.1103	11.63	0.1550	12.72	0.1253
1.067	767.7	12.16	0.2994	10.77	0.1491	10.87	0.2190	11.83	0.1687
1.067	859.7	10.03	0.5832	11.49	0.2298	10.38	0.3643	11.76	0.2686
1.067	951.7	0.89	0.6711	13.73	0.2171	8.35	0.5067	15.79	0.3115
1.219	123.7	18.34	0.1182	14.64	0.0652	16.00	0.0836	16.78	0.1011
1.219	215.7	16.43	0.1354	13.35	0.0754	13.87	0.0860	15.50	0.1223
1.219	307.7	15.49	0.1337	12.73	0.0778	12.42	0.0796	15.20	0.1293
1.219	399.7	14.61	0.1341	12.16	0.0758	11.26	0.0836	14.98	0.1324
1.219	491.7	13.77	0.1370	11.66	0.0755	11.18	0.0985	14.39	0.1208
1.219	583.7	13.28	0.1561	11.57	0.0860	11.39	0.1164	13.51	0.1219
1.219	675.7	12.87	0.1750	11.58	0.0860	11.58	0.1303	12.75	0.1278
1.219	767.7	12.44	0.2456	11.11	0.1018	11.56	0.1798	12.09	0.1671
1.219	859.7	12.37	0.5101	10.84	0.1297	12.79	0.2586	12.33	0.2517

Average Soil Density (g/cc)				
Depth (m)	Plot 1	Plot 2	Plot 3	Plot 4
0.152	1.398	1.435	1.580	1.406
0.305	1.517	1.576	1.639	1.304
0.457	1.715	1.679	1.500	1.529
0.610	1.864	1.597	1.684	1.661
0.762	1.672	1.552	1.493	2.051
0.914	1.682	1.745	1.772	1.860
1.067	1.620	1.678	1.618	1.604
1.219	1.702	1.576	1.550	1.555
1.372	1.474	1.635	1.446	1.538
1.524	1.637	1.510	1.340	1.526
1.676	1.722	1.398	1.392	1.496
1.829	1.786	1.229	1.602	1.656
1.981	1.576	1.223	1.674	1.706
2.134	1.648	1.610	1.775	1.755
2.286	1.720	1.677	1.742	1.831
2.438	1.815	1.750	1.806	1.885
2.591	1.803	1.808	1.775	1.824

Percent Sand, Silt, and Clay in Each Plot and at Each Depth					
Depth (cm)	Category	Plot 1	Plot 2	Plot 3	Plot 4
15.2	Sand	57.8	45.8	64.5	54.1
15.2	Silt	29.2	39.0	24.2	32.9
15.2	Clay	13.1	15.2	11.3	13.0
30.5	Sand	54.7	46.3	65.6	58.5
30.5	Silt	32.7	39.1	23.0	30.0
30.5	Clay	12.6	14.5	11.4	11.6
45.7	Sand	69.9	38.1	78.5	68.1
45.7	Silt	18.6	43.3	12.6	21.4
45.7	Clay	11.4	18.5	8.9	10.5
61.0	Sand	69.7	53.2	70.3	48.1
61.0	Silt	20.5	31.6	19.3	36.0
61.0	Clay	9.9	15.2	10.4	15.9
76.2	Sand	73.0	59.5	60.6	44.7
76.2	Silt	17.6	29.0	27.9	38.5
76.2	Clay	9.4	11.6	11.5	16.8
91.4	Sand	40.0	37.4	34.7	32.2
91.4	Silt	41.5	44.2	43.4	45.0
91.4	Clay	18.5	18.5	22.0	22.8
106.7	Sand	19.0	31.1	17.8	32.0
106.7	Silt	52.8	49.9	53.4	46.1
106.7	Clay	28.2	19.0	28.7	21.9
121.9	Sand	28.9	42.7	29.6	25.5
121.9	Silt	49.7	41.5	50.9	53.5
121.9	Clay	21.4	15.8	19.5	21.0
137.2	Sand	41.7	26.0	24.1	21.8
137.2	Silt	41.8	55.2	55.4	58.8
137.2	Clay	16.5	18.8	20.5	19.4
152.4	Sand	27.7	22.3	20.3	20.4
152.4	Silt	53.3	56.8	58.1	58.3
152.4	Clay	18.9	20.9	21.7	21.3
167.6	Sand	20.2	30.5	22.1	21.0
167.6	Silt	58.3	54.4	59.1	56.9
167.6	Clay	21.5	15.1	18.8	22.1
182.9	Sand	19.4	23.0	25.0	20.2
182.9	Silt	55.5	56.4	55.3	55.8
182.9	Clay	25.1	20.6	19.7	24.0
198.1	Sand	17.8	14.8	22.2	18.3
198.1	Silt	54.9	53.4	52.7	55.0
198.1	Clay	27.2	31.8	25.0	26.7
213.4	Sand	16.8	14.3	18.4	17.9
213.4	Silt	54.4	52.4	54.1	53.2
213.4	Clay	28.8	33.3	27.5	28.9
228.6	Sand	16.5	14.6	19.3	21.9
228.6	Silt	52.3	51.6	52.1	49.8
228.6	Clay	31.2	33.7	28.6	28.3
243.8	Sand	16.5	19.4	12.8	20.0
243.8	Silt	30.9	49.5	54.6	52.3
243.8	Clay	52.6	31.1	32.6	27.6
259.1	Sand	19.1	18.6	12.5	26.8
259.1	Silt	53.2	50.7	53.3	46.7
259.1	Clay	27.7	30.7	34.2	26.4

APPENDIX H

MOISTURE / DIELECTRIC RELATIONSHIP DATA

Frequency (MHz)	Average Permittivity in the Top Layer (Depth 0 m to 0.762 m)									
	0% VMC	5% VMC	10% VMC	15% VMC	20% VMC	25% VMC	30% VMC	35% VMC	40% VMC	45% VMC
80	4.31	7.34	9.59	12.55	15.89	21.42	22.92	24.44	26.57	27.13
84.6	4.08	7.12	9.35	12.26	15.60	21.19	22.65	24.13	26.30	26.92
89.2	4.11	7.07	9.32	12.24	15.52	21.09	22.59	24.06	26.22	26.78
93.8	4.02	6.96	9.20	12.10	15.43	21.03	22.50	23.90	26.11	26.61
98.4	3.75	6.64	8.91	11.83	15.12	20.75	22.29	23.75	25.92	26.59
103	3.61	6.48	8.72	11.65	14.92	20.55	22.07	23.60	25.79	26.38
107.6	3.50	6.36	8.64	11.60	14.91	20.56	22.11	23.55	25.66	26.26
112.2	3.42	6.25	8.53	11.49	14.76	20.47	22.01	23.40	25.63	26.27
116.8	3.14	5.98	8.24	11.20	14.46	20.25	21.86	23.21	25.39	25.99
121.4	2.98	5.80	8.05	11.05	14.32	20.07	21.61	23.08	25.36	26.01
126	2.96	5.76	8.02	11.03	14.31	20.10	21.77	22.99	25.25	26.04
130.6	2.90	5.65	7.95	10.95	14.16	20.06	21.63	22.97	25.15	25.77
135.2	2.76	5.49	7.78	10.82	13.99	19.78	21.51	22.76	25.13	25.37
139.8	2.56	5.27	7.52	10.50	13.66	19.51	21.35	22.55	24.94	25.50
144.4	2.55	5.24	7.47	10.47	13.65	19.63	21.11	22.33	24.68	25.23
149	2.64	5.29	7.50	10.52	13.66	19.41	21.15	22.28	24.37	25.18
153.6	2.76	5.38	7.59	10.57	13.59	19.40	21.15	22.27	24.47	25.08
158.2	2.67	5.21	7.44	10.34	13.46	19.16	20.87	22.17	24.35	24.64
162.8	2.67	5.19	7.38	10.28	13.26	19.01	20.79	21.76	23.89	24.96
167.4	2.73	5.23	7.37	10.27	13.22	19.01	20.66	21.71	23.96	24.32
172	2.80	5.03	7.20	10.08	13.02	18.75	20.58	21.63	23.67	24.18
176.6	2.77	5.16	7.27	10.12	13.05	18.63	20.47	21.40	23.47	24.07
181.2	2.80	5.14	7.26	10.11	12.86	18.69	20.32	21.28	23.37	24.04
185.8	2.88	5.20	7.24	10.09	12.86	18.56	20.32	21.27	23.28	23.98
190.4	2.89	5.16	7.24	9.97	12.76	18.53	20.24	20.99	23.41	23.70
195	2.88	5.12	7.16	9.90	12.58	18.19	20.09	20.92	23.10	23.72
199.6	2.74	4.93	6.97	9.74	12.33	18.29	19.84	20.65	23.29	23.59
204.2	2.73	4.91	6.91	9.69	12.25	18.23	19.83	20.74	22.93	23.33
208.8	2.65	4.84	6.83	9.63	12.23	17.98	19.93	20.50	22.71	23.93
213.4	2.68	4.79	6.83	9.52	12.04	17.80	19.65	20.61	22.64	23.58
218	2.51	4.65	6.67	9.40	11.93	17.84	19.70	20.45	22.70	22.92
222.6	2.58	4.69	6.68	9.45	11.96	17.97	19.88	20.36	22.63	22.95
227.2	2.44	4.53	6.51	9.34	11.69	17.48	19.63	20.15	22.35	23.07
231.8	2.23	4.33	6.35	9.07	11.47	17.51	19.51	20.13	22.23	22.80
236.4	2.25	4.33	6.35	9.13	11.48	17.34	19.64	20.16	22.20	22.54
241	2.23	4.31	6.31	9.07	11.37	17.41	19.39	19.72	22.22	22.62
245.6	2.15	4.24	6.26	9.10	11.44	17.48	19.51	19.91	22.06	22.65
250.2	2.07	4.14	6.20	9.05	11.24	17.48	19.35	19.63	21.44	22.11
254.8	1.85	3.92	5.94	8.80	11.05	17.00	18.97	19.34	21.50	21.93
259.4	2.06	4.10	6.15	8.93	11.06	17.29	19.17	19.35	21.52	22.21
264	2.04	4.10	6.17	8.84	11.04	16.86	19.13	19.32	21.45	22.02
268.6	1.93	3.96	6.00	8.86	10.81	16.85	19.17	18.91	21.30	21.86
273.2	2.11	4.14	6.16	8.98	10.98	16.86	18.80	19.01	21.36	21.59
277.8	1.81	3.82	5.90	8.65	10.65	16.67	18.46	18.84	20.55	21.33
282.4	1.92	3.92	5.95	8.79	10.59	16.58	18.74	18.59	21.02	20.93
287	2.22	4.19	6.26	8.94	10.80	16.73	18.60	18.46	20.47	21.11
291.6	2.10	4.02	6.05	8.80	10.50	16.32	18.72	18.37	20.49	21.00
296.2	2.14	4.07	6.08	8.73	10.39	16.31	18.28	18.52	20.51	21.02
300.8	2.42	4.33	6.26	8.99	10.56	16.17	18.38	18.06	20.46	20.95
305.4	2.23	4.13	6.09	8.85	10.46	16.29	18.16	18.27	20.30	20.83
310	2.28	4.12	6.06	8.75	10.33	16.41	18.12	18.15	20.15	20.66
314.6	2.27	4.07	6.09	8.74	10.16	15.96	18.21	18.28	20.24	20.85
319.2	2.20	3.98	5.91	8.54	9.97	16.16	17.96	17.91	19.97	20.58
323.8	2.38	4.14	6.10	8.71	10.16	16.19	18.48	17.91	20.36	21.03
328.4	2.16	3.91	5.78	8.52	9.88	16.19	18.14	18.27	20.64	20.96
333	2.06	3.85	5.75	8.33	9.71	16.03	18.07	18.08	20.19	21.03
337.6	2.18	3.90	5.78	8.51	9.76	16.09	18.58	18.39	20.66	21.16
342.2	2.04	3.73	5.65	8.30	9.63	16.09	18.34	18.37	20.80	21.32
346.8	1.86	3.56	5.51	8.16	9.50	16.12	18.32	18.45	20.99	21.52
351.4	1.80	3.49	5.42	8.05	9.34	16.46	18.46	18.42	20.67	21.70
356	1.69	3.35	5.27	7.97	9.17	15.92	18.54	18.75	20.94	21.53
360.6	1.71	3.39	5.28	7.97	9.11	16.06	18.64	18.76	20.94	21.88
365.2	1.45	3.15	5.10	7.88	9.03	16.11	18.38	18.52	20.88	21.65
369.8	1.28	2.92	4.94	7.54	8.62	16.02	18.14	18.41	20.85	21.54
374.4	1.33	2.99	4.94	7.71	8.71	15.85	18.40	18.55	20.94	21.61
379	1.37	3.00	4.96	7.71	8.74	16.01	18.31	18.65	21.02	21.53
383.6	1.33	3.00	4.88	7.68	8.72	16.04	18.16	18.20	20.63	21.40
388.2	1.42	3.08	4.95	7.72	8.61	15.79	17.99	18.36	20.66	21.38
392.8	1.42	3.09	5.07	7.83	8.58	15.91	17.87	18.23	20.53	21.37
397.4	1.48	3.12	5.06	7.78	8.62	15.71	17.74	18.22	20.58	21.23
402	1.70	3.32	5.21	7.95	8.67	15.90	17.73	18.53	20.75	21.41
406.6	1.83	3.46	5.36	8.03	8.75	15.72	17.71	18.31	20.64	21.35
411.2	2.07	3.67	5.57	8.13	8.91	15.85	17.76	18.48	20.80	21.50
415.8	2.03	3.64	5.52	8.04	8.73	15.76	17.58	18.32	20.66	21.36
420.4	2.12	3.73	5.62	8.17	8.69	15.70	17.63	18.25	20.69	21.42
425	2.48	4.05	5.85	8.44	8.88	15.73	17.80	18.61	20.98	21.74
429.6	2.50	4.08	5.91	8.39	8.83	15.88	17.63	18.53	21.00	21.74
434.2	2.67	4.25	6.07	8.50	8.92	16.02	17.82	18.75	21.19	21.96
438.8	2.67	4.23	6.03	8.43	8.94	15.96	17.84	18.76	21.23	21.98
443.4	2.77	4.30	6.08	8.57	8.99	16.02	17.92	18.94	21.35	22.13
448	2.80	4.33	6.10	8.63	8.91	16.05	17.98	18.97	21.46	22.24
452.6	2.70	4.24	6.02	8.47	8.88	16.06	17.97	19.00	21.45	22.23

Average Permittivity in the Top Layer (Depth 0 m to 0.762 m)										
Frequency (MHz)	0% VMC	5% VMC	10% VMC	15% VMC	20% VMC	25% VMC	30% VMC	35% VMC	40% VMC	45% VMC
503.2	1.34	2.98	5.00	7.95	8.19	15.56	17.15	18.23	20.38	21.09
507.8	1.31	2.97	5.01	7.97	8.25	15.52	17.10	18.17	20.31	21.02
512.4	1.31	2.96	5.05	8.02	8.31	15.45	17.02	18.11	20.21	20.91
517	1.31	2.97	5.04	8.13	8.35	15.43	16.99	18.08	20.18	20.88
521.6	1.34	2.99	5.15	8.16	8.33	15.36	16.92	18.02	20.13	20.82
526.2	1.36	3.10	5.19	8.09	8.41	15.33	16.90	18.00	20.10	20.80
530.8	1.47	3.17	5.32	8.17	8.47	15.33	16.89	18.01	20.12	20.83
535.4	1.58	3.28	5.37	8.34	8.57	15.35	16.94	18.07	20.18	20.89
540	1.72	3.45	5.53	8.43	8.65	15.44	17.02	18.15	20.29	21.03
544.6	1.81	3.55	5.59	8.40	8.72	15.43	17.05	18.21	20.36	21.09
549.2	1.97	3.71	5.76	8.50	8.79	15.54	17.16	18.34	20.51	21.26
553.8	2.14	3.81	5.86	8.57	8.95	15.63	17.28	18.46	20.67	21.44
558.4	2.28	3.98	5.94	8.63	9.00	15.71	17.38	18.60	20.83	21.60
563	2.40	4.09	6.01	8.69	9.10	15.81	17.50	18.72	20.99	21.78
567.6	2.47	4.16	6.14	8.78	9.13	15.88	17.59	18.84	21.11	21.90
572.2	2.60	4.27	6.14	8.78	9.22	15.99	17.70	18.97	21.26	22.05
576.8	2.65	4.38	6.27	8.85	9.29	16.06	17.80	19.08	21.38	22.21
581.4	2.75	4.46	6.31	8.88	9.39	16.14	17.90	19.19	21.52	22.37
586	2.76	4.38	6.26	8.84	9.42	16.15	17.90	19.21	21.53	22.32
590.6	2.78	4.43	6.23	8.88	9.44	16.17	17.95	19.25	21.60	22.43
595.2	2.75	4.45	6.33	8.90	9.48	16.19	17.95	19.27	21.61	22.48
599.8	2.75	4.47	6.31	8.89	9.48	16.13	17.90	19.22	21.54	22.46
604.4	2.73	4.42	6.29	8.86	9.54	16.08	17.85	19.17	21.57	22.40
609	2.66	4.45	6.26	8.78	9.50	16.00	17.76	19.09	21.39	22.27
613.6	2.60	4.42	6.29	8.79	9.53	15.89	17.66	18.97	21.34	22.28
618.2	2.59	4.42	6.25	8.81	9.54	15.83	17.58	18.91	21.34	22.22
622.8	2.55	4.38	6.23	8.75	9.54	15.69	17.46	18.75	21.11	22.07
627.4	2.55	4.43	6.35	8.74	9.55	15.60	17.36	18.70	21.11	22.05
632	2.52	4.47	6.31	8.73	9.57	15.54	17.27	18.62	20.94	21.95
636.6	2.53	4.48	6.34	8.72	9.57	15.42	17.16	18.48	20.94	21.82
641.2	2.56	4.57	6.40	8.71	9.58	15.34	17.08	18.43	20.89	21.94
645.8	2.58	4.63	6.44	8.68	9.58	15.26	17.01	18.37	20.88	21.84
650.4	2.65	4.68	6.47	8.69	9.60	15.22	17.01	18.36	20.87	21.88
655	2.71	4.74	6.51	8.70	9.63	15.20	16.97	18.38	20.91	21.92
659.6	2.81	4.85	6.53	8.69	9.64	15.17	16.99	18.37	21.01	22.13
664.2	2.85	4.88	6.57	8.68	9.67	15.17	17.00	18.39	21.07	22.20
668.8	3.00	4.97	6.64	8.71	9.71	15.23	17.10	18.59	21.27	22.43
673.4	3.09	5.09	6.66	8.73	9.76	15.30	17.17	18.67	21.42	22.67
678	3.18	5.10	6.68	8.73	9.80	15.36	17.30	18.74	21.72	22.81
682.6	3.32	5.18	6.72	8.77	9.87	15.49	17.48	19.00	21.93	23.23
687.2	3.37	5.22	6.74	8.79	9.92	15.59	17.59	19.22	22.20	23.43
691.8	3.44	5.27	6.76	8.80	9.97	15.72	17.79	19.35	22.33	23.78
696.4	3.54	5.30	6.78	8.83	10.04	15.82	17.94	19.56	22.70	23.90
701	3.66	5.41	6.83	8.90	10.14	16.04	18.21	19.95	23.08	24.72
705.6	3.68	5.36	6.81	8.88	10.17	16.11	18.30	19.97	23.31	24.55
710.2	3.75	5.43	6.81	8.90	10.24	16.30	18.51	20.26	23.50	24.96
714.8	3.78	5.43	6.82	8.90	10.29	16.42	18.67	20.44	23.89	25.08
719.4	3.85	5.46	6.85	8.95	10.38	16.61	18.88	20.75	24.15	25.32
724	3.83	5.40	6.79	8.92	10.39	16.63	19.03	20.77	23.94	25.20
728.6	3.87	5.41	6.80	8.92	10.44	16.79	19.14	21.07	24.38	25.57
733.2	3.90	5.45	6.80	8.94	10.50	16.86	19.39	21.28	24.57	25.61
737.8	3.92	5.42	6.79	8.93	10.53	16.97	19.41	21.25	24.51	25.52
742.4	3.92	5.44	6.78	8.93	10.55	17.03	19.47	21.37	24.71	25.76
747	3.97	5.48	6.80	8.94	10.58	17.18	19.75	21.67	24.79	25.77
751.6	4.02	5.48	6.81	8.93	10.60	17.16	19.76	21.71	24.91	25.84
756.2	3.98	5.44	6.75	8.87	10.56	17.13	19.78	21.77	24.95	25.72
760.8	4.07	5.53	6.81	8.91	10.63	17.33	20.13	22.06	25.08	26.00
765.4	4.18	5.59	6.85	8.93	10.65	17.41	20.27	22.25	25.34	26.13
770	4.18	5.57	6.83	8.89	10.63	17.36	20.13	22.23	25.14	25.96
774.6	4.23	5.61	6.84	8.89	10.65	17.56	20.48	22.47	25.46	26.12
779.2	4.29	5.65	6.85	8.87	10.65	17.58	20.55	22.73	25.46	26.25
783.8	4.36	5.68	6.88	8.88	10.67	17.80	20.82	23.03	25.60	26.24
788.4	4.42	5.72	6.89	8.88	10.69	17.97	21.03	23.08	25.55	26.31
793	4.47	5.74	6.89	8.87	10.70	18.15	21.38	23.20	25.66	26.27
797.6	4.53	5.77	6.92	8.89	10.75	18.33	21.53	23.44	25.80	26.31
802.2	4.57	5.78	6.92	8.89	10.78	18.54	21.74	23.61	25.72	26.35
806.8	4.63	5.80	6.95	8.91	10.84	19.02	22.14	23.71	25.69	26.25
811.4	4.66	5.82	6.94	8.93	10.90	19.53	22.22	23.83	25.69	26.22
816	4.69	5.84	6.95	8.95	10.97	19.54	22.33	23.72	25.68	26.19
820.6	4.72	5.84	6.96	8.97	11.04	20.01	22.41	23.89	25.55	26.02
825.2	4.77	5.88	7.01	9.04	11.17	20.49	22.62	23.87	25.56	26.05
829.8	4.80	5.88	7.02	9.08	11.27	20.66	22.66	23.88	25.45	25.98
834.4	4.76	5.85	6.98	9.07	11.34	20.81	22.58	23.76	25.30	25.81
839	4.77	5.85	6.98	9.11	11.46	20.84	22.56	23.66	25.22	25.66
843.6	4.81	5.86	7.02	9.19	11.62	21.21	22.52	23.71	25.11	25.61
848.2	4.77	5.83	6.99	9.21	11.72	20.96	22.50	23.55	24.98	25.43
852.8	4.77	5.81	6.99	9.24	11.82	21.00	22.38	23.41	24.78	25.33
857.4	4.68	5.73	6.92	9.23	11.88	20.88	22.13	23.22	24.61	25.04
862	4.71	5.74	6.96	9.30	12.04	20.98	22.09	23.12	24.50	24.96
866.6	4.68	5.71	6.93	9.31	12.14	20.98	22.03	23.02	24.34	24.79
871.2	4.69	5.70	6.94	9.36	12.25	20.86	21.94	22.93	24.19	24.65
875.8	4.63	5.65	6.92	9.36	12.33	20.75	21.81	22.73	24.02	24.50

Average Conductivity in the Top Layer (Depth 0 m to 0.762 m)										
Frequency (MHz)	0% VMC	5% VMC	10% VMC	15% VMC	20% VMC	25% VMC	30% VMC	35% VMC	40% VMC	45% VMC
80	0.003	0.020	0.037	0.052	0.063	0.088	0.091	0.091	0.096	0.094
84.6	0.003	0.020	0.038	0.053	0.064	0.091	0.092	0.092	0.098	0.096
89.2	0.003	0.021	0.039	0.054	0.065	0.092	0.094	0.094	0.100	0.097
93.8	0.004	0.022	0.040	0.055	0.066	0.096	0.096	0.094	0.101	0.097
98.4	0.004	0.023	0.041	0.057	0.067	0.096	0.099	0.098	0.103	0.102
103	0.004	0.023	0.041	0.058	0.068	0.097	0.099	0.099	0.106	0.103
107.6	0.005	0.025	0.043	0.059	0.071	0.100	0.102	0.101	0.106	0.104
112.2	0.005	0.026	0.044	0.061	0.071	0.101	0.103	0.100	0.107	0.106
116.8	0.005	0.026	0.045	0.062	0.072	0.104	0.106	0.103	0.110	0.106
121.4	0.006	0.027	0.045	0.063	0.073	0.104	0.106	0.104	0.112	0.110
126	0.006	0.028	0.047	0.064	0.075	0.107	0.109	0.106	0.113	0.112
130.6	0.007	0.029	0.048	0.066	0.075	0.110	0.111	0.108	0.114	0.112
135.2	0.007	0.029	0.048	0.067	0.076	0.108	0.112	0.108	0.117	0.109
139.8	0.007	0.030	0.049	0.066	0.076	0.109	0.116	0.110	0.119	0.115
144.4	0.007	0.031	0.050	0.068	0.077	0.114	0.114	0.109	0.118	0.113
149	0.008	0.032	0.051	0.069	0.078	0.112	0.116	0.110	0.116	0.115
153.6	0.009	0.033	0.052	0.070	0.078	0.113	0.118	0.111	0.119	0.116
158.2	0.009	0.033	0.052	0.070	0.080	0.114	0.119	0.114	0.121	0.115
162.8	0.009	0.034	0.053	0.071	0.079	0.114	0.121	0.111	0.118	0.120
167.4	0.010	0.035	0.053	0.072	0.079	0.116	0.119	0.113	0.123	0.116
172	0.009	0.034	0.053	0.072	0.080	0.117	0.124	0.114	0.121	0.118
176.6	0.011	0.036	0.054	0.073	0.081	0.118	0.124	0.115	0.122	0.118
181.2	0.011	0.037	0.055	0.075	0.080	0.120	0.124	0.116	0.123	0.121
185.8	0.012	0.037	0.055	0.075	0.081	0.120	0.128	0.118	0.125	0.122
190.4	0.012	0.038	0.057	0.075	0.082	0.122	0.128	0.117	0.130	0.123
195	0.013	0.039	0.057	0.076	0.081	0.121	0.130	0.119	0.128	0.125
199.6	0.012	0.038	0.057	0.076	0.081	0.125	0.131	0.118	0.133	0.126
204.2	0.013	0.039	0.057	0.077	0.081	0.127	0.133	0.122	0.131	0.126
208.8	0.012	0.040	0.057	0.078	0.083	0.126	0.136	0.120	0.131	0.133
213.4	0.013	0.040	0.059	0.078	0.082	0.124	0.134	0.124	0.133	0.131
218	0.013	0.041	0.059	0.079	0.083	0.130	0.139	0.125	0.135	0.127
222.6	0.014	0.042	0.060	0.080	0.084	0.132	0.143	0.123	0.136	0.131
227.2	0.014	0.042	0.060	0.081	0.082	0.128	0.141	0.125	0.134	0.132
231.8	0.013	0.042	0.060	0.079	0.082	0.129	0.140	0.124	0.134	0.130
236.4	0.014	0.043	0.061	0.081	0.083	0.126	0.144	0.128	0.137	0.130
241	0.016	0.045	0.063	0.083	0.083	0.131	0.142	0.124	0.139	0.133
245.6	0.016	0.046	0.064	0.085	0.085	0.132	0.145	0.127	0.136	0.134
250.2	0.017	0.047	0.065	0.086	0.085	0.136	0.144	0.127	0.134	0.132
254.8	0.016	0.046	0.063	0.085	0.084	0.130	0.140	0.123	0.135	0.130
259.4	0.019	0.050	0.067	0.087	0.085	0.135	0.145	0.126	0.137	0.134
264	0.020	0.052	0.069	0.088	0.087	0.132	0.146	0.128	0.139	0.136
268.6	0.021	0.052	0.069	0.091	0.086	0.132	0.148	0.126	0.139	0.135
273.2	0.025	0.056	0.073	0.093	0.089	0.135	0.145	0.130	0.141	0.136
277.8	0.023	0.054	0.072	0.090	0.088	0.134	0.144	0.129	0.137	0.135
282.4	0.025	0.057	0.073	0.094	0.089	0.136	0.149	0.129	0.144	0.137
287	0.029	0.061	0.078	0.096	0.092	0.138	0.150	0.132	0.142	0.140
291.6	0.029	0.060	0.077	0.097	0.090	0.136	0.152	0.133	0.144	0.140
296.2	0.030	0.062	0.078	0.097	0.091	0.138	0.152	0.136	0.146	0.143
300.8	0.034	0.066	0.081	0.101	0.093	0.139	0.154	0.136	0.149	0.147
305.4	0.033	0.065	0.081	0.102	0.094	0.142	0.155	0.138	0.151	0.148
310	0.034	0.066	0.082	0.101	0.093	0.146	0.156	0.141	0.153	0.150
314.6	0.034	0.066	0.083	0.102	0.093	0.143	0.159	0.143	0.154	0.152
319.2	0.033	0.065	0.081	0.101	0.092	0.146	0.159	0.142	0.156	0.152
323.8	0.036	0.068	0.084	0.103	0.095	0.148	0.164	0.144	0.159	0.157
328.4	0.034	0.066	0.081	0.103	0.093	0.150	0.164	0.147	0.162	0.158
333	0.033	0.066	0.082	0.100	0.091	0.149	0.164	0.147	0.161	0.158
337.6	0.034	0.066	0.081	0.103	0.092	0.152	0.168	0.151	0.165	0.162
342.2	0.032	0.065	0.081	0.102	0.091	0.153	0.167	0.152	0.164	0.161
346.8	0.030	0.063	0.080	0.101	0.091	0.153	0.167	0.152	0.164	0.161
351.4	0.029	0.062	0.079	0.100	0.089	0.154	0.168	0.153	0.166	0.161
356	0.028	0.061	0.078	0.100	0.088	0.153	0.167	0.153	0.165	0.161
360.6	0.029	0.062	0.079	0.101	0.089	0.155	0.169	0.154	0.167	0.162
365.2	0.027	0.061	0.078	0.102	0.089	0.155	0.168	0.154	0.166	0.161
369.8	0.027	0.060	0.079	0.100	0.087	0.155	0.167	0.154	0.164	0.160
374.4	0.028	0.062	0.080	0.103	0.089	0.156	0.167	0.155	0.165	0.162
379	0.030	0.064	0.082	0.105	0.091	0.157	0.169	0.157	0.166	0.164
383.6	0.031	0.065	0.082	0.106	0.092	0.159	0.169	0.161	0.170	0.166
388.2	0.033	0.068	0.084	0.107	0.093	0.161	0.171	0.162	0.173	0.169
392.8	0.036	0.070	0.088	0.111	0.096	0.162	0.173	0.165	0.175	0.171
397.4	0.037	0.072	0.090	0.112	0.098	0.165	0.175	0.167	0.177	0.175
402	0.040	0.075	0.091	0.113	0.100	0.167	0.178	0.168	0.180	0.177
406.6	0.043	0.077	0.094	0.115	0.102	0.171	0.181	0.174	0.187	0.183
411.2	0.045	0.079	0.096	0.117	0.104	0.173	0.183	0.177	0.191	0.187
415.8	0.047	0.082	0.099	0.118	0.105	0.175	0.185	0.181	0.194	0.192
420.4	0.050	0.085	0.101	0.121	0.107	0.178	0.187	0.186	0.198	0.195
425	0.052	0.086	0.101	0.122	0.108	0.184	0.191	0.188	0.203	0.199
429.6	0.054	0.087	0.103	0.123	0.110	0.184	0.195	0.193	0.205	0.202
434.2	0.055	0.088	0.104	0.123	0.111	0.186	0.196	0.195	0.207	0.203
438.8	0.055	0.088	0.104	0.123	0.112	0.188	0.196	0.196	0.208	0.206
443.4	0.055	0.089	0.104	0.125	0.113	0.190	0.197	0.196	0.211	0.206
448	0.056	0.089	0.105	0.125	0.113	0.192	0.198	0.200	0.213	0.208
452.6	0.055	0.088	0.104	0.125	0.114	0.192	0.197	0.199	0.210	0.208

Average Conductivity in the Top Layer (Depth 0 m to 0.762 m)										
Frequency (MHz)	0% VMC	5% VMC	10% VMC	15% VMC	20% VMC	25% VMC	30% VMC	35% VMC	40% VMC	45% VMC
544.6	0.065	0.106	0.127	0.144	0.145	0.198	0.201	0.206	0.221	0.219
549.2	0.064	0.104	0.125	0.142	0.145	0.198	0.201	0.206	0.220	0.221
553.8	0.063	0.102	0.123	0.140	0.144	0.199	0.202	0.208	0.223	0.221
558.4	0.062	0.102	0.122	0.139	0.145	0.200	0.204	0.209	0.224	0.222
563	0.062	0.101	0.121	0.138	0.145	0.202	0.205	0.212	0.227	0.226
567.6	0.061	0.100	0.120	0.137	0.146	0.203	0.207	0.212	0.227	0.225
572.2	0.059	0.097	0.117	0.135	0.144	0.202	0.206	0.212	0.229	0.224
576.8	0.056	0.094	0.113	0.132	0.142	0.201	0.204	0.210	0.225	0.225
581.4	0.053	0.091	0.110	0.129	0.141	0.199	0.203	0.209	0.225	0.225
586	0.055	0.093	0.112	0.132	0.143	0.202	0.207	0.212	0.228	0.224
590.6	0.053	0.090	0.110	0.130	0.143	0.201	0.204	0.213	0.227	0.226
595.2	0.050	0.088	0.107	0.126	0.141	0.198	0.203	0.208	0.225	0.226
599.8	0.051	0.089	0.108	0.127	0.143	0.200	0.205	0.211	0.225	0.229
604.4	0.054	0.093	0.111	0.130	0.145	0.204	0.209	0.215	0.234	0.232
609	0.053	0.092	0.110	0.129	0.146	0.202	0.207	0.214	0.230	0.230
613.6	0.055	0.095	0.113	0.131	0.147	0.205	0.211	0.218	0.236	0.238
618.2	0.059	0.099	0.116	0.133	0.151	0.208	0.215	0.222	0.246	0.243
622.8	0.061	0.102	0.119	0.135	0.152	0.211	0.220	0.225	0.245	0.247
627.4	0.066	0.107	0.122	0.138	0.156	0.216	0.224	0.233	0.255	0.256
632	0.069	0.110	0.125	0.141	0.159	0.218	0.229	0.237	0.256	0.258
636.6	0.075	0.116	0.130	0.145	0.162	0.223	0.234	0.240	0.268	0.265
641.2	0.077	0.118	0.131	0.146	0.164	0.226	0.236	0.248	0.272	0.279
645.8	0.080	0.121	0.133	0.148	0.166	0.229	0.241	0.251	0.281	0.280
650.4	0.084	0.124	0.136	0.151	0.170	0.236	0.248	0.258	0.285	0.288
655	0.087	0.127	0.138	0.153	0.172	0.239	0.250	0.264	0.292	0.293
659.6	0.088	0.127	0.138	0.153	0.173	0.241	0.258	0.267	0.300	0.304
664.2	0.089	0.127	0.138	0.154	0.174	0.242	0.258	0.269	0.304	0.305
668.8	0.090	0.128	0.139	0.155	0.176	0.247	0.264	0.279	0.309	0.312
673.4	0.092	0.130	0.140	0.157	0.178	0.254	0.269	0.283	0.317	0.319
678	0.090	0.126	0.137	0.155	0.177	0.253	0.273	0.282	0.320	0.318
682.6	0.090	0.126	0.137	0.155	0.178	0.259	0.277	0.289	0.323	0.325
687.2	0.089	0.124	0.136	0.154	0.178	0.258	0.277	0.293	0.323	0.323
691.8	0.087	0.121	0.133	0.153	0.177	0.262	0.282	0.290	0.320	0.323
696.4	0.085	0.118	0.131	0.151	0.176	0.260	0.281	0.294	0.323	0.317
701	0.084	0.117	0.130	0.151	0.178	0.270	0.287	0.300	0.324	0.324
705.6	0.079	0.112	0.125	0.147	0.174	0.262	0.281	0.290	0.318	0.310
710.2	0.077	0.109	0.123	0.146	0.174	0.267	0.284	0.294	0.313	0.307
714.8	0.073	0.105	0.119	0.144	0.172	0.268	0.283	0.293	0.313	0.299
719.4	0.072	0.103	0.118	0.143	0.172	0.271	0.283	0.296	0.306	0.294
724	0.067	0.099	0.114	0.140	0.170	0.264	0.281	0.286	0.295	0.282
728.6	0.066	0.097	0.112	0.139	0.170	0.270	0.282	0.290	0.292	0.278
733.2	0.064	0.095	0.111	0.138	0.169	0.267	0.284	0.289	0.288	0.272
737.8	0.064	0.095	0.111	0.138	0.170	0.272	0.285	0.286	0.285	0.267
742.4	0.063	0.094	0.110	0.138	0.171	0.275	0.285	0.286	0.281	0.263
747	0.065	0.096	0.112	0.140	0.174	0.285	0.294	0.292	0.279	0.260
751.6	0.066	0.096	0.112	0.141	0.175	0.284	0.294	0.290	0.277	0.257
756.2	0.066	0.096	0.113	0.142	0.176	0.286	0.295	0.292	0.274	0.255
760.8	0.070	0.100	0.116	0.145	0.180	0.299	0.307	0.298	0.276	0.255
765.4	0.073	0.102	0.118	0.148	0.184	0.308	0.312	0.301	0.273	0.254
770	0.076	0.104	0.121	0.150	0.187	0.311	0.314	0.303	0.275	0.255
774.6	0.079	0.107	0.123	0.153	0.191	0.323	0.321	0.305	0.271	0.252
779.2	0.082	0.110	0.126	0.156	0.194	0.330	0.327	0.308	0.271	0.249
783.8	0.085	0.112	0.128	0.159	0.198	0.342	0.331	0.308	0.269	0.249
788.4	0.087	0.114	0.130	0.161	0.201	0.352	0.334	0.307	0.268	0.247
793	0.089	0.116	0.132	0.163	0.204	0.361	0.338	0.305	0.264	0.244
797.6	0.090	0.117	0.133	0.165	0.207	0.365	0.336	0.301	0.257	0.242
802.2	0.092	0.117	0.134	0.167	0.210	0.371	0.333	0.294	0.254	0.236
806.8	0.092	0.118	0.134	0.168	0.212	0.379	0.326	0.288	0.251	0.234
811.4	0.090	0.116	0.133	0.168	0.213	0.379	0.316	0.277	0.242	0.227
816	0.090	0.115	0.133	0.169	0.217	0.376	0.312	0.274	0.238	0.224
820.6	0.088	0.114	0.132	0.169	0.218	0.370	0.303	0.264	0.233	0.222
825.2	0.087	0.112	0.131	0.169	0.220	0.362	0.290	0.256	0.227	0.214
829.8	0.083	0.109	0.128	0.167	0.220	0.349	0.278	0.245	0.220	0.207
834.4	0.079	0.105	0.125	0.165	0.219	0.334	0.266	0.236	0.212	0.201
839	0.074	0.100	0.121	0.163	0.218	0.319	0.255	0.226	0.203	0.195
843.6	0.071	0.098	0.119	0.162	0.220	0.303	0.245	0.216	0.199	0.189
848.2	0.065	0.092	0.114	0.159	0.219	0.290	0.231	0.207	0.190	0.182
852.8	0.061	0.088	0.111	0.157	0.215	0.275	0.222	0.199	0.185	0.176
857.4	0.055	0.082	0.106	0.154	0.212	0.261	0.211	0.191	0.177	0.172
862	0.052	0.079	0.104	0.153	0.212	0.249	0.203	0.185	0.172	0.167
866.6	0.047	0.076	0.101	0.151	0.213	0.238	0.194	0.177	0.167	0.163
871.2	0.044	0.073	0.099	0.150	0.210	0.228	0.186	0.169	0.164	0.160
875.8	0.041	0.070	0.097	0.149	0.211	0.220	0.180	0.166	0.161	0.157
880.4	0.039	0.068	0.096	0.149	0.208	0.212	0.176	0.163	0.158	0.157
885	0.038	0.068	0.096	0.150	0.214	0.207	0.172	0.159	0.157	0.154
889.6	0.038	0.068	0.096	0.151	0.214	0.200	0.168	0.158	0.157	0.154
894.2	0.038	0.068	0.097	0.154	0.216	0.198	0.165	0.157	0.156	0.156
898.8	0.039	0.069	0.098	0.156	0.220	0.195	0.164	0.155	0.158	0.158
903.4	0.040	0.070	0.099	0.158	0.223	0.191	0.163	0.155	0.158	0.158
908	0.042	0.072	0.102	0.163	0.229	0.192	0.164	0.158	0.159	0.162
912.6	0.045	0.075	0.105	0.167	0.232	0.190	0.164	0.158	0.163	0.165
917.2	0.047	0.077	0.108	0.170	0.240	0.190	0.164	0.159	0.165	0.167

Frequency (MHz)	Average Permittivity in the Middle Layer (Depth 0.762 m to 1.83 m)								
	0% VMC	5% VMC	10% VMC	15% VMC	20% VMC	25% VMC	30% VMC	35% VMC	40% VMC
80	4.40	7.32	9.55	12.17	17.11	21.85	25.05	27.16	28.81
84.6	4.16	7.07	9.28	11.87	16.79	21.58	24.65	26.79	28.52
89.2	4.19	7.01	9.20	11.81	16.72	21.50	24.63	26.82	28.43
93.8	4.09	6.87	9.08	11.68	16.60	21.36	24.48	26.67	28.45
98.4	3.86	6.59	8.74	11.37	16.29	21.08	24.22	26.45	28.17
103	3.69	6.38	8.56	11.18	16.11	20.89	23.96	26.24	28.04
107.6	3.60	6.27	8.45	11.09	16.03	20.95	23.99	26.24	27.98
112.2	3.50	6.18	8.32	10.98	15.95	20.91	23.99	26.26	27.81
116.8	3.23	5.86	8.00	10.68	15.62	20.55	23.64	25.93	27.70
121.4	3.08	5.67	7.85	10.50	15.46	20.40	23.55	25.83	27.68
126	3.06	5.64	7.79	10.48	15.44	20.33	23.51	25.78	27.56
130.6	2.99	5.53	7.68	10.36	15.34	20.30	23.54	25.61	27.53
135.2	2.87	5.39	7.52	10.17	15.12	20.09	23.09	25.50	27.41
139.8	2.65	5.14	7.28	9.94	14.81	19.86	22.86	25.29	27.15
144.4	2.64	5.08	7.18	9.83	14.77	19.72	22.86	25.20	26.89
149	2.73	5.15	7.22	9.86	14.77	19.70	22.73	25.14	26.87
153.6	2.86	5.24	7.31	9.93	14.80	19.71	22.53	24.78	26.88
158.2	2.75	5.09	7.12	9.70	14.52	19.38	22.33	24.78	26.56
162.8	2.75	5.04	7.07	9.61	14.37	19.25	22.23	24.45	26.28
167.4	2.84	5.09	7.06	9.61	14.28	19.14	22.09	24.08	26.24
172	2.70	4.93	6.88	9.34	14.03	18.81	21.58	24.15	25.83
176.6	2.85	5.01	6.93	9.47	14.01	18.85	21.68	24.03	25.66
181.2	2.89	5.03	6.93	9.40	13.87	18.61	21.44	23.85	25.53
185.8	2.96	5.09	6.95	9.35	13.88	18.53	21.19	23.69	25.39
190.4	2.98	5.03	6.89	9.29	13.70	18.49	21.21	23.44	25.33
195	2.98	4.98	6.80	9.21	13.57	18.20	21.04	23.21	25.15
199.6	2.81	4.82	6.62	8.99	13.33	17.96	20.70	23.15	24.68
204.2	2.82	4.80	6.59	8.94	13.21	17.90	20.64	22.85	25.00
208.8	2.73	4.69	6.52	8.80	13.06	17.83	20.43	22.66	24.81
213.4	2.75	4.70	6.45	8.79	13.06	17.74	20.28	22.73	24.08
218	2.60	4.54	6.32	8.63	12.85	17.48	20.19	22.69	24.31
222.6	2.65	4.54	6.31	8.65	12.80	17.65	20.05	22.29	24.43
227.2	2.52	4.42	6.14	8.48	12.67	17.36	19.82	22.68	24.28
231.8	2.32	4.19	5.99	8.26	12.61	17.13	20.03	22.38	24.02
236.4	2.32	4.22	5.97	8.26	12.47	17.02	19.80	21.85	23.86
241	2.30	4.18	5.97	8.27	12.43	17.20	19.72	21.88	23.82
245.6	2.24	4.12	5.89	8.14	12.42	17.05	19.71	21.94	23.53
250.2	2.17	4.04	5.79	8.17	12.30	16.77	19.06	22.21	23.60
254.8	1.93	3.79	5.58	7.84	12.04	17.02	19.37	21.44	23.06
259.4	2.15	3.98	5.76	8.06	12.18	16.74	19.16	21.67	23.34
264	2.12	3.94	5.74	8.03	12.19	16.86	19.12	20.90	23.08
268.6	2.01	3.85	5.64	7.91	12.04	16.56	18.81	21.47	22.33
273.2	2.19	4.06	5.75	7.99	12.00	16.44	18.89	20.96	22.63
277.8	1.88	3.73	5.49	7.80	11.66	16.34	18.26	20.73	22.05
282.4	2.00	3.82	5.57	7.76	11.85	16.15	18.36	20.90	21.75
287	2.29	4.10	5.84	7.95	11.99	16.15	18.46	20.31	21.65
291.6	2.17	3.93	5.63	7.86	11.66	15.74	17.91	19.80	21.35
296.2	2.22	3.96	5.63	7.84	11.71	15.83	17.72	19.89	21.16
300.8	2.47	4.28	5.89	8.09	11.88	16.06	17.69	20.36	21.42
305.4	2.32	4.04	5.71	7.79	11.47	15.63	17.55	19.84	21.14
310	2.35	4.05	5.69	7.76	11.45	15.52	17.56	19.51	21.19
314.6	2.31	4.00	5.63	7.73	11.36	15.46	17.85	19.73	20.67
319.2	2.25	3.91	5.48	7.53	11.02	15.05	17.18	19.45	20.61
323.8	2.44	4.07	5.67	7.67	11.36	15.51	17.39	19.91	21.10
328.4	2.19	3.84	5.45	7.49	11.20	15.24	17.60	19.67	21.15
333	2.13	3.74	5.30	7.38	11.15	15.25	17.73	19.70	21.15
337.6	2.23	3.85	5.36	7.38	10.97	15.06	17.82	20.12	21.52
342.2	2.08	3.67	5.23	7.30	10.73	15.10	17.45	19.97	21.39
346.8	1.92	3.48	5.05	7.09	10.89	15.13	17.59	20.23	21.44
351.4	1.86	3.46	4.99	6.97	10.70	15.09	17.59	20.20	21.87
356	1.73	3.28	4.78	6.91	10.60	14.79	17.94	20.53	21.70
360.6	1.75	3.30	4.88	6.86	10.53	14.92	17.87	20.38	22.14
365.2	1.52	3.06	4.65	6.60	10.36	14.90	17.80	20.50	21.78
369.8	1.32	2.92	4.43	6.46	10.04	14.56	17.81	20.33	21.79
374.4	1.36	2.94	4.49	6.49	10.28	14.64	17.86	20.54	21.80
379	1.41	2.98	4.57	6.48	10.37	14.86	18.17	20.48	21.85
383.6	1.38	2.95	4.47	6.52	10.22	14.55	17.74	20.18	21.53
388.2	1.48	3.01	4.59	6.56	10.20	14.89	17.46	20.17	21.58
392.8	1.48	3.02	4.59	6.56	10.00	14.42	17.60	20.10	21.51
397.4	1.53	3.07	4.61	6.57	10.25	14.42	17.80	20.07	21.41
402	1.77	3.32	4.87	6.74	10.33	14.59	17.68	20.12	21.53
406.6	1.88	3.40	4.94	6.86	10.38	14.25	17.46	19.98	21.46
411.2	2.12	3.66	5.15	6.96	10.39	14.43	17.68	20.23	21.63
415.8	2.08	3.63	5.11	6.91	10.41	14.28	17.49	20.05	21.54
420.4	2.20	3.68	5.18	6.94	10.33	13.98	17.35	20.07	21.57
425	2.52	4.03	5.47	7.27	10.33	14.14	17.74	20.40	21.92
429.6	2.54	4.04	5.48	7.29	10.53	14.34	17.77	20.41	21.96
434.2	2.74	4.20	5.63	7.41	10.66	14.41	17.94	20.59	22.19
438.8	2.73	4.20	5.64	7.35	10.60	14.36	17.89	20.66	22.23
443.4	2.79	4.27	5.74	7.39	10.71	14.49	18.11	20.79	22.38
448	2.87	4.31	5.71	7.44	10.55	14.51	18.21	20.92	22.51
452.6	2.75	4.15	5.59	7.33	10.53	14.53	18.23	20.95	22.49

Average Permittivity in the Middle Layer (Depth 0.762 m to 1.83 m)									
Frequency (MHz)	0% VMC	5% VMC	10% VMC	15% VMC	20% VMC	25% VMC	30% VMC	35% VMC	40% VMC
544.6	1.85	3.46	5.26	7.15	10.90	14.36	17.34	19.62	21.09
549.2	2.05	3.66	5.39	7.20	10.95	14.48	17.50	19.77	21.22
553.8	2.20	3.77	5.50	7.30	11.02	14.57	17.61	19.90	21.40
558.4	2.32	3.89	5.57	7.35	11.08	14.62	17.69	20.05	21.55
563	2.46	4.02	5.69	7.50	11.12	14.71	17.81	20.18	21.69
567.6	2.54	4.13	5.72	7.46	11.16	14.79	17.93	20.30	21.82
572.2	2.65	4.18	5.86	7.51	11.20	14.89	18.05	20.44	21.96
576.8	2.74	4.32	5.89	7.64	11.26	14.96	18.14	20.56	22.12
581.4	2.79	4.36	5.95	7.62	11.31	15.06	18.26	20.68	22.21
586	2.81	4.32	5.95	7.63	11.30	15.03	18.25	20.68	22.24
590.6	2.82	4.42	6.01	7.67	11.30	15.08	18.26	20.74	22.27
595.2	2.84	4.37	5.97	7.63	11.31	15.11	18.29	20.73	22.30
599.8	2.80	4.40	6.00	7.65	11.27	15.08	18.23	20.67	22.22
604.4	2.77	4.37	5.98	7.68	11.24	14.99	18.14	20.61	22.20
609	2.73	4.33	5.97	7.62	11.20	14.90	18.06	20.50	22.03
613.6	2.66	4.32	5.98	7.61	11.13	14.82	17.92	20.38	21.94
618.2	2.67	4.28	6.00	7.61	11.10	14.73	17.81	20.28	21.86
622.8	2.60	4.33	5.98	7.61	11.03	14.57	17.65	20.12	21.65
627.4	2.59	4.32	6.02	7.66	10.97	14.49	17.54	20.01	21.61
632	2.61	4.35	6.06	7.65	10.94	14.42	17.44	19.92	21.46
636.6	2.61	4.40	6.08	7.62	10.87	14.31	17.28	19.76	21.30
641.2	2.64	4.47	6.14	7.67	10.82	14.23	17.18	19.64	21.28
645.8	2.66	4.52	6.17	7.66	10.77	14.10	17.06	19.57	21.25
650.4	2.73	4.58	6.20	7.68	10.76	14.08	17.00	19.55	21.15
655	2.77	4.67	6.29	7.71	10.72	14.03	16.97	19.50	21.15
659.6	2.88	4.73	6.29	7.71	10.70	13.97	16.93	19.55	21.28
664.2	2.93	4.79	6.31	7.72	10.69	13.97	16.95	19.56	21.31
668.8	3.04	4.93	6.38	7.75	10.70	13.98	17.00	19.66	21.47
673.4	3.17	5.00	6.42	7.78	10.71	14.02	17.08	19.86	21.67
678	3.25	5.04	6.43	7.78	10.72	14.06	17.14	20.02	21.83
682.6	3.38	5.09	6.49	7.83	10.77	14.15	17.35	20.36	22.24
687.2	3.45	5.15	6.52	7.83	10.79	14.22	17.47	20.52	22.59
691.8	3.53	5.20	6.51	7.85	10.83	14.29	17.61	20.74	22.78
696.4	3.59	5.26	6.55	7.87	10.87	14.39	17.78	21.06	23.07
701	3.73	5.34	6.60	7.92	10.94	14.53	18.03	21.36	23.81
705.6	3.72	5.32	6.57	7.89	10.98	14.63	18.13	21.61	23.63
710.2	3.79	5.37	6.58	7.92	11.02	14.76	18.41	21.92	24.31
714.8	3.84	5.35	6.57	7.91	11.05	14.85	18.58	22.40	24.27
719.4	3.89	5.40	6.60	7.94	11.11	14.99	18.90	22.72	24.91
724	3.87	5.37	6.55	7.90	11.13	15.05	18.99	22.81	24.90
728.6	3.90	5.37	6.55	7.90	11.14	15.14	19.15	23.40	25.29
733.2	3.93	5.37	6.55	7.91	11.17	15.24	19.43	23.46	25.15
737.8	3.95	5.38	6.55	7.91	11.18	15.29	19.66	23.69	25.62
742.4	3.98	5.39	6.54	7.90	11.17	15.31	19.66	24.05	25.86
747	4.02	5.43	6.56	7.91	11.19	15.37	19.90	24.52	25.79
751.6	4.02	5.42	6.53	7.91	11.18	15.37	20.08	24.44	25.88
756.2	4.01	5.39	6.50	7.86	11.12	15.32	20.11	24.48	25.99
760.8	4.12	5.46	6.56	7.91	11.14	15.38	20.78	24.65	26.17
765.4	4.19	5.54	6.61	7.93	11.13	15.43	21.03	25.39	26.32
770	4.20	5.54	6.58	7.90	11.07	15.36	20.79	25.20	26.45
774.6	4.24	5.56	6.59	7.91	11.05	15.35	21.61	25.30	26.53
779.2	4.31	5.60	6.61	7.90	11.03	15.37	21.95	25.63	26.52
783.8	4.39	5.64	6.63	7.92	11.04	15.39	22.81	25.80	26.65
788.4	4.45	5.67	6.65	7.92	11.01	15.42	23.40	25.73	26.77
793	4.48	5.67	6.66	7.92	11.00	15.44	23.62	25.82	26.70
797.6	4.55	5.73	6.68	7.94	11.01	15.59	24.03	25.94	26.69
802.2	4.59	5.74	6.68	7.95	11.02	15.70	24.12	25.95	26.74
806.8	4.63	5.78	6.69	7.97	11.07	15.88	24.36	25.91	26.70
811.4	4.66	5.77	6.69	7.97	11.10	16.26	24.31	25.91	26.50
816	4.70	5.79	6.71	7.99	11.14	16.45	24.55	25.80	26.54
820.6	4.74	5.78	6.70	8.00	11.20	16.90	24.49	25.62	26.43
825.2	4.78	5.85	6.76	8.06	11.31	17.71	24.52	25.62	26.39
829.8	4.80	5.84	6.76	8.08	11.41	23.06	24.31	25.52	26.23
834.4	4.79	5.81	6.72	8.06	11.45	21.78	24.22	25.38	26.07
839	4.78	5.80	6.71	8.08	11.57	21.73	24.03	25.18	25.88
843.6	4.82	5.83	6.75	8.13	11.73	22.19	23.93	25.09	25.81
848.2	4.79	5.78	6.71	8.13	11.83	22.06	23.69	24.88	25.61
852.8	4.78	5.77	6.71	8.15	11.96	21.83	23.59	24.70	25.41
857.4	4.71	5.68	6.63	8.11	12.04	21.74	23.34	24.43	25.17
862	4.72	5.69	6.66	8.17	12.18	21.52	23.22	24.29	25.09
866.6	4.68	5.67	6.63	8.16	12.32	21.63	23.00	24.16	24.88
871.2	4.69	5.67	6.63	8.20	12.46	21.41	22.89	24.01	24.74
875.8	4.65	5.62	6.59	8.19	12.54	21.26	22.76	23.77	24.56
880.4	4.63	5.60	6.58	8.19	12.66	21.10	22.53	23.65	24.41
885	4.61	5.59	6.57	8.21	12.78	21.09	22.48	23.52	24.28
889.6	4.63	5.59	6.58	8.22	12.87	21.01	22.35	23.39	24.17
894.2	4.66	5.62	6.61	8.26	13.05	20.97	22.27	23.29	24.07
898.8	4.68	5.63	6.62	8.28	13.16	20.85	22.17	23.19	23.98
903.4	4.67	5.62	6.60	8.26	13.25	20.75	22.06	23.07	23.86
908	4.73	5.67	6.64	8.32	13.38	20.78	22.05	23.02	23.80
912.6	4.76	5.69	6.66	8.33	13.50	20.74	21.97	22.95	23.73
917.2	4.81	5.73	6.71	8.38	13.75	20.74	21.95	22.91	23.68

Average Conductivity in the Middle Layer (Depth 0.762 m to 1.83 m)									
Frequency (MHz)	0% VMC	5% VMC	10% VMC	15% VMC	20% VMC	25% VMC	30% VMC	35% VMC	40% VMC
80	0.003	0.017	0.034	0.057	0.092	0.122	0.132	0.135	0.141
84.6	0.003	0.017	0.035	0.057	0.094	0.124	0.137	0.139	0.140
89.2	0.004	0.018	0.036	0.059	0.095	0.126	0.137	0.140	0.145
93.8	0.004	0.019	0.038	0.060	0.096	0.128	0.139	0.145	0.145
98.4	0.004	0.019	0.038	0.061	0.098	0.131	0.142	0.146	0.149
103	0.004	0.020	0.039	0.062	0.099	0.134	0.145	0.149	0.152
107.6	0.005	0.021	0.040	0.064	0.100	0.135	0.145	0.151	0.152
112.2	0.005	0.022	0.042	0.065	0.102	0.136	0.146	0.153	0.153
116.8	0.005	0.022	0.042	0.066	0.104	0.138	0.148	0.154	0.156
121.4	0.006	0.023	0.043	0.068	0.104	0.141	0.153	0.154	0.158
126	0.007	0.024	0.045	0.069	0.107	0.141	0.154	0.158	0.159
130.6	0.007	0.025	0.045	0.070	0.108	0.142	0.157	0.157	0.160
135.2	0.007	0.025	0.046	0.070	0.108	0.147	0.154	0.160	0.163
139.8	0.007	0.026	0.047	0.072	0.108	0.148	0.155	0.164	0.166
144.4	0.008	0.027	0.048	0.072	0.110	0.145	0.159	0.165	0.164
149	0.008	0.028	0.048	0.073	0.112	0.147	0.158	0.165	0.165
153.6	0.009	0.029	0.050	0.074	0.114	0.148	0.155	0.159	0.165
158.2	0.009	0.029	0.050	0.074	0.113	0.152	0.159	0.167	0.171
162.8	0.010	0.029	0.051	0.075	0.113	0.151	0.159	0.166	0.169
167.4	0.010	0.030	0.051	0.076	0.113	0.150	0.161	0.162	0.170
172	0.010	0.030	0.051	0.074	0.114	0.150	0.160	0.170	0.171
176.6	0.011	0.031	0.052	0.078	0.114	0.154	0.164	0.169	0.170
181.2	0.012	0.032	0.053	0.078	0.114	0.152	0.163	0.171	0.171
185.8	0.012	0.032	0.054	0.077	0.116	0.152	0.161	0.171	0.175
190.4	0.013	0.033	0.055	0.079	0.116	0.156	0.164	0.171	0.176
195	0.013	0.034	0.055	0.079	0.116	0.155	0.167	0.172	0.177
199.6	0.012	0.033	0.055	0.079	0.117	0.156	0.168	0.178	0.175
204.2	0.013	0.034	0.055	0.079	0.116	0.156	0.170	0.176	0.179
208.8	0.013	0.034	0.056	0.080	0.117	0.159	0.169	0.177	0.183
213.4	0.014	0.035	0.056	0.080	0.119	0.161	0.169	0.178	0.175
218	0.013	0.035	0.057	0.082	0.119	0.161	0.173	0.183	0.180
222.6	0.014	0.036	0.057	0.083	0.119	0.164	0.173	0.176	0.185
227.2	0.014	0.036	0.058	0.082	0.121	0.163	0.170	0.186	0.186
231.8	0.014	0.035	0.058	0.081	0.123	0.159	0.178	0.183	0.183
236.4	0.015	0.037	0.059	0.083	0.120	0.158	0.173	0.180	0.185
241	0.017	0.039	0.062	0.085	0.121	0.164	0.176	0.181	0.185
245.6	0.017	0.040	0.062	0.085	0.124	0.164	0.176	0.182	0.181
250.2	0.018	0.040	0.063	0.089	0.125	0.161	0.169	0.189	0.184
254.8	0.017	0.039	0.062	0.085	0.122	0.167	0.176	0.179	0.179
259.4	0.020	0.043	0.066	0.089	0.125	0.162	0.172	0.185	0.184
264	0.021	0.044	0.067	0.090	0.127	0.164	0.175	0.177	0.186
268.6	0.022	0.045	0.069	0.092	0.127	0.162	0.173	0.185	0.178
273.2	0.025	0.049	0.071	0.094	0.127	0.162	0.176	0.182	0.183
277.8	0.023	0.047	0.070	0.093	0.124	0.163	0.171	0.181	0.180
282.4	0.025	0.049	0.072	0.094	0.130	0.162	0.174	0.185	0.182
287	0.030	0.054	0.077	0.097	0.131	0.163	0.178	0.183	0.184
291.6	0.029	0.053	0.076	0.098	0.128	0.160	0.175	0.181	0.185
296.2	0.030	0.054	0.076	0.098	0.130	0.163	0.176	0.187	0.188
300.8	0.034	0.059	0.080	0.102	0.131	0.168	0.180	0.193	0.192
305.4	0.033	0.058	0.080	0.101	0.131	0.166	0.181	0.193	0.194
310	0.034	0.059	0.081	0.101	0.133	0.167	0.183	0.193	0.196
314.6	0.035	0.059	0.081	0.102	0.134	0.169	0.187	0.197	0.198
319.2	0.034	0.058	0.080	0.101	0.130	0.167	0.186	0.201	0.203
323.8	0.036	0.060	0.083	0.103	0.137	0.173	0.191	0.206	0.207
328.4	0.034	0.059	0.082	0.103	0.137	0.173	0.196	0.207	0.210
333	0.033	0.058	0.080	0.102	0.138	0.175	0.198	0.210	0.212
337.6	0.034	0.059	0.081	0.102	0.137	0.176	0.203	0.215	0.216
342.2	0.033	0.057	0.080	0.102	0.136	0.178	0.204	0.217	0.219
346.8	0.031	0.055	0.079	0.101	0.141	0.180	0.207	0.217	0.220
351.4	0.030	0.055	0.078	0.100	0.140	0.181	0.208	0.220	0.218
356	0.029	0.054	0.076	0.101	0.141	0.181	0.209	0.219	0.220
360.6	0.029	0.054	0.079	0.100	0.141	0.184	0.214	0.223	0.219
365.2	0.028	0.053	0.078	0.099	0.143	0.184	0.213	0.219	0.220
369.8	0.028	0.054	0.077	0.101	0.141	0.185	0.211	0.219	0.217
374.4	0.029	0.055	0.079	0.102	0.145	0.187	0.215	0.219	0.220
379	0.030	0.057	0.082	0.103	0.149	0.188	0.214	0.221	0.221
383.6	0.032	0.058	0.082	0.106	0.149	0.189	0.218	0.226	0.228
388.2	0.034	0.060	0.085	0.108	0.150	0.191	0.224	0.229	0.230
392.8	0.036	0.063	0.088	0.110	0.151	0.194	0.223	0.231	0.232
397.4	0.038	0.065	0.089	0.111	0.155	0.195	0.222	0.233	0.237
402	0.041	0.068	0.093	0.113	0.157	0.198	0.229	0.239	0.241
406.6	0.044	0.070	0.094	0.115	0.158	0.202	0.238	0.249	0.251
411.2	0.046	0.073	0.097	0.117	0.160	0.205	0.239	0.248	0.255
415.8	0.048	0.076	0.099	0.119	0.163	0.208	0.243	0.255	0.257
420.4	0.051	0.078	0.101	0.120	0.165	0.212	0.251	0.261	0.264
425	0.053	0.080	0.102	0.122	0.166	0.217	0.252	0.264	0.268
429.6	0.054	0.081	0.103	0.124	0.169	0.218	0.254	0.267	0.274
434.2	0.055	0.082	0.104	0.124	0.170	0.222	0.258	0.274	0.277
438.8	0.056	0.083	0.105	0.125	0.171	0.225	0.266	0.274	0.277
443.4	0.056	0.083	0.106	0.125	0.174	0.226	0.263	0.274	0.279
448	0.056	0.084	0.106	0.126	0.175	0.231	0.265	0.277	0.280
452.6	0.056	0.082	0.105	0.125	0.176	0.231	0.265	0.276	0.278

Average Conductivity in the Middle Layer (Depth 0.762 m to 1.83 m)									
Frequency (MHz)	0% VMC	5% VMC	10% VMC	15% VMC	20% VMC	25% VMC	30% VMC	35% VMC	40% VMC
544.6	0.066	0.103	0.132	0.152	0.194	0.238	0.264	0.278	0.281
549.2	0.065	0.101	0.130	0.150	0.195	0.239	0.264	0.279	0.284
553.8	0.064	0.100	0.127	0.148	0.193	0.240	0.266	0.281	0.286
558.4	0.063	0.099	0.126	0.147	0.193	0.242	0.270	0.283	0.286
563	0.063	0.099	0.126	0.146	0.193	0.245	0.272	0.285	0.291
567.6	0.062	0.098	0.124	0.145	0.194	0.246	0.273	0.287	0.291
572.2	0.060	0.095	0.122	0.143	0.193	0.246	0.273	0.285	0.290
576.8	0.057	0.093	0.118	0.139	0.191	0.245	0.272	0.287	0.288
581.4	0.054	0.089	0.115	0.137	0.188	0.244	0.270	0.285	0.286
586	0.056	0.091	0.116	0.138	0.192	0.247	0.275	0.291	0.290
590.6	0.053	0.090	0.114	0.137	0.190	0.247	0.274	0.291	0.291
595.2	0.050	0.086	0.111	0.134	0.188	0.245	0.271	0.283	0.288
599.8	0.051	0.088	0.113	0.135	0.189	0.245	0.274	0.286	0.290
604.4	0.055	0.092	0.116	0.138	0.192	0.250	0.279	0.294	0.295
609	0.054	0.091	0.115	0.137	0.190	0.248	0.276	0.290	0.295
613.6	0.056	0.095	0.118	0.139	0.191	0.250	0.278	0.298	0.300
618.2	0.059	0.098	0.122	0.142	0.194	0.253	0.287	0.302	0.306
622.8	0.062	0.102	0.124	0.144	0.195	0.256	0.287	0.305	0.310
627.4	0.067	0.107	0.128	0.147	0.198	0.259	0.294	0.315	0.320
632	0.070	0.110	0.131	0.149	0.201	0.262	0.293	0.321	0.319
636.6	0.075	0.116	0.135	0.154	0.203	0.266	0.303	0.325	0.329
641.2	0.078	0.118	0.137	0.154	0.205	0.269	0.308	0.329	0.338
645.8	0.081	0.122	0.139	0.156	0.207	0.273	0.312	0.337	0.351
650.4	0.084	0.125	0.142	0.159	0.210	0.275	0.318	0.348	0.355
655	0.087	0.127	0.143	0.161	0.212	0.280	0.325	0.353	0.359
659.6	0.088	0.128	0.143	0.161	0.213	0.283	0.330	0.363	0.372
664.2	0.089	0.128	0.143	0.161	0.214	0.285	0.332	0.366	0.376
668.8	0.091	0.129	0.144	0.162	0.217	0.290	0.337	0.372	0.385
673.4	0.093	0.130	0.145	0.164	0.219	0.295	0.346	0.386	0.395
678	0.090	0.127	0.142	0.161	0.218	0.294	0.351	0.387	0.397
682.6	0.090	0.127	0.141	0.161	0.220	0.299	0.357	0.402	0.408
687.2	0.089	0.125	0.139	0.160	0.221	0.304	0.364	0.402	0.415
691.8	0.087	0.122	0.137	0.158	0.221	0.307	0.365	0.405	0.410
696.4	0.085	0.119	0.134	0.157	0.221	0.309	0.366	0.410	0.414
701	0.084	0.118	0.134	0.157	0.223	0.314	0.383	0.413	0.420
705.6	0.079	0.112	0.128	0.153	0.220	0.310	0.368	0.407	0.401
710.2	0.077	0.110	0.126	0.151	0.222	0.316	0.380	0.408	0.406
714.8	0.073	0.106	0.123	0.148	0.220	0.315	0.377	0.415	0.394
719.4	0.072	0.104	0.121	0.147	0.222	0.321	0.390	0.407	0.395
724	0.067	0.099	0.117	0.144	0.219	0.316	0.382	0.401	0.382
728.6	0.066	0.097	0.115	0.143	0.220	0.323	0.382	0.402	0.377
733.2	0.064	0.095	0.113	0.142	0.221	0.327	0.389	0.394	0.366
737.8	0.064	0.095	0.113	0.143	0.223	0.330	0.403	0.393	0.363
742.4	0.063	0.094	0.112	0.142	0.224	0.335	0.396	0.390	0.355
747	0.065	0.096	0.114	0.145	0.227	0.340	0.408	0.389	0.354
751.6	0.066	0.096	0.115	0.145	0.229	0.347	0.415	0.383	0.348
756.2	0.066	0.096	0.115	0.146	0.230	0.352	0.418	0.379	0.344
760.8	0.070	0.100	0.118	0.149	0.236	0.362	0.446	0.380	0.341
765.4	0.073	0.102	0.120	0.152	0.240	0.375	0.452	0.370	0.338
770	0.076	0.104	0.122	0.154	0.244	0.382	0.454	0.372	0.333
774.6	0.079	0.107	0.125	0.156	0.248	0.394	0.472	0.368	0.328
779.2	0.082	0.110	0.127	0.159	0.252	0.410	0.476	0.359	0.328
783.8	0.085	0.112	0.130	0.162	0.256	0.416	0.481	0.350	0.321
788.4	0.087	0.114	0.131	0.164	0.261	0.432	0.473	0.348	0.313
793	0.089	0.116	0.133	0.166	0.265	0.449	0.465	0.341	0.312
797.6	0.090	0.117	0.134	0.168	0.269	0.472	0.447	0.330	0.307
802.2	0.092	0.117	0.135	0.169	0.274	0.484	0.432	0.322	0.297
806.8	0.092	0.117	0.135	0.170	0.276	0.492	0.412	0.313	0.291
811.4	0.090	0.115	0.134	0.169	0.280	0.525	0.394	0.300	0.288
816	0.090	0.115	0.134	0.170	0.285	0.537	0.374	0.297	0.280
820.6	0.088	0.114	0.133	0.169	0.287	0.555	0.360	0.292	0.274
825.2	0.087	0.112	0.131	0.169	0.291	0.604	0.344	0.280	0.265
829.8	0.083	0.108	0.128	0.168	0.293	0.622	0.332	0.271	0.259
834.4	0.079	0.104	0.124	0.165	0.297	0.566	0.314	0.259	0.252
839	0.074	0.099	0.121	0.163	0.296	0.502	0.304	0.252	0.245
843.6	0.071	0.097	0.119	0.162	0.304	0.445	0.292	0.244	0.238
848.2	0.066	0.091	0.114	0.159	0.302	0.411	0.281	0.235	0.232
852.8	0.061	0.087	0.111	0.157	0.304	0.386	0.267	0.228	0.228
857.4	0.055	0.081	0.106	0.153	0.300	0.359	0.256	0.221	0.221
862	0.052	0.078	0.103	0.152	0.302	0.343	0.247	0.216	0.214
866.6	0.048	0.074	0.100	0.151	0.310	0.317	0.241	0.207	0.211
871.2	0.045	0.071	0.098	0.149	0.306	0.305	0.232	0.203	0.207
875.8	0.042	0.069	0.096	0.149	0.309	0.290	0.224	0.201	0.205
880.4	0.039	0.067	0.094	0.148	0.310	0.281	0.221	0.196	0.203
885	0.039	0.066	0.094	0.149	0.318	0.270	0.213	0.193	0.202
889.6	0.038	0.066	0.094	0.150	0.320	0.259	0.212	0.193	0.201
894.2	0.038	0.066	0.095	0.152	0.328	0.252	0.210	0.192	0.202
898.8	0.040	0.067	0.096	0.154	0.335	0.248	0.209	0.192	0.203
903.4	0.041	0.068	0.097	0.157	0.344	0.243	0.207	0.192	0.204
908	0.043	0.070	0.100	0.159	0.348	0.239	0.205	0.194	0.206
912.6	0.046	0.073	0.103	0.163	0.356	0.236	0.206	0.195	0.210
917.2	0.048	0.076	0.105	0.167	0.376	0.232	0.206	0.196	0.211

Frequency (MHz)	Average Permittivity in the Bottom Layer (Depth 1.83 m to 2.59 m)								
	0% VMC	5% VMC	10% VMC	15% VMC	20% VMC	25% VMC	30% VMC	35% VMC	40% VMC
80	4.57	8.84	11.29	14.09	17.51	22.12	24.34	29.49	31.11
84.6	4.37	8.58	10.99	13.75	17.16	21.75	24.08	28.77	30.76
89.2	4.39	8.49	10.89	13.66	17.03	21.72	24.06	28.71	30.76
93.8	4.30	8.36	10.71	13.49	16.94	21.57	23.73	28.76	30.63
98.4	4.03	8.02	10.37	13.15	16.53	21.05	23.37	28.32	30.00
103	3.88	7.86	10.15	12.94	16.33	20.97	23.29	28.25	29.79
107.6	3.82	7.70	10.04	12.82	16.34	20.86	23.27	28.21	29.84
112.2	3.68	7.57	9.88	12.73	16.21	20.87	23.11	28.13	29.95
116.8	3.42	7.27	9.55	12.40	15.86	20.45	22.87	27.69	29.49
121.4	3.26	7.05	9.39	12.18	15.66	20.33	22.78	27.59	29.42
126	3.27	7.03	9.28	12.15	15.60	20.31	22.81	27.46	29.42
130.6	3.22	6.91	9.17	12.01	15.48	20.17	22.60	27.43	29.37
135.2	3.05	6.72	9.00	11.84	15.30	19.98	22.53	27.19	29.12
139.8	2.86	6.47	8.71	11.55	14.95	19.62	22.17	26.63	28.77
144.4	2.84	6.41	8.62	11.46	14.91	19.47	22.13	26.72	28.60
149	2.94	6.46	8.64	11.46	14.85	19.42	22.06	26.53	28.55
153.6	3.07	6.53	8.70	11.49	14.87	19.30	22.06	26.47	28.29
158.2	2.93	6.34	8.47	11.26	14.53	19.00	21.63	25.80	27.89
162.8	2.96	6.29	8.41	11.12	14.36	18.78	21.55	25.69	27.63
167.4	3.03	6.31	8.40	11.08	14.30	18.58	21.21	25.59	27.36
172	2.90	6.12	8.16	10.80	14.01	18.31	20.88	25.00	27.02
176.6	3.02	6.20	8.21	10.86	13.97	18.36	20.88	24.76	26.63
181.2	3.07	6.19	8.15	10.75	13.82	18.06	20.66	24.43	26.51
185.8	3.17	6.22	8.13	10.72	13.74	17.88	20.22	24.22	26.16
190.4	3.17	6.17	8.06	10.59	13.64	17.71	20.37	24.01	26.40
195	3.16	6.07	7.99	10.48	13.46	17.47	20.06	23.74	26.13
199.6	3.03	5.95	7.77	10.27	13.12	17.20	19.89	23.42	25.73
204.2	3.01	5.88	7.73	10.21	13.06	17.01	19.78	23.34	25.21
208.8	2.92	5.77	7.57	10.04	12.90	16.78	19.61	23.13	25.46
213.4	2.94	5.74	7.53	10.01	12.86	16.65	19.51	22.93	25.18
218	2.80	5.62	7.39	9.84	12.62	16.48	19.52	22.75	25.13
222.6	2.84	5.63	7.40	9.83	12.66	16.38	19.43	22.46	24.96
227.2	2.70	5.47	7.25	9.68	12.46	16.24	19.53	22.07	25.68
231.8	2.50	5.23	7.05	9.53	12.27	16.17	19.36	22.28	24.65
236.4	2.50	5.27	7.03	9.49	12.22	16.09	19.26	21.90	24.74
241	2.50	5.20	7.01	9.48	12.22	15.79	19.40	21.56	24.82
245.6	2.42	5.16	6.95	9.40	12.15	15.73	19.53	21.68	24.65
250.2	2.36	5.07	6.88	9.41	12.05	15.82	19.72	21.05	24.66
254.8	2.14	4.87	6.63	9.20	11.81	15.51	19.44	21.06	24.01
259.4	2.33	5.05	6.81	9.36	11.99	15.47	19.66	21.14	24.38
264	2.32	5.00	6.76	9.28	11.94	15.23	19.44	20.85	24.10
268.6	2.22	4.91	6.66	9.19	11.72	15.13	19.82	20.68	23.28
273.2	2.38	5.05	6.83	9.35	11.96	15.08	19.15	20.13	23.23
277.8	2.08	4.76	6.50	9.07	11.50	14.69	19.35	19.80	23.10
282.4	2.19	4.84	6.55	9.08	11.59	14.42	20.03	19.17	22.45
287	2.50	5.08	6.77	9.31	11.63	14.62	18.71	19.62	22.69
291.6	2.35	4.95	6.68	9.19	11.35	14.48	18.85	18.92	21.57
296.2	2.43	5.00	6.67	8.97	11.57	14.21	19.21	18.77	21.74
300.8	2.69	5.21	6.85	9.26	11.55	14.12	19.30	18.40	21.86
305.4	2.51	4.97	6.70	9.08	11.18	13.91	19.09	18.39	21.42
310	2.54	5.00	6.63	9.04	11.20	13.82	18.59	17.83	21.03
314.6	2.54	4.98	6.59	8.90	11.05	13.35	18.54	17.70	21.65
319.2	2.44	4.86	6.42	8.88	10.83	13.16	18.68	17.43	20.78
323.8	2.63	4.97	6.64	8.95	11.08	13.62	19.03	17.25	21.69
328.4	2.40	4.72	6.33	8.73	10.67	13.23	18.92	17.31	21.23
333	2.32	4.66	6.23	8.53	10.57	12.76	18.99	16.84	21.88
337.6	2.39	4.71	6.32	8.60	10.50	13.10	19.21	17.48	21.84
342.2	2.25	4.61	6.12	8.43	10.32	12.74	19.14	17.72	22.53
346.8	2.10	4.37	6.00	8.34	10.28	12.49	19.21	17.61	22.27
351.4	2.05	4.31	5.89	8.28	10.06	12.15	19.14	17.51	22.49
356	1.90	4.18	5.70	8.06	9.91	12.11	19.68	17.95	22.75
360.6	1.93	4.19	5.73	8.13	9.80	11.98	19.48	18.07	22.63
365.2	1.71	3.94	5.59	7.82	9.57	12.03	19.38	18.15	22.65
369.8	1.52	3.76	5.30	7.77	9.55	11.55	19.28	18.15	22.22
374.4	1.59	3.83	5.45	7.81	9.56	11.78	19.25	18.53	22.27
379	1.59	3.84	5.41	7.76	9.56	11.64	18.75	18.61	22.17
383.6	1.56	3.83	5.37	7.74	9.36	11.06	18.56	18.25	21.96
388.2	1.65	3.90	5.43	7.85	9.38	11.45	18.51	18.43	21.78
392.8	1.65	3.87	5.40	7.82	9.37	11.11	18.35	18.18	21.60
397.4	1.72	3.95	5.46	7.96	9.43	11.04	17.86	18.21	21.50
402	1.95	4.13	5.69	8.11	9.53	11.03	17.67	18.36	21.46
406.6	2.08	4.30	5.79	8.20	9.39	10.91	17.64	18.33	21.39
411.2	2.30	4.46	5.96	8.20	9.44	10.79	17.47	18.45	21.47
415.8	2.24	4.41	5.93	8.10	9.37	10.84	17.28	18.45	21.27
420.4	2.36	4.50	5.99	8.24	9.40	10.62	17.11	18.50	21.30
425	2.69	4.81	6.32	8.59	9.58	10.55	17.13	18.93	21.57
429.6	2.72	4.80	6.31	8.35	9.49	10.40	17.09	18.96	21.50
434.2	2.90	4.95	6.39	8.57	9.38	10.53	17.15	19.31	21.70
438.8	2.89	4.95	6.40	8.55	9.56	10.41	16.97	19.37	21.73
443.4	3.00	5.01	6.48	8.69	9.61	10.56	16.99	19.68	21.86
448	3.02	5.04	6.44	8.69	9.30	10.15	16.98	19.87	22.08
452.6	2.93	4.97	6.40	8.52	9.34	10.15	16.94	19.89	21.80

Average Permittivity in the Bottom Layer (Depth 1.83 m to 2.59 m)									
Frequency (MHz)	0% VMC	5% VMC	10% VMC	15% VMC	20% VMC	25% VMC	30% VMC	35% VMC	40% VMC
544.6	2.01	4.36	6.24	8.67	9.86	11.04	14.91	18.64	19.74
549.2	2.22	4.50	6.23	8.77	9.94	11.16	14.98	18.76	19.90
553.8	2.34	4.59	6.31	8.76	10.01	11.21	14.95	18.99	20.08
558.4	2.47	4.74	6.49	8.84	10.02	11.30	15.00	19.16	20.20
563	2.60	4.84	6.49	8.89	10.06	11.33	15.06	19.27	20.31
567.6	2.69	4.93	6.59	8.81	10.09	11.40	15.10	19.39	20.49
572.2	2.80	5.01	6.67	8.85	10.15	11.51	15.11	19.64	20.61
576.8	2.89	5.11	6.76	8.88	10.20	11.60	15.12	19.60	20.72
581.4	2.95	5.12	6.78	8.87	10.24	11.70	15.25	19.91	20.86
586	2.94	5.16	6.71	8.86	10.24	11.68	15.20	19.82	20.80
590.6	3.00	5.17	6.74	8.88	10.27	11.78	15.11	19.87	20.90
595.2	3.01	5.20	6.77	8.86	10.27	11.80	15.14	19.95	20.98
599.8	2.95	5.17	6.71	8.78	10.27	11.85	15.03	19.85	20.87
604.4	2.92	5.17	6.78	8.79	10.26	11.82	14.89	19.70	20.76
609	2.88	5.17	6.73	8.71	10.20	11.77	14.79	19.62	20.63
613.6	2.83	5.13	6.76	8.70	10.19	11.74	14.63	19.45	20.43
618.2	2.79	5.17	6.73	8.66	10.17	11.66	14.48	19.27	20.33
622.8	2.77	5.09	6.75	8.63	10.10	11.62	14.32	19.09	20.03
627.4	2.76	5.23	6.76	8.60	10.04	11.55	14.15	18.82	19.83
632	2.76	5.21	6.80	8.57	10.02	11.53	14.02	18.69	19.74
636.6	2.73	5.31	6.82	8.54	10.00	11.46	13.88	18.51	19.42
641.2	2.79	5.33	6.82	8.51	9.94	11.37	13.72	18.26	19.29
645.8	2.81	5.34	6.85	8.48	9.88	11.28	13.55	17.95	19.07
650.4	2.89	5.42	6.86	8.48	9.87	11.30	13.48	17.96	18.94
655	2.96	5.51	6.91	8.46	9.86	11.25	13.40	17.81	18.82
659.6	3.06	5.55	6.94	8.44	9.82	11.20	13.29	17.69	18.79
664.2	3.08	5.58	6.95	8.42	9.81	11.19	13.22	17.72	18.74
668.8	3.23	5.65	6.97	8.43	9.82	11.19	13.18	17.63	18.75
673.4	3.36	5.75	7.01	8.44	9.81	11.20	13.11	17.73	18.80
678	3.43	5.76	6.99	8.41	9.81	11.19	13.12	17.80	19.00
682.6	3.50	5.79	7.04	8.44	9.82	11.29	13.17	17.92	19.00
687.2	3.62	5.85	7.05	8.43	9.84	11.30	13.19	18.04	19.20
691.8	3.69	5.90	7.06	8.42	9.86	11.34	13.22	18.33	19.55
696.4	3.75	5.92	7.07	8.43	9.89	11.40	13.25	18.51	19.81
701	3.91	6.00	7.11	8.47	9.94	11.49	13.28	18.76	19.92
705.6	3.91	5.95	7.06	8.43	9.97	11.59	13.35	19.17	20.85
710.2	3.96	5.99	7.08	8.43	10.02	11.65	13.41	19.53	20.72
714.8	4.00	5.97	7.05	8.41	9.99	11.71	13.41	20.08	20.73
719.4	4.07	6.03	7.10	8.44	10.05	11.72	13.54	19.87	19.82
724	4.03	5.97	7.02	8.39	10.07	11.84	13.60	20.63	19.62
728.6	4.10	5.97	7.01	8.37	10.05	11.86	13.52	20.60	18.28
733.2	4.10	5.97	7.01	8.37	10.09	11.94	13.58	19.45	17.84
737.8	4.12	5.97	6.99	8.35	10.07	11.92	13.49	19.83	16.87
742.4	4.15	5.96	6.99	8.33	10.08	11.91	13.43	17.95	14.70
747	4.19	6.00	7.00	8.33	10.07	11.93	13.38	16.42	13.24
751.6	4.19	6.01	6.99	8.31	10.01	11.89	13.21	15.37	11.27
756.2	4.20	5.96	6.94	8.24	9.98	11.78	13.06	13.85	10.57
760.8	4.28	6.02	6.99	8.28	9.99	11.82	12.92	12.87	8.86
765.4	4.36	6.08	7.02	8.28	9.93	11.73	12.67	11.49	8.64
770	4.37	6.05	6.99	8.23	9.91	11.63	12.48	11.02	7.41
774.6	4.44	6.10	7.00	8.22	9.86	11.50	12.39	9.53	6.42
779.2	4.48	6.11	7.00	8.20	9.80	11.46	12.09	8.38	5.84
783.8	4.55	6.14	7.02	8.20	9.78	11.45	11.77	7.52	5.00
788.4	4.61	6.17	7.02	8.18	9.75	11.34	11.54	6.69	4.36
793	4.66	6.17	7.02	8.16	9.72	11.24	11.24	6.23	3.69
797.6	4.72	6.21	7.04	8.17	9.69	11.16	11.00	5.40	3.41
802.2	4.75	6.22	7.03	8.16	9.70	11.12	10.80	4.82	3.07
806.8	4.78	6.23	7.05	8.17	9.71	11.07	10.65	4.45	2.90
811.4	4.83	6.24	7.05	8.16	9.68	11.05	10.24	4.03	2.56
816	4.86	6.25	7.05	8.15	9.69	11.07	9.82	4.08	2.45
820.6	4.88	6.24	7.05	8.16	9.75	11.00	9.81	3.71	2.26
825.2	4.95	6.29	7.10	8.20	9.76	11.08	9.57	3.16	2.06
829.8	4.95	6.30	7.09	8.21	9.84	11.10	9.21	2.97	2.07
834.4	4.94	6.26	7.06	8.18	9.85	11.19	9.14	2.79	1.96
839	4.92	6.25	7.05	8.20	9.91	11.31	8.82	2.85	1.94
843.6	4.98	6.28	7.08	8.24	10.01	11.26	8.51	2.48	1.87
848.2	4.94	6.24	7.06	8.22	10.03	11.46	8.43	2.39	1.94
852.8	4.92	6.22	7.05	8.24	10.13	11.53	8.17	2.45	1.95
857.4	4.84	6.15	6.98	8.21	10.19	11.66	7.96	2.32	1.95
862	4.86	6.16	7.01	8.25	10.32	11.76	7.73	2.23	2.02
866.6	4.84	6.13	6.98	8.22	10.32	11.22	7.50	2.24	2.00
871.2	4.84	6.13	6.99	8.26	10.41	11.30	7.35	2.19	2.09
875.8	4.79	6.09	6.95	8.24	10.46	11.18	6.98	2.25	2.22
880.4	4.77	6.07	6.94	8.24	10.57	11.21	6.73	2.33	2.44
885	4.77	6.07	6.93	8.23	10.56	10.68	6.47	2.11	2.26
889.6	4.76	6.06	6.94	8.24	10.57	10.16	6.31	2.28	2.50
894.2	4.80	6.10	6.96	8.27	10.62	9.67	5.76	2.39	2.59
898.8	4.83	6.10	6.97	8.26	10.66	9.36	5.63	2.54	2.71
903.4	4.82	6.09	6.95	8.24	10.62	8.59	5.45	2.40	2.79
908	4.87	6.13	6.99	8.27	10.58	7.98	5.19	2.44	2.95
912.6	4.91	6.15	7.00	8.27	10.54	7.04	4.91	2.60	3.07
917.2	4.95	6.19	7.04	8.31	10.56	6.84	4.72	2.66	3.26

Average Conductivity in the Bottom Layer (Depth 1.83 m to 2.59 m)									
Frequency (MHz)	0% VMC	5% VMC	10% VMC	15% VMC	20% VMC	25% VMC	30% VMC	35% VMC	40% VMC
80	0.003	0.022	0.043	0.076	0.110	0.147	0.169	0.187	0.195
84.6	0.003	0.022	0.044	0.078	0.111	0.149	0.171	0.194	0.199
89.2	0.004	0.024	0.045	0.079	0.114	0.150	0.173	0.196	0.199
93.8	0.004	0.025	0.047	0.082	0.115	0.153	0.179	0.196	0.204
98.4	0.004	0.025	0.048	0.083	0.117	0.157	0.183	0.201	0.210
103	0.005	0.026	0.049	0.084	0.120	0.157	0.184	0.199	0.214
107.6	0.005	0.027	0.051	0.087	0.120	0.160	0.188	0.203	0.215
112.2	0.006	0.028	0.052	0.088	0.123	0.160	0.193	0.207	0.215
116.8	0.006	0.029	0.053	0.090	0.125	0.165	0.195	0.212	0.222
121.4	0.006	0.030	0.054	0.092	0.127	0.163	0.195	0.209	0.221
126	0.007	0.031	0.056	0.093	0.130	0.168	0.199	0.217	0.226
130.6	0.007	0.032	0.057	0.096	0.131	0.170	0.205	0.213	0.229
135.2	0.007	0.032	0.058	0.097	0.129	0.169	0.204	0.214	0.228
139.8	0.007	0.033	0.058	0.097	0.132	0.168	0.205	0.219	0.231
144.4	0.008	0.034	0.060	0.099	0.135	0.169	0.208	0.220	0.228
149	0.009	0.035	0.061	0.100	0.135	0.174	0.209	0.217	0.229
153.6	0.010	0.036	0.062	0.102	0.135	0.170	0.212	0.219	0.236
158.2	0.009	0.036	0.063	0.102	0.134	0.173	0.209	0.215	0.241
162.8	0.010	0.037	0.064	0.102	0.135	0.172	0.218	0.222	0.235
167.4	0.010	0.038	0.065	0.105	0.137	0.168	0.221	0.225	0.232
172	0.010	0.038	0.064	0.105	0.137	0.171	0.222	0.215	0.242
176.6	0.011	0.039	0.066	0.106	0.140	0.172	0.224	0.219	0.233
181.2	0.012	0.040	0.066	0.106	0.137	0.174	0.219	0.218	0.241
185.8	0.012	0.040	0.067	0.107	0.136	0.170	0.224	0.223	0.234
190.4	0.013	0.041	0.068	0.108	0.139	0.173	0.231	0.221	0.255
195	0.013	0.042	0.069	0.109	0.142	0.175	0.226	0.225	0.251
199.6	0.013	0.042	0.069	0.110	0.139	0.176	0.238	0.227	0.254
204.2	0.013	0.042	0.070	0.111	0.142	0.172	0.236	0.230	0.247
208.8	0.013	0.043	0.069	0.111	0.142	0.176	0.239	0.235	0.260
213.4	0.014	0.043	0.070	0.111	0.142	0.172	0.236	0.230	0.261
218	0.014	0.043	0.071	0.113	0.143	0.172	0.248	0.236	0.263
222.6	0.015	0.045	0.072	0.115	0.144	0.174	0.250	0.232	0.267
227.2	0.015	0.045	0.073	0.115	0.145	0.176	0.262	0.229	0.283
231.8	0.014	0.044	0.073	0.116	0.147	0.174	0.250	0.239	0.261
236.4	0.015	0.046	0.074	0.116	0.144	0.173	0.248	0.236	0.269
241	0.017	0.048	0.076	0.118	0.146	0.170	0.250	0.227	0.267
245.6	0.017	0.049	0.078	0.120	0.149	0.170	0.252	0.234	0.269
250.2	0.018	0.050	0.079	0.123	0.150	0.176	0.260	0.228	0.270
254.8	0.017	0.049	0.077	0.123	0.145	0.174	0.254	0.225	0.260
259.4	0.020	0.053	0.081	0.124	0.150	0.170	0.259	0.231	0.265
264	0.021	0.054	0.083	0.125	0.150	0.169	0.252	0.229	0.265
268.6	0.023	0.055	0.084	0.127	0.148	0.169	0.253	0.229	0.255
273.2	0.026	0.058	0.088	0.131	0.154	0.167	0.243	0.223	0.256
277.8	0.024	0.057	0.086	0.129	0.149	0.164	0.248	0.223	0.255
282.4	0.026	0.059	0.088	0.132	0.153	0.164	0.261	0.221	0.252
287	0.030	0.063	0.091	0.134	0.151	0.165	0.237	0.227	0.259
291.6	0.030	0.063	0.093	0.135	0.150	0.166	0.244	0.226	0.253
296.2	0.031	0.065	0.093	0.131	0.157	0.166	0.249	0.228	0.259
300.8	0.035	0.068	0.096	0.137	0.156	0.164	0.254	0.229	0.265
305.4	0.034	0.067	0.097	0.138	0.154	0.167	0.251	0.235	0.267
310	0.035	0.068	0.097	0.138	0.156	0.166	0.250	0.236	0.270
314.6	0.035	0.069	0.098	0.138	0.156	0.163	0.252	0.240	0.274
319.2	0.035	0.068	0.096	0.140	0.154	0.163	0.254	0.246	0.280
323.8	0.037	0.070	0.100	0.142	0.160	0.170	0.260	0.249	0.284
328.4	0.035	0.069	0.098	0.143	0.158	0.170	0.260	0.259	0.292
333	0.034	0.068	0.098	0.140	0.158	0.165	0.262	0.259	0.292
337.6	0.035	0.069	0.099	0.142	0.157	0.173	0.263	0.276	0.302
342.2	0.033	0.068	0.098	0.142	0.159	0.171	0.262	0.281	0.294
346.8	0.031	0.066	0.097	0.145	0.163	0.171	0.263	0.289	0.300
351.4	0.030	0.065	0.097	0.146	0.162	0.168	0.260	0.300	0.299
356	0.029	0.065	0.096	0.144	0.161	0.171	0.255	0.303	0.292
360.6	0.030	0.065	0.097	0.147	0.162	0.173	0.256	0.310	0.298
365.2	0.028	0.064	0.098	0.145	0.162	0.176	0.250	0.311	0.289
369.8	0.028	0.064	0.097	0.149	0.166	0.174	0.246	0.316	0.294
374.4	0.029	0.066	0.100	0.150	0.168	0.179	0.244	0.314	0.294
379	0.031	0.068	0.101	0.150	0.171	0.180	0.247	0.316	0.293
383.6	0.032	0.070	0.102	0.153	0.170	0.177	0.246	0.327	0.296
388.2	0.034	0.072	0.104	0.155	0.171	0.183	0.244	0.330	0.305
392.8	0.037	0.074	0.107	0.156	0.174	0.183	0.243	0.336	0.307
397.4	0.039	0.077	0.109	0.160	0.177	0.185	0.248	0.340	0.306
402	0.042	0.079	0.112	0.161	0.178	0.187	0.253	0.344	0.318
406.6	0.044	0.082	0.114	0.162	0.178	0.188	0.255	0.357	0.330
411.2	0.047	0.084	0.116	0.161	0.179	0.189	0.259	0.366	0.331
415.8	0.049	0.086	0.118	0.162	0.181	0.193	0.259	0.367	0.336
420.4	0.052	0.089	0.120	0.166	0.183	0.195	0.262	0.375	0.347
425	0.053	0.090	0.122	0.168	0.185	0.197	0.270	0.388	0.351
429.6	0.055	0.091	0.123	0.165	0.186	0.199	0.269	0.389	0.354
434.2	0.056	0.092	0.123	0.167	0.186	0.203	0.271	0.395	0.357
438.8	0.056	0.093	0.124	0.168	0.189	0.205	0.275	0.394	0.362
443.4	0.057	0.093	0.125	0.170	0.192	0.209	0.277	0.401	0.365
448	0.057	0.094	0.124	0.170	0.192	0.212	0.281	0.402	0.369
452.6	0.056	0.093	0.125	0.169	0.196	0.216	0.276	0.399	0.362

Average Conductivity in the Bottom Layer (Depth 1.83 m to 2.59 m)									
Frequency (MHz)	0% VMC	5% VMC	10% VMC	15% VMC	20% VMC	25% VMC	30% VMC	35% VMC	40% VMC
544.6	0.067	0.117	0.155	0.186	0.233	0.272	0.273	0.389	0.375
549.2	0.065	0.115	0.152	0.184	0.233	0.273	0.274	0.391	0.377
553.8	0.064	0.113	0.150	0.183	0.230	0.277	0.275	0.397	0.381
558.4	0.064	0.112	0.148	0.180	0.233	0.280	0.279	0.400	0.387
563	0.064	0.112	0.147	0.179	0.234	0.282	0.282	0.405	0.394
567.6	0.063	0.111	0.145	0.180	0.236	0.284	0.284	0.409	0.395
572.2	0.060	0.108	0.142	0.176	0.234	0.287	0.285	0.407	0.399
576.8	0.057	0.105	0.139	0.174	0.232	0.286	0.285	0.414	0.402
581.4	0.054	0.102	0.136	0.172	0.233	0.286	0.284	0.407	0.402
586	0.056	0.104	0.138	0.172	0.235	0.288	0.288	0.418	0.408
590.6	0.055	0.102	0.136	0.169	0.234	0.290	0.288	0.418	0.407
595.2	0.051	0.099	0.132	0.167	0.233	0.287	0.286	0.415	0.407
599.8	0.052	0.101	0.134	0.168	0.233	0.290	0.288	0.418	0.411
604.4	0.055	0.105	0.136	0.170	0.234	0.292	0.292	0.427	0.418
609	0.054	0.104	0.135	0.169	0.232	0.290	0.291	0.427	0.423
613.6	0.057	0.107	0.137	0.169	0.235	0.291	0.293	0.430	0.432
618.2	0.060	0.111	0.141	0.172	0.237	0.292	0.296	0.438	0.436
622.8	0.063	0.114	0.142	0.172	0.236	0.292	0.298	0.439	0.450
627.4	0.068	0.118	0.146	0.175	0.237	0.295	0.303	0.452	0.459
632	0.071	0.122	0.148	0.177	0.240	0.297	0.306	0.458	0.458
636.6	0.076	0.127	0.151	0.181	0.243	0.299	0.309	0.461	0.470
641.2	0.079	0.129	0.153	0.181	0.243	0.300	0.312	0.473	0.480
645.8	0.082	0.131	0.154	0.183	0.244	0.302	0.316	0.493	0.498
650.4	0.085	0.135	0.157	0.185	0.246	0.305	0.320	0.492	0.506
655	0.088	0.137	0.158	0.186	0.249	0.307	0.323	0.499	0.526
659.6	0.090	0.137	0.158	0.186	0.249	0.309	0.326	0.514	0.529
664.2	0.090	0.137	0.158	0.187	0.250	0.310	0.331	0.514	0.534
668.8	0.092	0.138	0.158	0.187	0.252	0.314	0.335	0.536	0.565
673.4	0.094	0.138	0.159	0.190	0.254	0.319	0.343	0.547	0.578
678	0.092	0.135	0.157	0.187	0.254	0.320	0.345	0.556	0.585
682.6	0.091	0.135	0.156	0.188	0.256	0.323	0.349	0.579	0.630
687.2	0.091	0.133	0.155	0.187	0.257	0.327	0.354	0.599	0.653
691.8	0.088	0.130	0.152	0.186	0.258	0.329	0.357	0.600	0.670
696.4	0.086	0.128	0.150	0.185	0.258	0.332	0.362	0.618	0.683
701	0.086	0.126	0.149	0.185	0.261	0.337	0.371	0.652	0.753
705.6	0.080	0.121	0.145	0.181	0.259	0.337	0.371	0.651	0.735
710.2	0.078	0.119	0.143	0.181	0.261	0.340	0.377	0.678	0.816
714.8	0.075	0.115	0.140	0.179	0.260	0.341	0.381	0.699	0.865
719.4	0.073	0.113	0.138	0.177	0.262	0.348	0.384	0.781	0.949
724	0.069	0.109	0.135	0.175	0.260	0.346	0.382	0.778	0.993
728.6	0.067	0.107	0.133	0.175	0.262	0.350	0.393	0.830	1.024
733.2	0.065	0.105	0.131	0.174	0.263	0.351	0.395	0.904	1.055
737.8	0.065	0.105	0.132	0.174	0.264	0.357	0.404	0.915	1.066
742.4	0.065	0.104	0.131	0.175	0.265	0.359	0.408	0.959	1.084
747	0.067	0.106	0.133	0.177	0.269	0.364	0.415	0.989	1.085
751.6	0.067	0.106	0.133	0.178	0.272	0.370	0.427	1.006	1.075
756.2	0.068	0.106	0.133	0.178	0.271	0.372	0.430	1.015	1.058
760.8	0.072	0.110	0.136	0.181	0.276	0.377	0.442	1.006	1.040
765.4	0.075	0.112	0.138	0.184	0.280	0.385	0.458	1.001	1.027
770	0.077	0.114	0.140	0.186	0.281	0.390	0.463	0.989	0.990
774.6	0.080	0.116	0.143	0.189	0.285	0.400	0.466	0.972	0.966
779.2	0.084	0.119	0.145	0.191	0.290	0.404	0.478	0.950	0.937
783.8	0.086	0.122	0.148	0.194	0.293	0.408	0.491	0.932	0.906
788.4	0.089	0.123	0.150	0.196	0.296	0.417	0.499	0.909	0.875
793	0.091	0.125	0.151	0.198	0.299	0.425	0.509	0.892	0.841
797.6	0.092	0.126	0.152	0.200	0.304	0.435	0.518	0.868	0.818
802.2	0.093	0.127	0.154	0.202	0.307	0.441	0.524	0.848	0.792
806.8	0.093	0.127	0.154	0.203	0.309	0.452	0.531	0.833	0.776
811.4	0.091	0.125	0.153	0.203	0.314	0.464	0.546	0.819	0.757
816	0.091	0.125	0.153	0.204	0.317	0.470	0.556	0.808	0.736
820.6	0.090	0.124	0.152	0.204	0.319	0.480	0.559	0.791	0.718
825.2	0.088	0.122	0.151	0.205	0.325	0.493	0.571	0.768	0.695
829.8	0.085	0.119	0.149	0.204	0.327	0.506	0.580	0.756	0.690
834.4	0.080	0.115	0.145	0.202	0.330	0.515	0.585	0.749	0.673
839	0.076	0.111	0.142	0.201	0.333	0.529	0.593	0.745	0.666
843.6	0.073	0.108	0.141	0.202	0.338	0.552	0.605	0.730	0.649
848.2	0.067	0.103	0.136	0.199	0.341	0.563	0.612	0.721	0.641
852.8	0.062	0.099	0.134	0.198	0.344	0.582	0.618	0.720	0.633
857.4	0.056	0.094	0.129	0.195	0.343	0.592	0.623	0.708	0.624
862	0.053	0.091	0.127	0.196	0.347	0.614	0.628	0.692	0.621
866.6	0.049	0.088	0.125	0.195	0.353	0.652	0.628	0.689	0.595
871.2	0.046	0.085	0.123	0.195	0.359	0.669	0.632	0.674	0.592
875.8	0.043	0.083	0.122	0.195	0.361	0.691	0.631	0.669	0.592
880.4	0.041	0.081	0.121	0.195	0.363	0.710	0.630	0.658	0.584
885	0.040	0.080	0.120	0.197	0.372	0.735	0.625	0.636	0.560
889.6	0.040	0.080	0.121	0.198	0.379	0.749	0.621	0.629	0.554
894.2	0.040	0.081	0.122	0.201	0.387	0.770	0.612	0.615	0.537
898.8	0.041	0.082	0.124	0.204	0.393	0.777	0.604	0.607	0.527
903.4	0.042	0.083	0.125	0.206	0.403	0.785	0.596	0.583	0.514
908	0.044	0.085	0.128	0.210	0.414	0.786	0.583	0.563	0.502
912.6	0.047	0.088	0.131	0.214	0.426	0.785	0.571	0.553	0.489
917.2	0.050	0.091	0.134	0.218	0.434	0.784	0.557	0.535	0.479

APPENDIX I

MATLAB CODE: SIMULATION OF RADIO WAVE REFLECTIONS FROM DIELECTRIC PROFILES

```
% Soil Reflection Calculator

% This program calculates the dielectric properties of the soil from
% the reflection patterns in the coaxial cell.
% Written by Duane Needham
% June 22, 2003

% numeric constants
e = 8.854*10^-12;
u = 4*pi*10^-7;
d = 0.1524;

%constk %recalls frequency and permittivity values from file constk.m
%consts %recalls conductivity values from file "consts.m"

f = 1000000*K(:,1);
w = 2*pi*f*ones(1,13);

Bfree = 2*pi*f*(u*e)^0.5;
Zo = (u/e)^0.5*ones(size(f));

for x = 1:9,
    for y = 1:13,
        k(:,y) = K(:,(x-1)*13+y+1);
        s(:,y) = S(:,(x-1)*13+y+1);
    end

    gamma = ((j*w*u).*(s+j*w.*k*e)).^0.5;
    Zs = (j*w*u)./gamma;
% skin = 1./real(gamma(:,1))
% pause

    c1 = cos(0.349)*ones(size(f));
    c2 = cos(asin((sin(0.349)*Bfree)./imag(gamma(:,1))));
    r(:,1)=(Zs(:,1).*c2-Zo.*c1)./(Zs(:,1).*c2+Zo.*c1);

    for x = 2:13
        r(:,x)=(Zs(:,x)-Zs(:,x-1))./(Zs(:,x)+Zs(:,x-1)).*(1-
            r(:,1)).*(1+r(:,1));
    end

    refl = zeros(size(f));
    for x = 13:-1:1,
        refl = refl.*exp(-2*d*gamma(:,x))+r(:,x);
    end

    abs(refl)
    subplot(2,1,1),
```

```

    plot(f,abs( refl))
    xlabel('Frequency (MHz)')
    ylabel('Magnitude')
subplot(2,1,2),
    plot(f,unwrap(angle( refl)))
    xlabel('Frequency (MHz)')
    ylabel('Phase (rad)')
pause

%plot (real( refl), imag( refl))
% Title('Reflection from moisture profile')
% xlabel('Real component')
% ylabel('Imaginary component')
% pause
    unwrap(angle( refl))
    pause
end

```

APPENDIX J

FIELD MEASUREMENT REFLECTIONS

Frequency (MHz)	Magnitudes and Phases from Measured Reflection Coefficients							
	Profile #1		Profile #2		Profile #3		Profile #4	
	Magnitude	Phase (rad)	Magnitude	Phase (rad)	Magnitude	Phase (rad)	Magnitude	Phase (rad)
80	0.653	2.686	0.767	2.917	0.642	3.095	0.719	2.949
84.6	0.633	2.625	0.657	2.522	0.672	2.675	0.652	2.805
89.2	0.589	2.601	0.554	2.582	0.697	2.597	0.637	2.793
93.8	0.588	2.593	0.538	2.558	0.660	2.602	0.647	2.808
98.4	0.597	2.604	0.530	2.554	0.593	2.552	0.589	2.827
103	0.488	2.637	0.453	2.576	0.526	2.525	0.566	2.856
107.6	0.481	2.620	0.439	2.597	0.575	2.570	0.563	2.850
112.2	0.481	2.564	0.447	2.589	0.548	2.538	0.561	2.828
116.8	0.499	2.734	0.473	2.744	0.531	2.665	0.570	2.914
121.4	0.484	2.613	0.443	2.635	0.540	2.597	0.580	2.850
126	0.467	2.590	0.441	2.610	0.514	2.561	0.528	2.815
130.6	0.509	2.552	0.437	2.646	0.561	2.627	0.553	2.756
135.2	0.453	2.553	0.441	2.571	0.560	2.499	0.482	2.776
139.8	0.474	2.607	0.437	2.618	0.546	2.543	0.531	2.843
144.4	0.495	2.658	0.435	2.654	0.510	2.610	0.568	2.899
149	0.507	2.585	0.447	2.719	0.516	2.709	0.571	2.828
153.6	0.452	2.668	0.442	2.708	0.545	2.662	0.516	2.895
158.2	0.479	2.721	0.456	2.733	0.524	2.702	0.541	2.942
162.8	0.467	2.718	0.467	2.754	0.506	2.725	0.556	2.977
167.4	0.491	2.773	0.468	2.745	0.520	2.775	0.567	2.992
172	0.516	2.781	0.500	2.819	0.565	2.810	0.575	3.043
176.6	0.486	2.799	0.484	2.827	0.544	2.774	0.614	3.068
181.2	0.498	2.845	0.476	2.851	0.538	2.788	0.588	3.064
185.8	0.503	2.850	0.486	2.871	0.527	2.790	0.617	3.075
190.4	0.518	2.854	0.484	2.876	0.520	2.791	0.607	3.069
195	0.521	2.814	0.508	2.873	0.544	2.772	0.620	3.077
199.6	0.468	2.879	0.433	2.902	0.478	2.780	0.587	3.118
204.2	0.496	2.933	0.462	2.969	0.494	2.851	0.613	3.138
208.8	0.506	2.940	0.492	2.997	0.505	2.888	0.644	3.127
213.4	0.513	2.967	0.488	3.000	0.502	2.913	0.614	3.111
218	0.505	2.977	0.488	3.018	0.506	2.936	0.615	3.144
222.6	0.498	2.964	0.454	2.987	0.488	2.916	0.624	3.175
227.2	0.508	3.020	0.475	3.102	0.506	2.971	0.661	3.184
231.8	0.496	2.971	0.456	3.034	0.483	2.941	0.615	3.155
236.4	0.486	2.993	0.444	3.049	0.460	2.972	0.601	3.183
241	0.474	2.992	0.443	3.034	0.473	2.988	0.627	3.203
245.6	0.511	2.941	0.466	2.999	0.486	2.949	0.637	3.174
250.2	0.493	2.906	0.433	2.928	0.475	2.912	0.634	3.156
254.8	0.477	2.938	0.422	2.993	0.448	2.945	0.625	3.179
259.4	0.513	2.946	0.487	3.002	0.479	2.982	0.632	3.184
264	0.514	2.972	0.482	2.977	0.492	3.027	0.672	3.183
268.6	0.556	2.877	0.491	2.847	0.544	2.909	0.687	3.126
273.2	0.519	2.770	0.446	2.759	0.486	2.808	0.662	3.068
277.8	0.498	2.777	0.431	2.722	0.486	2.827	0.618	3.055
282.4	0.504	2.798	0.451	2.730	0.497	2.804	0.619	3.058
287	0.562	2.799	0.481	2.747	0.527	2.812	0.673	3.059
291.6	0.642	2.765	0.575	2.702	0.603	2.746	0.719	2.974
296.2	0.758	2.624	0.714	2.548	0.686	2.516	0.735	2.826
300.8	0.642	2.385	0.548	2.293	0.516	2.372	0.635	2.824
305.4	0.590	2.523	0.517	2.461	0.517	2.556	0.624	2.860
310	0.610	2.603	0.528	2.562	0.528	2.604	0.659	2.931
314.6	0.663	2.627	0.582	2.617	0.596	2.669	0.703	2.914
319.2	0.702	2.552	0.629	2.541	0.654	2.597	0.730	2.859
323.8	0.710	2.427	0.593	2.465	0.674	2.462	0.736	2.813
328.4	0.646	2.381	0.574	2.486	0.610	2.399	0.700	2.769
333	0.690	2.377	0.590	2.446	0.648	2.368	0.703	2.772
337.6	0.656	2.051	0.513	2.237	0.559	2.053	0.619	2.668
342.2	0.364	2.401	0.427	2.598	0.383	2.583	0.582	2.922
346.8	0.492	2.587	0.491	2.650	0.515	2.632	0.674	2.948
351.4	0.555	2.610	0.522	2.680	0.554	2.630	0.695	2.914
356	0.577	2.596	0.540	2.648	0.609	2.651	0.687	2.871
360.6	0.576	2.583	0.513	2.649	0.591	2.596	0.717	2.891
365.2	0.557	2.605	0.500	2.681	0.579	2.602	0.704	2.884
369.8	0.539	2.617	0.481	2.705	0.557	2.623	0.705	2.915
374.4	0.512	2.645	0.446	2.737	0.558	2.648	0.693	2.918
379	0.504	2.689	0.436	2.782	0.508	2.679	0.665	2.928
383.6	0.475	2.705	0.406	2.861	0.514	2.732	0.652	2.951
388.2	0.484	2.768	0.438	2.913	0.522	2.769	0.677	2.973
392.8	0.490	2.735	0.425	2.854	0.512	2.742	0.662	2.953
397.4	0.450	2.738	0.395	2.875	0.479	2.735	0.636	2.960
402	0.434	2.763	0.394	2.915	0.453	2.771	0.639	2.979
406.6	0.444	2.769	0.384	2.913	0.473	2.802	0.648	3.005

Magnitudes and Phases from Measured Reflection Coefficients								
Frequency (MHz)	Profile #1		Profile #2		Profile #3		Profile #4	
	Magnitude	Phase (rad)	Magnitude	Phase (rad)	Magnitude	Phase (rad)	Magnitude	Phase (rad)
544.6	0.534	2.548	0.533	2.720	0.546	2.639	0.639	2.869
549.2	0.514	2.550	0.515	2.715	0.548	2.632	0.643	2.863
553.8	0.501	2.540	0.524	2.732	0.520	2.633	0.636	2.874
558.4	0.488	2.564	0.524	2.708	0.514	2.627	0.635	2.882
563	0.502	2.584	0.530	2.700	0.519	2.660	0.619	2.877
567.6	0.542	2.593	0.560	2.657	0.552	2.659	0.648	2.882
572.2	0.578	2.488	0.594	2.567	0.576	2.595	0.635	2.831
576.8	0.535	2.368	0.531	2.438	0.555	2.509	0.626	2.816
581.4	0.482	2.362	0.483	2.445	0.500	2.507	0.602	2.817
586	0.438	2.355	0.454	2.443	0.482	2.519	0.603	2.850
590.6	0.430	2.414	0.422	2.486	0.462	2.562	0.577	2.841
595.2	0.401	2.426	0.409	2.513	0.438	2.600	0.572	2.880
599.8	0.389	2.451	0.386	2.512	0.441	2.644	0.567	2.893
604.4	0.387	2.448	0.388	2.491	0.453	2.674	0.544	2.914
609	0.388	2.403	0.393	2.462	0.450	2.649	0.559	2.922
613.6	0.393	2.317	0.386	2.369	0.473	2.620	0.562	2.924
618.2	0.385	2.238	0.395	2.300	0.469	2.549	0.572	2.879
622.8	0.383	2.130	0.399	2.212	0.473	2.461	0.551	2.833
627.4	0.367	2.051	0.383	2.148	0.460	2.367	0.556	2.770
632	0.367	2.018	0.406	2.153	0.438	2.305	0.536	2.748
636.6	0.366	2.032	0.406	2.150	0.432	2.272	0.530	2.723
641.2	0.371	2.057	0.413	2.181	0.427	2.294	0.499	2.711
645.8	0.382	2.126	0.434	2.201	0.420	2.306	0.512	2.728
650.4	0.394	2.180	0.447	2.259	0.444	2.365	0.528	2.778
655	0.417	2.256	0.480	2.279	0.475	2.391	0.557	2.804
659.6	0.437	2.292	0.488	2.296	0.517	2.432	0.569	2.819
664.2	0.495	2.345	0.506	2.287	0.560	2.411	0.605	2.807
668.8	0.509	2.308	0.503	2.272	0.607	2.371	0.640	2.805
673.4	0.532	2.252	0.503	2.238	0.614	2.271	0.659	2.759
678	0.503	2.227	0.473	2.249	0.594	2.242	0.642	2.723
682.6	0.495	2.287	0.446	2.286	0.577	2.255	0.636	2.739
687.2	0.484	2.330	0.431	2.354	0.553	2.282	0.620	2.744
691.8	0.471	2.371	0.438	2.419	0.561	2.319	0.626	2.776
696.4	0.487	2.417	0.430	2.464	0.573	2.370	0.631	2.803
701	0.504	2.456	0.427	2.491	0.561	2.364	0.659	2.838
705.6	0.494	2.443	0.435	2.535	0.572	2.388	0.651	2.841
710.2	0.499	2.451	0.439	2.546	0.570	2.382	0.667	2.842
714.8	0.493	2.435	0.427	2.529	0.555	2.381	0.682	2.842
719.4	0.470	2.416	0.411	2.519	0.545	2.380	0.664	2.825
724	0.441	2.394	0.383	2.514	0.518	2.380	0.660	2.801
728.6	0.419	2.398	0.355	2.527	0.505	2.401	0.649	2.834
733.2	0.396	2.392	0.338	2.541	0.478	2.381	0.638	2.815
737.8	0.400	2.406	0.328	2.578	0.472	2.395	0.623	2.834
742.4	0.378	2.381	0.323	2.561	0.458	2.404	0.602	2.816
747	0.369	2.380	0.320	2.592	0.460	2.419	0.602	2.842
751.6	0.365	2.389	0.325	2.605	0.462	2.427	0.588	2.828
756.2	0.378	2.405	0.337	2.612	0.465	2.399	0.604	2.857
760.8	0.383	2.365	0.349	2.570	0.480	2.357	0.609	2.837
765.4	0.385	2.325	0.346	2.520	0.486	2.343	0.624	2.844
770	0.372	2.296	0.334	2.516	0.460	2.307	0.623	2.827
774.6	0.351	2.304	0.328	2.515	0.444	2.299	0.611	2.826
779.2	0.332	2.300	0.326	2.508	0.442	2.293	0.612	2.817
783.8	0.322	2.309	0.309	2.484	0.424	2.286	0.596	2.821
788.4	0.312	2.315	0.302	2.459	0.417	2.257	0.628	2.828
793	0.302	2.292	0.285	2.434	0.399	2.227	0.599	2.808
797.6	0.298	2.260	0.290	2.408	0.376	2.218	0.599	2.779
802.2	0.306	2.236	0.303	2.409	0.377	2.214	0.587	2.773
806.8	0.309	2.190	0.326	2.385	0.363	2.176	0.595	2.756
811.4	0.346	2.195	0.350	2.355	0.375	2.173	0.595	2.734
816	0.373	2.162	0.370	2.322	0.391	2.145	0.637	2.712
820.6	0.402	2.142	0.398	2.333	0.414	2.122	0.635	2.668
825.2	0.430	2.137	0.428	2.343	0.452	2.126	0.672	2.657
829.8	0.470	2.150	0.448	2.333	0.460	2.110	0.687	2.639
834.4	0.467	2.136	0.462	2.356	0.480	2.084	0.708	2.607
839	0.476	2.140	0.442	2.346	0.495	2.099	0.699	2.580
843.6	0.467	2.132	0.449	2.380	0.502	2.103	0.715	2.565
848.2	0.454	2.178	0.430	2.417	0.476	2.110	0.680	2.548
852.8	0.433	2.209	0.420	2.461	0.481	2.161	0.670	2.558
857.4	0.411	2.239	0.414	2.503	0.473	2.228	0.650	2.564
862	0.406	2.300	0.415	2.540	0.479	2.274	0.647	2.602
866.6	0.409	2.397	0.410	2.584	0.487	2.346	0.616	2.613
871.2	0.430	2.490	0.400	2.666	0.538	2.386	0.622	2.663

Magnitudes and Phases from Measured Reflection Coefficients								
Frequency (MHz)	Profile #5		Profile #6		Profile #7		Profile #8	
	Magnitude	Phase (rad)	Magnitude	Phase (rad)	Magnitude	Phase (rad)	Magnitude	Phase (rad)
80	0.784	2.710	0.568	3.179	0.565	3.132	0.768	2.832
84.6	0.652	2.850	0.628	2.865	0.640	2.834	0.658	2.869
89.2	0.653	2.749	0.644	2.826	0.625	2.787	0.637	2.820
93.8	0.588	2.815	0.635	2.852	0.616	2.818	0.624	2.826
98.4	0.559	2.822	0.605	2.830	0.588	2.832	0.617	2.841
103	0.542	2.834	0.598	2.880	0.568	2.851	0.606	2.848
107.6	0.555	2.844	0.593	2.871	0.563	2.841	0.622	2.826
112.2	0.529	2.836	0.536	2.867	0.542	2.858	0.589	2.823
116.8	0.597	2.939	0.629	2.920	0.604	2.956	0.580	2.837
121.4	0.581	2.852	0.569	2.876	0.551	2.883	0.566	2.803
126	0.542	2.828	0.569	2.862	0.553	2.899	0.584	2.798
130.6	0.572	2.817	0.586	2.854	0.551	2.890	0.616	2.773
135.2	0.532	2.737	0.559	2.806	0.502	2.839	0.508	2.735
139.8	0.530	2.784	0.550	2.853	0.536	2.900	0.507	2.806
144.4	0.556	2.839	0.546	2.891	0.520	2.959	0.523	2.867
149	0.549	2.779	0.565	2.930	0.513	3.039	0.541	2.899
153.6	0.495	2.876	0.547	2.930	0.580	2.993	0.535	2.913
158.2	0.532	2.926	0.578	2.983	0.536	2.980	0.537	2.953
162.8	0.532	2.934	0.553	2.974	0.548	3.016	0.537	2.980
167.4	0.560	2.977	0.571	3.002	0.586	3.057	0.556	2.987
172	0.573	2.981	0.588	3.011	0.597	3.034	0.600	3.019
176.6	0.577	2.985	0.579	3.012	0.586	3.036	0.593	3.014
181.2	0.560	3.004	0.582	3.034	0.559	3.032	0.584	3.028
185.8	0.561	3.009	0.595	3.040	0.571	3.060	0.590	3.050
190.4	0.573	3.041	0.606	3.066	0.579	3.063	0.600	3.051
195	0.591	3.023	0.587	3.026	0.579	3.008	0.596	3.000
199.6	0.534	3.057	0.579	3.099	0.549	3.069	0.557	3.014
204.2	0.564	3.103	0.577	3.096	0.576	3.142	0.573	3.098
208.8	0.582	3.114	0.628	3.146	0.593	3.143	0.605	3.129
213.4	0.598	3.134	0.609	3.126	0.583	3.127	0.610	3.120
218	0.600	3.142	0.613	3.132	0.586	3.143	0.612	3.123
222.6	0.572	3.142	0.599	3.120	0.566	3.137	0.585	3.114
227.2	0.604	3.188	0.626	3.190	0.594	3.216	0.615	3.204
231.8	0.585	3.164	0.604	3.160	0.575	3.179	0.595	3.146
236.4	0.588	3.178	0.612	3.186	0.578	3.184	0.580	3.152
241	0.589	3.176	0.609	3.178	0.586	3.190	0.588	3.174
245.6	0.598	3.165	0.608	3.141	0.592	3.174	0.599	3.146
250.2	0.595	3.134	0.635	3.120	0.606	3.160	0.587	3.108
254.8	0.585	3.152	0.603	3.134	0.576	3.172	0.572	3.131
259.4	0.606	3.133	0.626	3.152	0.602	3.165	0.584	3.162
264	0.617	3.162	0.653	3.168	0.617	3.191	0.614	3.183
268.6	0.613	3.091	0.668	3.068	0.637	3.119	0.637	3.104
273.2	0.593	3.063	0.644	3.043	0.595	3.107	0.602	3.072
277.8	0.579	3.051	0.642	3.042	0.589	3.118	0.618	3.076
282.4	0.586	3.042	0.639	3.020	0.610	3.120	0.568	3.062
287	0.607	3.040	0.647	3.011	0.616	3.123	0.640	3.079
291.6	0.652	3.003	0.709	2.955	0.668	3.067	0.676	2.985
296.2	0.713	2.835	0.714	2.794	0.679	2.886	0.715	2.818
300.8	0.561	2.763	0.598	2.777	0.561	2.888	0.594	2.816
305.4	0.570	2.895	0.631	2.867	0.565	2.964	0.589	2.855
310	0.596	2.905	0.612	2.884	0.591	3.009	0.608	2.909
314.6	0.617	2.949	0.670	2.921	0.602	3.008	0.643	2.929
319.2	0.658	2.922	0.699	2.855	0.662	2.963	0.685	2.851
323.8	0.681	2.842	0.690	2.797	0.646	2.913	0.661	2.779
328.4	0.655	2.841	0.653	2.753	0.601	2.869	0.645	2.771
333	0.658	2.814	0.666	2.722	0.594	2.796	0.628	2.704
337.6	0.533	2.780	0.564	2.580	0.480	2.726	0.513	2.628
342.2	0.588	3.007	0.538	2.953	0.495	3.098	0.507	2.983
346.8	0.648	2.988	0.593	2.913	0.572	3.071	0.593	2.972
351.4	0.672	2.987	0.657	2.928	0.610	3.055	0.634	2.936
356	0.688	2.986	0.662	2.889	0.629	3.013	0.636	2.910
360.6	0.700	2.957	0.659	2.882	0.632	3.007	0.637	2.931
365.2	0.673	2.960	0.644	2.893	0.631	3.017	0.636	2.903
369.8	0.681	2.968	0.642	2.907	0.616	3.034	0.608	2.925
374.4	0.661	2.972	0.642	2.949	0.608	3.065	0.619	2.961
379	0.667	3.013	0.632	2.944	0.612	3.055	0.595	2.958
383.6	0.671	3.023	0.632	2.997	0.595	3.076	0.604	3.030
388.2	0.653	3.016	0.648	3.013	0.616	3.105	0.620	3.009
392.8	0.666	3.003	0.633	2.991	0.594	3.088	0.603	3.024
397.4	0.640	3.000	0.606	2.997	0.597	3.135	0.596	3.034
402	0.635	3.040	0.599	3.014	0.608	3.140	0.586	3.042
406.6	0.659	3.032	0.593	3.037	0.595	3.127	0.573	3.056

Frequency (MHz)	Magnitudes and Phases from Measured Reflection Coefficients							
	Profile #5		Profile #6		Profile #7		Profile #8	
	Magnitude	Phase (rad)	Magnitude	Phase (rad)	Magnitude	Phase (rad)	Magnitude	Phase (rad)
544.6	0.673	2.884	0.661	2.892	0.605	3.027	0.626	3.003
549.2	0.628	2.863	0.666	2.882	0.620	3.044	0.596	2.986
553.8	0.645	2.897	0.653	2.897	0.604	3.054	0.605	3.024
558.4	0.644	2.898	0.661	2.900	0.607	3.050	0.601	3.024
563	0.648	2.927	0.646	2.891	0.602	3.048	0.610	3.065
567.6	0.660	2.894	0.684	2.893	0.637	3.055	0.625	3.038
572.2	0.685	2.883	0.666	2.825	0.623	2.999	0.646	3.025
576.8	0.653	2.826	0.674	2.826	0.590	2.995	0.610	2.973
581.4	0.649	2.855	0.629	2.810	0.584	3.017	0.612	2.995
586	0.632	2.829	0.601	2.806	0.567	3.022	0.613	2.980
590.6	0.610	2.856	0.589	2.829	0.553	3.048	0.593	3.024
595.2	0.616	2.854	0.577	2.863	0.563	3.105	0.578	3.026
599.8	0.593	2.879	0.573	2.875	0.558	3.101	0.567	3.065
604.4	0.594	2.878	0.571	2.891	0.571	3.140	0.584	3.062
609	0.605	2.893	0.573	2.876	0.574	3.128	0.595	3.086
613.6	0.619	2.850	0.578	2.873	0.583	3.126	0.607	3.049
618.2	0.595	2.812	0.565	2.807	0.588	3.105	0.615	3.044
622.8	0.601	2.748	0.559	2.786	0.573	3.071	0.629	2.979
627.4	0.579	2.724	0.544	2.741	0.550	3.035	0.604	2.949
632	0.574	2.688	0.524	2.724	0.558	3.054	0.582	2.885
636.6	0.551	2.670	0.508	2.690	0.533	3.019	0.571	2.888
641.2	0.557	2.680	0.509	2.729	0.535	3.053	0.580	2.867
645.8	0.561	2.672	0.530	2.722	0.553	3.058	0.562	2.874
650.4	0.570	2.720	0.538	2.759	0.570	3.091	0.574	2.874
655	0.579	2.704	0.549	2.738	0.578	3.074	0.594	2.899
659.6	0.607	2.742	0.574	2.794	0.605	3.069	0.620	2.904
664.2	0.630	2.725	0.588	2.755	0.654	3.051	0.642	2.880
668.8	0.661	2.739	0.609	2.761	0.651	3.026	0.668	2.846
673.4	0.646	2.662	0.610	2.681	0.651	2.977	0.661	2.771
678	0.618	2.667	0.596	2.725	0.633	2.983	0.635	2.780
682.6	0.630	2.692	0.592	2.741	0.633	3.014	0.611	2.768
687.2	0.603	2.722	0.589	2.793	0.630	3.035	0.609	2.828
691.8	0.626	2.755	0.592	2.795	0.637	3.044	0.605	2.833
696.4	0.635	2.809	0.594	2.817	0.654	3.052	0.612	2.880
701	0.653	2.815	0.619	2.826	0.659	3.046	0.604	2.880
705.6	0.655	2.835	0.617	2.846	0.682	3.074	0.625	2.909
710.2	0.672	2.825	0.635	2.836	0.680	3.040	0.626	2.905
714.8	0.667	2.828	0.619	2.844	0.669	3.031	0.641	2.919
719.4	0.675	2.810	0.620	2.826	0.661	3.014	0.612	2.869
724	0.666	2.828	0.604	2.842	0.654	3.039	0.610	2.898
728.6	0.661	2.820	0.594	2.823	0.643	3.028	0.604	2.895
733.2	0.650	2.835	0.571	2.844	0.640	3.032	0.578	2.896
737.8	0.634	2.820	0.580	2.858	0.635	3.035	0.579	2.892
742.4	0.640	2.846	0.553	2.848	0.627	3.026	0.564	2.904
747	0.645	2.844	0.550	2.858	0.627	3.026	0.559	2.893
751.6	0.637	2.845	0.533	2.871	0.623	3.035	0.553	2.924
756.2	0.648	2.839	0.551	2.891	0.641	3.038	0.554	2.896
760.8	0.644	2.821	0.544	2.877	0.655	3.030	0.542	2.912
765.4	0.659	2.810	0.548	2.883	0.649	3.022	0.526	2.877
770	0.642	2.786	0.534	2.871	0.652	2.988	0.522	2.918
774.6	0.648	2.801	0.538	2.901	0.666	2.998	0.508	2.921
779.2	0.642	2.784	0.543	2.930	0.646	2.973	0.486	2.976
783.8	0.637	2.782	0.544	2.934	0.633	2.977	0.488	2.990
788.4	0.635	2.754	0.526	2.913	0.617	2.966	0.498	3.035
793	0.641	2.755	0.543	2.918	0.630	2.978	0.495	3.023
797.6	0.626	2.713	0.507	2.902	0.608	2.972	0.497	3.047
802.2	0.626	2.721	0.520	2.904	0.604	2.967	0.496	3.018
806.8	0.602	2.687	0.508	2.910	0.588	2.939	0.507	3.054
811.4	0.616	2.691	0.527	2.908	0.610	2.946	0.501	2.996
816	0.638	2.657	0.519	2.866	0.596	2.911	0.514	3.018
820.6	0.634	2.649	0.560	2.873	0.615	2.943	0.528	2.972
825.2	0.679	2.634	0.546	2.823	0.619	2.910	0.534	2.962
829.8	0.692	2.637	0.570	2.816	0.638	2.908	0.563	2.923
834.4	0.700	2.594	0.569	2.794	0.621	2.866	0.556	2.932
839	0.710	2.614	0.589	2.783	0.616	2.856	0.569	2.898
843.6	0.715	2.608	0.575	2.765	0.632	2.871	0.575	2.923
848.2	0.710	2.634	0.592	2.787	0.616	2.885	0.575	2.892
852.8	0.706	2.631	0.572	2.807	0.602	2.889	0.563	2.943
857.4	0.676	2.657	0.576	2.839	0.605	2.926	0.568	2.945
862	0.697	2.670	0.568	2.866	0.606	2.933	0.554	2.978
866.6	0.691	2.693	0.567	2.921	0.609	2.979	0.586	3.015
871.2	0.724	2.715	0.596	2.932	0.629	2.982	0.602	3.051

APPENDIX K

MATLAB CODE: PROFILE RESTORATION ALGORITHM

```
% Soil Dielectric Profile Restoration Algorithm

% This program calculates a 2-layer dielectric profile of soil from two
reflection coefficients.
% Written by Duane Needham
% June 25, 2003

% *****
% EM numeric constants
e = 8.854*10^-12;
u = 4*pi*10^-7;
Zo = (u/e)^0.5;
l = 0.304;
N1 = 10;    %number of profiles

% *****
%const1; %recalls data in "const1.m"
%*****
f = 1000000*A(:,1);
w = 2*pi*f;
for x1 = 1:N1,
    M = A(2,2*x1);
    p = A(2,2*x1+1);
    r = ((M.*cos(p))+(j*M.*sin(p)));
%    r = A(2,2*x1)+j*A(2,2*x1+1);
    Zin = Zo*0.94*(1+r)/(1-r);

% Start with permittivity and conductivity values of soil at 20% VMC
s(x1) = 0.15;
k(x1) = 14;

% initialize variables
gamma = zeros(1,9);
Zs = zeros(1,9);
d = zeros(1,9);

for x2 = 1:3000,
gamma(1) = ((j*w(2)*u).*(s(x1)+j*w(2)*k(x1)*e)).^0.5;
gamma(2) = ((j*w(2)*u).*(s(x1)+j*w(2).*(k(x1)-0.001)*e)).^0.5;
gamma(3) = ((j*w(2)*u).*(s(x1)+j*w(2).*(k(x1)+0.001)*e)).^0.5;
gamma(4) = ((j*w(2)*u).*((s(x1)-0.00001)+j*w(2).*k(x1)*e)).^0.5;
gamma(5) = ((j*w(2)*u).*((s(x1)+0.00001)+j*w(2).*k(x1)*e)).^0.5;
gamma(6) = ((j*w(2)*u).*((s(x1)-0.00001)+j*w(2).*(k(x1)-
0.001)*e)).^0.5;
gamma(7) = ((j*w(2)*u).*((s(x1)-
0.00001)+j*w(2).*(k(x1)+0.001)*e)).^0.5;
```

```

        gamma(8) = ((j*w(2)*u).*(s(x1)+0.00001)+j*w(2).*(k(x1)-
0.001)*e)).^0.5;
        gamma(9) =
((j*w(2)*u).*(s(x1)+0.00001)+j*w(2).*(k(x1)+0.001)*e)).^0.5;

        for x3 = 1:9,
            Zs(x3) = (j*w(2)*u)./gamma(x3);
            d(x3) = abs(Zs(x3)-Zin);
        end

        d1 = min(d);
        for x3 = 1:9,
            if d1 == d(x3)
                adj = x3;
            end
        end
        if adj == 2
            k(x1) = k(x1)-0.01;
        end
        if adj == 3
            k(x1) = k(x1)+0.01;
        end
        if adj == 4
            s(x1) = s(x1)-0.001;
        end
        if adj == 5
            s(x1) = s(x1)+0.001;
        end
        if adj == 6
            s(x1) = s(x1)-0.001;
            k(x1) = k(x1)-0.01;
        end
        if adj == 7
            s(x1) = s(x1)-0.001;
            k(x1) = k(x1)+0.01;
        end
        if adj == 8
            s(x1) = s(x1)+0.001;
            k(x1) = k(x1)-0.01;
        end
        if adj == 9
            s(x1) = s(x1)+0.001;
            k(x1) = k(x1)+0.01;
        end
    end
end

Zin
Zs(1)
k'
s'
MC = (k-2.1967)./0.5661;
k = 0.5844.*MC+3.1069;
s = -0.00006*MC.^2 + 0.005*MC + 0.0036;

for x1 = 1:N1
    g = ((j*w(1)*u).*(s(x1)+j*w(1)*k(x1)*e)).^0.5;
    Z = (j*w(1)*u)./g;
end

```

```

r = (Z-Zo*0.94)./(Z+Zo*0.94);

M = A(1,2*x1);
p = A(1,2*x1+1);
r1 = ((M.*cos(p))+(j*M.*sin(p)));
r1 = (r1-r)./exp(-2*g*x1)./(1-r)./(1+r);

%r1 = (A(1,2*x1)+j*A(1,2*x1+1)-r)./exp(-2*g*x1)./(1-r)./(1+r);
Zin = Zo*(1+r1)/(1-r1);

% Start with permittivity and conductivity values of topsoil

% initialize variables
gamma = zeros(1,9);
Zs = zeros(1,9);
d = zeros(1,9);

for x2 = 1:3000,
gamma(1) = ((j*w(1)*u).*(s(x1)+j*w(1)*k(x1)*e)).^0.5;
gamma(2) = ((j*w(1)*u).*(s(x1)+j*w(1).*(k(x1)-0.001)*e)).^0.5;
gamma(3) = ((j*w(1)*u).*(s(x1)+j*w(1).*(k(x1)+0.001)*e)).^0.5;
gamma(4) = ((j*w(1)*u).*((s(x1)-0.00001)+j*w(1).*(k(x1)*e)).^0.5;
gamma(5) = ((j*w(1)*u).*((s(x1)+0.00001)+j*w(1).*(k(x1)*e)).^0.5;
gamma(6) = ((j*w(1)*u).*((s(x1)-0.00001)+j*w(1).*(k(x1)-
0.001)*e)).^0.5;
gamma(7) = ((j*w(1)*u).*((s(x1)-
0.00001)+j*w(1).*(k(x1)+0.001)*e)).^0.5;
gamma(8) = ((j*w(1)*u).*((s(x1)+0.00001)+j*w(1).*(k(x1)-
0.001)*e)).^0.5;
gamma(9) =
((j*w(1)*u).*((s(x1)+0.00001)+j*w(1).*(k(x1)+0.001)*e)).^0.5;

    for x3 = 1:9,
        Zs(x3) = (j*w(1)*u)./gamma(x3);
        d(x3) = abs(Zs(x3)-Zin);
    end

    d1 = min(d);
    for x3 = 1:9,
        if d1 == d(x3)
            adj = x3;
        end
    end
    if adj == 2
        k(x1) = k(x1)-0.01;
    end
    if adj == 3
        k(x1) = k(x1)+0.01;
    end
    if adj == 4
        s(x1) = s(x1)-0.001;
    end
    if adj == 5
        s(x1) = s(x1)+0.001;
    end
    if adj == 6

```

```
        s(x1) = s(x1)-0.001;
        k(x1) = k(x1)-0.01;
    end
    if adj == 7
        s(x1) = s(x1)-0.001;
        k(x1) = k(x1)+0.01;
    end
    if adj == 8
        s(x1) = s(x1)+0.001;
        k(x1) = k(x1)-0.01;
    end
    if adj == 9
        s(x1) = s(x1)+0.001;
        k(x1) = k(x1)+0.01;
    end
end
end

end
Zin
Zs(1)
k'
s'
```

VITA 

Duane Lee Needham

Candidate for the Degree of

Doctor of Philosophy

Thesis: NON-CONTACT PREDICTION OF SOIL MOISTURE PROFILES USING
RADIO WAVE REFLECTION

Major Field: Biosystems Engineering

Biographical:

Personal Data: Born in Minden, Nebraska on February 24, 1975, the son of Dale L., and Gwen Y. Needham.

Education: Graduated from Minden High School, Minden, Nebraska, May, 1993; received a Bachelor of Science degree in Agribusiness from the University of Nebraska—Lincoln, Lincoln, Nebraska, May, 1998; received a Master of Science Degree in Biosystems Engineering from Oklahoma State University, Stillwater, Oklahoma, July, 2000; completed the requirements for the Doctor of Philosophy Degree with a major in Biosystems Engineering from Oklahoma State University, August, 2003.

Professional Experience: Graduate Assistant, Biosystems and Agricultural Engineering Department, Oklahoma State University, June, 1998 to August, 2003; Student Assistant, Nebraska Tractor Testing Laboratory, University of Nebraska-Lincoln, October, 1996 to May, 1998; Member American Society of Agricultural Engineers.